UNIVERSITY OF LIÈGE

Faculty of Medicine

University Hospital of Liège (CHU de Liège)

Doctoral thesis under international joint supervision with:

The University of Melbourne – Faculty of Medicine, Dentistry and Health Sciences

Royal Victorian Eye and Ear Hospital (RVEEH)

Doctoral Thesis in Medicine

Atraumatic Electrode Insertion and Frequency Mapping Optimization: Surgical and Functional Innovations for Enhanced Cochlear Implant Outcomes

Submitted by

Dr Guillaume Gersdorff

Promotor:

Prof. Philippe Lefebvre

(University of Liège – CHU de Liège)

Co-Promotor:

A/Prof. Jean-Marc Gérard

(The Royal Victorian Eye and Ear Hospital – University of Melbourne)

Thesis conducted under the framework of an international joint PhD agreement

Faculty of Medicine – University of Liège

Doctoral School of Health Sciences (EDSS)

Academic Year: 2025 – 2026

ACKNOWLEDGEMENTS

A doctoral thesis is a demanding journey, marked by doubt, effort, enthusiasm, and self-transcendence. But above all, it is a path shaped by encounters, by silent or decisive support, and by the transmission of knowledge and values. This thesis is as much the result of a collective endeavour as it is of a personal commitment. To all those who, at one time or another, crossed my path and helped me bring this project to fruition, I wish to express my deepest and most sincere gratitude.

First and foremost, I wish to warmly thank Professor Philippe Lefebvre, promoter of this thesis, whose role was instrumental at every stage of this journey. It is thanks to his vision, his intellectual generosity, and his unwavering trust that this work was able to be conceived, to grow, and ultimately to come to life. His support has been steadfast, both scientifically and personally. He inspired in me a passion for research, the joy of collaboration, the discipline of rigour, and the pride in work well done. He encouraged me to aim higher, to push my limits, and to build with a long-term perspective. He supported me with unwavering determination in my international project, enabling me not only to carry out part of this thesis in Australia, but also to complete a surgical fellowship there. Thanks to him, future projects and international collaborations are now possible, for which I am profoundly grateful.

My deepest appreciation also goes to Professor Jean-Marc Gérard, co-promoter of this multicentric thesis, who has trained me in surgery with exemplary rigour and inspiring humanity. He has imparted far more than surgical technique: he instilled in me a passion for precision in every gesture, confidence in the operating theatre, and calm in the face of complexity. He introduced me to the fields of otologic and otoneurosurgical practice with passion, exacting standards, and kindness. His welcome in Australia, both warm and efficient, allowed me to quickly integrate into a new and demanding environment while developing both my clinical and scientific skills in English. Thanks to him and Professor Lefebvre, I now have the privilege of participating in multicentre research projects and contributing to a truly international research dynamic.

I also extend my sincere thanks to Professor Stephen O'Leary and Professor Robert Briggs for welcoming me into their team in Melbourne. Their patience, their pedagogy, and their outstanding scientific and surgical expertise have greatly enriched my skill set and helped shape a professional identity that is open-minded, rigorous, and future-oriented.

I warmly thank Dr Phoebe Ramos for her constant commitment to all of our scientific and surgical projects. In Australia, I had the great fortune to discover not only an outstanding collaborator, remarkable in her precision and professionalism, but also a loyal and invaluable friend.

I am deeply grateful to Professor Naïma Deggouj, whose teaching at the Catholic University of Leuven played a pivotal role in shaping my academic and professional trajectory. Through her scientific excellence, intellectual rigor, and inspiring enthusiasm for clinical research, she instilled in me a deep appreciation for scientific inquiry and provided the methodological foundations that continue to guide my work today.

I would also like to express my heartfelt gratitude to all my colleagues at the CHU of Liège, who welcomed me with open arms, kindness, curiosity, and respect. You have created an

environment that fosters progress, dialogue, and mutual inspiration. You are present every day in my surgical and clinical training, and I am deeply aware of how fortunate I am to be part of this team.

Now, with particular emotion, I wish to thank my father, Professor Michel Gersdorff. For as long as I can remember, he has embodied excellence, rigour, and intellectual curiosity. Long before I became aware of it myself, he instilled in me a passion for medicine, for work done with care, and for knowledge as both a quest and a responsibility. Above all, however, he offered me a precious relationship, filled with shared moments, deep conversations, sincere exchanges, and a rare sense of complicity. These moments, between father and son, between doctors, between researchers, have shaped who I am and continue to carry me forward. They are life's treasures, which I cherish deeply. His calm, his serenity, and his unwavering belief in merit and continuous growth have formed the bedrock upon which I have built myself.

To my family, I wish to extend my heartfelt thanks. To my parents, my brothers, and my sisters, who have always supported me unconditionally, believed in me even through periods of doubt, and helped me navigate the most complex moments with their gentle, steadfast presence and non-judgmental listening. Their love and trust have been my most solid foundation.

And then, there is Pauline, my lovely wife. You have been by my side since the very beginning of my medical studies, and you have never ceased to support me. You have shared my enthusiasm, my long writing nights, my absences, my doubts, always with grace and strength. You followed me to Australia, to the other side of the world, with quiet determination and rare elegance. You transformed this experience into a unique chapter of our life, filled with discovery, laughter, tenderness, and love. You are my balance, my refuge, my light. And today, you have given me the greatest gift of all: our son, Oscar. May he one day discover for himself the joy of learning, the richness of sharing, and the pride of surpassing himself. I hope to pass on to him, as best I can, all the values that this thesis has helped awaken and strengthen in me.

Finally, I thank all those who, through a word, a glance, a conversation, have helped make this scientific journey a profoundly human one. This thesis is, in part, also yours.

PREFACE

The word “sense,” derived from the Latin sensus, refers to the faculty of perception. As early as Antiquity, Aristotle reflected on how smell, taste, touch, hearing, and sight enable us to apprehend our surroundings. The integration of sensory signals is fundamental to survival, to the understanding of the world, and to action.

The senses are the windows through which human beings perceive the world. Acting as true interfaces between the individual and the environment, they allow us to grasp even the subtlest nuances of reality. Vision reveals forms, colors, and movement; touch connects us to textures, temperatures, and contours; smell and taste, closely intertwined, immerse us in a realm of flavors and fragrances, often charged with memories and emotions. These various sensory modalities shape our perceptual experience in complementary and indispensable ways. Among them, hearing holds a unique position. It captures fleeting air vibrations and transforms them into sound, voices, melodies. This subtle sense links the individual to the living world: from rustling leaves to thunder, from the regularity of footsteps to the unique timbre of a familiar voice. Hearing is not limited to a passive role of reception. It enables expression, the sharing of ideas, the transmission of emotions, and cultural creation. It is a vector of humanity.

The auditory system functions to generate an internal representation of the acoustic environment, that is, to construct perception from elementary sensations. This ability is vital for all living organisms, from the simplest to the most complex.

In the animal kingdom, auditory strategies are diverse and demonstrate remarkable adaptive plasticity. Certain species, such as bats and dolphins, rely on echolocation to navigate their environment. They emit and analyze ultrasounds, with frequencies exceeding 20 kHz, far beyond human capability [1]. Other animals, such as elephants, communicate using infrasound (<20 Hz), capable of traveling across several kilometers [2]. In songbirds, hearing is specialized for identifying the complex patterns of birdsong, which play a crucial role in reproduction and territorial behavior.

In humans, hearing developed in close conjunction with the emergence of language. The so-called “linguistic staircase” hypothesis posits a co-evolution of vocal and auditory capacities, which progressively facilitated the increasing complexity of human language [3]. This adaptive dynamic enabled the fine discrimination of sounds, a critical advantage for communication. In turn, language shaped cognition, memory, social interaction, and cultural transmission. This co-evolutionary process was accompanied by neurological transformations. Verbal exchanges contributed to the strengthening of connections between auditory, linguistic, and emotional brain areas. Human hearing does not merely register sound signals: it interprets them, contextualizes them, and links them to intentions and emotions. It lies at the heart of social dynamics and cultural constructs.

From an anthropological perspective, the evolution of the human auditory system reflects selective pressures favoring the detection of salient sounds within three-dimensional environments. The capacity to localize a sound source, to recognize a call, or to detect danger proved crucial. In Homo sapiens, this evolution is particularly evident in the increased sensitivity to frequencies between 500 and 4000 Hz, the range characteristic of human speech [4]. Insights from paleogenetics and paleoanthropology further support this evolutionary perspective. The FOXP2 gene, strongly implicated in language capacities, plays a key role in the development of auditory and vocal skills [5]. Its presence in modern humans, and in closely

related forms in certain hominids, suggests an evolutionary convergence toward optimized hearing for verbal communication. Moreover, the analysis of ear bone structures in hominid fossils reveals similarities with current anatomical configurations, indicating a continuous evolutionary trajectory toward auditory specialization.

The anatomical organization of the human ear reflects this specialization. The pinna, through its shape, effectively captures and amplifies vocal sounds. Sound vibrations are transmitted by the ossicles to the cochlea, where hair cells ensure the mechano-transduction of acoustic signals into neural signals. These are then conveyed to the auditory cortex via the cochlear nerve. The auditory cortex, organized hierarchically, processes acoustic information through both parallel and sequential pathways, enabling the precise discrimination and recognition of rapid and complex acoustic patterns that underlie phoneme identification. The semantic interpretation and comprehension of speech, however, emerge from higher-order processing within distributed cortical language networks involving temporo-frontal regions [6].

This capacity to analyze the frequency and temporal variations of sounds also enables precise coordination of social interactions. It constituted a decisive evolutionary lever in the development of articulated language, music, and, more broadly, symbolic cognition.

Thus, human hearing extends far beyond a simple sensory modality. It represents a complex evolutionary interface linking biological, cognitive, social, and cultural dimensions of communication. Studying its evolution provides insight into the neural systems that support human language. Although spoken language has likely been evolutionarily favored because it allows communication while freeing the hands for other actions, language itself is not limited to the auditory modality. In individuals with deafness, signed languages support full cognitive, emotional, and social development through visual-manual communication. However, the absence of auditory input leads to structural and functional adaptations of the brain, reflecting the plasticity of neural systems involved in human communication.

TABLE OF CONTENT

I. Introduction 11
1. Physiology of Hearing 11
1.1. The Outer Ear 12
1.2. The Middle Ear 13
1.3. The Inner Ear 15
1.3.1 Macroscopic Anatomy 15
1.3.2. Microscopic Anatomy 19
1.3.2.1. Basilar membrane and Organ of Corti 19
1.3.2.2. Inner Hair Cells 21
1.3.2.3. Outer Hair Cells 22
1.3.2.4. Nerve fibers 23
1.4. The Auditory Nerve and Central Auditory Processing 25
1.5. Conclusion 27
2. Hearing Loss 28
2.1 General Introduction to Deafness 28
2.2 Classification of Hearing Loss 28
2.2.1. Types of Hearing Loss 29
2.2.2. Degrees of Hearing Loss 30
2.3. Functional Consequences of Hearing Loss 30
2.3.1. Impact on Development in Children 30
2.3.2. Cognitive, Social, and Emotional Consequences in Adults 30
2.3.3. Central Auditory Damage and Neural Plasticity 31
3. Hearing Aids 31
3.1. General Overview of Hearing Aids 31
3.2. Objectives and Principles 31
3.3. Current Limitations and Future Perspectives 32
4. The Cochlear Implant 33
4.1. Cochlear Implant Components 33
4.1.1. Overview of Cochlear Implant Components 34
4.1.2. External Component: Signal Capture and Transmission 34
4.1.3. Internal Component: Signal Reception and Auditory Stimulation 35
4.1.4. Conclusion 36
4.2. Electrical Signal Transmission to the Cochlea 36
4.3. Cochlear Implant Surgery: Techniques and Advances 40

4.3.1 Introduction 40
4.3.2. Surgical Procedure 40
4.3.2.1. Anesthesia and Initial Preparations 40
4.3.2.2. Surgical Access and Implantation 40
4.3.2.3. Mastoidectomy and Cochlear Access 40
4.3.2.4. Cochleostomy and Electrode Insertion 42
4.3.2.5. Receiver/Stimulator Placement 43
4.3.3. Electrode Array Insertion 43
4.3.4. Intraoperative Electrophysiological Monitoring and Surgical Refinements 44
4.3.5. Hearing Preservation Strategies 44
4.3.6. Conclusion 44
5. Atraumatic Cochlear Implant Surgery 45
5.1. Introduction 45
5.2. Principles of Atraumatic Electrode Insertion 45
5.3. Surgical Approaches 48
5.3.1 Anatomical Landmarks of the Cochlear Hook Region 48
5.3.2. Implications of Anatomical Variability on Surgical Access 49
5.3.3 Surgical Approaches to the Scala Tympani 50
5.3.3.1. Round Window (RW) Approach 50
5.3.3.2. Extended Round Window (eRW) Approach 51
5.3.3.3. Cochleostomy (CS) Approach 51
5.3.3.4. Comparative Evidence: Anatomical and Clinical Studies 53
5.3.3.5. Clinical Outcomes and Hearing Preservation 53
5.3.3.6. Technical Considerations and Recommendations 54
5.3.3.7. Conclusion 54
5.4. Electrode Array Design: Straight versus Perimodiolar Arrays 55
5.4.1. Introduction 55
5.4.2. Design Principles and Surgical Challenges 55
5.4.3. Lateral Wall (LW) Electrodes 56
5.4.4. Perimodiolar and Mid-Scala (PM/MH) Electrodes 57
5.4.5. Sheath-Based Perimodiolar Electrodes 58
5.4.6. Functional Outcomes and Programming 59
5.4.7. Comparative Outcomes Across Studies 60
5.4.8. Toward Precision Surgery 61
5.4.9. Conclusion 62
5.5. Rationale and Future Directions 62
5.5.1. The Role of Detailed Cochlear Anatomy 62

5.5.2. Intraoperative Monitoring and Robotic Assistance 63
5.5.3. Towards Personalized CI Surgery and Programming 63
5.5.4. Conclusion 63
II. Objectives of the Work: Rationale of our Approach to Rehabilitate Hearing Loss with CI 65
III. Atraumatic Surgery: Strategies to Improve Cochlear Health Preservation 67
3.1 Before insertion Phase: Optical Coherence Tomography (OCT) 67
3.1.1 State of the Art 67
3.1.1.1. Cochlear Anatomy and Microanatomy 67
3.1.1.1.1. Cochlear Anatomy 67
3.1.1.1.2. Modiolus and Spiral Ganglion 68
3.1.1.1.3. Rosenthal's Canal 71
3.1.1.1.4. Round Window Membrane 72
3.1.1.1.5. Hook Region 74
General Description and Clinical Significance 74
Anatomical Structures and Microarchitecture 76
Scala Tympani Orientation and Spatial Configuration 77
Bony Landmarks: Secondary Spiral Lamina and Crista Fenestrae 78
Role and Configuration of the Secondary Spiral Lamina 79
Imaging Insights and the Round Window Arch 80
Osseous Spiral Lamina and Spiral Ligament Relationships 81
Cochlear Partition Bridge 81
Lateral Wall Configuration and Functional Implications 82
Surrounding Vascular and Ductal Structures 82
Clinical Relevance and Summary 83
3.1.1.1.6. Scala Tympani and Cochlear Duct Length 83
3.2 During the Insertion Phase: Robotic-Assisted Cochlear Implant Surgery (RACIS) 101
3.2.1 State of the Art 101
3.2.1.1. Interindividual Variability in Cochlear Implant Outcomes 101
3.2.1.2. Performance Heterogeneity: Perceptual and Neurobiological Factors 102
3.2.1.3. Robotic-Assisted Cochlear Implant Surgery 105
3.2.1.3.1. Introduction and Evolutionary Context of Cochlear Implantation 105
3.2.1.4. General Philosophy of RACIS 106
3.2.2 Robotic Platforms for Surgical Assistance: Principles and Classification 107
3.2.2.1. Existing Robotic Systems and Design Philosophies 107
3.2.3 Robot-Assisted Procedure: Insertion Mechanisms, Safety, and Trauma 108
3.2.4 Clinical and Functional Outcomes of RACIS 118

3.2.4.1 **Clinical Feasibility and Surgical Complications** 118
3.2.4.2 Audiological Performance and Quality of Electrode Placement 119
3.2.5 **Conclusion and Perspectives** 125
3.2.5.1 **RACIS and Cochlear Health** 126
IV. Postoperative Optimization: Frequency-to-Place Mismatch 160
4.1. State of the Art 160
4.1.1. Electrode Position within the Cochlea 160
4.1.2. Matching Electrode Position to Cochlear Frequency Maps 168
4.1.3. Anatomy-Based Frequency Reallocation in Cochlear Implantation: Theoretical Foundations and Clinical Implications 169
4.2 Special Case: Single-Sided Deafness (SSD) 183
V. Conclusions and Perspectives 194
VI. Conflict of Interest Statement 197

I. Introduction

1. Physiology of Hearing

Hearing is the sensory ability to perceive sound, allowing humans to extract critical information from the surrounding environment. Initially essential for survival, such as detecting predators or locating prey, hearing has evolved to support more complex functions in humans, including verbal communication and the appreciation of music. These capacities are made possible by the auditory system, which collects and transduces acoustic vibrations into electrical signals that are interpreted by the brain.

Auditory perception begins with the external ear capturing sound waves and culminates in the brain's interpretation of these signals. This intricate process involves a series of well-coordinated anatomical and physiological mechanisms, spanning the peripheral and central auditory pathways [7].

Anatomically, the auditory system is divided into three distinct but complementary components: the external ear, the middle ear, and the inner ear. Sound waves are first gathered by the pinna (external ear) and funneled through the auditory canal. The specific morphology of the pinna enhances sound localization, while the auditory canal selectively amplifies certain frequencies, particularly those critical for speech perception.

These airborne vibrations subsequently reach the tympanic membrane (eardrum), causing it to oscillate. This mechanical transformation of sound waves is pivotal, initiating the chain of transmission through the ossicular chain in the middle ear. The malleus (hammer), incus (anvil), and stapes (stirrup) act in concert to amplify and convey these vibrations to the cochlea of the inner ear.

The cochlea, a fluid-filled spiral structure, serves as the primary organ of hearing. It converts mechanical vibrations into neural signals through a process known as mechano-electrical transduction. When vibrations reach the cochlear fluids, they induce movements in the basilar membrane and associated structures. These movements, which involve not only passive mechanics but also active amplification mechanisms, influence the deflection of hair cell stereocilia. This deflection leads to the depolarization of hair cells and the subsequent generation of action potentials in the auditory nerve.

Human hearing typically spans a frequency range from approximately 20 Hz to 20 000 Hz in young adults with normal auditory function, although spectral sensitivity progressively declines from adolescence onward. Very low frequencies near 20 Hz are perceived primarily as vibrations rather than distinct sounds, with effective auditory perception generally beginning around 40 Hz. Auditory sensitivity is greatest between 1 and 5 kHz, a range that is critical for speech perception. This remarkable capacity for acoustic discrimination relies on the high anatomical and physiological complexity of the auditory pathway.

Sensory transduction is a fundamental principle common to all sensory systems. Each sensory modality relies on specialized receptor organs that convert external physical or chemical stimuli into invariant physiological signals, predominantly action potentials. These signals are processed in parallel and independently by the central nervous system. Except for the olfactory bulb and retina, all sensory receptor organs project to brainstem nuclei. These nuclei then relay information to the thalamus, which acts as the primary relay station to the cerebral cortex.

Each thalamic nucleus dedicated to a sensory modality projects to a specific primary sensory cortex. Adjacent to these primary regions are secondary sensory cortices, which integrate inputs from both the thalamus and the primary sensory cortex and which interact with the complex brain circuits involved in auditory cognition and language processing. In the auditory, visual, and somatosensory systems, this thalamo-cortical organization follows a similar pattern. Topographically organized thalamic nuclei project to primary cortical areas, while non-topographic nuclei project to secondary regions, which subsequently engage broader associative cortical networks involved in higher-order sensory integration and cognitive processing [8,9].

This hierarchical and spatial organization of the auditory pathway underpins the brain's ability to process, interpret, and respond to the rich spectrum of auditory stimuli encountered in everyday life.

1.1. The Outer Ear

The external ear serves as the initial interface in the auditory processing chain, functioning as a directional acoustic antenna. It consists of the auricle (pinna) and the external auditory canal, both of which play essential roles in capturing and modifying airborne sound waves before they reach the tympanic membrane. The pinna not only collects sound but also enhances some frequencies and diffracts it, particularly favoring frequencies originating from the front of the listener (Fig.1). This anatomical configuration supports spatial hearing by facilitating the localization of sound sources.

In many mammalian species, the pinnae are mobile, allowing dynamic orientation toward sound sources and thus enabling active auditory exploration of the environment. In humans, however, the pinnae are relatively immobile. Despite this anatomical limitation, the brain partially compensates through the interpretation of acoustic cues shaped by the outer ear's geometry and the diffraction of sound around the head and torso.

The external auditory canal further contributes to auditory perception by guiding sound waves toward the tympanic membrane and amplifying specific frequency bands. The pinna enhances frequencies near 5 kHz by a few decibels, while the canal boosts those around 2.5 kHz by approximately 10 dB. Together, the head and external ear produce a cumulative amplification ranging between 5 and 20 dB across the 0,5 –7 kHz frequency range (Fig.1) [10,11]. This spectral shaping is especially relevant for speech comprehension, as it aligns with the frequency range critical for human vocal communication.

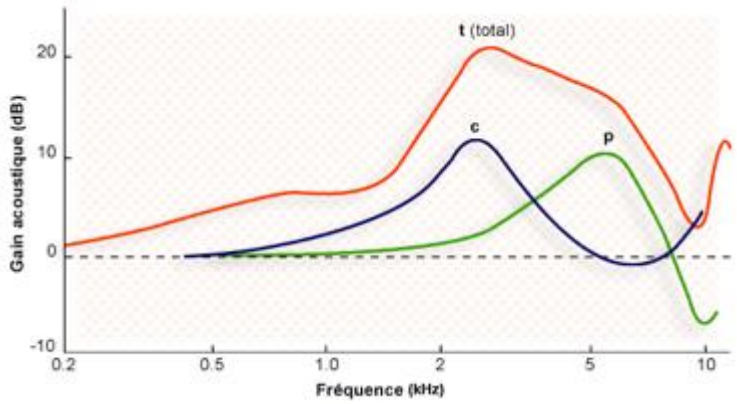

Figure 1. The contribution of the pinna (p, green) and the external auditory canal (c, blue) to the amplification of sound vibrations, expressed as acoustic gain, is depicted for a 45° azimuth in the horizontal plane. At a frequency of 3 kHz, the combined effect of these structures (t, red) yields an overall gain of approximately 20 dB, corresponding to a tenfold increase in the amplitude of the incoming acoustic signal. From the educational website Journey into the World of Hearing (cochlea.eu) [12].

Beyond amplification, the external ear plays a pivotal role in spatial hearing. The filtering effect induced by its anatomical structure varies with the location of the sound source relative to the head and ear axis, primarily affecting high-frequency components. These source-dependent alterations in the spectral and temporal characteristics of the sound wave provide the auditory system with essential cues for sound localization. These cues are mathematically modeled as Head-Related Transfer Functions (HRTFs), which describe how sound is filtered by the listener's anatomy before reaching the eardrum. HRTFs are widely applied in signal processing, particularly in the development of spatial audio technologies [13,14].

The auditory system leverages these spatial cues to localize sound sources even in acoustically complex environments. This capability is crucial in scenarios involving multiple overlapping sound streams, such as crowded social settings. Known as the cocktail party effect, this phenomenon allows listeners to focus attention on a specific speaker despite background noise, facilitating intelligible speech perception under low signal-to-noise conditions.

In conclusion, although the external ear's role is often considered secondary to that of the middle and inner ear in terms of signal transduction, it is mandatory for effective auditory function. It provides mechanical protection to the tympanic membrane, contributes significantly to the amplification of mid-to-high frequency sounds, and delivers critical spatial information necessary for auditory scene analysis and source localization.

1.2. The Middle Ear

The middle ear plays a critical role in the auditory system by serving as the primary structure for sound transmission from the external environment to the inner ear. Structurally, it is an air-filled cavity located within the temporal bone and includes the tympanic membrane, the ossicular chain (malleus, incus, stapes), the oval and round windows, and the auditory (Eustachian) tube (Fig.2).

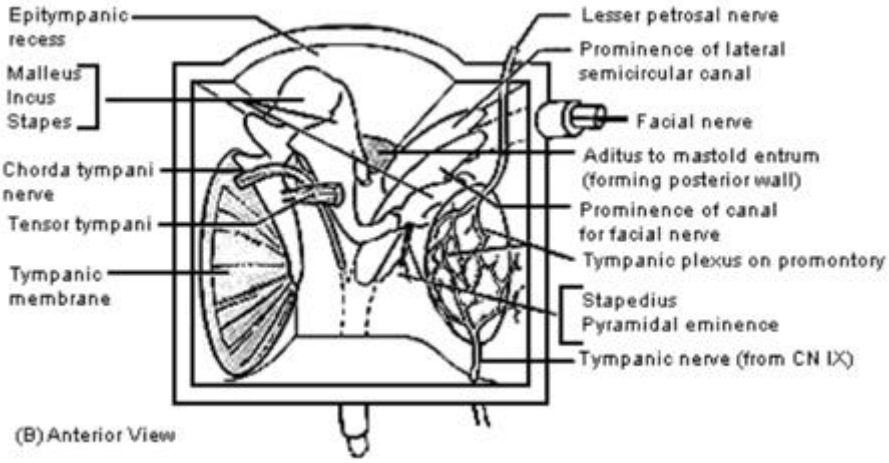

Figure 2. Illustrative diagram of the middle ear cavity shown without the anterior wall. From Clinically Oriented Anatomy (Moore and Dalley) [15].

The tympanic membrane captures airborne sound waves and transmits these vibrations to the ossicular chain. This chain operates as a mechanical lever that amplifies the signal nearly twentyfold before transmitting it via the stapes footplate to the oval window of the cochlea, thereby inducing fluid waves in the perilymph.

A primary function of the middle ear is to ensure impedance matching between the air-filled external auditory canal and the fluid-filled cochlea. Without this adaptation, most acoustic energy would be reflected due to the mismatch between the low-impedance air and the high-impedance cochlear fluid [11,16]. This impedance transformation is achieved mainly through three mechanisms: the lever action of the ossicles, the cone-shaped tympanic membrane and, more significantly, the surface area differential between the large tympanic membrane and the much smaller stapes footplate. This system is especially efficient in the frequency range of human speech, enabling the transfer of a significant proportion of the incoming acoustic energy to the cochlear fluids. Most experimental and modeling studies estimate this transfer efficiency to range between approximately 10% and 30%, depending on sound frequency, although some authors have reported values approaching up to about 46% [17].

In addition to sound transmission, the middle ear provides a protective reflex mechanism that safeguards the inner ear from acoustic overstimulation, particularly at low frequencies. This protection involves the stapedius muscle, which contracts in response to intense sounds, typically above 80 dB HL, with a latency of about 150 ms, or 25–35 ms at higher intensities [16,18]. The contraction increases the stiffness of the ossicular chain, reducing the energy transmitted to the cochlea. However, this reflex is limited in scope:

- It attenuates sound by only 10–20 dB and is effective only up to ~2000 Hz.
- Its effect diminishes after several minutes due to muscular fatigue.
- It does not respond effectively to impulsive sounds.
- Its frequency range is mostly limited to below 1–2 kHz.

This ossicular reflex may also serve a role in attenuating self-generated sounds such as speech or mastication, thereby preventing internal noise from overwhelming cochlear input [19].

Anatomically, the middle ear comprises three interconnected compartments:

1. Middle ear Cavity: A cuboidal space housing the three ossicles. It is bounded by six walls (Fig.2):
    - Lateral wall: Dominated by the tympanic membrane, with the manubrium of the malleus embedded.
    - Medial wall: Separates the middle and inner ear, featuring the promontory (basal cochlear turn), the lateral semicircular canal, and the facial nerve canal.
    - Inferior wall: Adjacent to the jugular vein bulb.
    - Superior wall (tegmen tympani): Lies beneath the temporal lobe.
    - Anterior wall: Contains the tympanic opening of the Eustachian tube.
    - Posterior wall: Leads to the mastoid antrum via the aditus ad antrum.
2. Auditory (Eustachian) Tube: A bony-cartilaginous canal that connects the tympanic cavity to the nasopharynx. It opens during swallowing and yawning to equalize air pressure across the tympanic membrane by adjusting the middle ear air volume.
3. Mastoid Air Cells: A network of air-filled spaces within the mastoid process, varying in size and volume. The mastoid antrum is the largest and most consistent cell, serving as a key anatomical and functional component in pressure regulation and middle ear aeration.

Together, these structures enable the middle ear to fulfill its dual functions: effective transmission of acoustic energy and protective modulation of sound intensity. The intricate anatomy and biomechanics of the middle ear underscore its central role in auditory perception and homeostasis.

1.3. The Inner Ear

1.3.1 Macroscopic Anatomy

The inner ear, or *labyrinth*, is a complex structure embedded within the petrous portion of the temporal bone, also known as the otic capsule. It consists of two concentric systems: a bony labyrinth and a membranous labyrinth. The bony labyrinth is a rigid, fluid-filled cavity that houses the membranous labyrinth. It is divided into two primary sensory components: the vestibular system posteriorly (responsible for balance) and the cochlea anteriorly (responsible for hearing) (Fig.3).

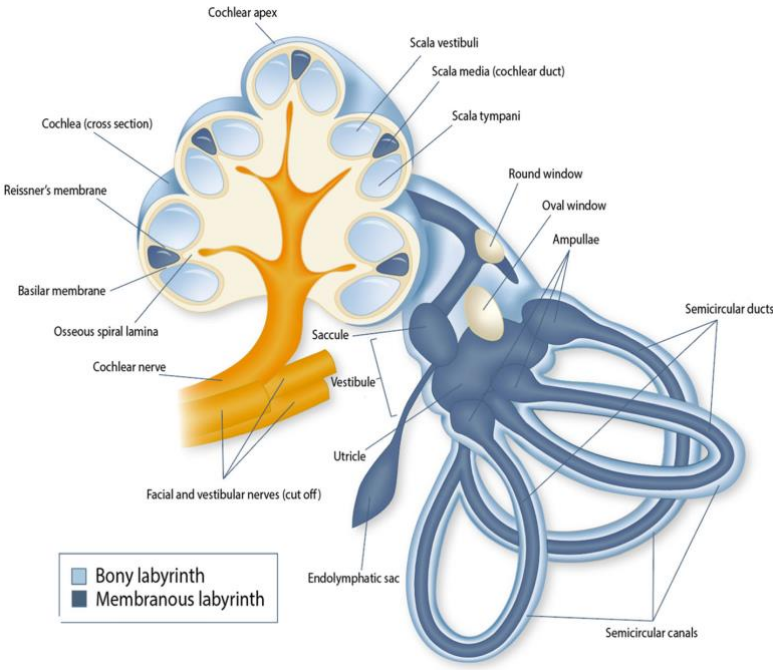

Figure 3. A diagrammatic illustration of the inner ear highlights its two main components: the bony and membranous labyrinths. The bony labyrinth, situated within the petrous part of the temporal bone, contains perilymph and includes the cochlea, vestibule, and semicircular canals. Enclosed within this structure is the membranous labyrinth, which holds endolymph. In the cochlear region, the membranous portion consists of the scala media, or cochlear duct, which houses the auditory sensory organ. The scala media is bordered inferiorly by the basilar membrane and osseous spiral lamina, and superiorly by Reissner's membrane. Within the vestibule, the membranous labyrinth includes the saccule and utricle, endolymph-filled sacs responsible for balance. The saccule, typically smaller, is positioned in the lower (inferior) vestibule, while the utricle resides in the upper (superior) portion. The endolymphatic duct emerges from the posteromedial vestibule, travels through the osseous vestibular aqueduct, and connects to the endolymphatic sac, which is partly located in the aqueduct and partly within the dura of the posterior cranial fossa. The three semicircular canals, horizontal, posterior, and superior, contain corresponding membranous ducts that terminate in the utricle via widened regions known as ampullae. Together, the saccule, utricle, and semicircular ducts play key roles in maintaining balance and spatial orientation. Reproduced from de Pont et al. (2020) [20].

The bony labyrinth is filled with perilymph, a fluid similar in composition to cerebrospinal fluid. Suspended within this cavity is the membranous labyrinth, which follows the contours of the bony shell and is filled with endolymph, a potassium-rich fluid essential to electrochemical signal transduction. These two fluids are confined to separate compartments, providing the electrochemical and hydrostatic environments necessary for sensory function.

The cochlea, located in the anterior portion of the labyrinth, is the sensory organ of hearing. Its structure resembles a spiral snail shell (hence the name *limaçon* in French), making about two and a half turns around a central axis called the modiolus, a hollow bony core from which the fibers of the cochlear nerve originate. This spiral conformation allows a compact yet functionally extensive sensory surface.

Anatomically, the cochlea is composed of three coiled ducts that run longitudinally through its spiral:

- the scala vestibuli (upper duct),
- the scala tympani (lower duct),
- and the scala media (middle duct or cochlear duct).

The scala vestibuli and scala tympani are filled with perilymph and communicate at the helicotrema, an opening at the cochlear apex. The scala media, positioned between the two, is filled with endolymph and forms a closed triangular duct separated by two membranes (Fig.4):

- the Reissner's membrane (separating it from the scala vestibuli), and
- the basilar membrane (separating it from the scala tympani).

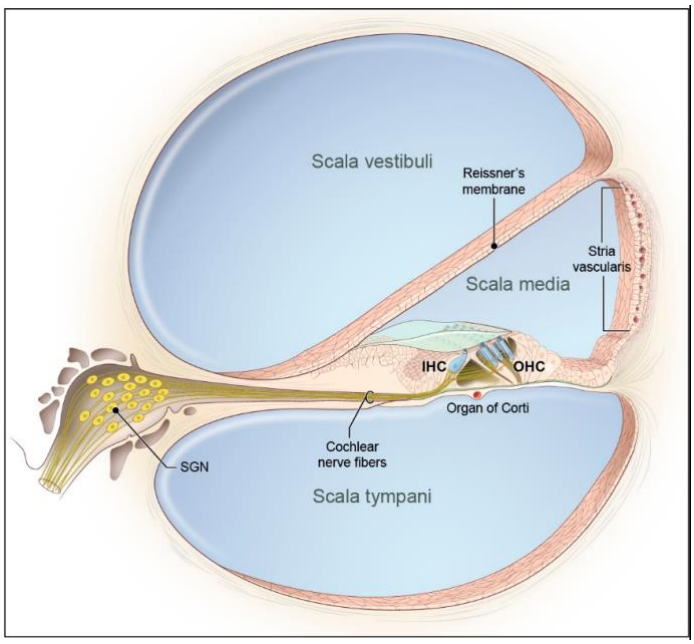

Figure 4. Illustration of a cross-sectional view of the cochlea, highlighting the organ of Corti and spiral ganglion neurons (SGNs). Reproduced from Tona et al. (2020) [21].

The organ of Corti is composed of several types of supporting cells, along with a single row of inner hair cells (IHCs) and three distinct rows of outer hair cells (OHCs) [21].

Within the scala media, resting on the basilar membrane, lies the organ of Corti, the fundamental structure for auditory transduction. This organ houses inner and outer hair cells, which are the mechanosensory cells responsible for converting fluid-induced vibrations into electrical signals. These cells are innervated by fibers of the auditory nerve, which transmit temporal, frequency- and intensity-specific information to the central auditory system.

Sound transmission begins when airborne vibrations enter the external auditory canal and cause displacement of the tympanic membrane. These vibrations are relayed by the ossicular chain (malleus, incus, stapes) to the oval window, where the stapes footplate is anchored. The movement of the stapes initiates a pressure wave in the perilymph of the scala vestibuli. This wave travels along the cochlea, passes through the helicotrema into the scala tympani, and is finally released by the round window, a pressure-relief membrane located at the base of the scala tympani (Fig.5).

At the basal end of the cochlea, two key openings are sealed by membranes:

- The oval window, which is in contact with the stapes, surrounded by the annular ligament, and leads into the scala vestibuli.

- The round window, which terminates the scala tympani and acts as a compliant boundary to dissipate hydraulic energy.

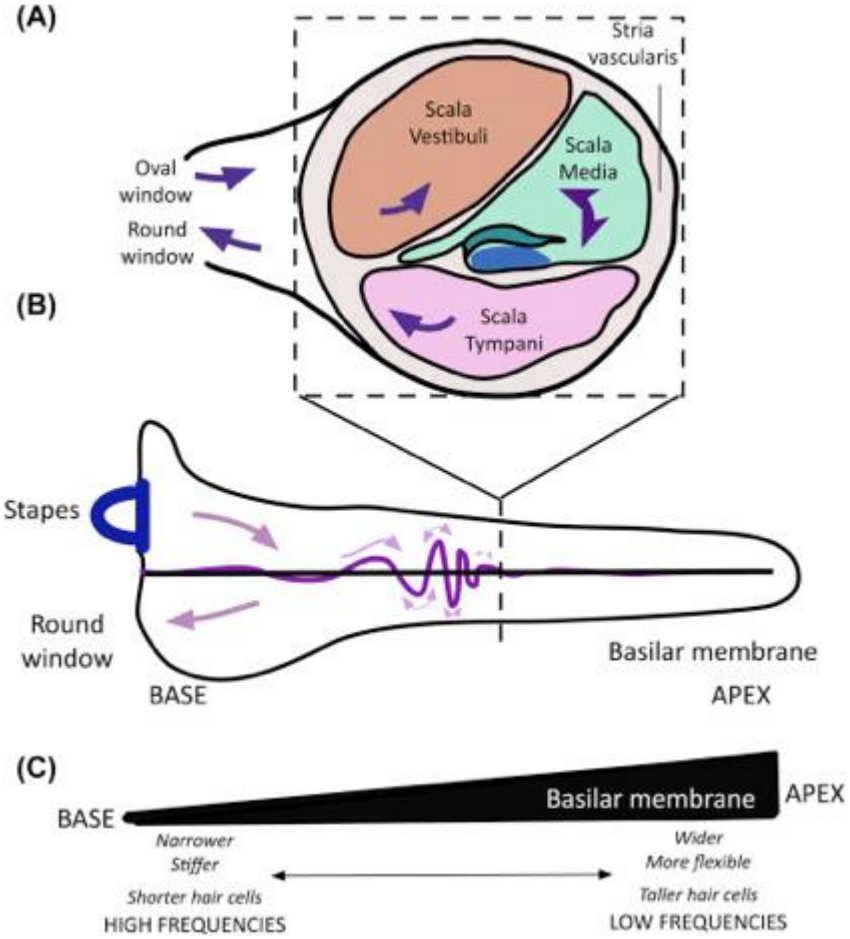

Figure 5. Structure of the Cochlea.
(A) A transverse section of the cochlea reveals its three internal chambers: the scala vestibuli, scala media, and scala tympani. Sound-induced vibrations enter through the oval window and are released through the round window. The basilar membrane, which supports the sensory hair cells, is located at the base of the scala media.
(B) A side view of the cochlea demonstrates the development of a traveling wave along the basilar membrane.
(C) The basilar membrane exhibits variations in stiffness and width along its length, which confer its frequency-specific mechanical properties. The stiffer and narrower base responds preferentially to high-frequency sounds, whereas the wider, more flexible apex is tuned to low-frequency stimuli. From Conn's Translational Neuroscience (Bizley) [22].

A bony spiral lamina projects from the modiolus and partially separates the cochlear cavity into upper and lower chambers. The basilar membrane extends from its free edge and supports the organ of Corti. The progressive widening and softening of this membrane from base to apex establishes a tonotopic gradient: high frequencies are detected at the base, where the membrane is narrow and stiff, while low frequencies are detected near the apex, where it is wider and more flexible.

The cochlear duct terminates blindly at the apex, but the scala vestibuli and scala tympani are continuous through the helicotrema. This continuity permits the transmission of pressure waves and enables the complex hydromechanical phenomena necessary for the frequency-specific excitation of the organ of Corti.

In summary, the cochlea is an exquisitely organized sensorineural transducer. It receives mechanical vibrations from the middle ear, converts them into electrical activity via the hair cells, and encodes them along a spatially organized frequency map. This neural information is then transmitted by the cochlear nerve to the auditory cortex, where it is interpreted as sound [23].

1.3.2. Microscopic Anatomy

1.3.2.1. Basilar membrane and Organ of Corti

The organ of Corti (Fig.6), located within the cochlea, serves as the primary sensory structure for hearing, responsible for transducing mechanical stimuli into electrical signals. Resting on the basilar membrane, it is composed of three main components: sensory cells (inner and outer hair cells), afferent and efferent nerve fibers innervating these cells, and supporting cells along with associated structures such as the tectorial membrane.

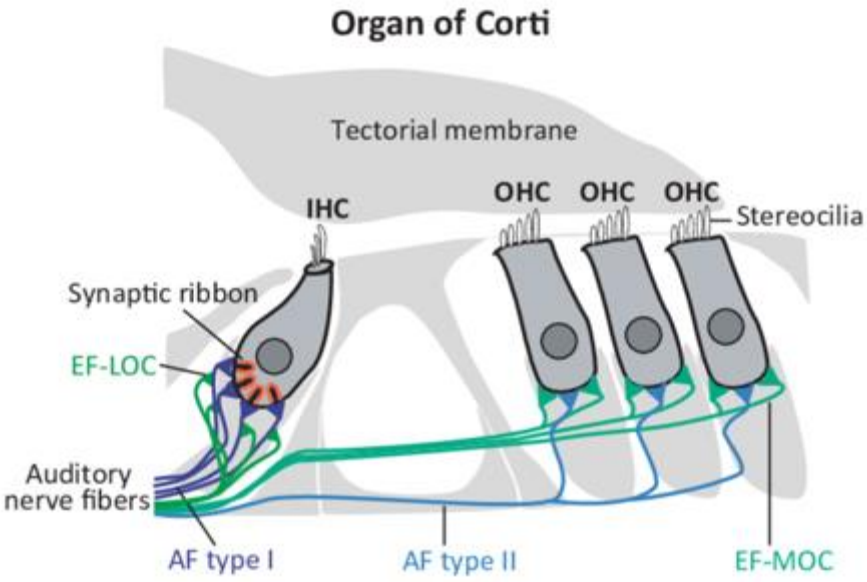

Figure 6. Schematic representation of the adult organ of Corti, the specialized sensory epithelium of the cochlea, illustrates its intricate cellular and neural architecture. This structure comprises two distinct types of mechanosensory cells: IHCs and OHCs. The IHCs serve as the primary transducers, converting mechanical stimuli into frequency-specific electrical signals that are relayed to higher-order auditory centers. In contrast, OHCs function predominantly to enhance cochlear sensitivity and frequency selectivity by amplifying sound-induced vibrations, thereby facilitating the activation of IHCs. Two classes of afferent nerve fibers are associated with the organ: type I and type II. Approximately 90–95% of afferent innervation consists of type I fibers, which establish synaptic connections exclusively with IHCs. Type II fibers, by contrast, selectively innervate the OHCs. In addition to this afferent input, the hair cells receive efferent innervation originating from the superior olivary complex within the brainstem. During early development, efferent projections emerge from the region of the superior olive and convey modulatory signals from central auditory nuclei back to the cochlea. Specifically, lateral olivocochlear (LOC) efferent fibers (EF-LOC) target type I afferent fibers beneath the IHCs via axodendritic synapses, exerting an indirect influence on sensory signal transmission. In parallel, medial olivocochlear (MOC) efferent fibers (EF-MOC), which arise from regions adjacent to the medial superior olive, form direct synaptic contacts with OHCs. These EF-MOC fibers play a pivotal role in modulating cochlear amplification by regulating OHC electromotility. Reproduced from Rüttiger et al. (2017) [24].

In the human cochlea, approximately 3,500 IHCs and between 9,000 and 12,500 OHCs are present [25,26]. These cells are named for the stereocilia located at their apical pole, which mediate mechanoelectrical transduction. The structural arrangement of stereocilia differs between cell types: those of the IHCs are aligned in parallel rows, whereas OHC stereocilia form a distinctive "V" pattern (Fig. 7). The total number of hair cells is established early during embryonic development, by approximately the 10th gestational week in humans. Importantly, these cells do not regenerate once damaged, resulting in permanent hearing loss [25,26].

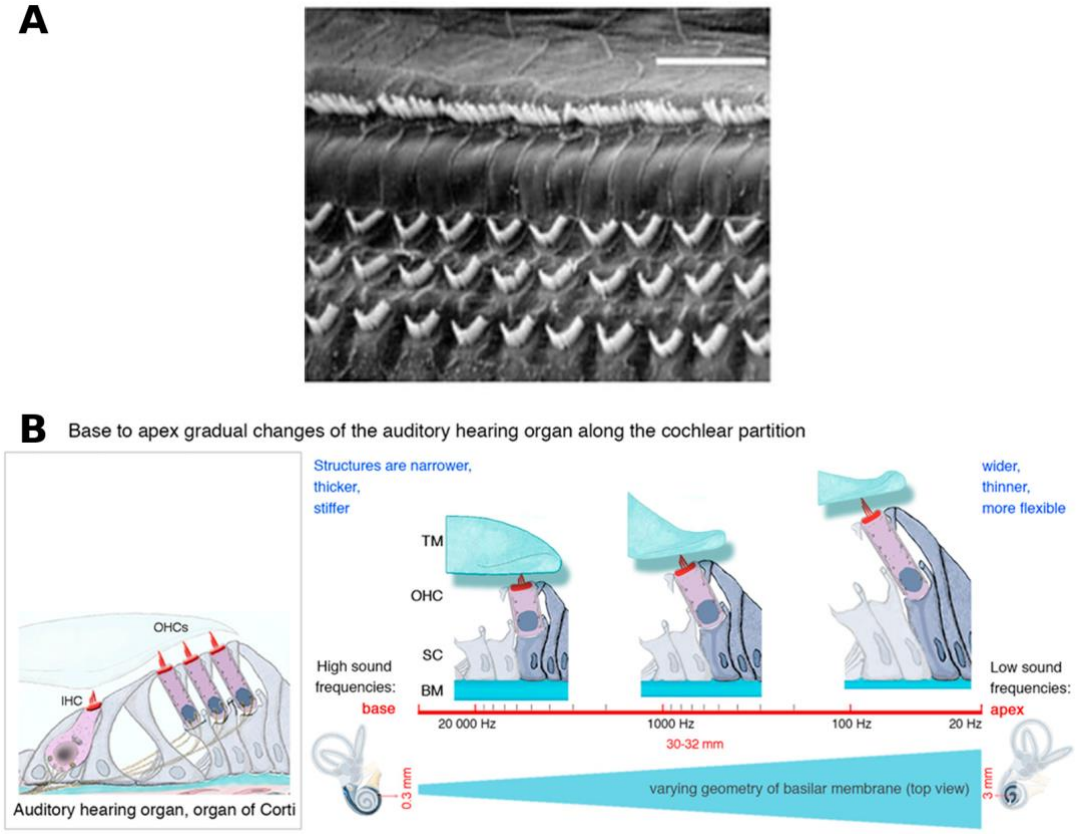

Figure 7. Cellular organization of the organ of Corti and its base-to-apex gradient. (A) Scanning electron micrograph of the surface of the organ of Corti, showing the single row of inner hair cell stereocilia at the top and the three rows of outer hair cell stereocilia below. Scale bar: 15 µm. Image by Marc Lenoir, INSERM Montpellier, from "Journey into the World of Hearing", www.cochlea.eu [12]. (B) The auditory sensory organ, the organ of Corti, consists of a single row of precisely arranged IHCs, three rows of OHCs, and various types of surrounding supporting cells. Along the length of the cochlea, the hair cells, the underlying basilar membrane (BM), and the overlying tectorial membrane (TM) are structurally and functionally specialized to detect specific sound frequencies, establishing a cochlear tonotopy that is preserved up to the auditory cortex. The structural and mechanical properties of the cochlea vary from base to apex: the basal region contains shorter and stiffer hair cells, while the apical region harbors longer and more compliant ones. Consequently, the base primarily encodes high-frequency sounds (up to 20 kHz in humans), whereas the apex is tuned to low frequencies (around 20 Hz in humans). Reproduced from Delmaghani and El-Amraoui (2020) [27].

Humans can perceive acoustic frequencies ranging from 20 Hz to 20 000 Hz. The basilar membrane, which extends approximately 34 mm in length, exhibits graded mechanical properties along its longitudinal axis: it is narrower and stiffer at the base (about 0.1 mm) and becomes wider and more compliant toward the apex (up to 0.5 mm). This mechanical gradient underlies the spatial distribution of frequency responses, a phenomenon known as passive tonotopy. First described by Von Békésy, this principle posits that high-frequency sounds

primarily stimulate the basal turn of the cochlea, whereas low-frequency sounds elicit responses near the apical end (Fig. 5) [23].

Sound-induced vibrations, transmitted through the ossicular chain to the oval window, generate fluid motion within the perilymph. This motion causes localized displacement of the basilar membrane at a site corresponding to the stimulus frequency. The resulting shearing motion between the organ of Corti and the tectorial membrane deflects the stereocilia, thereby activating mechanosensitive potassium (K^+) channels located at their tips [25]. Functionally, the cochlea operates as a bank of frequency-tuned filters that decompose complex acoustic signals into elementary frequency components [28].

The intricate structural organization of the inner ear is fundamental to the remarkable auditory performance observed in mammals, including sensitivity to low-intensity sounds and discrimination across a wide frequency spectrum. The physical, morphological, and molecular properties of hair cells vary systematically along the cochlear axis, such that each hair cell is selectively tuned to a specific frequency, its characteristic frequency. Collectively, hair cells constitute a continuous tonotopic map from apex to base, which is essential for the spectral decomposition of complex sounds into their pure tone constituents within the cochlea.

1.3.2.2. Inner Hair Cells

IHCs, which are pear-shaped in morphology, are arranged in a single row along the inner side of the tunnel of Corti (Fig. 7). Each cell possesses approximately 100 stereocilia, organized into three rows of increasing height and immersed in endolymph. These cells are the primary site of mechanoelectrical transduction and are responsible for transmitting auditory information to the neurons of the spiral ganglion [29–32].

Deflections of the basilar membrane cause bending of the stereocilia toward the stria vascularis. This mechanical stimulation opens ion channels, allowing an influx of potassium ions (K+) due to an inverted potassium gradient characteristic of the endolymphatic environment rich in K+. The resulting depolarization activates basal calcium channels, leading to the release of glutamate. This neurotransmitter binds to glutamate receptors (GLUR) located on the postsynaptic terminals of the ribbon synapse, which interface with afferent fibers of the auditory nerve, thereby triggering the generation of action potentials [28,32–34].

The amount of glutamate released at the synapse is proportional to the amplitude of basilar membrane displacement, allowing for precise encoding of sound intensity [28]. Additionally, this process follows a temporal pattern that depends on the frequency of the auditory stimulus. For low-frequency sounds, IHCs can follow the acoustic signal cycle by cycle, generating a receptor potential characterized by alternating depolarization and repolarization phases, referred to as the alternating current (AC) component, which remains phase-locked to the stimulus frequency.

However, at frequencies above approximately 1000 Hz, IHCs can no longer track each individual cycle of the acoustic waveform. In this frequency range, phase locking at the level of single auditory nerve fibers becomes incomplete, and temporal encoding relies on the volley principle, whereby groups of auditory nerve fibers collectively represent the stimulus periodicity despite the inability of individual fibers to fire on every cycle. As a result, the AC component of the receptor potential progressively diminishes while the direct current (DC) component increases. At even higher frequencies, such as those around 5000 Hz, only slow

fluctuations in the stimulus envelope are encoded, and the receptor potential becomes predominantly DC. In this regime, phase-locked firing is lost, and action potentials are mainly elicited at stimulus onset rather than being synchronized with the fine temporal structure of the sound.

This frequency-dependent temporal coding capability of IHCs is essential for accurate pitch perception [33,34].

1.3.2.3. Outer Hair Cells

OHCs, numbering approximately 10,000 to 12,000 per cochlea, are arranged in three rows forming a V-shaped pattern on the outer side of the tunnel of Corti. Each cell possesses three rows of stereocilia, with the tallest ones anchored in the tectorial membrane. Unlike IHCs, OHCs exhibit contractile properties, granting them an active role in modulating the mechanical input to the cochlea. This mechanism, known as electromotility, enables OHCs to alter the tension between the basilar membrane and the tectorial membrane, thereby influencing the mechanical stimulation transmitted to the IHCs [29–31,35].

When an acoustic stimulus reaches the cochlea, it generates a traveling wave along the basilar membrane. The deflection of the stereocilia induces depolarization of the OHCs, resulting in their shortening. Conversely, repolarization leads to elongation. This cycle of contraction and elongation, driven by the motor protein prestin, amplifies the vibrations of the basilar membrane over a narrow region of the organ of Corti, thereby enhancing cochlear sensitivity and frequency selectivity. This process, referred to as active tonotopy, can provide amplification gains of up to 50 dB [29–31,35]. Such active amplification operates primarily for low to moderate sound intensities. Above a threshold of approximately 90 dB SPL, the cochlea reverts to a passive mechanical behavior, as originally described by von Békésy [23]. Cochlear active mechanisms are essential for three fundamental auditory functions: the detection of low-level sounds, fine frequency discrimination, and the nonlinear response of the basilar membrane to variations in sound intensity. Frequency selectivity arises from the tonotopic organization of the cochlea, where each location along the basilar membrane corresponds to a specific characteristic frequency, reflecting a precise spatial coding of frequency.

In addition to spatial coding, temporal coding also contributes to frequency encoding, notably through phase locking, in which auditory nerve fibers fire action potentials in synchrony with the phase of the incoming sound wave.

Cochlear nonlinearity manifests as a compressive relationship between stimulus intensity and the amplitude of basilar membrane vibration. At low intensities (up to ~20 dB SPL), active mechanisms provide amplification of 40 to 50 dB, yielding an almost linear response. Between 30 and 90 dB SPL, this gain gradually decreases, resulting in a compressive response (Fig. 8). Above 90 dB SPL, the response becomes entirely passive, mirroring the pattern described by von Békésy. This nonlinear compression is particularly pronounced at the base of the cochlea, whereas in the apical regions, the effect is more attenuated and does not always occur precisely at the characteristic frequency [19]. Other phenomena further illustrate this nonlinearity, including two-tone suppression, where the response to one tone is reduced by the presence of a second, closely spaced tone, and the generation of combination tones, also known as distortion products [11].

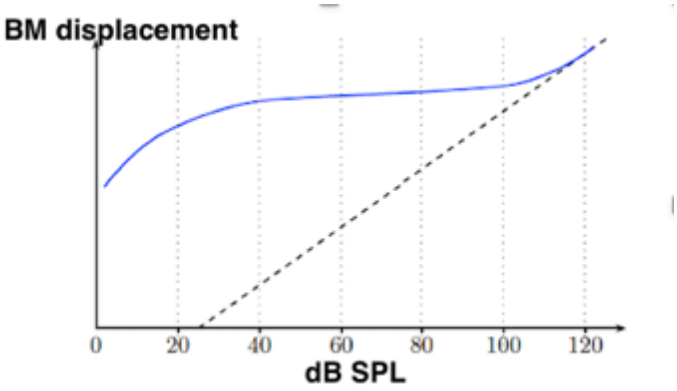

Figure 8. Simplified illustration of the basilar membrane's response to a pure tone. A 8 kHz stimulus is applied to the cochlea, and the curve displays the displacements measured at the location on the basilar membrane corresponding to its 8 kHz characteristic frequency. Reproduced from Johnstone et al. (1986) [36].

1.3.2.4. Nerve fibers

IHCs are the primary sensory receptors of the organ of Corti. Each IHC establishes specialized glutamatergic connections, known as ribbon synapses, with approximately 10 to 30 type I afferent nerve fibers [37]. These myelinated fibers account for approximately 95% of the auditory nerve fibers [37,38], forming a redundant network around each IHC that ensures robust and parallel transmission of auditory signals [37,38]. In contrast, each type I fiber innervates only a single IHC.

Type II fibers, on the other hand, are unmyelinated, much less numerous (constituting only 5% of the auditory nerve fibers), and project toward the OHCs (Fig. 6) [37,38]. A single type II fiber typically innervates about ten OHCs, which reflects their primarily motor, rather than sensory, function, mediated through efferent pathways from the central nervous system. These efferent fibers arise from the olivocochlear system in the superior olivary complex and reach the cochlea through the auditory nerve, passing partly through the vestibular nerve before joining the cochlear nerve, as illustrated in Fig. 6 and functionally demonstrated by the suppression of otoacoustic emissions during contralateral acoustic stimulation. Thus, while IHCs activate afferent fibers, OHCs receive efferent signals that modulate their mechanical properties. This efferent control likely plays a feedback role in the regulation of OHC active mechanisms.

Type I fibers exhibit precise tonotopic responses, each possessing a characteristic frequency at which the response threshold is minimal. This frequency–intensity relationship is depicted by a tuning curve, indicating that a fiber is only activated when the stimulus exceeds a threshold at its characteristic frequency (Fig. 9). As stimulus intensity increases, the fiber's firing rate follows a sigmoid-shaped rate-level function and ultimately reaches a saturation plateau, reflecting the intensity-response function [39]. The dynamic range of most fibers lies between 20 and 50 dB SPL, supporting fine discrimination of sound intensity. Importantly, several fibers can share the same characteristic frequency but differ in their activation thresholds, a feature that underlies the functional heterogeneity necessary for encoding dynamic auditory ranges [40].

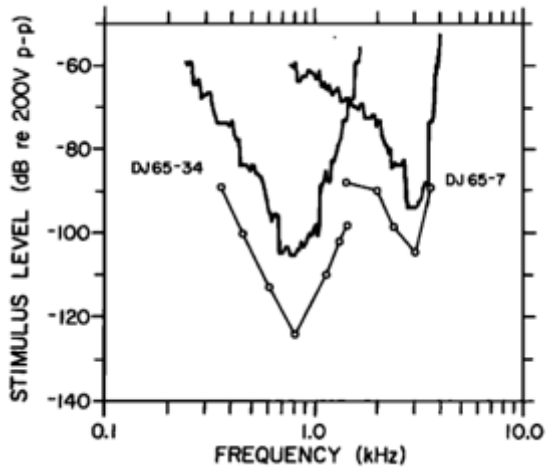

Figure 9. Frequency tuning curves derived from average firing rate and neural synchrony.
The solid curves represent tuning curves obtained from the average firing rate. The lines connecting the open circles correspond to synchrony-based tuning curves and indicate the stimulus levels required to reach a synchronization index equal to 20% of the maximum value observed for the corresponding frequency in that unit. Reproduced from Johnson (1980) [41].

In the absence of OHCs, the activation threshold of auditory nerve fibers increases by 40 to 50 dB, and their frequency selectivity becomes degraded [40,41]. This frequency specificity is also reflected at the neural level. Analogous to the concept of characteristic frequency along the basilar membrane, each nerve fiber has a characteristic frequency that approximately matches that of the basilar membrane at the site of synaptic contact, supporting a precise anatomo-functional matching.

Liberman (1978) proposed a functional classification of type I fibers based on their spontaneous discharge rates:

- Low-threshold fibers: > 20 spikes/s, low activation thresholds, ~60% of the population.
- Medium-threshold fibers: 0.5–20 spikes/s, ~25%.
- High-threshold fibers: < 0.5 spikes/s, activated only at high intensities, ~15% [40].

This classification enables the auditory nerve to encode a broad range of sound intensities at the periphery. The spatial distribution of type I fibers around IHCs is non-random: low- and medium-threshold fibers tend to innervate the modiolar side of the cell, whereas high-threshold fibers are located on the pillar side, near supporting cells, suggesting a functional specialization based on synaptic location [39,42,43].

Historically, it was hypothesized that spontaneous firing rate correlated with fiber diameter, with high-spontaneous-rate fibers having larger diameters. However, this view was later challenged by observations indicating that small-diameter fibers can also exhibit high spontaneous rates [39,44].

Ribbon synapses between IHCs and spiral ganglion neurons exist in two morphological types: simple and complex plaques [44]. Complex synapses, characterized by widened synaptic clefts and a high density of synaptic vesicles, are typically associated with fibers exhibiting low or medium spontaneous discharge rates. In contrast, simple plaques are more commonly observed

in fibers with high spontaneous rates, suggesting variability in synaptic release and transduction properties.

Functional diversity among fibers may arise from:

- The density and distribution of Cav1.3 calcium channels in the presynaptic active zones, which regulate calcium influx essential for vesicle exocytosis,
- The size and organization of GLUR receptor aggregates at the postsynaptic membrane, which determine response kinetics and sensitivity [45].

This structural and molecular diversity supports precise encoding of auditory information at the earliest stages of sensory transduction.

In addition to encoding frequency and intensity, auditory nerve fibers are capable of tracking fine temporal structures of sound stimuli through a phenomenon known as phase-locking. This refers to the tendency of action potentials to occur at specific phases of a periodic stimulus, typically near the rising phase. Phase-locking is especially robust for low-frequency pure tones (< 1 kHz in humans) [46]. At higher frequencies, the ability to synchronize declines due to the limitation imposed by the neuronal refractory period (~1 ms).

Although degraded at successive levels, temporal coding is partially preserved in ascending auditory pathways, with decreasing precision in more central auditory nuclei [47,48]. This temporal synchrony plays a key role in pitch perception (by encoding stimulus periodicity) and in spatial localization (through interaural phase differences) [49]. Notably, phase-locking can occur even at sound intensities below the behavioral hearing threshold in some fibers.

Thus, frequency encoding in the auditory system relies on two complementary mechanisms: tonotopy (place-frequency coding) and phase-locking (temporal coding), the latter being effective mainly at lower frequencies.

Regarding intensity coding, each IHC is contacted by multiple afferent fibers with distinct activation thresholds and spontaneous firing rates. Each fiber increases its firing rate with stimulus intensity until reaching saturation [50]. Because the dynamic range of a single auditory nerve fiber is limited, perceived loudness is not encoded by any individual fiber alone but rather through spatial (population) coding, whereby the central auditory system integrates the distributed activity of multiple fibers innervating the same IHC, and, at higher sound levels, across neighboring cochlear regions, to estimate stimulus intensity.

1.4. The Auditory Nerve and Central Auditory Processing

The auditory nerve, also known as the vestibulocochlear nerve (eighth cranial nerve), plays a pivotal role in transmitting acoustic signals from the peripheral sensory receptors to the central auditory pathways. It is formed by the union of axons originating from the spiral ganglion neurons, comprising the cochlear component, and those from the vestibular ganglion. In humans, the spiral ganglion contains approximately 35,000 neurons [32], each relaying specific information encoded by the sensory hair cells.

The dendrites of these neurons establish direct synaptic contacts with hair cells, predominantly IHCs via type I afferent fibers, while their axons converge toward the cochlear nuclei within

the brainstem. This synaptic connection marks the initial stage of central auditory processing [37,38].

Within the auditory nerve, fibers are arranged in a strict tonotopic organization: fibers arising from the apical region of the cochlea, which encode low frequencies, are located centrally, whereas those from the basal region, tuned to high frequencies, are distributed peripherally [51]. This frequency-based topography mirrors the spatial distribution of hair cells along the cochlear spiral, as the characteristic frequency of each fiber is directly determined by the site of the hair cell it innervates [52]. Such tonotopy is preserved throughout all subsequent stages of the auditory pathway, extending to the auditory cortex (Fig. 10).

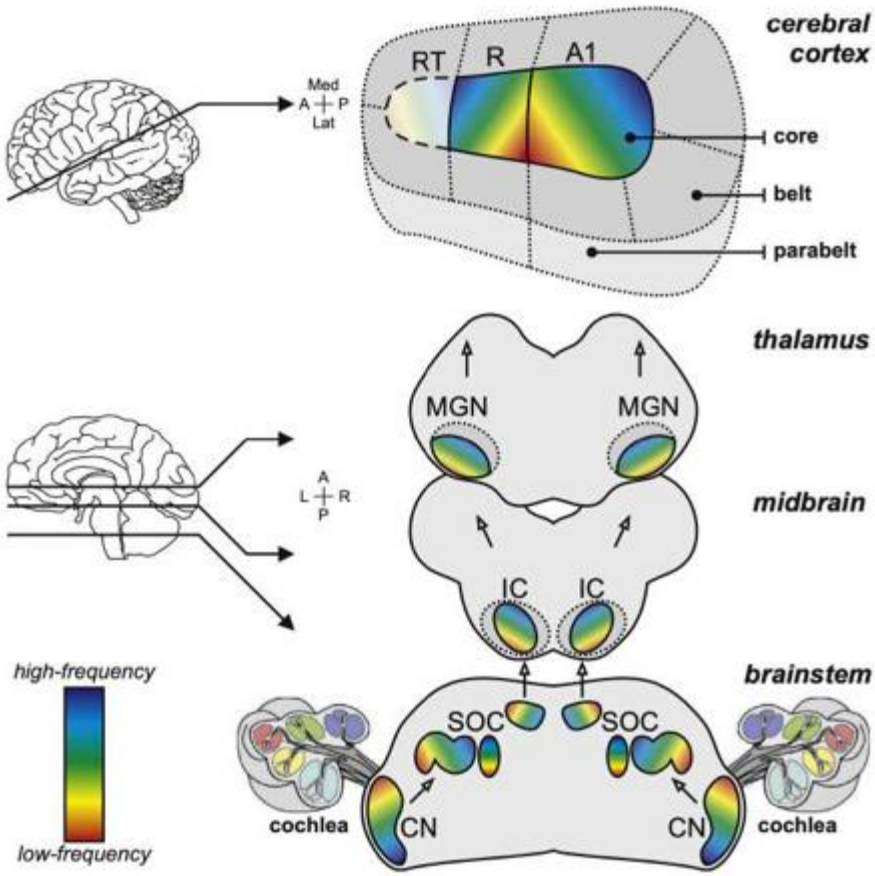

Figure 10. Tonotopic organization along the ascending auditory pathway, from the cochlea to the auditory cortex. Each relay station within the auditory system exhibits a frequency-based spatial arrangement. A1 = primary auditory field, R = rostral field, RT = rostrotemporal field, CN = Cochlear Nuclei, SOC = Superior Olivary Complex, IC = Inferior Colliculus, and MGN = Medial Geniculate Nucleus. The 'belt' and 'parabelt' regions represent components of the secondary auditory cortex. Reproduced from Saenz and Langers (2014) [53].

Following their exit from the cochlea, axons of the spiral ganglion neurons traverse the cochlear root of the vestibulocochlear nerve. They course through the internal auditory meatus, accompanied by the vestibular root of the eighth cranial nerve, the facial nerve, the labyrinthine artery, and the auditory veins. These fibers then reach the cerebellopontine angle and enter the brainstem to establish their first synapse within the cochlear nucleus.

Auditory information is subsequently relayed through a complex hierarchical network: the brainstem (cochlear nucleus, superior olivary complex, lateral lemniscus), the midbrain

(inferior colliculus), the diencephalon (medial geniculate body of the thalamus), and finally, the primary auditory cortex, located in Heschl's gyrus within the temporal lobe (Fig. 10). Compared to other sensory systems, the auditory pathway is characterized by a higher degree of complexity within its subcortical processing stages.

From the level of the cochlear nucleus, projections become bilateral, with a predominance of contralateral pathways. Each central auditory structure thus receives input from both ears, ensuring essential binaural integration. The auditory signal ascends through three to five successive relays, each specialized in decoding, modulating, or interpreting distinct features of the auditory information [54,55].

Two major functional pathways are traditionally distinguished within the central auditory system. The primary (lemniscal) pathway, which is rapid and highly specific, relies on large myelinated fibers that transmit acoustic signals directly to the primary auditory cortex. Conversely, the non-primary (extralemniscal) pathway is more diffuse and integrates multisensory information related to functions such as arousal, emotional responses, and autonomic regulation. At each processing level, auditory nuclei maintain a tonotopic organization consistent with the cochlear frequency map.

Importantly, auditory processing is not exclusively ascending. The auditory cortex also sends numerous descending projections to subcortical structures, from the thalamus down to the cochlear nucleus [56]. These efferent pathways, referred to as corticofugal tracts, follow similar routes as their ascending counterparts and exert modulatory feedback upon lower-order centers, including the hair cells themselves. This top-down control enables dynamic contextual modulation of auditory responses, enhancing the signal-to-noise ratio, sound localization and facilitating selective auditory attention [57,58]. Furthermore, the auditory system operates as part of a broader large-scale cortical network. Extensive bidirectional interactions exist between auditory cortical areas and regions involved in language processing. Auditory perception is also closely linked to higher cognitive processes such as attention, working memory, and executive control. Through these distributed networks, auditory signals can be interpreted within a predictive and cognitive framework, enabling complex functions such as speech perception, linguistic decoding, auditory scene analysis, and adaptive attentional modulation.

1.5. Conclusion

The cochlea plays a fundamental role in the initial processing of acoustic signals by performing a spectral decomposition based on frequency and intensity. Frequency analysis is governed by the spatial location of depolarized inner hair cells, which determines the specific auditory nerve fibers activated. In parallel, sound intensity is encoded through the amplitude and temporal synchronization of hair cell depolarization [59].

This tonotopic organization (i.e., the spatial mapping of frequencies along the cochlear partition) is remarkably preserved throughout the successive relay stations of the central auditory system, up to the primary auditory cortex. Such preservation ensures a faithful transmission of frequency-specific information. In contrast, the phase-locking of neuronal responses to the carrier frequency, which remains robust at the level of the cochlear nucleus, progressively diminishes along the central auditory pathway and is ultimately absent in the thalamo-cortical system.

2. Hearing Loss

2.1 General Introduction to Deafness

Deafness, defined as a partial or complete loss of auditory perception, represents the most common sensory disorder in humans. It may be unilateral or bilateral and can affect individuals at any stage of life.

This auditory deficit is now recognized as a major global public health concern. According to the World Health Organization (WHO), approximately 1.5 billion people worldwide experience some degree of hearing impairment, with 466 million suffering from disabling hearing loss, including 34 million children [60]. Congenital deafness affects nearly one in 500 newborns [61]. Another estimate reports over 360 million affected individuals, comprising 328 million adults and 32 million children [62].

Epidemiological data indicate that neonatal hearing loss affects approximately 1 to 2 per 1000 live births globally [63,64], with a reported incidence of 0.6 to 1.2 per 1000 live births in France based on neonatal screening data [65,66]. By the age of eight, the prevalence of severe to profound bilateral hearing loss is estimated at 0.58 per 1000 children [67].

The etiologies of hearing loss are diverse. In congenital cases, approximately 70% are due to genetic causes [60,68]. Among adults, around 25% of hearing loss cases are also related to genetic mutations [68]. Environmental, multifactorial, or acquired causes throughout life also contribute significantly to the burden.

In children, congenital deafness has serious implications for development, potentially delaying the acquisition of spoken language and impairing social and emotional development, particularly in cases of bilateral hearing loss, whereas unilateral hearing loss may also have developmental consequences, although these are generally less severe [60,69]. In adults, hearing loss may lead to social isolation, psychological disturbances, and, in older adults, is associated with a more pronounced cognitive decline [70,71].

Given its increasing prevalence and wide-ranging impact, hearing loss demands heightened public health attention, both in terms of early screening strategies and the implementation of effective preventive and therapeutic approaches.

2.2 Classification of Hearing Loss

Deafness, whether unilateral or bilateral, can be classified based on several clinical and audiological criteria, including the type of lesion (conductive, sensorineural, or mixed), the degree of hearing loss, the age of onset, the presence or absence of syndromic features, and its etiology (genetic or acquired) (Fig. 11).

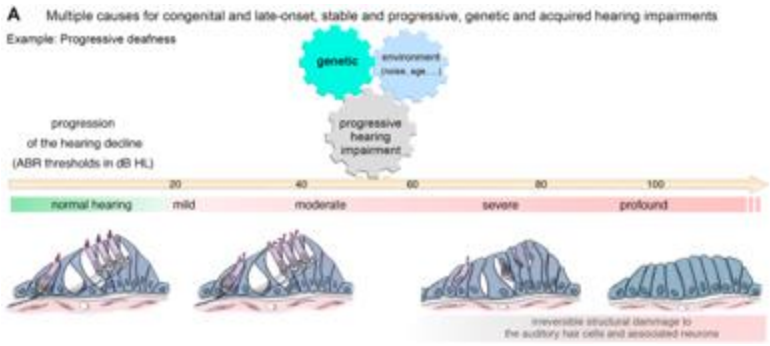

Figure 11. Possible causes of hearing loss.
Hearing loss is typically categorized by severity: mild (21–40 dB HL), moderate (41–70 dB HL), severe (71–90 dB HL), or profound (>90 dB HL). It may arise from genetic factors, noise exposure, or age-related degeneration. Regardless of its etiology, hearing impairment can occur at any point after birth and may progress at highly variable rates and magnitudes between individuals. Reproduced from Delmaghani and El-Amraoui (2020) [27].

The clinical and functional consequences of hearing loss vary widely across individuals, necessitating a precise classification system. It may be defined by its origin (congenital or acquired), the period of onset (childhood or adulthood), the degree of auditory deficit, and its temporal pattern, whether stable, fluctuating, progressively worsening, or, in rare cases, spontaneously improving.

2.2.1. Types of Hearing Loss

Hearing loss is classically categorized into two principal types:

- **Conductive hearing loss**, which results from a dysfunction of the external or middle ear structures (including the auricle, auditory canal, tympanic membrane, ossicular chain, or Eustachian tube). This form of hearing impairment arises from inadequate transmission of sound waves to the cochlea. The associated auditory threshold elevation is typically moderate, with losses reaching up to 60 dB. Audiometric evaluation reveals elevated thresholds in air conduction while bone conduction remains within normal limits, allowing for a clear diagnostic distinction. Self-perception of one's own voice is generally preserved.
- **Sensorineural hearing loss**, also referred to as perceptive hearing loss, is attributable to damage within the inner ear, the auditory nerve, or the central auditory pathways. These impairments are frequently associated with pathologies directly impacting the organ of Corti, encompassing injury to sensory cells, neural fibers, or the supporting structures critical to the inner ear's functional integrity. Sensorineural hearing loss may be cochlear (labyrinthine) or retrocochlear, involving neural pathways up to the auditory cortex. This type of hearing loss produces a parallel elevation of thresholds in both air and bone conduction. It is often irreversible and may be caused by genetic mutations, exposure to ototoxic agents, acoustic trauma, or age-related degeneration (presbycusis).

In certain cases, individuals exhibit **mixed hearing loss**, which combines both conductive and sensorineural components.

2.2.2. Degrees of Hearing Loss

The severity of hearing loss is classified according to the average air conduction thresholds at 500, 1000, 2000, and 4000 Hz, according to the classification proposed by the Bureau International d'Audiophonologie (BIAP), as follows: normal hearing is defined as thresholds ≤ 20 dB HL; mild hearing loss ranges from 21 to 40 dB HL; moderate hearing loss from 41 to 70 dB HL; severe hearing loss from 71 to 90 dB HL; profound hearing loss exceeds 90 dB HL; and total deafness, or anacusis, is defined by thresholds above 120 dB HL. The functional consequences of hearing loss vary widely. Mild deficits impair the perception of soft sounds, while profound hearing loss significantly hinders speech discrimination, particularly in children undergoing language acquisition. In this context, the impact on language development follows a continuum: mild hearing loss may result in delayed language acquisition, whereas severe to profound hearing loss may prevent the normal development of oral language in the absence of appropriate auditory rehabilitation, such as acoustic amplification or cochlear implantation.

2.3. Functional Consequences of Hearing Loss

Beyond its physiological dimension, hearing loss exerts profound effects on development, cognition, communication, and social integration. These consequences are influenced by multiple factors, including the age of onset, the degree and laterality of the hearing loss, the timing of its occurrence, and the presence or absence of timely and appropriate intervention.

2.3.1. Impact on Development in Children

In children, particularly in cases of bilateral congenital hearing loss or deafness arising within the first two years of life, the impact is especially significant on oral language acquisition. This early prelingual period represents a critical window for cognitive and socio-emotional development. Sensory deprivation at this stage may lead to delayed or absent language acquisition, impairing not only verbal communication but also literacy skills such as reading and writing [60,69]. Furthermore, childhood hearing impairment can disrupt multiple developmental domains, potentially resulting in behavioral disturbances, social withdrawal, relational difficulties, diminished academic performance, and, ultimately, more complex pathways to social and professional integration [72].

2.3.2. Cognitive, Social, and Emotional Consequences in Adults

In adults, hearing loss primarily manifests as a communication disorder, particularly in challenging acoustic environments such as noisy settings. This difficulty in speech comprehension often leads to progressive social isolation. The resulting isolation is strongly associated with increased risk of anxiety and depression, reduced self-esteem, and a gradual disengagement from social and recreational activities. In the elderly population, hearing impairment is now recognized as a modifiable risk factor for cognitive decline. Several longitudinal studies have demonstrated an association between presbycusis and accelerated deterioration in memory, executive function, and attentional processes, thereby contributing to the development of dementia [70,71].

2.3.3. Central Auditory Damage and Neural Plasticity

Although most forms of hearing loss stem from damage to peripheral auditory structures (external, middle, or inner ear), central consequences also arise. Prolonged auditory deprivation, especially when occurring early in life, can lead to functional reorganization of the central auditory pathways, including cortical remapping. These plasticity mechanisms, while sometimes compensatory (e.g., enhanced visual or tactile processing), may also complicate auditory rehabilitation, particularly in cases of delayed cochlear implantation. Importantly, early childhood represents a critical window for auditory-driven language development. Adequate auditory stimulation during the first years of life, particularly before the age of two, is essential for the normal maturation of cortical networks supporting oral language. In the absence of sufficient auditory input during this sensitive developmental period, irreversible alterations in language-related neural circuits may occur, significantly limiting later spoken language acquisition.

3. Hearing Aids

3.1. General Overview of Hearing Aids

Sensorineural hearing loss constitutes a major sensory disability, arising from irreversible damage to the inner ear, particularly involving the loss or dysfunction of sensory hair cells. These lesions, which are typically permanent, severely compromise auditory function and exert profound consequences on both functional abilities and socio-emotional well-being. In this context, auditory rehabilitation emerges as a clinical imperative, although its implementation remains notably complex.

Among the available rehabilitative strategies, the use of external hearing aids represents the most commonly adopted approach to mitigate this deficit. However, due to the intrinsic nature of sensorineural hearing loss, these devices do not restore normal hearing but can provide a functional level of auditory perception that allows detection of sounds and, in many cases, effective speech perception. In individuals with mild to moderate hearing loss, acoustic amplification frequently leads to good to very good functional outcomes. The improvement achieved through amplification therefore often enables meaningful communication abilities, although it remains different from the auditory capabilities of a normal-hearing individual. Nevertheless, even modest auditory gains may lead to meaningful improvements in the quality of life of individuals with hearing impairment, given the substantial impact of hearing loss on autonomy, communication, and social inclusion.

In cases of severe hearing loss, however, acoustic hearing aids may become insufficient to provide adequate speech perception, and implantable solutions such as cochlear implants may be required. Within the scope of this work, the focus will be limited to external hearing aids. Implantable devices, including cochlear implants, middle ear implants, and bone-conduction systems, will not be addressed in the present chapter.

3.2. Objectives and Principles

The primary objective of external hearing aids is to compensate for auditory deficits by modifying the acoustic signal in such a way that it becomes accessible to individuals with hearing impairment. In contrast to implantable devices, these aids do not require surgical intervention and rely exclusively on air conduction to transmit sound.

The fundamental role of an external hearing aid is to restore, insofar as possible, auditory function, particularly the audibility and intelligibility of speech. Hearing loss typically induces two principal forms of distortion: intensity and frequency. Through amplification, hearing aids can restore the audibility of soft sounds. However, they can only partially compensate for certain impairments, such as the broadening of auditory filters, a phenomenon directly linked to the irreversible damage of hair cells. Modern hearing aids incorporate advanced signal-processing strategies that can partially mitigate these distortions when they are not too pronounced. This widening of auditory filters reduces frequency selectivity and tends to worsen as sound intensity increases. When cochlear damage and the resulting distortions become more marked, however, these mechanisms remain only partially effective.

In cases of severe hearing loss, and in some cases of moderate hearing loss, although sufficient amplification is necessary to ensure sound perception, the increased intensity may simultaneously degrade the hearing-impaired listener's ability to discriminate between frequencies. Despite their benefits, hearing aids cannot restore normal hearing. They serve as valuable but inherently limited tools. In light of these constraints, the fitting of a hearing aid must pursue three essential objectives: (1) to restore audibility by selectively amplifying soft sounds, thereby rendering them perceptible and harmonizing auditory perception thresholds; (2) to protect against the phenomenon of loudness recruitment by limiting the amplification of intense sounds, thus avoiding their aggressive character and enhancing their tolerability; and (3) to adapt the dynamic range of sound by compressing the conversational sound window (30–70 dB SPL) so that it fits within the residual dynamic auditory range of the aided patient [73].

3.3. Current Limitations and Future Perspectives

Despite these remarkable developments, the processing capacities of modern hearing aids remain limited when compared to the inherent complexity of the human auditory system. One significant component of modern hearing aid signal processing is multiband amplification and compression, which is essential for tailoring gain to frequency-specific hearing losses. This functionality is now available in technologically advanced contemporary hearing aids, but it requires high filter selectivity across numerous channels, placing substantial demands on computational power.

Another technical constraint lies in the sampling frequency. While some state-of-the-art devices now reach sampling rates of up to 16 kHz, many remain restricted to 8 or 11 kHz. This limitation hinders the accurate rehabilitation of high-frequency sounds, frequencies that are often the first to be affected in hearing loss. Nevertheless, as high-frequency components play a relatively secondary role in speech intelligibility in good sounds environment, this restriction is considered clinically acceptable in most cases.

In summary, while current digital hearing aids already support sophisticated functionalities, including feedback suppression, speech enhancement, dynamic compression, and directional microphone systems, the potential for further refinement remains vast. Continued advances in computational power, the integration of more versatile chipsets, and the development of increasingly efficient algorithms are expected to lead to more precise, personalized, and effective auditory rehabilitation, bringing performance ever closer to the natural functioning of the human inner ear.

4. The Cochlear Implant

4.1. Cochlear Implant Components

In patients with severe-to-profound sensorineural hearing loss, conventional hearing aids often prove inadequate for restoring satisfactory speech understanding, both in quiet and in noisy environments, in the deaf ear. In this context, cochlear implantation has emerged as a major therapeutic alternative. Introduced in the 1970s for bilateral profound HL, the cochlear implant (CI) has progressively become the reference solution for the rehabilitation of profound deafness worldwide [74].

Currently, the indication for cochlear implantation is based on a thorough audiological assessment and strict clinical criteria. In adults, bilateral implantation is considered on a case-by-case basis, taking into account the patient's expectations and the potential benefits in terms of spatial perception and speech comprehension in noise [74]. In the pediatric population, medical societies recommend early bilateral implantation to restore functional binaural hearing and prevent the deleterious effects of auditory deprivation [75,76].

Initially reserved for anacusic patients, cochlear implantation criteria have gradually expanded over the decades. Today, candidates include individuals with bilateral or unilateral severe, and sometimes moderate, hearing loss who do not achieve adequate speech intelligibility despite optimally fitted hearing aids. An intelligibility score of less than 50% for monosyllabic words at 65 dB HL is generally considered a threshold beyond which cochlear implantation may provide superior benefit [77,78]. More recently, referral guidelines such as the so-called "60/60" rule have been proposed to improve the early identification of potential candidates: this rule recommends referring an adult for cochlear implant candidacy evaluation when the best-ear unaided monosyllabic word score is ≤60% and the unaided pure-tone average of the better ear is ≥60 dB HL [79].

The fundamental principle of cochlear implantation lies in the direct electrical stimulation of the auditory fibers via surgical insertion of a multichannel electrode array into the scala tympani of the cochlea. This approach bypasses the defective sensory structures of the inner ear, delivering an encoded electrical signal to the auditory fibers [80]. The objective is to provide the brain with an acoustic representation that closely approximates physiological hearing, particularly through accurate frequency (via channel number) and temporal (via stimulation rate) coding. Following implantation, the patient must undergo intensive auditory and speech therapy to learn how to decode and interpret these novel signals.

Technological advances over the past decades have markedly improved cochlear implant outcomes. It is now common to see implant recipients capable of making phone calls or engaging in conversations in noisy environments, achievements that were unimaginable thirty years ago. However, this progress is not solely attributable to hardware innovation; it also reflects the refinement of candidate selection criteria. Whereas only individuals with total deafness were initially eligible, current audiometric indications have progressively broadened to include patients with residual low-frequency hearing.

This evolution raises important questions about the boundary between acoustic amplification and cochlear implantation. In some cases, cochlear implant users outperform acoustically aided patients, particularly regarding speech perception in challenging listening environments such as noise or telephone conversations. These observations call into question the optimal threshold

for recommending cochlear implantation over conventional amplification. Therefore, objective comparative evaluation between the two rehabilitative strategies remains a key clinical challenge.

Lastly, it is important to emphasize that cochlear implants can be safely and effectively used in both adults and children, regardless of age, provided the indication is appropriate. Cochlear implantation is a multidisciplinary intervention requiring coordinated expertise in surgery, audiology, speech therapy, and psychology to ensure optimal functional outcomes and successful auditory integration [80,81].

4.1.1. Overview of Cochlear Implant Components

The cochlear implant is a high-tech neuroprosthetic device designed for patients with severe to profound sensorineural hearing loss. Unlike conventional hearing aids, which amplify sound, the cochlear implant bypasses the damaged hair cells by directly stimulating the auditory nerve through electrical signals. It consists of two main units: an external component responsible for capturing and processing sound signals and an internal, surgically implanted component that ensures the transmission of electrical signals to the cochlea.
The following figure (Fig.12) illustrate the structure and arrangement of the external and internal components of the cochlear implant, highlighting their complementarity and their role in the implantation and auditory stimulation process.

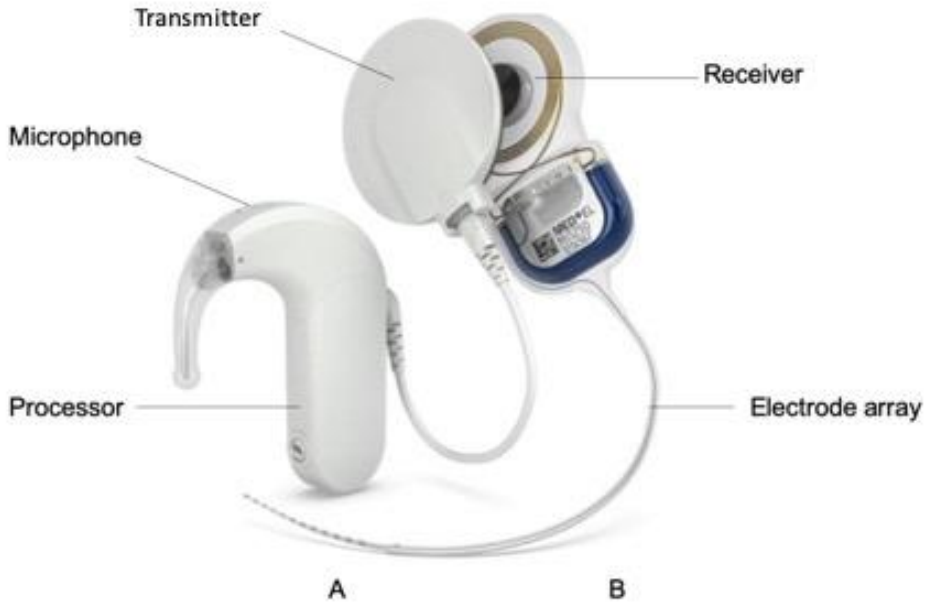

Figure 12. (a) The external component of the cochlear implant. (b) The internal component of the cochlear implant. Adapted from MED-EL product imagery, courtesy of MED-EL; the labels were added by the author.

4.1.2. External Component: Signal Capture and Transmission

The external component of the cochlear implant is removable and worn by the patient. It comprises several essential elements:

-The Microphone: Typically located on a behind-the-ear processor, the microphone captures ambient sounds and converts them into electrical signals. In certain cases, particularly in pediatric patients or in the presence of auricular malformations, the microphone can be relocated to the external antenna.
- The Speech Processor: This miniaturized microcomputer processes and analyzes the sounds detected by the microphone. It applies a specific coding algorithm that transforms these acoustic signals into a set of electrical instructions designed to selectively stimulate the intracochlear electrodes. The processor operates on disposable batteries or a rechargeable power source and allows adjustment of settings according to the listening environment (quiet settings, ambient noise, music).
- The External Antenna: Positioned on the scalp and held in place by a magnet, the antenna transmits the coded signal to the internal implant via transcutaneous electromagnetic coupling. This technology eliminates the need for a percutaneous cable, thereby reducing the risk of infection. Certain cochlear implant devices, specifically single-unit processors worn off-the-ear, combine the antenna, processing unit, battery, and microphone into a single external housing. This module attaches directly to the implant via magnetic coupling. This streamlined configuration eliminates the necessity for a behind-the-ear component and connecting cables, which can significantly enhance user comfort, aesthetic appearance, and ease of use.

4.1.3. Internal Component: Signal Reception and Auditory Stimulation

The internal component is surgically implanted beneath the skin in the temporal bone and directly connected to the cochlea. It consists of multiple elements encased in biocompatible materials to ensure long-term functionality and compatibility with biological tissues:
- The Receiver-Stimulator: Implanted under the skin, this device receives and decodes the information transmitted by the external antenna. It then converts these signals into electrical impulses, which are subsequently delivered to the implanted electrodes.
- The Electrode Array: A critical component of the device, the electrode array is delicately inserted into the scala tympani of the cochlea during surgery. Depending on the model, it contains between 12 and 22 electrodes distributed tonotopically to selectively stimulate different regions of the cochlea corresponding to various sound frequencies. The distribution and flexibility of the electrode array are crucial parameters for preserving cochlear structures and optimizing auditory restoration.
- The Ground Electrode: Generally positioned on the surface of the receiver-stimulator or below the temporal muscle, this electrode completes the electrical circuit and optimizes current distribution for stimulation.

Recent innovations aim to further enhance the effectiveness of cochlear implants. For example, new generations of ultra-flexible or shorter electrode arrays allow for more atraumatic insertion, reducing the risk of intracochlear damage and improving the preservation of residual hearing. Furthermore, advancements in signal coding technology provide more precise sound reproduction and improved speech comprehension, even in noisy environments. Beyond conventional systems, fully implantable cochlear implants, also referred to as Totally Implantable Cochlear Implants (TICI), are currently under development. These devices integrate the microphone, processor, power source, and stimulating components entirely under the skin, thereby eliminating all external hardware. Although still facing technical challenges related to power consumption, signal acquisition, and long-term reliability, TICI systems represent a promising future direction aimed at continuous hearing, improved cosmetics, and enhanced patient autonomy.

4.1.4. Conclusion

The cochlear implant function relies on a close interaction between two components: an external unit that captures and processes sound and an internal unit that converts these signals into electrical impulses that stimulate the auditory nerve. The design and optimization of these components are essential to improving auditory outcomes for patients and ensuring their optimal adaptation to various sound environments.

4.2. Electrical Signal Transmission to the Cochlea

The cochlear implant is a sophisticated medical device designed to restore hearing in individuals with severe to profound sensorineural hearing loss. It restores auditory perception in severe to profound sensorineural hearing loss by bypassing damaged hair cells and directly stimulating the auditory nerve." [82]

As previously described, the implant consists of two complementary components. The external component includes microphones that capture ambient sound, an audio processor that performs frequency-based analysis of the acoustic signal, and a power supply.

The processor decomposes the incoming signal into multiple frequency bands, typically between 12 and 22, based on a model inspired by the 24 critical bands defined in human psychoacoustics [83]. These bands correspond to the natural resonant frequencies of the cochlea and are essential for reproducing a faithful auditory perception. This spectral segmentation preserves the cochlea's inherent tonotopic organization.
Each frequency band is then processed to extract key acoustic features. This processing yields three fundamental parameters: (i) the spectral content, determined by the number of active bands; (ii) signal intensity; and (iii) the temporal dynamics of intensity, represented by the stimulus envelope.
Two principal signal processing approaches are employed to perform spectral analysis and envelope extraction. The first relies on a bank of band-pass filters to isolate frequency bands, followed by envelope extraction via rectification (elimination of the signal's negative oscillations) and subsequent smoothing of the filter output [84]. The second method utilizes the Fast Fourier Transform (FFT), grouping and weighting spectral lines according to the required number of frequency channels to derive the signal envelope. Frequencies below 100 Hz and above 8,000 Hz are typically filtered out, as they are generally considered non-essential for speech understanding or environmental sound identification.
In parallel with signal analysis, dynamic range compression is applied to each frequency band individually, particularly to modulate ambient sound intensity and short-duration impulse noises. This compression process aligns the acoustic dynamic range with the electrical dynamic range of the auditory nerve. The electrical stimulation range is easily adjustable during audiological programming sessions to optimize patient comfort. It is defined between two personalized thresholds: the threshold of perception (T) and the maximum comfortable level (MCL).

Coding strategies vary across cochlear implant manufacturers, including differences in stimulation rate (pulse frequency) and the number of simultaneously activated electrodes. However, one fundamental principle remains consistent: sound intensity is conveyed through electrical pulses delivered to the auditory nerve, while frequency is encoded spatially by the position of electrodes along the cochlea. This tonotopic arrangement is preserved through

localized and sequential electrode stimulation. Without sufficient selectivity, inter-electrode (inter-channel) interference may degrade frequency resolution. Sound intensity coding can be achieved by modulating the amplitude of the pulses, their duration, or a combination of both, depending on the specific technological design of each manufacturer [85].

Sound coding strategies are numerous and continuously evolving. They may be designed to adapt to spectral characteristics, such as the tonotopic arrangement of electrodes and spectral filtering, temporal characteristics, such as stimulation rate and inter-channel synchronization, or a combination of both. Hybrid strategies, such as ACE (Advanced Combination Encoder) or n-of-m, are widely implemented. These algorithms are developed to enhance speech recognition in noisy environments, improve telephone communication, and even support music perception. Current advancements are oriented toward smarter implants, featuring adaptive electrodes, real-time stimulation based on acoustic scene analysis, and robotic-assisted implantation procedures.
The processed signal is transmitted via a radiofrequency link to an internal antenna, which is held in place by a magnet. This antenna is connected to a subcutaneous receiver-stimulator that demodulates the incoming information before relaying it to the electrode array. The implanted array contains multiple electrodes distributed along the scala tympani and positioned in close proximity to the modiolus. This configuration aims to optimize the stimulation of spiral ganglion fibers by maximizing the electrophysiological coupling between the electrodes and the target neural structures (Fig.13).

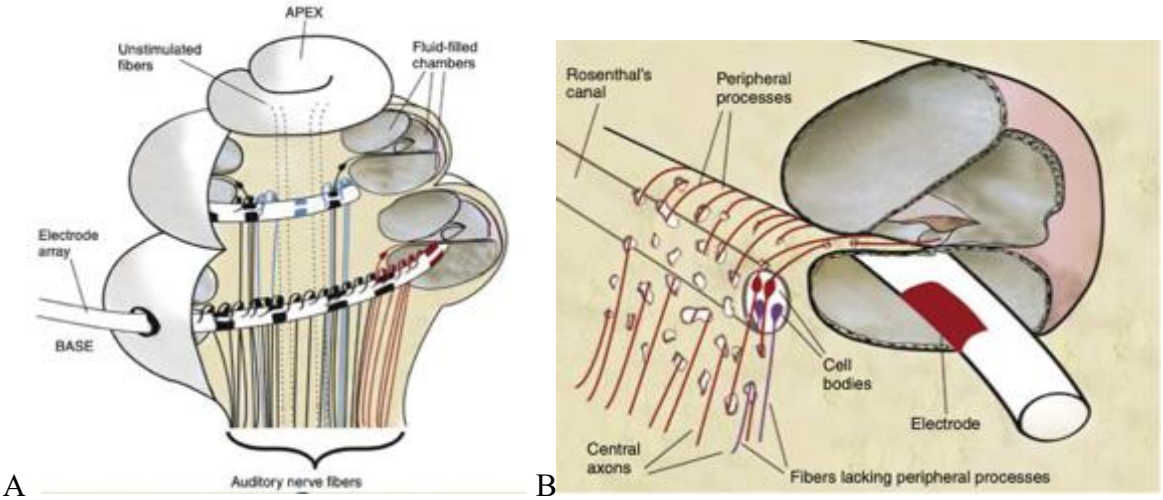

Figure 13. Localization of an electrode array within the cochlea. (A) Cross-sectional view of a cochlea. The electrode array is inserted into the scala tympani. (B) Visualization of a single electrode. Its position adjacent to the auditory nerve fibers allows direct access to the dendrites and somata of the spiral ganglion neurons located within Rosenthal's canal. Reproduced from Macherey and Carlyon (2014) [82].

The total number of electrodes is generally designed to correspond to the number of frequency bands processed by the external audio processor, ensuring a direct correspondence between spectral decomposition and cochlear stimulation sites. This mapping helps preserve spectral resolution and improves the representation of frequency contrasts in the encoded signal.
The intracochlear stimulator selects which electrodes to activate based on the corresponding frequency band, and for each selected electrode modulates both the current intensity and its temporal dynamics. This modulation is driven by the temporal and spectral characteristics of the acoustic signal, which are continuously analyzed in real time by the processor, ensuring efficient encoding of auditory information.

Once implanted within the scala tympani, a perilymph-filled duct, the electrode array delivers electrical stimulation that propagates through the conductive cochlear fluids toward the auditory nerve fibers located in the modiolus. The electrical pulses are biphasic (sometimes triphasic) to prevent electrolysis and electrode degradation, and the alternating polarity helps preserve neuronal tissue integrity [86]. Each pulse consists of a positive (anodic) phase followed by a negative (cathodic) phase, maintaining a net-zero mean current. To ensure this neutrality, the pulse waveform can be symmetrically modulated in both duration and amplitude.

Depending on the manufacturer's system design, loudness may be encoded either by modulating pulse amplitude or by varying pulse duration. Some systems primarily adjust pulse amplitude while maintaining constant duration, whereas others encode intensity through duration modulation with relatively stable amplitude. In practice, effective stimulation usually results from a balanced interaction between these two parameters.

The active electrode generates the current waveform, while the return electrodes complete the circuit by conducting an oppositely polarized current. This flow induces an electric field within the cochlea, most of which propagates through the scala tympani, although part may cross the osseous spiral lamina. Within this region lie the cell bodies of spiral ganglion neurons, whose axonal processes form the auditory nerve. When the electric field reaches sufficient intensity, it can depolarize neuronal membranes, triggering a cascade of action potentials along the auditory nerve.

Neuronal stimulation can be achieved using several modes. The monopolar mode, which involves an intracochlear active electrode and an extracochlear return electrode, produces a widely diffused current capable of recruiting numerous nerve fibers, albeit with reduced spatial selectivity. Bipolar mode offers an alternative, delivering current between two intracochlear electrodes. This configuration generates a localized electric field between the electrodes, resulting in more targeted activation of auditory fibers. Increasing the spacing between the electrodes can stimulate a broader population of fibers, though this does not necessarily improve spatial selectivity, as current spread may still engage wide cochlear regions even with closely spaced contacts (Fig.14).

Other, less commonly used configurations include the tripolar mode, in which the active electrode is flanked by two return electrodes that symmetrically distribute the compensatory current, thereby narrowing the stimulation field. The common ground mode, in contrast, employs all inactive electrodes as simultaneous return paths. The efficacy of these modes depends on electrode topography and the specific stimulation parameters employed [87–89] (Fig.14).

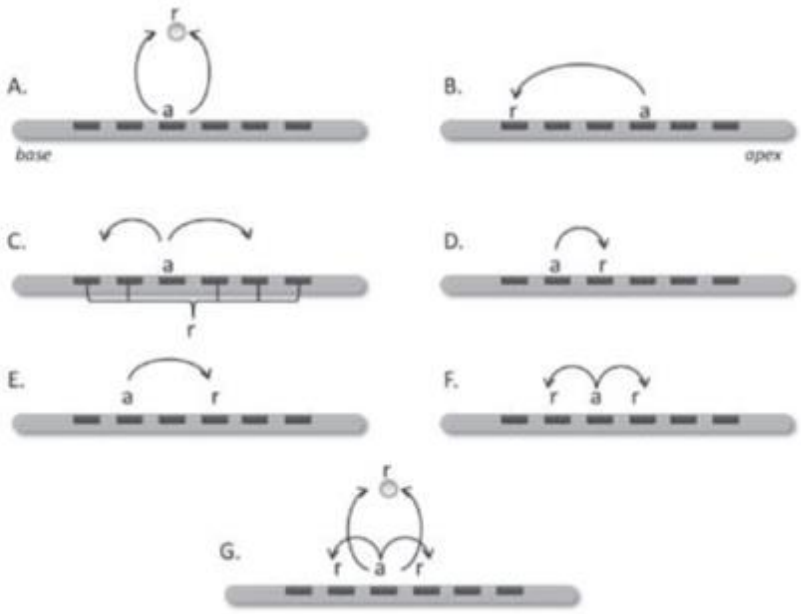

Figure 14. Representation of different stimulation modes. The active electrode is indicated by the letter 'a' and the return electrode by 'r'. A) Monopolar mode with an extracochlear return electrode. B) Monopolar mode with an intracochlear return. C) Common Ground mode. D) Bipolar mode. E) Bipolar +1 mode. F) Tripolar mode. G) Hybrid mode based on tripolar configuration with an extracochlear return electrode. From Objective Measures in Cochlear Implants (Hughes) [87].

The design of the electrode array can also influence stimulation efficacy. Straight electrodes rest against the lateral wall of the cochlea while pre-curved electrodes wrap around the modiolus and offer increased proximity to spiral ganglion neurons, thereby enhancing stimulation selectivity. Techniques such as the "Advanced-Off-Stylet" (AOS) method have been developed to optimize insertion while minimizing direct contact with cochlear walls [90–92].

At the neurophysiological level, electrical stimulation fundamentally differs from natural acoustic stimulation. It activates large populations of auditory nerve fibers simultaneously, without distinction based on fiber type or activation threshold. Electrical stimulation is thus considered 'non-selective'. Most fibers are Type I, normally categorized by sensitivity (low, medium, high), though this classification becomes irrelevant under electrical activation. Type II fibers, which are far fewer in number, have not yet been shown to play a significant role in auditory perception.
Moreover, electrical stimulation primarily activates auditory nerve afferent fibers that transmit information to the brain. However, the spread of electrical current within the cochlea may reduce the spatial selectivity of stimulation, potentially degrading the temporal and spectral encoding of the signal and thereby reducing auditory precision. Several mechanisms described contribute to this limitation, including the broad spread of electrical excitation within the cochlea, artificial synchronization of neural firing across populations of auditory nerve fibers, reduced fidelity of natural temporal coding, and interactions between adjacent stimulation channels.

Finally, the functional state of the auditory nerve is dynamic. It is influenced by various factors such as patient age, duration of deafness, presence of inflammatory or degenerative conditions, and long-term implant use [93]. These variables directly affect the quality of the 'electrode-neuron interface,' defined as the capacity of an injected current to elicit a meaningful neural

response [82]. Fine-tuning stimulation parameters, personalizing mapping protocols, and conducting regular assessments can help mitigate functional decline, although biological limits to auditory plasticity remain.

4.3. Cochlear Implant Surgery: Techniques and Advances

4.3.1 Introduction

Cochlear implantation is a surgical procedure designed to restore hearing in patients with severe to profound hearing loss. Over the past three decades, this technique has been refined, particularly regarding surgical approaches, receiver/stimulator management, and cochlear access. Advances in materials and surgical methods have significantly improved functional outcomes while reducing the risk of complications.

4.3.2. Surgical Procedure

4.3.2.1. Anesthesia and Initial Preparations

The procedure is performed under general anesthesia with the assistance of an operative microscope and facial nerve neuromonitoring to minimize the risk of nerve damage. Antibiotic prophylaxis is recommended to reduce the risk of infection. The duration of surgery typically ranges from 1.5 to 3 hours, depending on the surgeon's experience, the patient's anatomical complexity, and the surgical technique used.

4.3.2.2. Surgical Access and Implantation

The skin incision is made behind the ear after local anesthesia. A short postauricular incision, usually oriented vertically, is preferred as it preserves the vascular supply of the skin flap. If a previous postauricular incision exists, it can be reused or slightly extended.

A musculoperiosteal flap is then elevated to expose the mastoid bone. A periosteal incision with an anterior base allows the creation of a subperiosteal pocket for the receiver/stimulator without involving the temporalis muscle.

The receiver/stimulator is placed in a posterior and slightly superior position relative to the postauricular incision, approximately 45 degrees relative to the canthomeatal line. It is crucial to position the receiver/stimulator sufficiently posterior to the postauricular incision to prevent it from being directly under the auditory processor. This positioning ensures adequate soft tissue coverage and prevents excessive pressure between the internal implant and the external processor. A template can be used before the surgical incision to determine the optimal posterior distance from the postauricular fold.

4.3.2.3. Mastoidectomy and Cochlear Access

The surgery proceeds with a mastoidectomy, a critical step that exposes the external semicircular canal and the short process of the incus [94]. The mastoidectomy is initiated at Henle's spine and progresses posteriorly and inferiorly. Identification of the middle fossa dura, sinodural angle, and sigmoid sinus is recommended. Dissection then proceeds medially toward

the mastoid antrum, ensuring removal of all aerated cells outside these anatomical landmarks. If an operative microscope has not yet been introduced, it becomes indispensable at this stage (Fig.15).

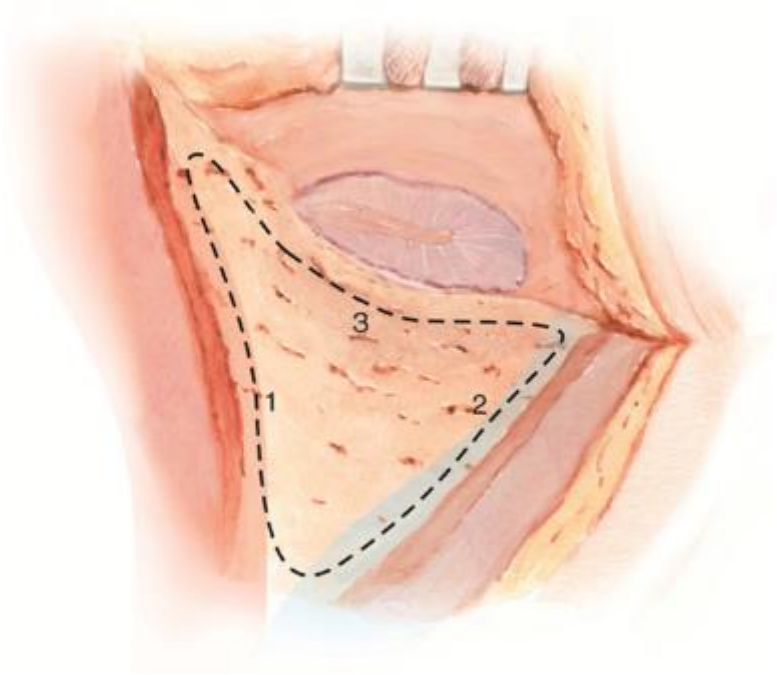

Figure 15. Identification of the mastoid surgical landmarks. Following a retroauricular skin incision, an anteriorly based musculoperiosteal flap has been elevated, exposing the mastoid cortex of the temporal bone. Anteriorly, the mastoid continues toward the bony external auditory canal, at the medial end of which the tympanic membrane can be identified. The three lines delineating the boundaries of the cortical mastoidectomy are indicated: the temporal line (1), the sigmoid sinus (2) and the posterior wall of the external auditory canal (3). From the Atlas of Middle Ear Surgery (Gersdorff and Gérard) [95].
Once the mastoid cortex is uncovered, drilling should begin with a large cutting burr along the temporal line in an anteroposterior trajectory to reveal the middle fossa plate (1). A second drilling line is then performed posteriorly to delineate the sigmoid sinus (2), and a third line is placed immediately behind the posterior wall of the external auditory canal to complete the orientation (3) [95].

Precise identification of the facial recess and facial nerve is a key step (Fig.16). Thinning of the external auditory canal allows better visualization of retrofacial air cells. The facial nerve must be located just after its second genu, ensuring that a thin protective bony layer remains over it.

Most surgeons opt for a posterior tympanotomy through the facial recess to access the round window and promontory [96]. The facial recess is a small triangular surgical space located between the vertical segment of the facial nerve and the chorda tympani. It is laterally bounded by the incus buttress and provides access to the middle ear from the mastoid cavity, particularly to the round window niche. Its opening should be as wide as possible to optimize visualization of the stapes tendon, round window, and underlying cochlea. The opening extends from the posterior incudal ligament superiorly to the emergence of the chorda tympani inferiorly. The lower section is crucial for observing the round window niche, while the upper section ensures an optimal electrode insertion angle.

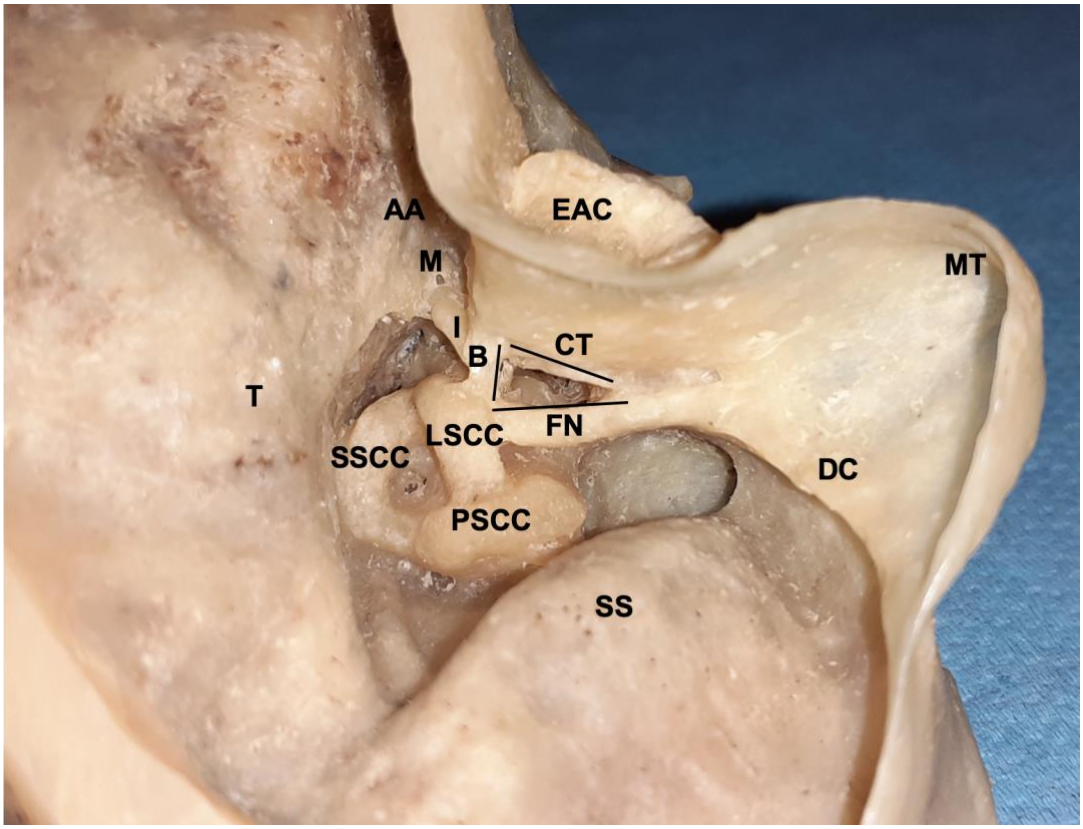

Figure 16. Temporal bone dissection of a right ear in the supine surgical position. Following mastoidectomy, a posterior tympanotomy has been performed through the facial recess, a triangular corridor bounded medially by the mastoid segment of the facial nerve, laterally by the chorda tympani and superiorly by the incus buttress. This approach exposes the posterior middle ear and allows direct visualisation of the promontory and the round window region, the key landmarks for cochlear implantation. AA, aditus ad antrum; B, incus buttress; CT, chorda tympani; DC, digastric crest; EAC, external auditory canal; FN, facial nerve; I, incus; LSCC, lateral semicircular canal; M, malleus; MT, mastoid tip; PSCC, posterior semicircular canal; SS, sigmoid sinus; SSCC, superior semicircular canal; T, tegmen (meninges). Own figure: specimen dissected by the author. For scale, the incus buttress measures 4 mm, the visible segment of the chorda tympani 7 mm and the visible mastoid segment of the facial nerve 9 mm, measured directly on the specimen.

The facial recess reaches adult size at birth, and in infants, the round window niche may be positioned more posteriorly relative to the facial nerve compared to adults. This anatomical configuration may affect the surgical angle and exposure during cochlear implantation in pediatric patients.

4.3.2.4. Cochleostomy and Electrode Insertion

A meticulous and atraumatic exposure of the round window niche is essential to ensure optimal visualization of the round window membrane and to limit mechanical trauma prior to electrode insertion.

Once the round window is identified, an opening is created to allow electrode array insertion into the cochlea. This step requires extreme precision to preserve cochlear structures and optimize implant performance.

Three main approaches are used for cochlear entry:

- **Traditional cochleostomy:** A 0.6–1.2 mm opening is created in the anteroinferior portion of the round window.
- **Round window insertion:** An incision is made in the round window membrane, allowing direct insertion.
- Extended cochleostomy: The lower ring of the round window membrane (crista fenestra) is identified, and 0.8–2 mm of underlying bone is removed for better access.

The use of lubricants, such as hyaluronic acid or glycerol, varies among surgeons. Before opening the endosteum, it is crucial to eliminate bone dust as much as possible through irrigation. If a lubricant is injected into the scala tympani, it may facilitate the evacuation of residual bone particles.

4.3.2.5. Receiver/Stimulator Placement

Once an appropriate site is identified, a bony bed is created to accommodate the thickest portion of the receiver/stimulator, preventing postoperative displacement. The depth and configuration of this cavity depend on the implant model but generally range from 2 to 3 mm. A groove is created to accommodate the electrode array and extends to the mastoid cavity.

In very young children, particularly those under one year old, skull thickness is often limited, requiring surgeons to adapt the preparation of the implant bed. When the bone is too thin, placing the device directly on the dura is a common and well-tolerated option. Various surgical teams adopt different strategies, such as maintaining a small bony island or removing the bone entirely, depending on their preferences and experience [97,98].

In conventional approaches, the implant is mechanically secured to the skull. However, many surgeons now favor less invasive fixation strategies. Avoiding extensive drilling or a formal bony bed may reduce the risk of surgical complications, while remaining safe in routine practice. If no bony bed is created, a well-fitted subperiosteal pocket is essential to prevent implant migration. Additionally, a bony ridge or fixation point should be added anteriorly to prevent forward displacement.

Finally, a channel is drilled from the implant housing to the mastoid cortex, ensuring secure electrode passage into the mastoid cavity. Some surgeons prefer maintaining a bony bridge at the groove-mastoidectomy interface for added stability.

Once the implant is positioned and tested, the incision is closed in multiple layers, and a compressive dressing is applied to minimize hematoma risk [97,98].

4.3.3. Electrode Array Insertion

Electrode array insertion is based on a set of general principles aimed at minimizing intracochlear trauma and ensuring optimal functional outcomes. The array should be advanced in a slow, gradual, and delicate manner, with proper orientation of the electrode contacts to follow the scala tympani. Unnecessary movements should be avoided throughout the insertion process.

If resistance is encountered, gentle corrective maneuvers may be performed, such as a slight withdrawal of the array followed by minimal readjustment to restore an appropriate trajectory,

without applying excessive force. Over-insertion should be avoided, as advancing the electrode beyond the intended depth or the manufacturer's recommendations may lead to suboptimal frequency–place alignment along the basilar membrane and potentially alter sound perception.

Once the desired depth is reached, the electrode should be adequately secured, and the excess lead carefully coiled to prevent postoperative displacement and ensure long-term stability.

4.3.4. Intraoperative Electrophysiological Monitoring and Surgical Refinements

Intraoperative electrophysiological tests are performed to verify the integrity of the device and ensure proper electrode positioning. These tests include Neural Response Telemetry (NRT), Auditory Response Telemetry (ART) or Neural Response Imaging (NRI) depending on the manufacturer, and allow assessment of auditory nerve stimulation via the implant [99]. Advances in surgical techniques and improvements in imaging tools have contributed to greater implantation precision and a significant reduction in postoperative complications.

4.3.5. Hearing Preservation Strategies

Hearing preservation has become an increasingly achievable and desirable goal in cochlear implantation procedures. Maintaining residual acoustic hearing, with or without amplification, enhances speech perception in noisy environments and improves music appreciation. It is estimated that hearing preservation is possible in approximately 80% of cases when considered in the surgical strategy [100,101].

The atraumatic approach, also known as "soft surgery," is based on several key principles:

1. Precise identification of the round window membrane.
2. Optimal cochleostomy placement, ideally inferior to the mid-portion of the round window membrane.
3. Meticulous removal of bone dust and blood through irrigation before opening the round window membrane.
4. Low-speed and progressive bone drilling to minimize trauma. The endosteum should be adequately exposed before entering the round window membrane.
5. Avoiding aspiration of perilymph.
6. Perioperative corticosteroid administration. Some surgeons prefer intratympanic injections before electrode insertion, others apply steroids directly onto the electrode array, while some opt for systemic administration before, during, or after the procedure. However, direct injection into the cochlea is generally discouraged when hearing preservation is a goal.
7. Controlled low speed and gradual electrode array insertion, allowing perilymph displacement to minimize trauma.

4.3.6. Conclusion

Cochlear implantation represents a significant advancement in the management of profound hearing loss. Thanks to the progress in surgical techniques, instrumentation, and hearing preservation strategies, functional outcomes continue to improve. However, this surgery

requires high precision, specialized expertise, and rigorous postoperative monitoring to ensure optimal benefits while minimizing potential complications.

5. Atraumatic Cochlear Implant Surgery

5.1. Introduction

As outlined in Section 4, the indications for cochlear implantation have progressively broadened, and contemporary practice places a growing emphasis on the preservation of native cochlear function.

Modern cochlear implantation aims not only to restore auditory input but also to maximize speech perception, enhance musical appreciation, and enable effective electro-acoustic stimulation (EAS) by maintaining residual low-frequency hearing. These goals have stimulated critical changes in both surgical technique and electrode design, with an overarching emphasis on minimizing intracochlear trauma.

Current best practices involve slow, controlled insertions using thin, flexible arrays designed to conform to cochlear anatomy. These "soft surgery" techniques aim to avoid injury to delicate structures such as the stria vascularis, BM, and surrounding neural tissues [102]. Innovations in electrode design now allow for full insertions, limiting mechanical and inflammatory injury risks [103].

Despite these refinements, suboptimal insertions remain a challenge. Historically, straight electrodes were inserted through the RW; however, limited visibility, unfavorable anatomy, and early resistance at the modiolus often hindered full insertion. Meta-analytic data from Hoskison et al. reveal a 17.6% overall cochlear trauma rate, with BM elevation and rupture observed in 5.2% of cases. Notably, 84.4% of trauma involved translocation from the ST to the SV, and 5.2% reached grade 4 severity with both SV entry and OSL fracture [104].

Although standardized insertion protocols and robotic assistance may mitigate such risks, key limitations persist. Most studies lack audiometric correlation, rely on cadaveric specimens, and exhibit considerable heterogeneity in electrode design. Moreover, trauma detection is more reliable histologically (28.9%) than radiologically (13.3%), underscoring the limitations of current imaging modalities [104].

As surgical candidates become increasingly diverse, with varying cochlear anatomies and residual hearing profiles, minimally traumatic, anatomically guided electrode insertion becomes essential. Achieving this requires a synergistic approach combining advanced imaging, intraoperative monitoring, electrode innovation, and individualized surgical planning.

5.2. Principles of Atraumatic Electrode Insertion

The preservation of residual hearing, whether partial or complete, has become a cornerstone objective in contemporary CI surgery. Achieving this goal critically depends on minimizing

intracochlear trauma during electrode insertion, as both hearing preservation and long-term implant performance are significantly influenced by the quality of insertion.

Atraumatic electrode insertion, particularly one that ensures full placement of the electrode array within the scala tympani (ST), is essential. This is especially true along the initial segment of the basal turn, where anatomical vulnerability is greatest. Translocation of the array into the scala vestibuli (SV) is strongly associated with poorer auditory outcomes and should be systematically avoided [105,106]. To mitigate insertion trauma, the trajectory must align closely with the longitudinal axis of the ST, avoiding contact with delicate structures such as the osseous spiral lamina (OSL) and the BM. The relationship between insertion angle, cochlear curvature along the lateral wall, and insertion forces underscores the importance of maintaining a linear, controlled insertion path, preferably at low, constant speeds, which can be facilitated through robotic or motorized assistance.

Mechanical trauma can lead to direct structural damage to critical elements such as the organ of Corti, the vascular networks of the spiral ligament (SL), neural fibers within the OSL, and the neuronal populations housed in Rosenthal's canal. In particular, rupture of the scala media may precipitate immediate and irreversible auditory loss, often followed by secondary complications including inflammation, fibrosis, and ossification [107]. Furthermore, electrode translocation involving perforation of the BM, SL, or OSL not only increases the physical distance between the electrode contacts and target neurons, reducing stimulation efficiency, but also exacerbates chronic inflammatory responses, potentially triggering progressive cochlear degeneration [107]. A precise three-dimensional understanding of the cochlear microanatomy, especially the ST and its adjacent landmarks, is therefore indispensable for reducing trauma and improving surgical outcomes [107].

Electrode insertion can be achieved either via the round window (RW) or through a surgically created cochleostomy (CS). Irrespective of the chosen approach, the critical surgical goal remains the same: complete insertion of the array within the ST while preserving essential intracochlear structures such as the BM and OSL. These structures are pivotal in maintaining cochlear ionic homeostasis and ensuring the electrochemical gradients required for normal hair cell function [108]. Numerous clinical and histopathological studies have demonstrated that preservation of these barriers is positively correlated with better postoperative auditory thresholds and speech perception outcomes [109,110].

Despite these precautions, scalar translocation remains a common and largely unpredictable complication. This phenomenon, wherein the electrode unintentionally migrates from the ST to the SV, is associated with significantly reduced speech comprehension and diminished preservation of residual acoustic hearing [105,109,110]. Recent evidence emphasizes the importance of optimizing the insertion vector, particularly in the basal turn, to minimize structural disruption and reduce the likelihood of translocation [111,112].

Outcomes are consistently superior when the electrode remains confined within the ST [105,106]. Therefore, surgical strategies should prioritize atraumatic techniques not only to support hair cell preservation [113] but also to maintain the viability of future regenerative therapies and EAS applications [114].

Robotic-assisted insertion techniques have shown promise in achieving precise electrode placement with stable force profiles and consistent insertion velocities. These attributes are essential in minimizing intracochlear damage. In this work, the term "robotic-assisted insertion"

refers to a surgeon-controlled motorized insertion performed via a surgical telemanipulator, and not to an autonomous robotic system such as the HEARO®, as no independent decision-making or trajectory execution is involved; the device acts as a stabilized mechanical extension of the surgeon's hand, providing motion scaling, tremor filtering, increased precision of movements and reproducibility. Nevertheless, scalar deviations continue to occur in both manual and robot-assisted procedures, reflecting the inherent complexity of intracochlear navigation [115].

A key ambition of contemporary CI surgery is to preserve residual low-frequency hearing for acoustic stimulation while delivering electric stimulation to higher-frequency regions. This electro-acoustic hybrid configuration has demonstrated superior results in speech recognition, musical perception, and sound quality. Realizing such benefits requires detailed anatomical insight, particularly of the basal turn and hook region, where variability is most pronounced.

Trauma mitigation serves not only to preserve cochlear microarchitecture but also to facilitate future therapeutic interventions for sensorineural hearing loss. Non-linear insertion trajectories have been associated with greater damage to intracochlear structures, including the BM, OSL, and SL, thereby diminishing both structural and functional outcomes in stiff electrodes.

According to Starovoyt et al. [116], most insertion-related trauma occurs during the first 180° of the cochlea. Maintaining strict alignment with the natural curvature of the ST is essential to avoid iatrogenic injury. A primary obstacle to achieving this is the absence of real-time visual feedback. Surgeons rely solely on external landmarks, such as the RW or CS site, without intraoperative visualization of the electrode path. Conventional imaging techniques lack the resolution to delineate fine cochlear anatomy intraoperatively, particularly in the hook region.

Although improved electrode flexibility and soft-surgical techniques have reduced overall trauma rates, studies still report trauma in up to 40% of insertions. This underscores the need for integrated intraoperative technologies such as Optical Coherence Tomography (OCT) and electrocochleography (ECochG), which, when combined with robotic-assisted systems, further enhance surgical precision and reproducibility [116].

Optical coherence tomography is a non-contact, non-destructive optical imaging technique based on low-coherence interferometry of backscattered near-infrared light. It produces cross-sectional images of tissue at micrometre-scale resolution and, unlike computed tomography, resolves the soft-tissue structures of the hook region through the intact round window membrane, including the osseous spiral lamina, the crista fenestra and the spiral ligament [116]. Systematic imaging of a series of human cochleae has allowed these structures and their variability to be mapped into an atlas of the hook region, which provides the anatomical reference against which an intraoperative image can be interpreted [117].

Electrocochleography records the electrical activity generated by the cochlea in response to an acoustic stimulus delivered to the ear, principally the cochlear microphonic, which originates mainly from the outer hair cells, together with the response of the auditory nerve [118]. During cochlear implantation, this response can be recorded repeatedly, or continuously, from the electrode array itself as the insertion proceeds, which provides the surgeon with real-time functional feedback on the impact of each insertion step [119]. A marked change in the amplitude or in the morphology of the response signals an intracochlear event that may be traumatic, and allows the insertion to be interrupted or redirected before the trauma becomes irreversible.

Modern CI systems aim to optimize both hearing preservation and speech understanding. Electrode design must therefore satisfy several competing requirements: (1) minimal insertion trauma; (2) sufficient depth for broad frequency coverage; (3) proximity to the spiral ganglion (SG); and (4) anatomical adaptability. These goals are further complicated by inter-individual differences in cochlear duct length, RW orientation, and the spatial configuration of the basal turn.

High-resolution synchrotron imaging studies by Starovoyt et al. [116] reveal substantial microanatomical variability among cochleae, emphasizing the need for personalized surgical and programming strategies. Even minor deviations in insertion trajectory or depth can result in mismatched neural stimulation patterns and suboptimal hearing outcomes.

Histological analyses provide additional support. Carlson et al. [113] and Ibrahim et al. [114] demonstrated that non-linear insertion vectors are significantly correlated with structural damage, particularly to the BM, OSL, and SL. These injuries trigger inflammatory cascades that result in fibrosis, ossification, and the eventual deterioration of auditory and vestibular function. Notably, even when the electrode reenters the ST after an initial deviation, trauma may have already occurred, underscoring the importance of an accurate initial trajectory.

Together, these findings argue strongly in favor of slow, robotically tailored and guided insertions that respect the native anatomy of the ST. Such individualized strategies, guided by preoperative imaging and intraoperative monitoring, represent the current frontier in minimizing cochlear trauma and optimizing long-term auditory outcomes.

5.3. Surgical Approaches

Variability in CI outcomes is influenced by multiple factors, including surgical technique. In particular, the choice between the RW, peri-round window (PRW), and CS approaches plays a critical role in determining electrode trajectory, the likelihood of intracochlear trauma, and the preservation of residual hearing. A thorough understanding of cochlear anatomy, particularly of the hook region and RW niche, is essential for optimizing electrode placement and minimizing insertion-related complications.

5.3.1 Anatomical Landmarks of the Cochlear Hook Region

The round window membrane (RWM), located in the basal turn of the cochlea, offers a natural and direct access route to the ST through the hook region. However, its visibility is inconsistent: it is only partially exposed in 50–80% of cases and may be entirely absent in up to 8% of temporal bones [120]. Anatomical variations, including bony overhangs, crests, and the crista fenestrae, may obscure the RWM or alter the electrode insertion path [120–124].

Atturo et al. [125] reported a reduced oval window–round window (OW–RW) distance in smaller cochleae, increasing the risk of injury to the SL and OSL. Similarly, a high-riding crista fenestrae or a narrow inferior niche can obstruct atraumatic electrode placement [122,124]. Notably, the vertical clearance between the crista fenestrae and the BM is limited to an average of 0.9 mm (range: 0.8–1.1 mm), emphasizing the need for meticulous surgical precision [124].

Cochleostomy, a surgical opening into the cochlea, remains technically demanding due to considerable inter-individual anatomical variability [122,126]. Even for seasoned surgeons, consistently identifying safe insertion sites is challenging. The RW annulus remains the most

dependable anatomical landmark for cochlear access [121,122], although the RW's shape and rotational axis vary significantly across patients, unpredictably affecting the spatial orientation of internal cochlear elements such as the SL, BM, and OSL [122,123].

Preoperative computed tomography (CT) imaging is indispensable to guide the safest surgical trajectory, particularly in cases of atypical RW anatomy or a constricted hook region [122]. A longer OW-RW distance typically provides a broader operative corridor for atraumatic electrode placement [125]. Larger cochleae are often associated with a wide SL arch, facilitating easier access and favoring extended or anterior-inferior cochleostomy (eCO or AICO) approaches, with reduced risk to adjacent structures [122]. In contrast, smaller cochleae or narrow hook regions restrict access and elevate the risk of trauma, particularly to the lateral SL [124,126,127]. Hence, preoperative imaging is essential for assessing spatial constraints and optimizing surgical strategy. For patients with residual hearing and small cochleae, the RW approach is preferred for its minimal invasiveness [122].

Contrast-enhanced computed tomography (CECT) improves the delineation of bony structures surrounding the RW. The round window arch (RWA), a dense and bilaterally symmetrical structure of probable embryological origin, does not appear to provide mechanical support to intracochlear tissues. In contrast, the porous secondary spiral lamina (SSL) plays a structural role by supporting both the BM and the SL [107]. Differentiating these elements is vital to minimize intracochlear trauma and guide electrode positioning.

The RWM thus serves as a critical entry point for a range of otologic procedures, including cochlear implantation, therapeutic delivery, and diagnostic exploration. The RW approach, in particular, has garnered attention for offering an anatomically favorable trajectory into the ST. This direct pathway minimizes mechanical disruption and enhances postoperative hearing preservation potential.

These modalities further refine anatomical assessment, particularly in cases of RW anomalies or hook region constraints [122]. The OW- RW distance is increasingly recognized as a predictive metric for RW approach suitability [122,125], reinforcing the need for individualized surgical planning.

5.3.2. Implications of Anatomical Variability on Surgical Access

The anatomical constraints of the RW region have direct surgical consequences. A narrow or obscured RW niche may necessitate bone removal or a shift to an alternative approach, such as the eRW or CS, both of which introduce their own risks. Modifications such as anterior enlargement of the RW or removal of the crista semilunaris and anterior bony lip have been proposed to facilitate insertion of slim perimodiolar electrodes (SPE), especially in anatomically restricted RW niches [125,128].

The curvature of the SL cannot be visualized intraoperatively but significantly affects insertion trajectory. For this reason, preoperative imaging is indispensable for assessing cochlear dimensions and planning the surgical approach [122]. Particularly in small cochleae with residual hearing, the RW approach remains preferable due to its less invasive nature and reduced trauma risk [122,125].

Prominent anatomical features such as bony crests, crista fenestrae, and overhangs can obstruct insertion and deflect the electrode toward the modiolus or BM. In 10% of specimens, a

projection (CF-B) was found on the inferior ST wall, requiring surgical modification to allow atraumatic insertion [124].

5.3.3 Surgical Approaches to the Scala Tympani

5.3.3.1. Round Window (RW) Approach

The RW approach provides direct access to the ST with minimal bone removal (bony overhang) and is well-suited for soft surgical techniques.

Although the RW approach provides a trajectory closer to the natural entry vector of the scala tympani, it cannot be considered strictly aligned with the ST axis due to the anatomical curvature of the hook region. This orientation nonetheless reduces the likelihood of contacting critical intracochlear structures, such as the BM, SL, and OSL [129,130]. However, anatomical variations, including a shortened vertical segment of the RWM or an elevated crista fenestrae, may still deflect the electrode toward the modiolus or into the SV [125,128].

In such scenarios, Pringle et al. [131] recommend partial removal of the bony overhang of the RW, particularly its posterior–superior portion, to straighten the insertion trajectory and minimize modiolus contact. Even when the vertical segment of the RWM is sufficiently elongated, a prominent crista fenestrae can still redirect the electrode array (EA) medially toward the modiolus prior to descending into the ST. This anatomical barrier may compromise insertion linearity and increase the risk of trauma.

Non-linear insertions have been observed more frequently with the RW approach and are strongly correlated with structural damage. In two RW cases characterized by non-linear trajectories, the electrode contacted the modiolus, with one instance resulting in significant trauma - specifically, an OSL fracture [120]. These findings confirm that modiolar contact and non-linear trajectories increase the risk of intracochlear trauma and scalar deviation. In addition, electrode stiffness plays a critical biomechanical role: straight and flexible arrays tend to naturally follow the hook region into the scala tympani, whereas stiffer arrays, particularly those incorporating a sheath or stylet, less readily conform to the cochlear curvature, thereby increasing the likelihood of a non-linear, traumatic trajectory.

Moreover, the RW approach may be associated with a reduced angular insertion depth, potentially limiting cochlear coverage in certain patients [120]. Nevertheless, when anatomical conditions are favorable, RW insertions can achieve complete ST positioning with minimal trauma. In contrast, narrowed or distorted RW regions increase the likelihood of non-linear insertions, thereby elevating the risk of modiolus contact and associated complications [120].

Histological and fluoroscopic evidence supports the RW approach as generally less traumatic. However, Zhou et al. [120] reported modiolus contact in three out of five RW insertions, with one case resulting in an OSL fracture - an event undetectable via fluoroscopy. These data underscore the importance of preoperative planning and trajectory optimization to minimize insertion-related injury.

Although the RW route is frequently selected for cochlear implantation due to its direct access to the ST, it may be contraindicated in the presence of anatomical anomalies or limited membrane visibility. Additionally, electrode insertion through the RWM may compromise its

physiological role as a pressure-relief mechanism, raising concerns regarding its universal applicability [120,122].

5.3.3.2. Extended Round Window (eRW) Approach

Anterior or anteroinferior enlargement of the RW niche may improve trajectory in anatomically challenging cases. While this approach may offer a straighter path for insertion, it increases the risk of SL damage, especially if the electrode is misdirected toward the SM or SV [126,128]. SPEs often require this extension for appropriate placement, given their stiffness and tendency to deviate in tight spaces [125].

The use of slim perimodiolar electrodes typically necessitates a two-handed technique. Insertion via the RW may be limited by the narrow RW anatomy, particularly in inferior access trajectories. In such cases, eRW may be preferable, although at the cost of increased risk to cochlear microstructures [125].

5.3.3.3. Cochleostomy (CS) Approach

Cochleostomy (CS) entails drilling a new opening into the cochlea, typically inferior or anteroinferior to the RWM, and is generally employed when the RW is inadequately exposed. However, the high inter-individual anatomical variability complicates the identification of consistent and safe CS sites [122,126]. Improper placement - particularly in superior or anterior positions - significantly increases the risk of trauma to the BM or scala media [126,128]. Historically, the stapes head served as a surgical landmark, but due to the anatomical inconsistency of the round window niche (RWN), this method is no longer recommended.

Anteroinferior drilling aligned with the RWM offers a safer and more reliable trajectory into the ST, while superior placements elevate the risk of BM damage [128]. Inferior CS, performed via the crista fenestra, enables ST access without violating the BM or scala media but often requires extensive drilling and may compromise critical adjacent structures such as the inferior cochlear vein (ICV) and cochlear aqueduct, with potential consequences for sensory cell viability and stria vascularis function. Moreover, both anterior-inferior cochleostomy (AICO) and inferior cochleostomy (ICO) approaches may endanger the tympanic nerve, which was sacrificed in cadaveric studies (Fig.17).

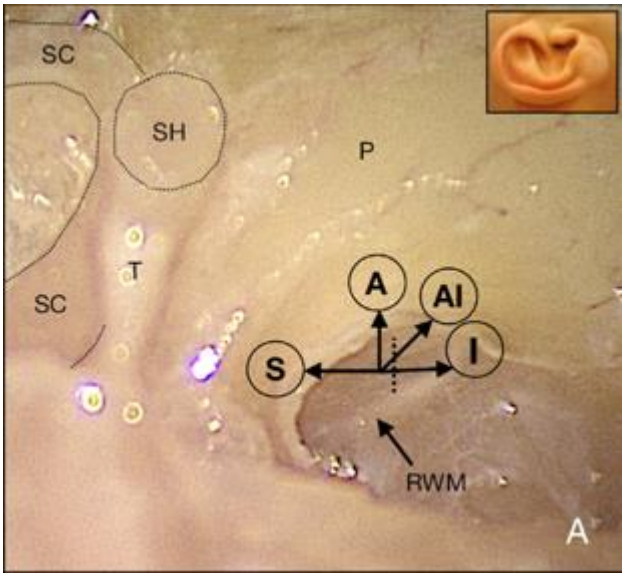

Figure 17. Right ear positioned for surgery, illustrating potential cochleostomy locations and the optimal entry site. The pinna is shown to indicate the orientation of the surgical view: the patient is in the supine position and the ear is a right ear. The bony overhang of the RWN has been removed, allowing clear visualization of both the stapes and the RWM. Several possible cochleostomy entry points are indicated in relation to the RWM. The image provides excellent exposure of the membrane. A dashed line marks a proposed incision site in the RWM for insertion of the electrode array, which would pass near the OSL. The oval window (OW), which is closed by the footplate of the stapes, lies immediately above and slightly anterior to the round window. The distance between the inferior margin of the OW and the superior margin of the RWM itself, and not that of the bony margin of the niche, is less than 3 mm; this short and constant distance makes the stapes a reliable landmark for locating the round window when the niche is difficult to identify. Abbreviations: A, anterior; AI, anteroinferior; I, inferior; OSL, osseous spiral lamina; OW, oval window; P, promontory; RWM, round window membrane; RWN, round window niche; S, superior; SC, stapes crura; SH, stapes head; T, stapes tendon. Reproduced from Pringle and Konieczny (2021) [131].

Li et al. [122] and Atturo et al. [125] emphasized that only very inferiorly placed cochleostomies reliably reach the ST while avoiding injury to the BM or OSL. Nevertheless, these approaches pose technical challenges due to limited exposure and the proximity of vascular structures. Li et al. further identified the anteroinferior margin of the RWM or adjacent otic capsule as the most favorable CS site. This location allows for direct ST access, assuming the insertion follows the longitudinal axis of the scala.

Zhou et al. [120] reported that anteroinferior CS yielded the greatest angular depth of insertion (487°), compared to 413° for the postero-inferior RW (PRW) approach and 375° for the RW itself, with no modiolar contact or OSL fractures observed in CS and PRW groups. Moreover, inferior CS was associated with a reduced risk of damaging vascular structures such as the CA and ICV [122].

Although the CS technique offers controlled cochlear access and may reduce modiolar contact due to its linear trajectory, it is not always feasible due to anatomical limitations. In some cases, attempts to insert the electrode through the horizontal portion of the RWM may result in BM trauma or misplacement into the scala vestibuli or vestibule. A short vertical RWM segment or an elevated crista fenestrae can further complicate the insertion path [120].

Despite its advantages, CS carries inherent risks, including acoustic trauma, hemorrhage, bone dust contamination, and inadvertent injury to the OSL or BM [116,125,128]. Starovoyt et al. [116] noted that although CS enables precise access to the basal cochlea, the drilling process

itself may cause unavoidable damage to delicate structures such as the BM and OSL. These findings support the continued preference for the RW approach whenever anatomical conditions permit.

5.3.3.4. Comparative Evidence: Anatomical and Clinical Studies

Briggs et al. [132], in cadaveric studies, demonstrated that both RW and CS approaches permit atraumatic lateral wall (LW) electrode insertions. However, RW insertions were more frequently associated with modiolar contact and tip fold-over. Similarly, Addams-Williams et al. [133] observed that well-executed CS resulted in localized inflammation without inducing neuronal loss.

Comparative clinical data remain equivocal. Gudis et al. [134] reported similar scalar translocation rates in 130 RW-based insertions compared to CS procedures, while Richard et al. [135] emphasized that trauma risk exists with either approach when anatomical boundaries are not respected. Zhou et al. [120] corroborated these findings, reporting no modiolar contact or OSL fracture in CS and PRW insertions, whereas 3 of 5 RW insertions exhibited modiolar contact.

Meta-analyses and systematic reviews offer conflicting interpretations. Havenith et al. [129] found no significant difference in hearing preservation between RW and CS techniques; however, methodological variability across studies limits definitive conclusions. In contrast, Wanna et al. [130] reported superior hearing outcomes with RW and PRW insertions. Starovoyt et al. [116] cautioned that CS, due to the requirement for drilling, poses increased risk to the BM and OSL, reinforcing the preference for RW access when feasible.

Insertion trajectory also influences electrode positioning and trauma risk. Briggs et al. [132] noted more frequent perimodiolar positioning at the basal turn with RW approaches, while CS enabled greater angular insertion depth (255° vs. 240°). Zhou et al. [120] further demonstrated that CS achieved the greatest depth of insertion (487°), followed by PRW (413°) and RW (375°). Regardless of technique, the Cochlear slim straight electrode performed effectively when cochlear anatomy was favorable [120].

Non-linear insertions were consistently associated with increased trauma, particularly in cases where the EA contacted the modiolus. These observations highlight the necessity of minimizing angular deviation to preserve cochlear structures and optimize functional outcomes.

5.3.3.5. Clinical Outcomes and Hearing Preservation

Preservation rates and audiologic outcomes vary. Adunka et al. [136] and Briggs et al. [132] found no significant differences in hearing preservation between RW and CS. Havenith et al. [129] compiled data from 16 studies involving 170 patients, showing preservation rates of 0 - 40% for CS and 13–59% for RW, with threshold shifts of 10–30 dB at 125–500 Hz.

RW insertions are associated with lower stimulation thresholds due to proximity to the modiolus, but inconsistent electrode positioning can impair stimulation uniformity [132]. According to Hoskison et al. [104], RW insertion with straight electrodes reduces trauma rates.

Although RW access avoids drilling and facilitates full ST insertion, modiolus contact can impair linearity and increase trauma risk. In contrast, CS offers controlled access but poses risks to delicate structures and may be contraindicated in small cochleae with residual hearing [125].

5.3.3.6. Technical Considerations and Recommendations

When anatomical conditions are favorable, the alignment of the RW approach with the ST allows for atraumatic electrode insertion, especially in patients with small cochleae or residual hearing [125]. Nevertheless, certain anatomical constraints, such as a high-positioned crista fenestrae or a narrow vertical segment of the RW membrane (RWM), may necessitate alternative routes such as the extended RW (eRW) or CS [128].

A key challenge arises from the anatomical curvature of the OSL, which remains invisible during surgery. This unpredictability complicates intraoperative trajectory control and underscores the importance of detailed preoperative imaging. High-resolution CT and three-dimensional (3D) reconstruction of the hook region have become essential for precise surgical planning and for guiding electrode placement [122,123].

When the RW is unsuitable, anteroinferior CS positioned at the divergence point between the BM/OSL and the vertical RWM segment provides a safe and effective insertion route [122,128]. Posteroinferior enlargement is generally preferred to minimize trauma, while anterior or superior extensions should be avoided due to their association with increased injury risk [128].

Advanced imaging techniques, particularly 3D reconstructions of the cochlear hook region, enhance anatomical understanding and intraoperative orientation, allowing for individualized surgical planning [122,123,137]. However, conventional CT and MRI still do not reliably delineate the fine microanatomy of the hook region, which would require automated segmentation and robust CT/MRI co-registration, approaches that remain limited in routine clinical practice. These limitations underscore the potential value of higher-resolution intraoperative imaging modalities, such as OCT, for real-time visualization of the hook microanatomy. Ultimately, the selection of the insertion approach should be tailored to the patient's anatomy, the electrode array design, and specific hearing preservation goals.

5.3.3.7. Conclusion

The choice of surgical approach for cochlear implantation must be individualized based on cochlear anatomy, electrode design, and functional hearing goals, and the presence of cochlear pathology (e.g., otosclerosis, ossification). While both RW and CS can achieve successful outcomes, the RW route offers a favorable balance of surgical ease, safety, and hearing preservation provided anatomical constraints are respected. Extended RW and anteroinferior CS approaches serve as viable alternatives in anatomically complex cases, albeit with increased technical demands. Advanced imaging, meticulous planning, and precise execution remain essential for minimizing trauma and optimizing long-term outcomes. Despite extensive research, there remains no universal consensus on the ideal trajectory. Further randomized trials with standardized anatomical documentation are needed to refine surgical strategy selection.

Table 1. Comparative summary of the surgical approaches to the scala tympani.

Approach	Principle	Main advantages	Main risks and limitations
Round window (RW)	Direct access to the scala tympani through the round window membrane, with minimal removal of the bony overhang.	Trajectory closest to the natural entry vector of the scala tympani; no drilling; generally less traumatic; lower stimulation thresholds owing to modiolar proximity [132].	Not strictly aligned with the axis of the scala tympani because of the curvature of the hook region; modiolar contact and non-linear insertions reported, with one osseous spiral lamina fracture [120]; possibly reduced angular insertion depth; limited when the membrane is poorly visible or the anatomy is atypical [131].
Extended round window (eRW)	Anterior or anteroinferior enlargement of the round window niche.	Straighter insertion path in anatomically difficult cases; frequently required for slim perimodiolar electrodes [125].	Increased risk of injury to the spiral ligament, particularly if the array is misdirected towards the scala media or the scala vestibuli [126,128].
Cochleostomy (CS)	Drilling of a new opening into the cochlea, usually inferior or anteroinferior to the round window membrane.	Controlled and linear access; greatest angular insertion depth reported (487°, versus 413° for the posteroinferior round window and 375° for the round window) and no modiolar contact in that series [120].	High inter-individual anatomical variability, which complicates the identification of a safe site [122,125]; risk of acoustic trauma, haemorrhage, bone dust contamination and injury to the osseous spiral lamina or the basilar membrane [116,125,128]; may be inadvisable in small cochleae with residual hearing [125].

5.4. Electrode Array Design: Straight versus Perimodiolar Arrays

5.4.1. Introduction

Electrode array (EA) design in cochlear implantation is driven by three fundamental goals: atraumatic insertion, optimal placement within the ST, and alignment with the cochlear tonotopic organization. The primary categories of EAs include LW electrodes, straight and flexible, and perimodiolar (PM) or mid-scala (MH) electrodes, which are pre-curved to approximate the modiolus and stimulate the SG neurons.

5.4.2. Design Principles and Surgical Challenges

The ideal EA should ensure atraumatic insertion, be easily handled by surgeons, support re-implantation if needed, and allow complete insertion without complications. Mechanical properties such as stiffness, diameter, and curvature critically affect how an electrode interacts with cochlear structures. Stiffer or thicker electrodes can increase pressure within the cochlea, reducing blood flow and raising trauma risk, particularly in apical regions where residual hearing is often preserved. Larger-diameter electrodes may ensure better proximity of the contacts to the auditory neurons but can also raise intracochlear pressure and exacerbate trauma [90].

Variations in CDL, RW angle, cochlear curvature, and hook region morphology demand a patient-specific approach. The selection of electrode type, insertion depth, and frequency allocation must be tailored based on detailed anatomical assessment.

For example, the slim peri-modiolar electrode model (Cochlear Ltd ®) uses a flexible sheath designed to reduce modiolus trauma, though challenges remain due to its straight shape and volume [116].

Insertion depth must also be considered. Full insertion is not always possible due to anatomical variations in the RW, cochlear anomalies, or ossification.
BM rupture can occur with forces as low as 88 millinewtons- imperceptible during surgery [115]. Therefore, careful preoperative planning - including evaluation of the hook region trajectory, and the use of tools like OCT, fluoroscopy, ECochG, robotic insertion, and force-sensing systems is vital [116,117,124–126].

5.4.3. Lateral Wall (LW) Electrodes

Lateral wall (LW) electrodes, also referred to as straight electrodes, are increasingly favored for cochlear implantation due to their atraumatic properties and anatomical adaptability. Positioned along the outer curvature of the scala tympani, these electrodes follow the natural cochlear contour and stimulate the organ of Corti (OoC), which spans the full length of the cochlear duct [90]. Compared with perimodiolar arrays, this lateral positioning may reduce the risk of scalar translocation and facilitate deep apical insertion. In some electrode designs, this configuration has been associated with reduced intracochlear trauma and improved preservation of delicate intracochlear structures, thereby potentially enhancing residual hearing preservation and minimizing trauma.

One of the key advantages of LW electrodes lies in their flexibility regarding insertion depth, particularly with some MED-EL lateral wall arrays designed for extended cochlear coverage. Their lateral trajectory allows for modulation of insertion depth to avoid intracochlear trauma, yet still supports deep insertions when appropriate. This feature renders LW electrodes especially suitable for a wide range of cochlear morphologies and contributes to their ease of mapping and consistent targeting of the OoC [90].

The atraumatic profile of LW electrodes is supported by biomechanical data showing low insertion forces and improved curvature conformance [102,103]. These properties have translated into clinically significant outcomes. For instance, in a comparative study of electrode types from Advanced Bionics (Valencia, CA, USA), the SlimJ (Advanced Bionics' slim LW array) achieves higher hearing preservation than the Mid-Scala electrode (54% vs. 41%, $p = 0.04$), with an even larger difference in EAS candidates (66% vs. 42%, $p = 0.006$) [138]. SlimJ has also shown advantages in terms of post-operative anatomical positioning, including improved PTA thresholds (22.6 vs. 36.8 dB HL, $p = 0.015$) and lower scalar translocation rates (16.1% vs. 34.8%, $p = 0.019$) [139]. Because scalar translocation predicts poorer auditory performance, these findings reinforce SlimJ's atraumatic behavior. However, SlimJ presents a higher incidence of basal electrode deactivation (46% vs. 32%, $p = 0.03$) [138]. This may reflect a tendency for extracochlear placement or migration, a recognized limitation of straight arrays when post-insertion imaging is not routinely employed. Such findings emphasize the importance of intraoperative monitoring and post-operative imaging to confirm optimal electrode positioning.

Overall, slim lateral wall electrodes provide excellent cochlear coverage, are more adaptable to cochlear size variations, and are associated with reduced trauma and enhanced hearing preservation [90,102,103]. However, despite differences in electrode design between

manufacturers, large differences in functional outcomes between major cochlear implant systems (e.g., MED-EL and Cochlear) have generally not been consistently demonstrated, likely because multiple interacting factors (electrode design, number of active contacts, fitting parameters and stimulation strategie), also influence postoperative performance. Nevertheless, limitations in proximity to the spiral ganglion neurons, particularly in the basal turn, and risks of basal deactivation underscore the need for individualized electrode selection based on patient anatomy and hearing goals.

5.4.4. Perimodiolar and Mid-Scala (PM/MH) Electrodes

PM and MH electrode arrays, both pre-curved for close modiolar positioning, have been developed to optimize neural excitation by reducing stimulation thresholds and improving spatial selectivity of SG cell activation [90]. These arrays are primarily designed to cover the basal turn and typically achieve an insertion depth of approximately 380°- 420° [90,140]. However, this limited angular depth may impair proper tonotopic alignment, particularly in patients with longer cochleae [140].

Despite their electrophysiological benefits, PM and MH arrays are associated with the highest rates of scalar translocation among electrode designs [90,126]. This risk is principally attributed to the use of stiff internal stylets required to maintain the pre-curved shape during insertion. The rigidity conferred by these stylets increases the likelihood of trauma at the 180° mark of the basal turn, particularly by perforating delicate intracochlear structures such as the SL and OSL [90,115]. Skinner et al. [106] and Aschendorff et al. [105] have documented frequent intraoperative complications, including tip fold-over and cross-scalar placement, even in cases with thorough preoperative imaging. These misplacements can significantly compromise speech perception and vestibular integrity [90,141].

Fixed curvatures inherent to pre-curved electrodes often fail to match individual cochlear anatomies, particularly in tightly coiled or morphologically atypical cochleae [90]. This mismatch may result in the electrode pressing excessively against the modiolus, leading to insertion trauma, or being positioned too far from neural targets, thereby diminishing stimulation efficiency. Improper orientation after stylet withdrawal further increases the risk of BM contact, especially in MH arrays [90].

Among these, the Mid-Scala electrode has demonstrated a particularly high incidence of scalar translocation. The electrode's stiff tip, maintained by the stylet during initial advancement, frequently leads to SL penetration near the basal turn's 180° region. Even with design refinements such as slimmer profiles in models like Contour Advance and Mid-Scala, the prevalence of translocation events has not shown consistent decline [90,115]. In response, surgical strategies aimed at reducing trauma, such as controlled insertion velocities and gradual stylet withdrawal, have been proposed. However, these approaches lack universal standardization and vary considerably among surgical teams, contributing to heterogeneity in patient outcomes [90].

When translocation occurs, electrodes may deviate from the intended scala tympani into the SV, where they can cause damage to cochlear structures such as the OSL and SL. This misplacement fosters pathological changes, including fibrosis and new bone formation within the scala media and SV, phenomena that have been directly correlated with poor CNC (consonant-nucleus-consonant) word recognition scores [141]. Furthermore, such trauma may

not only reduce auditory performance but also provoke vestibular disturbances, thereby affecting the overall functional outcome of cochlear implantation [90,141].

In conclusion, although perimodiolar and mid-scala arrays offer clear electrophysiological advantages through modiolar proximity, their mechanical design and insertion techniques carry a significant risk of scalar translocation and intracochlear trauma. An individualized approach to surgical technique, alongside further refinement of electrode design, remains crucial to improving the safety and efficacy of cochlear implantation.

5.4.5. Sheath-Based Perimodiolar Electrodes

Slim perimodiolar electrode arrays (SPEs) represent a recent advancement in CI technology, offering enhanced flexibility and anatomical conformity. These electrodes are up to 60% thinner than conventional PM arrays, a design aimed at improving residual hearing and vestibular function preservation [90]. Their reduced diameter and increased pliability also enable closer proximity to the SG neurons, particularly in the basal turn of the cochlea, potentially enhancing stimulation efficiency.

However, despite these benefits, SPEs present notable surgical challenges. Their insertion is technically demanding and associated with an increased risk of complications, particularly tip fold-over and scalar translocation. Tip fold-over is a significant complication that may go unnoticed intraoperatively unless real-time imaging, such as fluoroscopy, is employed, especially when only apical electrodes are involved [90]. When identified, tip fold-over typically requires electrode repositioning or reinsertion, a maneuver that may compromise intracochlear structures and thereby jeopardize residual hearing preservation strategies. Scalar translocation, defined as the misplacement of the electrode array from the ST to the SV, has profound implications for functional outcomes.

In a clinical study involving sheath-based SPE insertions via a CS approach, Floris et al. [128] reported a tip fold-over rate of 4.3% (1 out of 23 cases) and eight instances of scalar translocation. Notably, one case involved a direct insertion into the SV, while the remaining seven exhibited translocation after the placement of two electrodes. Functional outcomes were significantly better in patients whose arrays remained entirely within the ST. These patients demonstrated a mean pure tone average (PTA) shift of +4.4 dB and a hearing preservation (HP) rate of 77.2%. Conversely, cases with scalar translocation showed a markedly higher PTA shift of +17.9 dB and poorer speech perception at the 12-month follow-up (58% vs 65%) [128].

These findings underscore the critical importance of accurate scalar positioning in optimizing post-operative auditory performance. As such, the extended round window (eRW) approach, rather than the CS approach, is increasingly favored for SPE insertion. The eRW technique, as recommended by Floris et al. [128], facilitates atraumatic placement of the array into the ST and reduces the risk of both tip fold-over and translocation.

Despite advancements in soft surgical techniques and refined electrode design, intracochlear trauma remains a persistent concern, occurring in up to 40% of cases. The adoption of minimally invasive strategies, such as the RW insertion technique combined with perimodiolar arrays, aims to mitigate this risk.

In summary, while slim perimodiolar electrodes offer anatomical and presumed functional advantages, their successful deployment hinges on meticulous surgical technique and the judicious choice of insertion approach. The extended round window technique has emerged as a preferred method to safeguard cochlear structures and optimize clinical outcomes.

5.4.6. Functional Outcomes and Programming

Electrode array (EA) design and placement accuracy are critical determinants of CI outcomes. While speech perception scores such as CNC and AzBio do not consistently differ between electrode types under standard conditions, nuanced factors such as hearing preservation, electrode positioning, and histopathological changes can significantly influence long-term auditory performance [139].

In comparative analyses, Patro et al. [139] reported no significant difference in CNC or AzBio scores between perimodiolar Mid-Scala arrays and lateral wall SlimJ arrays. However, SlimJ arrays demonstrated a substantial advantage in hearing preservation (50.0% vs. 24.4%, $p = 0.002$) and reduced translocation rates in preserved cases (16.7% vs. 37.2%, $p = 0.048$), highlighting the importance of atraumatic insertion. Furthermore, patients with better preoperative hearing achieved superior postoperative outcomes, regardless of electrode type, confirming that preoperative thresholds are a strong prognostic factor for CI success [138].

Despite these advantages, SlimJ arrays also showed higher basal deactivation and greater performance variability in noise ($p = 0.006$), potentially reflecting placement inconsistencies or anatomical mismatches [138]. Histological findings provide further insight: trauma to the BM can incite fibrous tissue and new bone formation, both detrimental to CI performance. Kamakura et al. [141] demonstrated that ossification in the scala media and scala vestibuli was directly associated with decreased CNC word scores, whereas fibrous tissue volume had no significant effect. Flexible electrodes and minimally traumatic surgical techniques have been shown to better preserve vestibular function, underscoring the need for anatomical preservation [90].

Intraoperative misalignment of electrode arrays remains a prevalent issue. Postoperative imaging by Skinner et al. [106] revealed that final EA positioning frequently deviated from preoperative planning. Intraoperative misplacements, including tip foldover, scalar translocation, and extracochlear insertions - often went undetected at the time of surgery. These discrepancies highlight the critical role of real-time imaging and precise trajectory control to ensure accurate EA placement and mitigate functional impairment.

Electrode activation data further support these findings. While average programming parameters such as threshold and comfort levels did not differ significantly across electrode types, notable variability was observed across individual channels. Deactivation rates were significantly higher with SlimJ arrays (46% vs. 32%; $p = 0.03$), particularly at basal contacts, likely due to poor auditory performance or suboptimal positioning. This may reflect a higher incidence of extracochlear or migrated electrodes associated with straight arrays, although confirmatory imaging remains limited [138].

Importantly, despite consistent average programming profiles, the assumption that perimodiolar proximity uniformly reduces current demands is challenged by the variability observed across electrode contacts [138]. Meanwhile, PM (perimodiolar) designs have been associated with superior long-term CNC scores, independent of confounding factors such as

age, gender, or baseline PTA, suggesting a potential benefit in speech encoding efficiency over time [140].

5.4.7. Comparative Outcomes Across Studies

The design and positioning of CI electrode arrays are critical factors influencing postoperative auditory outcomes. Several studies have sought to compare the performance of different electrode models from Advanced Bionics™, notably the precurved Mid-Scala (MS) and the straight SlimJ (SJ) arrays, in both adult and pediatric populations.

A large multicenter retrospective study evaluated 320 CI recipients (205 adults, 115 children) implanted with either the MS or SJ arrays. The primary endpoints included HP, speech perception as measured by Bamford-Kowal-Bench (BKB) scores, and key stimulation parameters such as threshold and comfort levels, and the number of deactivated electrodes [138]. Results demonstrated statistically equivalent speech perception scores across all listening conditions between the two arrays (e.g., male speaker in quiet: 78% for SJ vs. 73% for MS; $p = 0.26$), with no significant interaction between array type and preoperative hearing levels. However, the SJ array exhibited greater variability under more challenging acoustic conditions, particularly in the presence of background noise (male speaker in noise; $p = 0.006$), which may reflect differences in anatomical placement or programming requirements. Importantly, preoperative auditory thresholds were independently associated with postoperative performance, regardless of electrode type, underscoring the predictive value of residual hearing [138].

Further supporting these findings, a separate retrospective analysis involving 237 adult recipients (136 ears with MS, 101 with SJ) compared speech recognition outcomes using CNC words and AzBio scores in quiet and noise at 6 and 12 months post-implantation [139]. No statistically significant differences were observed between the two electrode types. At 12 months, mean CNC scores were 51.9% (MS) versus 48.8% (SJ; $p = 0.363$), while AzBio in quiet yielded 60.6% and 62.3% respectively ($p = 0.684$). AzBio in noise also showed no significant divergence (27.4% vs. 28.3%; $p = 0.843$). Multivariate analysis revealed that younger age at implantation, higher daily CI usage, and superior preoperative PTA were significantly associated with improved speech perception outcomes, whereas electrode type itself did not emerge as a significant predictor [139].

In contrast, Pennington-FitzGerald et al. focused on the influence of electrode design and length on long-term speech outcomes in adult CI recipients using electrode arrays from three different manufacturers (Cochlear Americas, MED-EL, and Advanced Bionics), which were subsequently grouped according to their intracochlear design rather than by brand [140] .Their study demonstrated that PM arrays, which are designed to lie closer to the modiolus, were associated with significantly better CNC word recognition scores at both 6 and 24 months post-implantation ($P = 0.023$), and outperformed MS electrodes specifically at 12 months ($P = 0.036$) [112]. Notably, a shorter electrode length was inversely correlated with improved CNC scores at 6, 12, and 24 months. Crucially, multivariate analysis confirmed that PM design was an independent predictor of better auditory outcomes, even after controlling for patient demographics and baseline audiologic metrics [140].

Together, these findings suggest that while electrode type may not universally dictate speech perception outcomes, specific designs such as PM arrays can confer significant advantages under certain conditions. Moreover, variables such as preoperative hearing, age at implantation,

and CI usage remain robust independent predictors of success, highlighting the need for individualized electrode selection strategies based on anatomical and audiological profiles.

5.4.8. Toward Precision Surgery

No single EA design can accommodate the broad anatomical variability observed in CI candidates. Differences in cochlear duct length (CDL), RW angle, cochlear curvature, and hook region geometry necessitate an individualized surgical strategy. High-resolution imaging modalities, including CT and OCT, combined with intraoperative monitoring and advanced insertion systems, robotic or guided, facilitate more precise electrode placement [116,117,124,125].

From a surgical and clinical standpoint, array selection (PM (perimodiolar), LW (lateral wall)) must balance anatomical compatibility, residual hearing preservation, functional outcomes, and surgical insertion technique, which critically influences intracochlear trajectory and trauma risk. Cochlear size, as assessed preoperatively, critically influences array choice. However, multivariate analyses indicate that electrode length is strongly correlated with electrode design, making it challenging to disentangle the respective contributions of intracochlear position and array length to postoperative functional outcomes. Moreover, several additional factors must be considered. Ideally, the electrode array should conform to the cochlea's natural place–frequency map. Consequently, patients with longer cochlear duct lengths may derive greater benefit from longer electrode arrays. Electrode array selection should therefore always be guided by a nuanced, individualized clinical approach [140].

Preservation of residual low-frequency hearing is another decisive factor. Slim, flexible LW electrodes - such as Flex24 or Flex28 - offer less traumatic insertion paths, making them ideal for EAS in patients with preserved hearing. Clinical data underscore the superiority of the SlimJ array in this context, demonstrating improved hearing preservation and better AzBio in noise scores (38.7% vs. 25.1%, $p = 0.042$), which highlights its relevance in real-world acoustic environments [139]. In contrast, Mid-Scala electrodes, which incorporate a stylette, have been associated with increased trauma risk and scalar translocation, despite intentions for atraumatic insertion [139].

PM arrays, typically shorter and positioned closer to the modiolus, offer more focused stimulation of spiral ganglion cells and reduce current spread. This makes them particularly advantageous in cases requiring robust neural recruitment, such as profound deafness or diffuse neural degeneration from autoimmune or ototoxic causes [140]. However, the higher risk of insertion trauma and scalar translocation, especially in anatomically tight cochleae, must be considered. Surgical planning must thus navigate the trade-offs between insertion depth, scalar location, and expected performance outcomes [140].

Etiology of hearing loss further refines electrode selection criteria. Patients with autoimmune, infectious, or ototoxic etiologies may present with more widespread neural degeneration, potentially favoring PM arrays due to their closer proximity to neural targets. Conversely, patients with idiopathic or genetic etiologies may tolerate longer LW arrays with reduced risk [140]. However, it should be acknowledged that the primary targets of cochlear implant stimulation, neuronal cell bodies versus more distal auditory nerve fibers near the organ of Corti, remain a subject of debate in the literature.

In cases prioritizing full insertion and complete neural engagement, PM arrays may be preferred despite their increased risk of trauma. Yet when residual hearing is to be preserved, especially in low frequencies, LW designs offer safer profiles [140]. The apparent superiority of one design over another depends heavily on patient-specific factors, highlighting the necessity of a precision medicine approach.

This nuanced, individualized strategy - anchored in anatomical imaging, functional goals, and risk-benefit analysis, reflects a paradigm shift in cochlear implantation. It emphasizes the integration of audiologic profiling with imaging data to inform array selection and insertion strategy. The heterogeneity of postoperative outcomes across array types and cochlear anatomies, as evidenced in recent studies, further reinforces the need for detailed preoperative planning and tailored surgical interventions [140].

5.4.9. Conclusion

In conclusion, cochlear implantation has moved beyond a one-size-fits-all model. Precision surgery and customized fitting strategies, anchored in detailed anatomical and functional mapping, are essential to maximize the auditory potential of each patient. Electrode positioning, insertion trajectory, and frequency-place alignment are interdependent variables that must be individually optimized to ensure long-term success. Despite technological advances, insertion trauma and suboptimal placement remain challenges. Future success in cochlear implantation hinges on precision surgery guided by high-resolution imaging, intraoperative tools, and detailed patient-specific planning.

5.5. Rationale and Future Directions

As CI technology advances, the field is steadily transitioning from a standardized surgical model toward a precision-based, anatomically guided, patient-specific surgical planning. This evolution is driven by the recognition that interindividual anatomical variability, particularly within the cochlear hook region and the ST, can significantly impact insertion trajectory, scalar location, trauma risk, and ultimately, auditory outcomes.

5.5.1. The Role of Detailed Cochlear Anatomy

Achieving atraumatic and functionally effective implantation requires accurate three-dimensional mapping of the cochlear base, including the ST and its adjacent microstructures. Variations in the RW orientation, basal turn curvature, and spiral ligament morphology necessitate individualized surgical planning. Anatomical studies have underscored that even minor deviations in insertion angle or electrode trajectory may result in translocation, basilar membrane rupture, or damage to the osseous spiral lamina - compromising residual hearing and long-term outcomes.

To address these challenges, advanced imaging modalities are essential. High-resolution techniques, such as CECT, micro-CT, and synchrotron radiation phase-contrast imaging (SR-PCI), have emerged as powerful tools for evaluating cochlear microanatomy. These modalities enable precise measurements of CDL, hook region topography, and scala tympani dimensions, thereby enhancing surgical accuracy and postoperative assessment [112].

SR-PCI, in particular, offers unprecedented visualization of intracochlear structures without the artifacts introduced by staining or histological sectioning. Parameters derived from SR-PCI,

such as θST (insertion angle relative to the scala tympani) and WST (width of the scala tympani), are being explored as novel metrics to guide atraumatic electrode insertion. As shown by Micuda et al. [142], these individualized measurements can directly inform surgical decision-making and electrode design, ultimately reducing the risk of frequency-to-place mismatch and promoting hearing preservation.

Finally, the findings of Canfarotta et al. underscore the importance of inner ear morphology, particularly ST volume, as a determinant of low-frequency hearing preservation in the early postoperative phase [143].

5.5.2. Intraoperative Monitoring and Robotic Assistance

In parallel, real-time intraoperative technologies are gaining prominence. Electrocochleography (ECochG) provides electrophysiological feedback during insertion, allowing the detection of changes in cochlear electrophysiological responses that may indicate intracochlear trauma, such as sudden decreases in cochlear microphonic amplitude, or loss of ongoing responses, potentially associated with basilar membrane contact, rupture, or scalar translocation. Similarly, OCT offers high-resolution imaging of cochlear microstructures in situ, facilitating trajectory verification and damage prevention in real time.

The integration of these feedback mechanisms with robotic-assisted electrode insertion holds immense promise. Robotic platforms provide precise control of insertion speed, angle, and force, reducing variability between surgeons and enhancing reproducibility across cases. Combined with intraoperative monitoring and imaging, robotic surgery is poised to become a cornerstone of minimally traumatic, customized cochlear implantation.

5.5.3. Towards Personalized CI Surgery and Programming

The next frontier in cochlear implantation lies in the convergence of anatomy-driven surgical planning, patient-specific electrode design, and individualized programming strategies. Rather than applying uniform stimulation maps, future CIs will rely on neuro-tonotopic alignment, adjusting stimulation sites and rates based on imaging-derived models of SG cell distribution and cochlear morphology.

Processor advancements and hybrid EAS technologies will also play a pivotal role. Personalized signal-coding strategies, including place-based frequency allocation and dynamically adjusted stimulation rates, can optimize pitch perception and reduce spectral distortion. Beyond improving speech recognition, music appreciation, spatial localization, and overall listening comfort, these individualized approaches may also facilitate postoperative rehabilitation. By reducing the extent of neural plasticity required for adaptation, patient acclimatization becomes more straightforward. Likewise, clinical management is simplified, enabling more efficient follow-up and potentially improving the feasibility of remote fitting and tele-audiology workflows.

5.5.4. Conclusion

Cochlear implantation is evolving into a discipline of individualized precision medicine progressing from millimetric toward micrometric surgical accuracy. Success increasingly depends on a synergistic understanding of cochlear anatomy, electrode mechanics, and neural

excitation profiles. Emerging technologies, such as ECochG, OCT, and robotic insertion, are transforming both preoperative planning and intraoperative execution.

To fully realize the potential of these advances, future CI systems must integrate customizable electrode arrays, imaging-based navigation tools, and neural interface modeling. Programming protocols should abandon rigid defaults in favor of data-driven, anatomy-informed algorithms tailored to each patient's unique inner ear architecture.

Ultimately, this approach will redefine cochlear implantation not merely as a surgical procedure, but as a dynamic, patient-centered therapeutic strategy, designed to maximize hearing outcomes through science-guided precision.

II. Objectives of the Work: Rationale of our Approach to Rehabilitate Hearing Loss with CI

Hearing loss constitutes a major global public health issue. In 2016, it ranked among the four most prevalent conditions and represented the third leading cause of Years Lived with Disability according to the Global Burden of Disease study [144]. By 2017, disabling hearing loss affected 6.1% of the global population, significantly impairing not only communication but also cognitive health, occupational integration, and overall quality of life [145]. CI has emerged as an effective and cost-efficient means of restoring hearing; however, fewer than 10% of eligible individuals currently benefit from this intervention [146,147]. One of the main barriers to its broader adoption remains the risk of residual hearing loss, often attributable to intra-cochlear trauma incurred during surgery.

CI surgery is progressively shifting toward a more conservative paradigm, with a focus on preserving the delicate intracochlear microstructures. This evolution is driven by the development of hybrid strategies such as electro-acoustic stimulation (EAS), which combines acoustic amplification for low frequencies with electrical stimulation for high frequencies. Despite technical advancements, including flexible electrodes and "soft surgery" techniques, more than 30% of patients still experience insertion-related trauma and loss of residual hearing, thus limiting access to combined stimulation strategies [104]. The anatomical complexity and interindividual variability of the hook region surrounding the round window contribute to this vulnerability. In response, a paradigm of personalized cochlear implantation is emerging, relying on refined anatomical knowledge and real-time intraoperative guidance.

Our research project proposes a multimodal and integrated approach that includes: optical coherence tomography (OCT) to visualize cochlear microanatomy in real time and guide surgical decision-making; robotic-assisted cochlear implant surgery (RACIS), performed with the RobOtol® system, for slow and reproducible insertions compatible with advanced measurements; 3D planning and surgical navigation for automated and patient-specific insertion trajectories; and postoperative frequency allocation to optimize auditory stimulation maps.

OCT overcomes the resolution limits of conventional CT scan imaging by providing direct visualization of the proximal scala tympani region. It can guide the choice of surgical approach (round window versus cochleostomy), optimize the insertion axis and depth, and reduce the risk of misdirection toward the modiolus or basilar membrane, which is particularly critical when using rigid or precurved electrode arrays with limited conformability. The RobOtol® robotic system is employed for automated electrode insertion with extremely high precision control compared to surgeon's hands for speed, depth, and angle. Together, these tools support a personalized implantation approach. Our objective is to map optimal electrode locations, develop semi-automated surgical planning, and implement it through real-time navigation and imaging.

A final and central component of this individualized strategy lies in postoperative frequency reallocation. The spatial alignment between electrode position and the patient's perceived frequencies is often suboptimal, particularly when individual anatomy or actual insertion deviates from theoretical tonotopy. Such mismatch may delay auditory rehabilitation and hinder speech understanding, especially in complex acoustic environments. The integration of patient-specific tonotopic maps based on imaging data allows realignment of stimulation channels with

natural frequency regions. This strategy aims to accelerate the post-activation learning curve, improve auditory clarity in the early weeks, and enhance long-term functional outcomes.

III. Atraumatic Surgery: Strategies to Improve Cochlear Health Preservation

This chapter is based on three original studies, all of which are now published and of which the candidate is the first author. Section 3.1 corresponds to Article 1 (Gersdorff G, Ramos P, Wijewickrema S, O'Leary S, Lefèbvre PP, Gerard JM. High-resolution intraoperative guide for cochlear implant surgery using optical coherence tomography. Audiol Neurotol; doi:10.1159/000552581; received 6 October 2025, accepted 13 February 2026, published online 6 August 2026). Section 3.2 corresponds to Article 2 (Gersdorff G, Peigneux N, Duran U, Camby S, Lefebvre PP. Impedance and Functional Outcomes in Robotic-Assisted or Manual Cochlear Implantation: A Comparative Study. Audiol Neurotol. 2025;30:80–88; doi:10.1159/000540577) and to Article 3 (Gersdorff G, Nopp P, Camby S, Lefebvre P. Impact of Robotic-Assisted Electrode Array Insertion on Neural Health and Hearing Outcomes in Cochlear Implant Recipients. Audiol Neurotol; doi:10.1159/000552800; received 3 December 2025, accepted 21 May 2026, published online 24 August 2026).

The candidate is the first author of the three studies presented in this chapter. He conceptualized the optical coherence tomography study, collected the data and drafted the manuscript (Article 1), and reviewed the clinical records, contributed to the clinical evaluation and drafted the manuscripts of Articles 2 and 3. The detailed contribution of each co-author is given in the Author Contributions section of the corresponding publication.

3.1 Before insertion Phase: Optical Coherence Tomography (OCT)

3.1.1 State of the Art

3.1.1.1. Cochlear Anatomy and Microanatomy

3.1.1.1.1. Cochlear Anatomy

As previously described in the general anatomical sections, the cochlea is a highly complex sensory organ embedded within the petrous temporal bone. In the present section, the focus is specifically placed on anatomical features that are critical for surgical planning and electrode insertion during cochlear implantation.

The human cochlea is a very small (4 mm × 7 mm × 10 mm) and complex organ, deeply embedded inside the human skull bone, prohibiting direct visualization of its internal structure [107]. It is embedded within the densest part of the petrous temporal bone, making both imaging and surgical access extremely challenging [107].

Intracochlear dimensions may vary not only between people but also within individuals (e.g., cochlear duct length: varies between 25–35 mm) [107,148]. The organ of Corti (OoC), the Rosenthal's canal (RC), and cochlear volume all exhibit variability in shape, size, and proportion across individuals [107]. Certain dimensions such as the length of the OoC and RC can affect the ideal insertion depth of the electrode array during cochlear implantation [107,148].

There is a wide range of anatomical variations, including differences in length, coiling pattern, overall size, and shape of the cochlea [107,148]. In some individuals, the cochlea may exhibit incomplete coiling or a broader base, impacting the angle and depth of insertion. Consequently, the electrode insertion angle may not always align optimally with individual anatomical variations [149].

The height of the basal turn ranges from 1.6 mm to 2.6 mm (mean: 2.1 mm; SD: 0.2 mm) [107]. This dimension, along with the cochlear duct diameter and turn count, plays a role in planning electrode trajectories.

Taken together, these anatomical variations highlight the necessity of individualized surgical strategies, in which electrode selection, insertion depth, and trajectory must be adapted to each patient's specific cochlear morphology.

3.1.1.1.2. Modiolus and Spiral Ganglion

The modiolus is a central pillar of the cochlea containing Rosenthal's canal, which houses the cell bodies of spiral ganglion (SG) neurons. Its trunk diameter in the second turn is less than 1 mm, making it particularly vulnerable to trauma during deep electrode insertions, especially when using pre-curved arrays [150,151]. The modiolus is covered superficially by fragile blood vessels and canaliculi, essential for perilymph homeostasis. Even minimal mechanical forces can potentially damage this delicate structure [107,150].

Anatomically, the RC and SG form a two-turn helico-spiral. There is no clear correlation between the angular rotation of the basilar membrane (BM) and the length of the RC, the latter largely reflects interindividual cochlear size differences. Notably, the BM does not extend beyond the basal end of the SG, and within the basal turn, SG neurons are clustered in groups without filling the entire RC lumen. At the round window (RW), the RC is thinner and terminates at its proximal rim, while apically, the RC and SG end in a bulbous structure located adjacent to the scala tympani of the third cochlear turn [150–152] (Fig.18).

Synchrotron radiation phase-contrast imaging (SR-PCI) has been selected here because it provides high-resolution three-dimensional visualisation of the intracochlear microanatomy. The colour-segmented reconstructions make the spatial relationships between several delicate structures easier to grasp, including the basilar membrane, the spiral ganglion, the peripheral dendrites, Rosenthal's canal, the spiral ligament, the osseous spiral lamina, the cochlear aqueduct and the round window membrane. They also allow these structures to be viewed from different three-dimensional perspectives, which is particularly valuable given the substantial inter-individual anatomical variability of the inner ear.

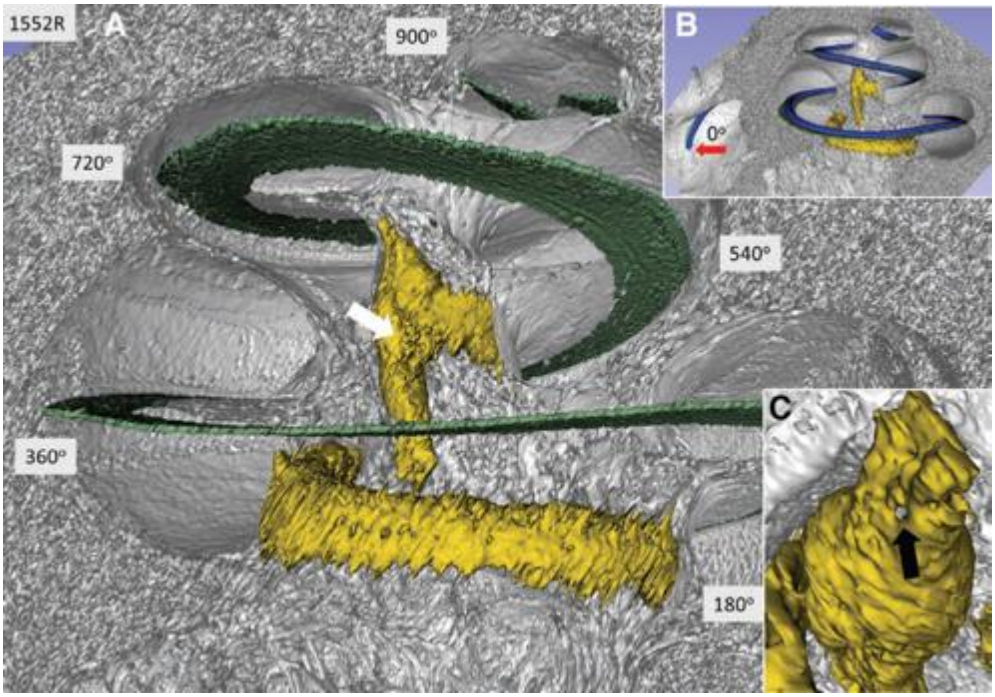

Figure 18.
A. Using synchrotron radiation phase-contrast imaging (SR-PCI) combined with 3D reconstruction, the basilar membrane (green), peripheral dendrites (yellow), and spiral ganglion (yellow) are visualized after color segmentation and cropping from a medial perspective. The image illustrates the tight anatomical relationship between the spiral ganglion and the medial wall of the scala tympani. Additionally, a group of unidentified ganglion cells is seen projecting toward the basal modiolus (indicated by the white arrow).
B. The length of the basilar membrane was assessed from its basal origin at the scala vestibuli opening (highlighted by the red arrow), which corresponds to the proximal edge of the round window membrane, extending to the helicotrema. Reproduced from Li et al. (2020) [150].
C. At the apex, the spiral ganglion terminates in an expanded structure or "bulb" containing a central cavity (black arrow)[150].

In the basal turn, SG cell bodies cluster in groups and do not fill the entire RC volume, making individual neurons hard to delineate. The RC thins near the RW and terminates there at its proximal rim. More apically, it becomes densely populated with SG neurons [150].

SR-PCI studies have revealed that the RC and SG terminate in a bulbous thickening shaped like a mini-helix with a distinct rotational profile [150]. This apical SG bulb was found to be twisted, indicating that the number of SG turns corresponds to that of the BM. In the apical region, the spiral ganglion is characterized by a marked spatial compression relative to the organ of Corti, with a large population of neurons located above one cochlear turn. These neurons correspond to approximately 40% of the organ of Corti (OC) length but only 20% of the SG, concentrated within a short segment of about 2.5 mm [150,153]. The apical SG tip could sometimes exhibit a hollow center, extend up to 720°, and include neurons projecting into the third cochlear turn [150].

The average length of the RC/SG is approximately 13.69 mm, with a rotational span of 630° to 720°, extending well beyond the second turn [151]. This finding is consistent with SR-PCI reconstructions reported by Li et al., who measured a mean SG length of 14.01 mm (SD: 0.8 mm) in eight specimens [150]. SG cells reach 720° and innervate the apical regions of the cochlea, projecting fibers into the third turn [152]. Before the advent of synchrotron imaging,

it was established that the OoC spans the full length of the cochlea, while the SG extends only up to 1.75 to 1.85 turns, corresponding to approximately 660° of rotation. Histological images of the human mid-modiolar section confirm that SG cells can extend into the end of the middle turn [150,154,155] (Fig.19).

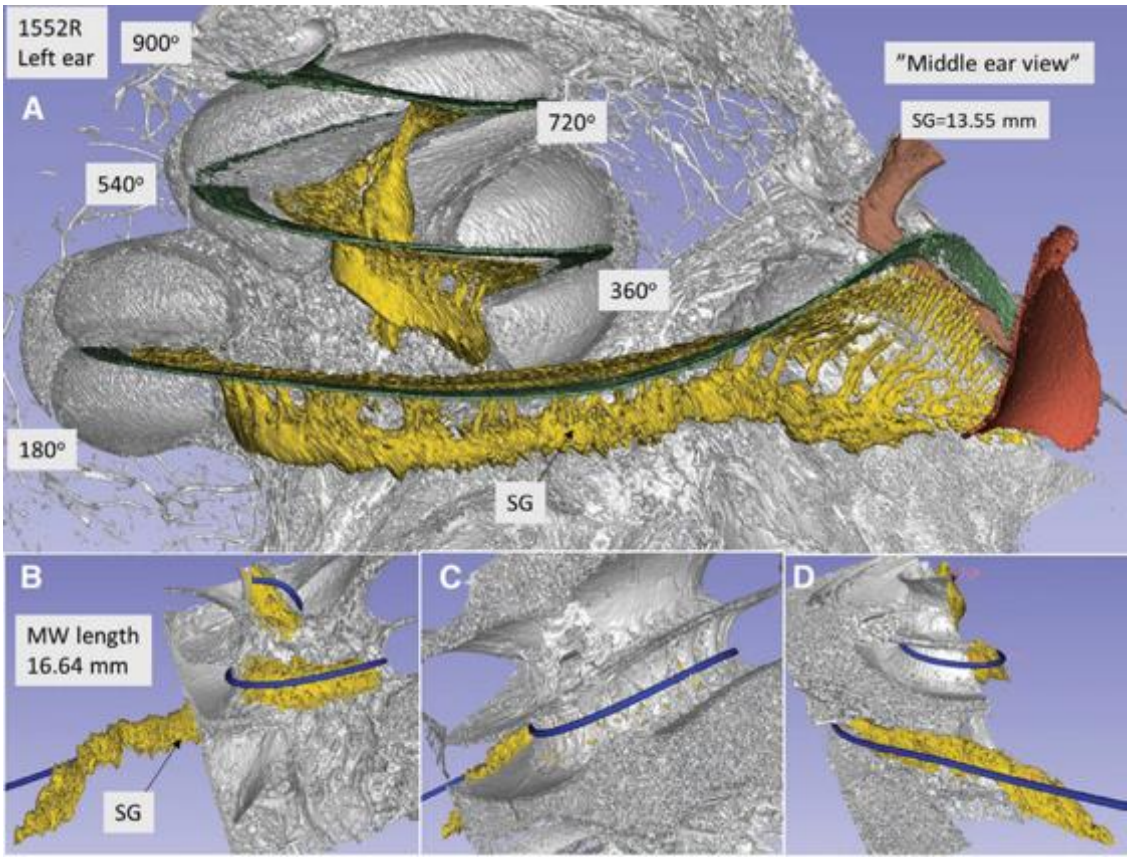

Figure 19.
A. As in the previous depiction, SR-PCI and 3D reconstruction provide a detailed visualization of the cochlea from a middle ear perspective. After segmentation and cropping, the basilar membrane (green), peripheral dendrites (yellow), and spiral ganglion (yellow) are displayed. The basal portions of both the basilar membrane and the spiral ganglion extend to the round window membrane (RWM). Reproduced from Li et al. (2020) [150].
B–D. The contour of the medial wall (MW) of the modiolus, which faces Rosenthal's canal, was delineated and its dimensions measured (illustrated by the blue line).
Abbreviations: MW, medial wall; RC, Rosenthal's canal; RWM, round window membrane; SR-PCI, synchrotron radiation phase-contrast imaging [150].

Morphometrically, the BM extends from the proximal rim of the RWM to the cochlear apex, with an average angular rotation of 904° and a mean length of 33.4 mm (SD: 1.5 mm) [107,150,152]. Its width increases approximately threefold from base to apex.

In the hook region, the BM adopts a serpentine course, and the distance to the SG is minimal at the base and progressively increases along the first cochlear turn (~360°) [150]. Both the basal ends of the BM and SG reach the RW membrane [107]. Around the completion of the first cochlear turn (~360°), SG dendrites transition from a predominantly radial orientation in the basal turn to a helical-spiral trajectory in more apical turns, which may contribute to discrepancies between excitation location and frequency perception. Electrodes placed near the BM exhibit minimal mismatch between frequency-pitch and insertion angle or depth, compared to those placed along the modiolus [152,156].

3.1.1.1.3. Rosenthal's Canal

The Rosenthal's canal does not consistently begin at the level of the RWM, which has implications for electrode trajectory during cochlear implantation [150,151]. Misalignment of the electrode relative to the cochlear structures can increase the likelihood of trauma to adjacent bony elements such as the osseous spiral lamina (OSL) and secondary spiral lamina (SSL), rather than directly affecting the RC itself [127,151]. This suggests that precise electrode positioning is critical to avoid unnecessary damage, particularly to the OSL and SSL, which are more susceptible during initial insertion when the RC is not immediately encountered at the RWM level [127] (Fig.20).

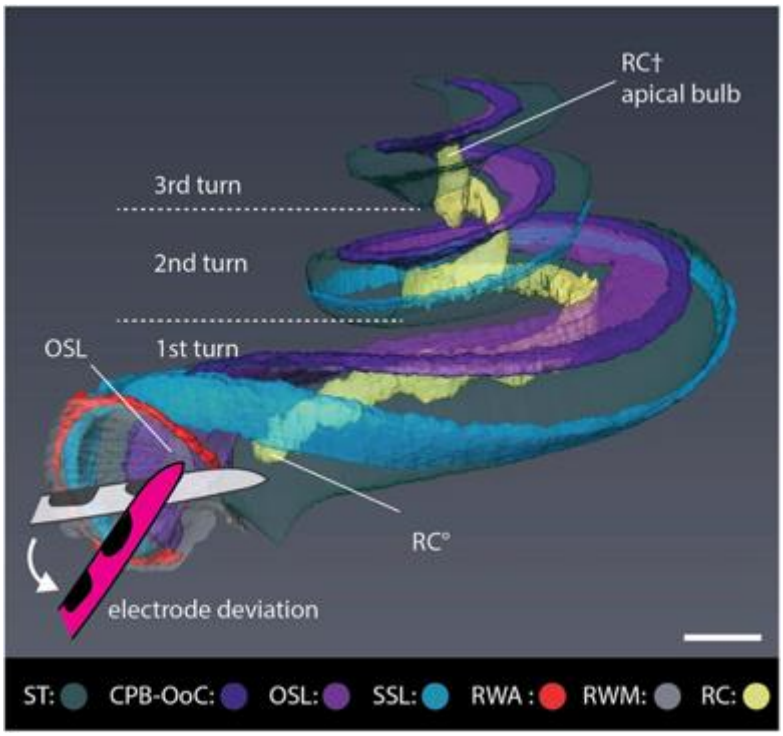

Figure 20.
Three-dimensional anatomical representation of the deviation of the proximal electrode relative to the osseous spiral lamina (OSL) and Rosenthal's canal. A schematic illustration of the electrode's proximal deflection is overlaid on a CECT-derived 3D, showing that the OSL is more susceptible to impact or damage than the proximal segment of RC (denoted RC). Additionally, the distal extremity of RC (RC†), also referred to as the apical bulb, is situated adjacent to the scala tympani (ST) of the cochlea's third turn.
Abbreviations: CPB-OoC, cochlear partition bridge–organ of Corti complex; OSL, osseous spiral lamina; RC, Rosenthal's canal; RWA, round window arch; RWM, round window membrane; SSL, secondary spiral lamina; ST, scala tympani. Scale bar: 1 mm. Reproduced from Starovoyt et al. (2023) [107].

Previous studies have raised concerns that the proximal region of Rosenthal's canal may be vulnerable to trauma during CI electrode insertion [150]. Traditionally, the maximal insertion depth of the electrode array has been limited to the second cochlear turn, based on findings suggesting that the apical end of the RC does not extend into the third turn [150].

However, more recent imaging has shown that the RC may in fact reach beyond the second turn, with the "apical bulb" consistently located adjacent to the ST in the third cochlear turn [150]. This implies that deeper insertions, up to the third turn, could be beneficial for stimulating low-frequency regions, potentially improving auditory outcomes in CI patients [150].

Emerging evidence suggests that trauma during CI electrode insertion is more likely to affect the OSL than the proximal portion of Rosenthal's canal [150]. This is particularly relevant since the RC does not always originate immediately at the level of the RWM, potentially reducing its exposure to direct mechanical damage during early stages of insertion [150].

Thus, while prior surgical guidelines limited insertion depth based on the assumption that Rosenthal's canal and its associated neural structures were vulnerable to trauma and did not extend far toward the apex, thereby emphasizing the risk of injury in the basal turn, newer imaging data suggest that the OSL may actually present a higher risk site for trauma in the proximal cochlear segment [150].

Spiral ganglion (SG) neurons are housed within Rosenthal's canal, which extends through approximately 1.75 turns of the cochlea [90]. This anatomical distribution is critical for CI design and strategy, as electrode arrays must be aligned with the tonotopic organization of the auditory neural pathway rather than strictly limited to the spatial extent of SG cell bodies to achieve effective stimulation. The understanding of SG cell location within the RC helps inform not only electrode length and insertion angle, but also the potential for trauma, especially in deeper cochlear regions while recognizing that apical stimulation may rely on excitation of peripheral neural projections extending beyond the RC [90].

3.1.1.1.4. Round Window Membrane

The RWM, approximately 70 μm thick, plays multiple physiological roles in the inner ear [157]. It contributes to immune defense, facilitates molecular exchange between the middle and inner ear, and dissipates acoustic energy from the ossicular chain [157]. Studies show that substances like antibiotics, local anesthetics, corticoids and cationic ferritin can traverse the RWM depending on the properties of its outer epithelium [158].

Histological findings have identified gland-like structures within the RWM's rim that secrete glycoprotein material containing scavenger cells, highlighting its role in waste clearance. Capillaries, lymphatic channels, and venous structures containing leukocytes are also present within this area [157,159].

Anatomical measurements indicate high variability in RWM diameter, ranging from 0.48 mm to 2.7 mm, which can influence electrode array (EA) selection during cochlear implantation [157]. Individual variability in the length of the vertical and horizontal portions of the RW contributes significantly to the anatomical diversity observed in RW shapes [160]. According to Singla et al., the mean height and width of the RW are approximately 1.62 ± 0.77 mm and 1.15 ± 0.39 mm, respectively [161]. Atturo et al. reported that the surface area of the human RW can vary between 0.99 mm^2 and 3.20 mm^2, emphasizing the need for customized surgical approaches [123].

The inferior margin of the RW is defined by the crista fenestrae (CF), a bony ridge attached to the lower edge of the RWM [160]. The variable height and configuration of the CF may render direct RW insertion technically difficult or even impossible [123,160].

The RWM is frequently obscured by a bony overhang, which often complicates surgical visibility. Structurally, the RWM is not perfectly round but rather an ovoid, curved membrane [160]. There are significant anatomical variations in the RW niche, including differences in the

configuration of the tegmen and the anterior and posterior posts [161]. The RWM may be partially concealed by an obliquely oriented ridge of bone projecting from the promontory, which commonly impairs visualization during surgery [160,161]. This overhanging edge is narrowest at its free margin and broadens medially, with an average width of 2.1 mm (range: 1.9–2.4 mm) [161]. Due to uneven growth of the walls forming the RW niche, the size and orientation of the entrance vary considerably, leading to highly variable exposure of the true membrane depending on the surgical approach [123]. In order to fully visualize the RWM, the removal of the bony overhang is often necessary. When this is done, the membrane can be exposed in up to 93% of cases, thus allowing either a standard RW or an extended RW approach [123]. Additionally, the RWM may be located very superiorly relative to the edge of the overhanging bone, further complicating the approach and necessitating precise anatomical knowledge to optimize access [131] (Fig.21).

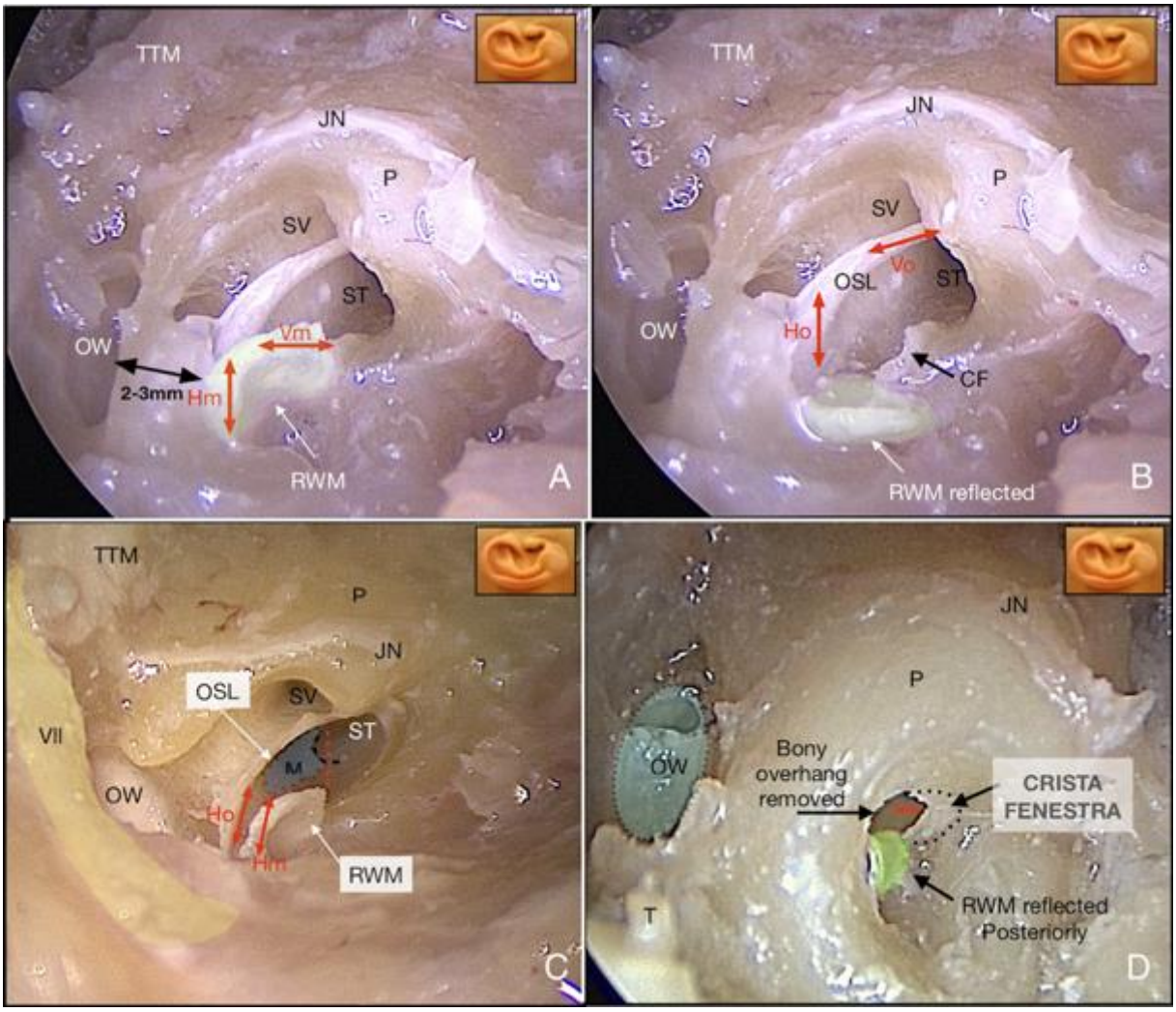

Figure 21.
Surgical exposure of a right ear illustrating dissection of the RW region and promontory (P).
(A) The round window niche (RWN) and the bony promontory have been excised to reveal the RWM, shown in light green, along with the proximal portion of the cochlea's basal turn. The separation between the oval window (OW) and the RWM measures approximately 2 to 3 mm.
(B) The RWM (light green) is retracted posteriorly, following removal of the bony promontory to further expose the initial segment of the basal turn.
(C) With the promontory removed, both the RWM and the adjacent scalae of the basal turn are visible. The horizontal portions of the RWM (Hm) and the osseous spiral lamina (Ho) are in very close proximity (highlighted by red arrows). The ST extends inferiorly past the lower margin of the RWM (indicated by a red dashed line)

before arching upward. The modiolus (M), marked in grey, defines the anteromedial boundary of the ST, with its contour indicated by a black dashed line. Reproduced from Pringle and Konieczny (2021) [131].
(D) The overhanging bone of the RWN has been removed. The RWM, now colored dark green, is again reflected posteriorly. The high CF is evident, resulting in a reduced vertical segment of the RWM.
Abbreviations: Hm, horizontal portion of the RWM; Ho, horizontal portion of the OSL; JN, Jacobson's nerve; OSL, osseous spiral lamina; SV, scala vestibuli; T, stapedial tendon; TTM, tensor tympani muscle; VII, facial nerve; Vm, vertical portion of the RWM; Vo, vertical portion of the OSL [131].

The RWM typically emerges from the free edge of the CF. When the CF is prominent, it reduces the effective size of the RW, complicating surgical access and increasing the difficulty of electrode insertion [107]. In such cases, deflection of the electrode toward the basilar membrane or the modiolus is more likely [162].

Recent studies have provided quantitative data on RW dimensions. Jain et al. reported an average RW height of 0.69 ± 0.25 mm, while Singla et al. reported 1.62 ± 0.77 mm, and Angeli et al. described a range from 0.60 to 1.04 mm (mean: 0.77 mm) [135]. In the present study, RW height varied from 0.707 to 2.155 mm, with a mean of 1.500 ± 0.432 mm. While absolute RW height is not always the most critical factor, the proportion of the CF relative to RW height has greater surgical implications. A tall CF can obstruct direct access and require modification of the insertion path. These anatomical differences must be carefully evaluated preoperatively to minimize trauma and ensure successful CI outcomes [116,162].

3.1.1.1.5. Hook Region

General Description and Clinical Significance

The hook region represents the most basal portion of the cochlear duct, forming a distinctive fish hook–like curvature in three dimensions [122,125]. This curvature reflects both axial and tangential bends, giving the region a complex 3D orientation that changes significantly over short distances [122]. It constitutes a critical anatomical zone at the entry of the cochlea and is prominent on the medial wall of the middle ear. This region is complex and highly variable across individuals, particularly in terms of spatial relationships and morphology, which holds significant implications for surgical access and residual hearing preservation [125] (Fig.22).

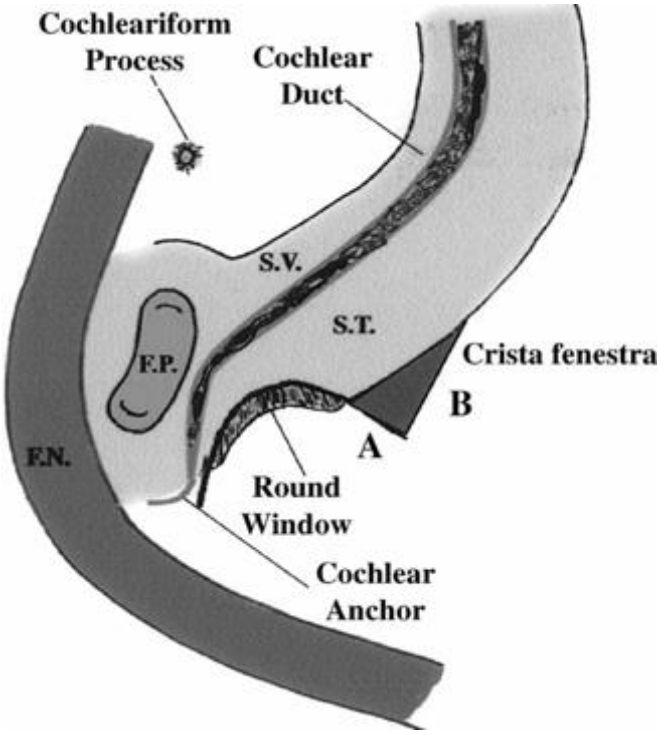

Figure 22.
An axial schematic representation illustrating the vestibule, the basal turn of the cochlea, and the facial nerve. The diagram also highlights two key dimensions of the crista fenestra: its thickness (labelled as measurement A) and its longitudinal span (measurement B). The values indicated correspond to the average anatomical measurements of the crista fenestra.
Abbreviations: S.T., scala tympani; S.V., scala vestibuli; F.N., facial nerve; F.P., stapes footplate. Reproduced from Briggs et al. (2005) [126].

The hook region marks the convergence of several key anatomical structures: the OSL, spiral ligament (SL), and BM. It contains the cul-de-sac of the endolymphatic space, produces a medial prominence in the middle ear, and serves as the typical entry site during cochlear implantation [125]. The ST maintains a relatively straight trajectory up to the first cochlear turn but becomes more curved deeper within the cochlea [125].

Variations include differences in the degree of curvature, relative spacing of the oval and round windows, and hook width and depth. The distance between the OW and RW can differ by more than 1 mm, and the area between them may vary by over 100% in size [125] (Fig.23).

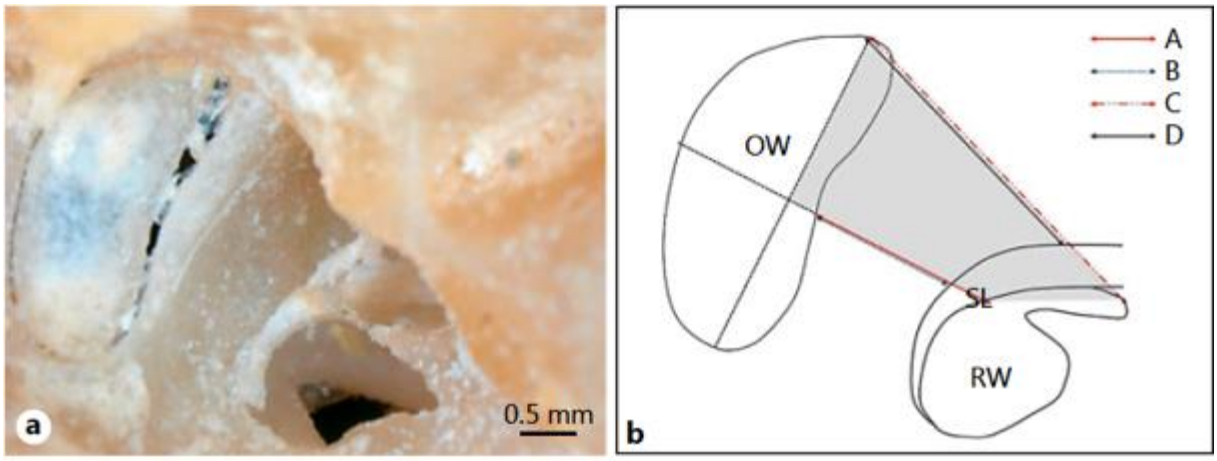

Figure 23.
a. Medial view of a left human temporal bone following microdissection. The image reveals the lateral wall of the vestibule as well as the basal portion of the cochlea, commonly referred to as the "hook" region. Reproduced from Atturo et al. (2014) [125].
b. Schematic illustration showing the reference lines employed in the analysis. The dimensions of the shaded region and the associated distances may vary by over 100% in size [125]. A: vertical distance from the midportion of the OW to the superior margin of the RW; B: vertical distance from the same reference point to the SL; C: linear distance between the anterior borders of the OW and RW; D: point at which this anterior OW–RW axis intersects the SL, indicating its relative position along this trajectory.

The shape and rotation of the RW niche, as well as the relationship of the SL to the RW, are particularly unpredictable. The SL connects to the anterior, superior, and posterior rims of the RW before merging with the OSL at the “cul-de-sac” of the hook region [125].

Advanced 3D imaging techniques, such as contrast-enhanced micro-CT and synchrotron radiation imaging, have shown that the shape of the cochlear hook is frequently non-planar, with laterally open angulations and asymmetries that affect the approach to the scala tympani [107,125]. These findings highlight the anatomical complexity and variability of the hook region, which are critical considerations in cochlear implantation planning [125].

Anatomical Structures and Microarchitecture

Anatomically, the hook region contains the “cul-de-sac” of the endolymphatic space, where the OSL, SL, and BM converge. This area also includes the RWM and associated bony prominences, such as the CF and SSL [122,127,163]. Additional structures in this region include the cochlear aqueduct (CA), inferior cochlear vein (ICV), and the beginning of the ST, which can all be influenced by drilling or insertion angle [122,164].

The OSL arches outward from the anterior part of the RW niche, following a fish hook-like curvature where the ST also widens. These dynamic structural relationships, between SSL, SL, and OSL, help maintain the tension and positioning of the BM near the RW [125].

Micro-CT studies have shown that trauma in the hook region often involves the SL, SSL, or BM, especially during difficult insertions [124]. Two bony protrusions unique to this region, the SSL (at the superior margin of the RWM) and the CF (anteroinferior to the RWM), can narrow the proximal ST and deviate the electrode trajectory [116,125].

A two-dimensional optical coherence tomography (OCT) scan through the RWM revealed that several key cochlear structures, namely the proximal OSL, BM, SL, and SSL, were often not visualized due to the shadowing effect from the dense bone of the cochlear capsule [116]. RWM thickness showed significant variability (0.118 mm to 0.060 mm), and the true ST width after refractive index correction was ~677 µm [116].

Histological analysis and 3D reconstructions have revealed that the SSL has a porous microarchitecture, contrasting with the dense cortical bone of the round window arch (RWA). The SSL connects to the basal attachment of the SL approximately 270° from the RWM center [107].

Scala Tympani Orientation and Spatial Configuration

The ST in this region follows an initial straight path that shifts orientation as it approaches the first cochlear turn. It begins running inferiorly, anteriorly, and medially relative to the RWM, with the modiolus forming the anteromedial boundary [122,125].

In the proximal hook region, a crucial anatomical transition occurs: the BM, SL, SM, and OSL rotate approximately 90°, shifting from a horizontal to a vertical orientation. These components run anteriorly from the posterior margin of the RWM, and the gap between them narrows significantly at the horizontal plane [122,125]. OCT and synchrotron imaging reveal this angular transition as a bottleneck for insertion, particularly with stiffer arrays [117,122] (Fig.24).

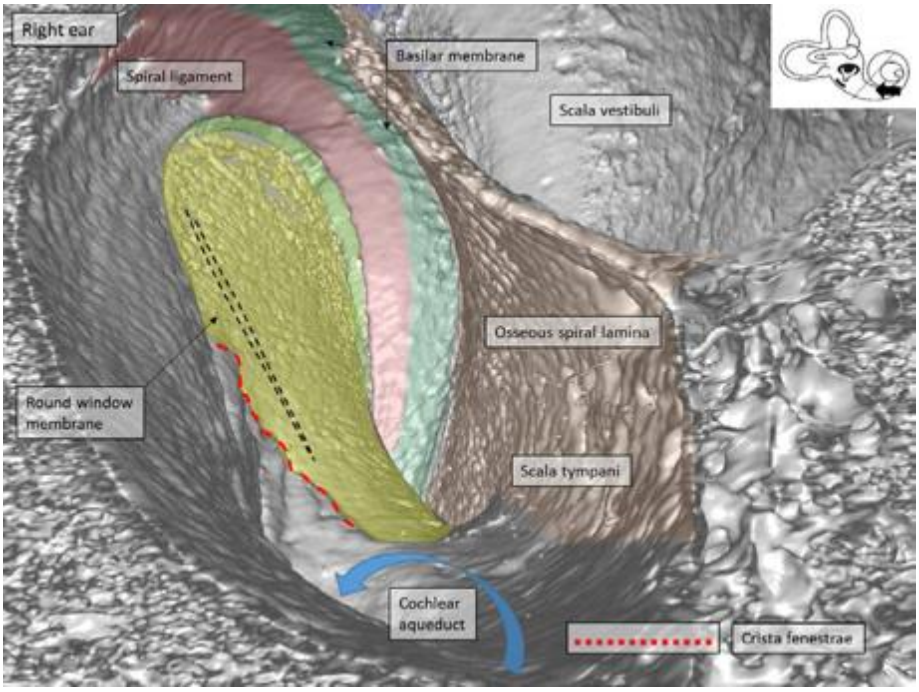

Figure 24.
Synchrotron radiation phase-contrast imaging (SR-PCI) combined with three-dimensional (3D) reconstruction of a right human cochlea, shown as a color-enhanced image. The round window membrane is visualized from within the scala tympani (see inset). The basilar membrane is laterally supported by the spiral ligament and the secondary spiral lamina, both depicted in red. The cochlear aqueduct opens onto the floor of the scala tympani at the inner surface of the crista fenestrae, indicated by the red dashed line. Reproduced from Schart-Morén et al. (2019) [124].

Superior to the horizontal segment of the RWM, the ST is particularly narrow. As one moves anteriorly and inferiorly through the hook region, the width and height of the ST increase, and the distance between the RWM and intracochlear structures becomes more pronounced [125,165]. This change in volume permits a smoother curvature for electrode trajectory if the array passes correctly through the centerline of the ST [165]. Reproduced from Schart-Morén et al. (2019) [124].

The ST is separated from other cochlear compartments by three distinct structures:

- The **OSL**: a rigid bony plate
- The **cochlear partition bridge (CPB)**: a soft-tissue support structure
- The **BM**: flexible and vibratory [107]

Bony Landmarks: Secondary Spiral Lamina and Crista Fenestrae

Two notable bony landmarks within the proximal ST are the **SSL**, a bony or cartilaginous protrusion at the superior rim of the RWM, and the **CF**, a bony crest at the anteroinferior rim [122,127,163]. These structures must be navigated during cochlear implant insertion, as they can obstruct the electrode's pathway or cause deflection into critical structures such as the BM or modiolus [122,125,163].

The SSL is now recognized to extend as far as the second cochlear turn (370°–572°), beyond its previously assumed limits near the RWM [107]. Its porous microarchitecture and anatomical relationships suggest that it supports BM stiffness and may contribute to high-frequency hearing [107,127]. However, it also poses a trauma risk, particularly in mid- and high-frequency regions [107].

The CF varies significantly between individuals and can obstruct access to the ST and RWM. Angeli et al. found that it may represent 23% to 50% of the RW diameter (mean 1.31 mm) [166]. In some cases, the CF must be drilled to ensure proper visualization or access [125,162,166].

Kumar et al. reported CF presence in 79.2% of cases, while Roland et al. identified bony obstruction in 30% of temporal bones [165,166]. Clifford and Gibson described the CF as a sharp ridge (as little as 0.2 mm) [160].

In a cadaveric study, CF-A, defined as the inferior bony edge of the RW, was observed in 95% of cases, with an average height of 0.6 ± 0.3 mm, accounting for approximately 40% of the RW height [162]. Based on its relative height, CF-A was classified into three categories (Fig.25):

- Category A1: height <33% of RW (42.1% of cases)
- Category A2: height between 33–66% of RW (47.38%)
- Category A3: height >66% of RW (10.52%)

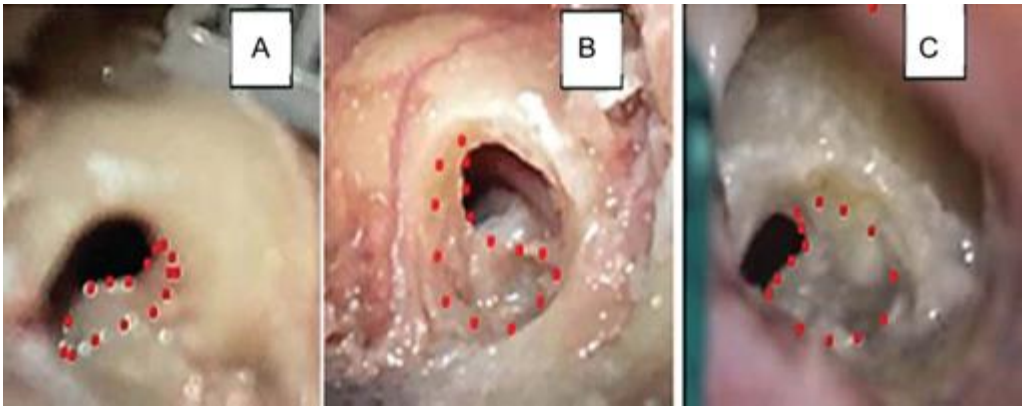

Figure 25.
Variants of Crista Fenestra type A.
(A) Subtype A1, (B) Subtype A2, and (C) Subtype A3 are presented, illustrating the morphological differences among the three configurations. Reproduced from Baki et al. (2021) [162].

A second anatomical variant, CF-B, is a bony projection located on the inferior wall of the scala tympani just behind the RWM. This structure was present in 10% of specimens, divided equally between small (B1) and large (B2) prominences [162].

Role and Configuration of the Secondary Spiral Lamina

The **SSL** surrounds the posterior and superior margins of the RW and anchors the BM laterally through the basilar crest [127]. It typically remains disconnected from the superior rim of the RW, creating a "free" bony region whose size may vary and influence the ease of atraumatic electrode insertion [125,127] (Fig.26).

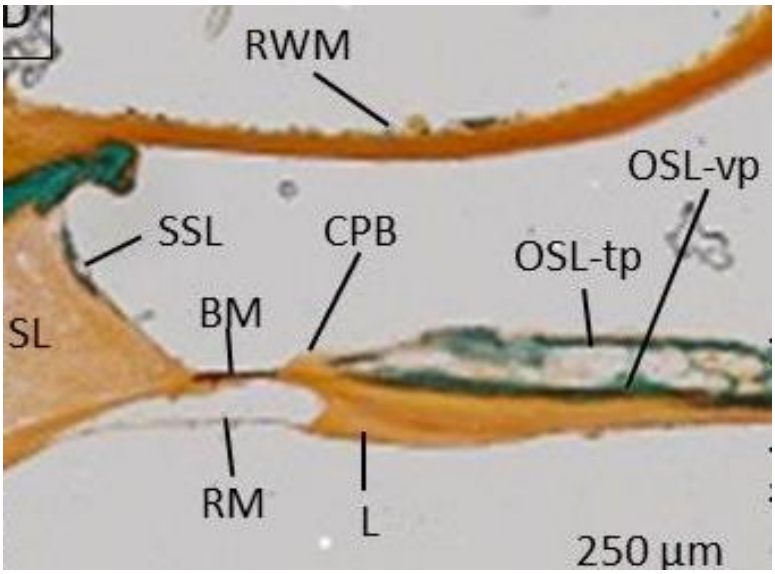

Figure 26.
Histological section stained with Masson-Goldner, serving as an anatomical reference for interpreting structures observed in the OCT images.
Abbreviations:RWM, round window membrane; OSL-tp, osseous spiral lamina, tympanic plate; OSL-vp, osseous spiral lamina, vestibular plate; CPB, cochlear partition bridge; BM, basilar membrane; OoC, organ of Corti; SSL, secondary spiral lamina; SL, spiral ligament; L, spiral limbus; RM, Reissner's membrane. Reproduced from Kerkhofs et al. (2022) [117].

Extending from the caudal end of the RW up to the second turn, the SSL contributes to increased stiffness of the BM, a property that may be important for high-frequency sound processing [127]. *While relatively underdeveloped in humans, the SSL may still contribute to BM suspension and high-frequency filtering within the hook region* [127].

Histological analysis and 3D reconstruction have shown that the SSL has a porous microarchitecture and attaches to the basal SL approximately 270° from the RWM center [107]. This configuration suggests that the SSL plays a structural and functional role beyond its classical description, especially in mid- and high-frequency regions where electrode trauma to the SSL can lead to fibrosis or ossification [107].

Imaging Insights and the Round Window Arch

Advanced imaging, particularly **contrast-enhanced computed tomography (CECT)**, has enabled clearer visualization and differentiation of key cochlear hook region structures, including the **SSL** and **RWA**.

The **RWA** is a newly described, arch-like bony structure located along the superior margin of the RWM. Composed of dense cortical bone and symmetrical in shape, it contrasts with the more porous and functionally supportive SSL [107] (Fig.27). It may represent a remnant of embryological development and potentially acts as a partial barrier between the RWM and BM, a function previously attributed to the SSL [107].

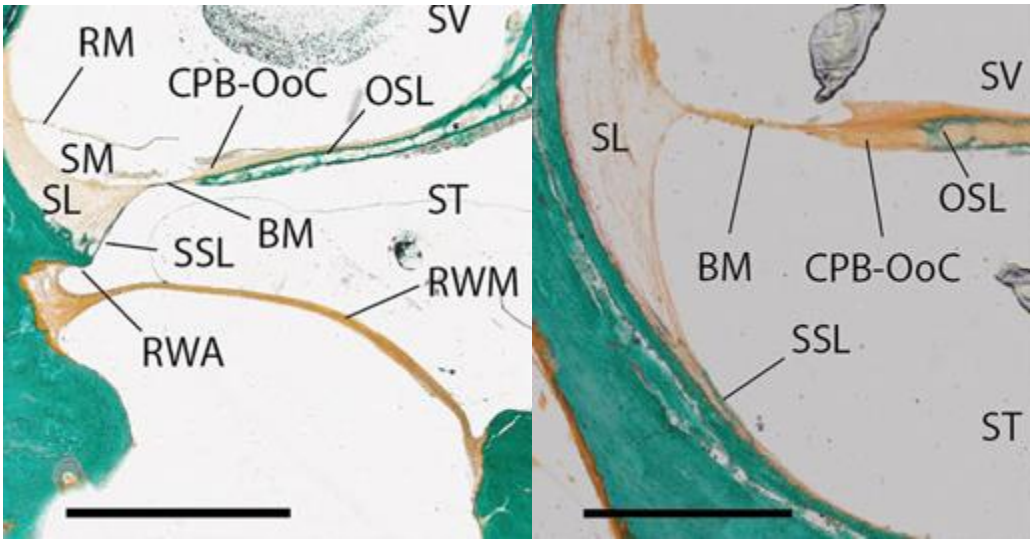

Figure 27.
Masson–Goldner-stained histological sections. The transbasal views (left) reveal the porous nature of the SSL, in contrast to the RWA, which is composed of dense cortical bone. The transmodiolar sections (right) show the anatomical location of the SSL at the basal insertion of the SL, situated approximately 270° from the central axis of the RWM.
Abbreviations: BM, basilar membrane; CPB-OoC, cochlear partition bridge-organ of Corti complex; OSL, osseous spiral lamina; RC, Rosenthal's canal; RM, Reissner's membrane; RWA, round window arch; RWM, round window membrane; SL, spiral ligament; SM, scala media; SSL, secondary spiral lamina; ST, scala tympani; SV, scala vestibuli. Scale bar: 1 mm for the three-dimensional rendering and the transbasal section, 0.5 mm for the transmodiolar section. Reproduced from Starovoyt et al. (2023) [107].

This distinction, **SSL:** porous, BM-supportive vs. **RWA:** dense, non-supportive, is essential for accurate interpretation of imaging and surgical navigation [107].

OCT imaging further confirms that dense bone in the cochlear capsule often casts shadows that obscure visualization of structures like the proximal OSL, BM, and SSL [116]. Nevertheless, accurate measurements of RWM thickness and ST width remain essential for planning electrode insertion trajectories and avoiding trauma [116].

Osseous Spiral Lamina and Spiral Ligament Relationships

The **OSL** runs parallel to the global plane of the RWM. Anterior to the RW niche, it curves upward and outward in a fish hook shape, where the ST also expands [122,125]. The **SL**, attached to the lateral cochlear wall, defines the SSL at the superior rim of the RWM and joins the anterior, superior, and posterior rims of the RW before merging with the OSL at the hook's "cul-de-sac" [125,127].

The BM is suspended between the SL and SSL and anchored to the lateral wall via the **basilar crest**. This junction, known as the **lateral wall/ligament fusion point (LLFP)**, marks the onset of cochlear function and is located near the posterior RWM margin [122,127].

The SL also lies adjacent to the **CPB** and exhibits variable curvature and rotation patterns that contribute to the anatomical complexity of the hook region [125]. The SL's configuration significantly affects the BM's positioning and motility, making it highly relevant to surgical planning and insertion strategies.

Auditory nerve fibers travel between the tympanic (OSL-tp) and vestibular (OSL-vp) plates of the OSL. These projections, together with the complex 3D relations of the OSL and SL, underline the surgical risks of intracochlear trauma if insertion is not carefully guided [107].

Cochlear Partition Bridge

The **CPB** is a soft tissue structure located between the OSL and the BM. It provides lateral support to the spiral limbus (L) and serves as a foundation for the OoC, which lies atop both the BM and the CPB (Fig.28).

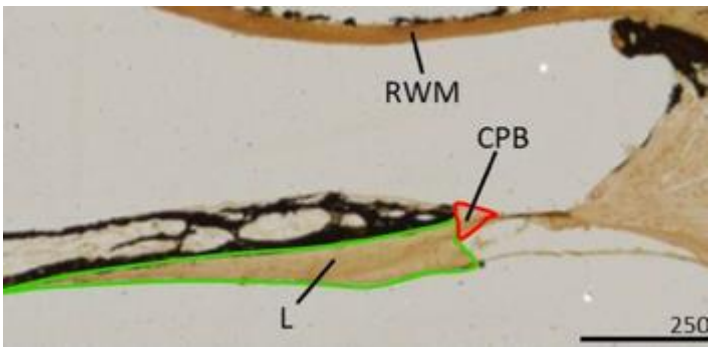

Figure 28. Histological section stained with von Kossa/von Gieson, highlighting the anatomical positions of the CPB and the spiral limbus (L). Reproduced from Kerkhofs et al. (2022) [117].

In the human cochlea, the CPB becomes progressively wider from base to apex [122]. It plays a critical mechanical role in coupling the vibratory motion of the BM with sensory structures. Any trauma to this region during cochlear implantation may compromise the support and alignment of the OoC, affecting auditory function [107].

Precise knowledge of this structure is vital for minimizing damage during electrode insertion, particularly when navigating the hook region's tight spaces and varying anatomy [107].

Lateral Wall Configuration and Functional Implications

The **lateral wall**, including the SL and its surface facing the ST, is notably reshaped in the hook region. As it curves around the RW, it narrows into a sickle-like structure that wraps along the posterior RW circumference (Fig.29).

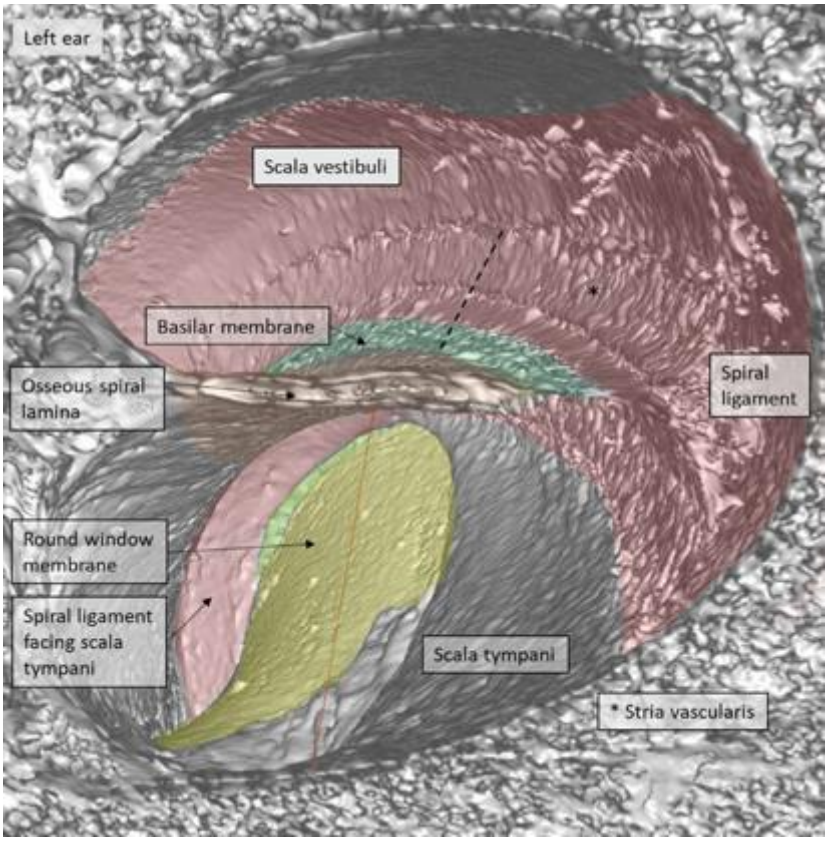

Figure 29.
Anterior view of the round window and surrounding soft tissue structures within the hook region of a left human temporal bone, visualized using SR-PCI following image cropping. Reproduced from Schart-Morén et al. (2019) [124].

At its posterior end, it merges with the OSL, creating a scaffold that supports the BM. This confluence contributes to maintaining BM tension and mobility in the hook region, which is crucial for cochlear transduction and proper propagation of sound waves [122].

Given the variability in lateral wall shape and its implications for electrode guidance and tissue preservation, this area deserves special attention in atraumatic surgical strategies [125].

Surrounding Vascular and Ductal Structures

Several important vascular and ductal structures surround the RW and ST in the hook region:

- The ductus reuniens lies adjacent to the posterior RWM margin

- The CA and ICV are closely associated with the inferior RW rim [122,164,167]

The internal aperture of the CA is typically located at anterior-inferior aspect of the RW niche, near the CF. It opens into the ST floor, just anterior to the anterior edge of the RW [122,164,167].

The ICV and other accessory canals drain blood from the cochlea, SG, and middle ear toward the jugular foramen [167].

Clinical Relevance and Summary

The ST in the hook region is bordered by three key structures: the bony **OSL**, the soft-tissue CPB, and the vibratory BM. Their close proximity and delicate nature make the hook region particularly susceptible to trauma during CI insertion [122,126,127].

Understanding this microanatomy is essential for optimizing CI placement and preserving residual hearing. Damage to the SL, SSL, or CF can have long-term consequences, including fibrosis, ossification, and degraded auditory performance [107,124,166].

In surgical practice, the hook region demands high-resolution preoperative imaging, careful trajectory planning, and atraumatic techniques to minimize the risk of insertion-related complications. Detailed knowledge of individual anatomical variability, especially in the SSL, CF, and RW niche configuration, is crucial for successful and safe electrode placement [107,125,162,163,165,166].

3.1.1.1.6. Scala Tympani and Cochlear Duct Length

Canfarotta et al. investigates the influence of ST volume, CDL, and angular insertion depth (AID) on early hearing preservation following cochlear implantation with lateral wall electrode arrays (Fig.30). They highlighted that the mean ST volume was 40.4 mm^3 (range: 31.2–50.5 mm^3), and was significantly greater in males (42.4 mm^3 vs. 38.7 mm^3 in females, $p = 0.005$). The mean CDL was 36.8 mm (range: 33.6–40.1 mm), and ST volume was strongly correlated with CDL ($r = 0.74$, $p < 0.001$) [143].

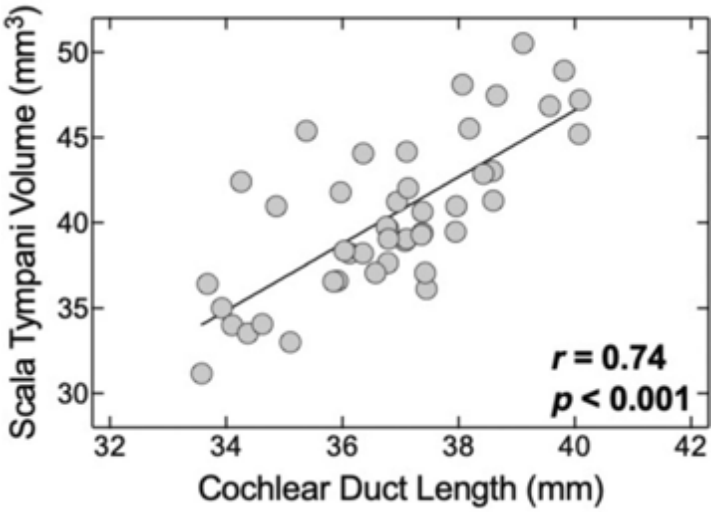

Figure 30.
An increased volume of the scala tympani is associated with a greater cochlear duct length. The fitted regression line, as shown in the panel, illustrates this correlation. Reproduced from Canfarotta et al. (2025) [143].

Spiegel et al. study investigates the anatomical variability of the human cochlea, with a particular focus on CDL, utilizing a novel tablet-based imaging software, OTOPLAN. Accurate measurement of CDL is essential in CI, as it directly informs the selection of electrode array length and contributes to minimizing insertion-related complications while optimizing auditory outcomes.

Their retrospective analysis was performed on 108 high-resolution preoperative CT scans of patients implanted with either FLEX28™ or FLEXSOFT™ electrodes manufactured by MED-EL [168]. Across the entire cohort, the mean CDL was found to be 36.2 ± 1.8 mm, with values ranging from 30.4 to 40.2 mm, indicating a variation of over 30%. A significant sex-related difference was observed, with males exhibiting longer cochleae (36.5 ± 0.2 mm) than females (35.8 ± 0.3 mm; $p = 0.037$). However, no statistically significant differences in CDL were observed with respect to the side of the ear or the age of the patient. Only two cochleae (1.8%) were shorter than 32 mm [168].

Comparison with prior studies revealed that the CDL values obtained were consistent with those reported using alternative methodologies, such as direct histological sectioning, three-dimensional reconstructions, or CT-based spiral coefficient modeling. Nevertheless, the CDL estimates in several other studies employing OTOPLAN were slightly lower (typically between 32.4 and 34.0 mm). The observed trend of longer cochleae in male patients also aligns with findings from the broader literature [168].
Therefore, this study highlights the considerable interindividual variation in cochlear anatomy and the clinical relevance of incorporating such variability into the preoperative planning of CI [168].

This study by Micuda et al. presents the most comprehensive morphologic analysis to date of the ST in the human cochlea using SR-PCI. Key anatomical metrics included the ST cross-sectional diameter (DST), area (AST), width (WST), and a novel metric termed ST tilt (θST), which assesses the orientation of the cochlear partition (Fig.31). The AID of cochleae ranged from 810° to 1043°, with ST volumes between 47.1 and 82.4 mm^3, revealing significant inter-individual variability. On average, DST decreased from base to apex, from 1.12 mm at 90° to 0.56 mm at 720°, and 0.51 mm at 810°. At 720°, the smallest cochlea still presented a DST of 0.4 mm, indicating that even the narrowest anatomies can accommodate a standard 0.4 mm electrode up to two turns [142].
AST similarly declined along the cochlear spiral, with mean values dropping from 1.67 mm^2 at 90° to 0.65 mm^2 at 720°. Importantly, the area ratio AST/ASV (scala vestibuli) transitioned from >1 to <1 around 180°, indicating the scala tympani becomes relatively smaller than the scala vestibuli in the apical turns [142].

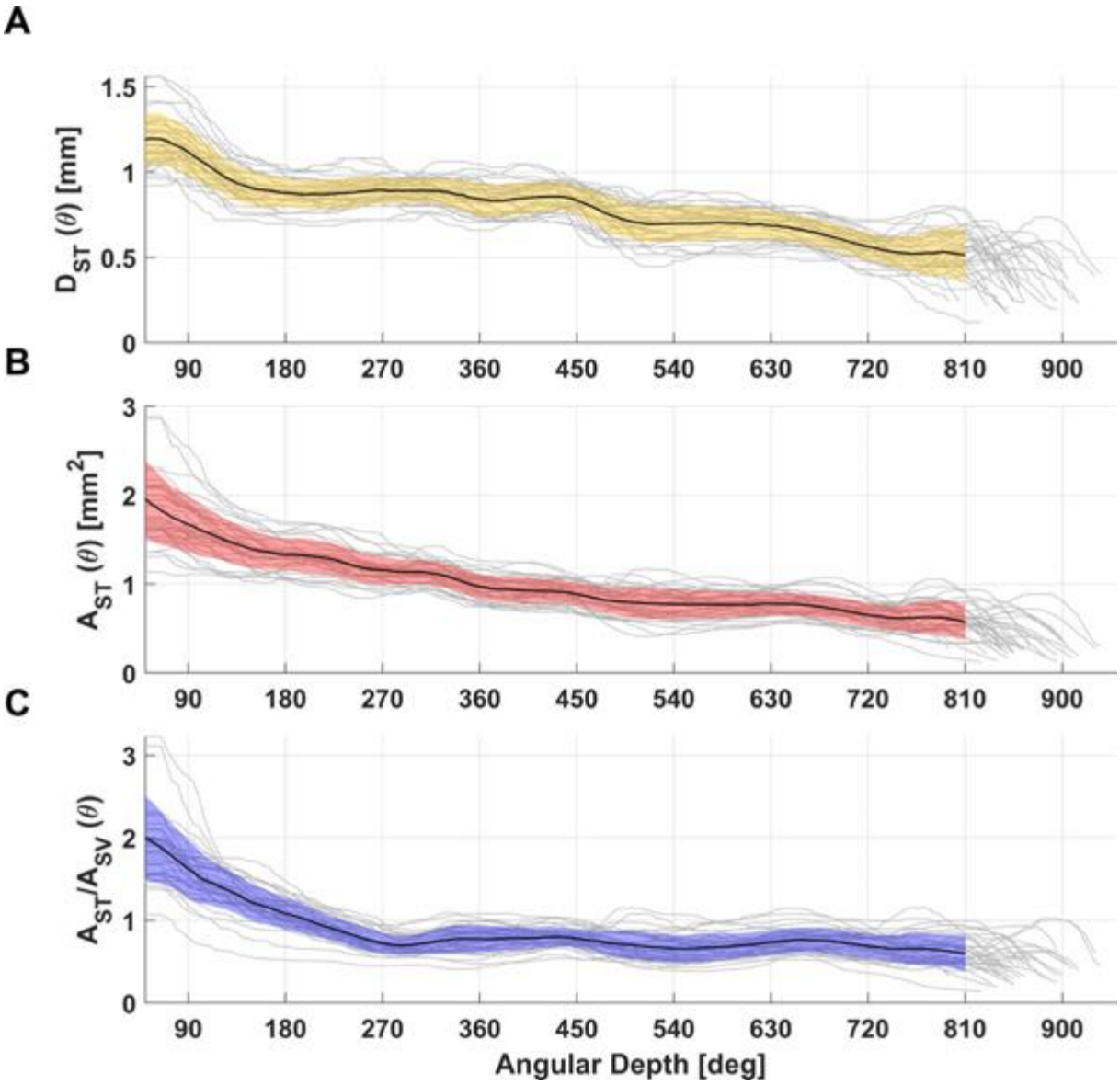

Figure 31.
(A) Cross-sectional diameter of the ST plotted as a function of angular depth, denoted DST(θ), defined by the diameter of the largest circle that fits within each ST cross-section across 35 cochleae (grey traces). The average profile (black line) and the associated standard deviation (yellow band) are displayed. In the smallest cochlea, the diameter reaches 0.4 mm at 720°.
(B) Cross-sectional area of the ST along the cochlear angular trajectory, represented as AST(θ), calculated based on the pixel count within each ST cross-section for all 35 samples (grey). The mean AST (black line) and ±1 standard deviation (red band) are shown. Reproduced from Micuda et al. (2024) [142].
(C) Ratio of AST to the cross-sectional area of the scala vestibuli (ASV) at each angular depth. Values are presented for all 35 cochleae, with the mean (black line) and ±1 standard deviation (blue band). Notably, the ratio falls below 1 beyond 180°, indicating a relative reduction in the ST compared to the SV [142].

The WST showed a non-linear trend, decreasing through the basal turn before slightly increasing in the second turn. θST displayed periodicity across the cochlear spiral, with its most rapid change between 0° and 180°, a decrease from 50.2° at the RW to an average of 4.7° at 180° [142] (Fig.32).

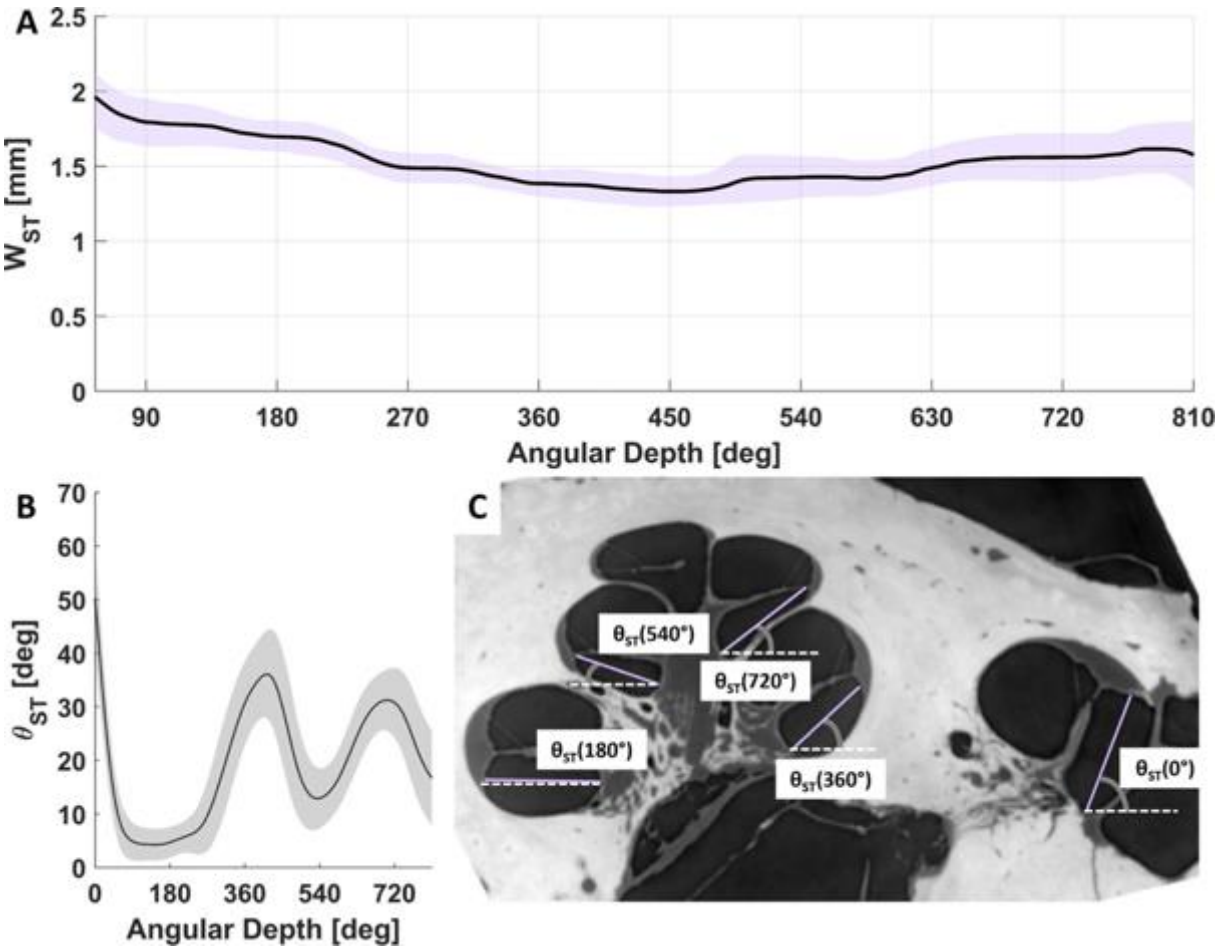

Figure 32.
(A) The mean width along the long axis of the scala tympani (WST) as a function of angular depth is represented by a black line, with ±1 standard deviation indicated in purple.
(B) The average inclination angle of the scala tympani (θST) at each angular position is shown as a solid line, with the grey band denoting ±1 standard deviation. Reproduced from Micuda et al. (2024) [142].
(C) A mid-modiolar cross-section illustrates the measurement geometry: the WST axis is marked in purple (solid line), the x–y plane representing the basal plane is shown as a dashed white line, and the corresponding tilt angle (θST) is indicated in grey at the respective angular depth [142].

Article 1

Journal: Audiology and Neurotology. Peer-reviewed. Published: Gersdorff G, Ramos P, Wijewickrema S, O'Leary S, Lefèbvre P, Gerard JM. High-resolution intraoperative guide for cochlear implant surgery using optical coherence tomography. Audiol Neurotol. 2026. doi:10.1159/000552581. PMID: 42560936.

Audiology and Neurotology

Research Article

Audiol Neurotol
DOI: 10.1159/000552581

Received: October 6, 2025
Accepted: February 13, 2026
Published online: September ▪▪▪, 2026

High-Resolution Intraoperative Guide for Cochlear Implant Surgery Using Optical Coherence Tomography

Guillaume Gersdorff[a, b, c] Phoebe Ramos[a, b] Sudanthi Wijewickrema[a]
Stephen O'Leary[a, b] Philippe Lefèbvre[c] Jean-Marc Gerard[a, b]

[a]Department of Surgery (Otolaryngology), University of Melbourne, East Melbourne, VIC, Australia; [b]Royal Victorian Eye and Ear Hospital, East Melbourne, VIC, Australia; [c]University Hospital of Liege Liège, Belgium

Keywords
Optical coherence tomography · Cochlear implant · Hearing preservation

Abstract

Introduction: Despite advances in soft surgery, intracochlear trauma during cochlear implant (CI) electrode insertion still occurs, potentially damaging cochlear microstructures and affecting hearing outcomes or future treatments. While the round window membrane (RWM) approach is generally less traumatic, the hook region's complex anatomy can still cause mechanical injury, often due to limited visual guidance. Preoperative imaging and intraoperative optical coherence tomography (OCT) could reduce trauma by offering high-resolution, real-time visualization of cochlear microstructures. ***Methods:*** Eight fresh-frozen human temporal bones (TB1–TB8) were included. The first 6 specimens (TB1–TB6) underwent micro-CT scanning with manual segmentation to establish detailed anatomical baselines and served for OCT-micro-CT co-registration. Following a standard cochlear implantation approach, intracochlear structures behind the RWM were visualized using a microscope-integrated OCT system, with additional imaging performed via an anteroinferior cochleostomy to compare access routes. Electrode insertions were performed under OCT guidance in selected specimens, while feasibility of intraoperative workflow and insertion dynamics was assessed in TB7–TB8 under fluoroscopic control. ***Results:*** OCT images were successfully obtained for each TB, with proper RWM exposure being crucial. The OCT microscope enabled scanning of the RWM and scala tympani (ST) from various axes, depths, and angles at a surgical working distance, improving assessment of proximal ST anatomy. OCT appears reliable for evaluating microanatomy through the RWM, guiding CI electrode selection, approach, and proximal array course modification during insertion. By visualizing critical structures and inferring deeper ones, it supports preoperative imagery-based planning and may reduce the risk of intracochlear damage. ***Conclusion:*** Intraoperative OCT imaging enhances the precision of the cochlear opening site and electrode insertion axis. By integrating OCT, CI surgery could shift from a largely blind procedure to one with significant visual guidance, reducing surgical trauma and improving post-operative hearing preservation. © 2026 S. Karger AG, Basel

karger@karger.com
www.karger.com/aud

© 2026 S. Karger AG, Basel

Correspondence to:
Guillaume Gersdorff, gersdorff.guillaume@gmail.com

Introduction

Modern cochlear implantation increasingly prioritizes minimally invasive techniques to preserve cochlear structures, protecting delicate intracochlear structures and reducing inflammatory responses. This shift reflects growing recognition that electrode insertion can impact not only immediate auditory outcomes but also long-term cochlear health and future treatment options. This holistic approach not only enhances overall cochlear implant (CI) performance but also broadens future therapeutic possibilities.

Hearing preservation has become a central goal in modern cochlear implantation, aiming to minimize trauma to intracochlear structures and maintain the delicate neural and mechanical elements of the cochlea. Preserving cochlear health has multiple advantages, including improved speech understanding in noise, enhanced music appreciation, and more accurate sound localization [1]. Patients benefit significantly from hearing preservation strategies, regardless of their level of preoperative hearing. Those with substantial residual hearing postoperatively achieve notably higher speech perception scores compared to those without [2]. Furthermore, even patients with no measurable residual hearing preoperatively show improved outcomes when cochlear implantation is performed using atraumatic techniques, which are associated with better overall auditory performance [3, 4].

Despite advancements such as soft surgery techniques, including robotic-assisted insertion and the use of softer electrodes, intracochlear trauma remains a concern, occurring in up to 32% of implantations [5]. This high incidence is largely attributed to anatomical variations, particularly in the round window (RW) and hook region [6–12]. The entry path into the scala tympani (ST) via the round window membrane (RWM) is anatomically complex, especially in its proximal portion, which exhibits a three-dimensional fishhook-like curvature. This so-called "hook region" contains the cul-de-sac of the endolymphatic space, where the osseous spiral lamina (OSL) changes orientation and merges with the spiral ligament (SL) and basilar membrane (BM). Additionally, bony structures such as the secondary spiral lamina (SSL) and crista fenestra (CF) can further complicate electrode insertion by narrowing the RWM and deflecting the electrodes toward the BM and modiolus.

The anatomical complexity and variability of the hook region present a persistent challenge in CI surgery, reinforcing the need for a detailed, precise, three-dimensional understanding of this space and a personalized surgical approach to minimize mechanical trauma. A major challenge in current surgical practice is the absence of direct visual feedback during electrode insertion [13]. With some electrode designs, particularly perimodiolar arrays using an insertion sheath or stylet, there is a higher susceptibility to deflection toward the basilar membrane (BM) and modiolus, further complicating navigation of the hook region. Current clinical imaging techniques, such as CT scans, lack the resolution required to reliably assess intracochlear microanatomy. Even micro-CT scans often fall short to fully define this anatomy, requiring synchrotron imaging for complete delineation [7, 8].

Optical coherence tomography (OCT), a safe and non-invasive high-resolution imaging modality widely used in ophthalmology and dermatology, offers a potential solution. Based on interferometry, OCT provides real-time imaging with a resolution of 1–15 μm, allowing for the visualization of cochlear structures through the RWM [12, 14, 15]. By enabling direct visualization of the surgical path, OCT has the potential to transform cochlear implantation from a largely blind procedure into one guided by individualized anatomy, reducing the risk of damaging essential intracochlear structures.

This study examines the use of microscope-integrated OCT to visualize intracochlear microanatomy in fresh human temporal bones. Prior to dissection, micro-CT imaging was performed to generate detailed anatomical reference data, including the orientation, dimensions, and spatial relationships of key cochlear structures. OCT was then used to evaluate the visibility of these structures through the intact RWM in a controlled cadaveric setting. The primary aim was to determine whether OCT could reliably provide qualitative and semi-quantitative assessment of intracochlear anatomy in a surgical context, particularly in the hook region, and support surgical decision-making, including electrode array (EA) selection (straight vs. perimodiolar) and the choice of insertion approach (RW vs. cochleostomy), based on individual anatomy. If proven reliable, OCT could further enhance intraoperative decision-making by enabling tailored electrode selection and optimization of the insertion trajectory, with the aim of minimizing insertion-related trauma and improving preservation of residual hearing, an increasingly important goal in modern cochlear implant surgery. This study investigated the feasibility of microscope-integrated OCT for visualizing intracochlear anatomy and guiding EA insertion.

Materials and Methods

A total of eight fresh-frozen human temporal bones (TB1–TB8) were used and obtained from anonymous donors through Science Care (AZ, USA). The first 6 temporal bones (TB1–TB6) are analyzed to establish and correlate anatomical baselines. Each specimen is scanned using micro-computed tomography (μCT50, Scanco Medical AG, Brüttisellen, Switzerland). Images data were converted from ISQ to DICOM format, and anatomical measurements and segmentation were performed using 3D Slicer providing high-resolution measurements of cochlear microstructures.

Segmentation and anatomical measurements were performed by a single trained observer using standardized protocols to ensure consistency across specimens. A standard cochlear implantation approach was performed on each specimen. The facial nerve and chorda tympani were preserved in all cases.

After optimal RWM exposure, each middle and inner ear was inspected under a surgical microscope to confirm the absence of damages. Stapes mobility and RW reflex integrity were assessed using both direct microscopy and OCT.

Initial OCT imaging was performed through the posterior tympanotomy using conventional ophthalmologic surgical microscopes equipped with integrated OCT modules. The first six specimens (TB1–TB6) were scanned using the OPMI LUMERA 700 with RESCAN 700 OCT (Carl Zeiss Meditec AG, Jena, Germany). This system operates with axial resolutions of 5.5 μm (2.9 mm depth) and 11.1 μm (5.8 mm depth). It offers 2 imaging modes: real-time (live surgical view) and capture (freeze and scan).

In all cases, the OCT scanning axis was aligned with the presumed axis of the ST and oriented perpendicular to the RWM. The full surface of the RWM was scanned, providing detailed visualization of the hook region, including the CF and adjacent microstructures and videos and pictures were taken.

Subsequently, in the first six temporal bones (TB1–TB6), a blue-lined anteroinferior cochleostomy (±1.5 mm^2) was performed adjacent to the RWM in each bone without breaching the endosteum. OCT imaging was then repeated through the cochleostomy. This dual-window imaging approach allowed for comparison of RWM and cochleostomy access routes.

Electrode insertion through the RWM was performed in TB1 and TB6 using the CI22 (slim straight) and CI32 (slim perimodiolar) arrays (Cochlear Ltd.), under OCT guidance with the OPMI LUMERA 700 microscope equipped with the RESCAN 700 OCT system (Carl Zeiss Meditec AG, Jena, Germany). The reliability of OCT in supporting atraumatic electrode placement was assessed. For TB7 and TB8, 32-electrode feasibility insertions through the RWM were assessed under fluoroscopic guidance, allowing real-time evaluation of electrode trajectory and insertion behavior. These 2 temporal bones were imaged with the EnFocus Spectral Domain OCT system (Leica Microsystems GmbH, Wetzlar, Germany), which operates with axial resolutions of ≤4 μm (5.0 mm depth) and ≤9 μm (11.1 mm depth), offering both real-time and volumetric imaging modes."

Results

Assess Cochlear Microanatomy

The ST axis was successfully identified in all 6 specimens, and the anatomical landmarks, including the CF, SL, and OSL, were visible in all scans (shown in Fig. 1). Importantly, OCT revealed considerable anatomical variability within the hook region. This was exemplified by the angle between the RWM and the OSL, which varied from 34.9° to 88.7° despite the limited sample size. This variability, as well as the agreement between OCT and micro-scan measurements, is illustrated in Figure 2. Likewise, the RWM diameter showed substantial variation, ranging from 1.25 to 2.9 mm.

The comparison illustrated in Figure 2 is provided as a representative example of anatomical concordance between OCT and micro-CT; a systematic quantitative comparison across all specimens was beyond the scope of this feasibility study. Across the analyzed specimens, OCT-derived measurements showed overall consistency with micro-CT anatomical trends, particularly regarding round window dimensions and general orientation of the proximal ST. While absolute values occasionally differed between modalities, the relative anatomical relationships were preserved. Variability in angular measurements was observed and is likely related to differences in imaging planes, acquisition angles, and optical properties of the tissues. Additionally, complete measurement datasets could not be obtained in all specimens due to variability in visualization conditions through the RWM.

Predict the Electrode Type

The RW was scanned at multiple sites to identify the most favorable entry point. In all cases, the anteroinferior quadrant consistently represented the widest and most linear proximal segment of the ST (shown in

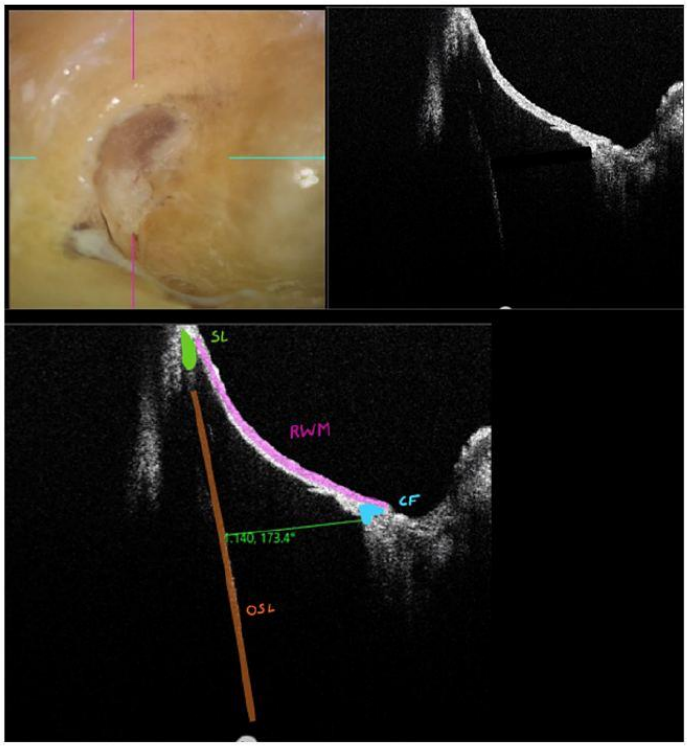

Fig. 1. OCT imaging of the right ear showing the round window membrane (RWM) in pink, the crista fenestra (CF) in blue, spiral ligament (SL) in green, and osseous spiral lamina (OSL) in orange. The image allows precise evaluation of the ST axis and diameter, providing orientation landmarks essential for atraumatic electrode insertion planning.

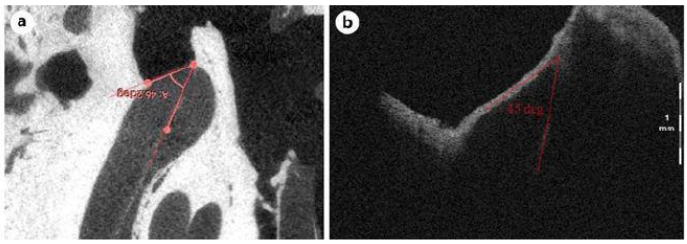

Fig. 2. a Anatomical micro-scan of the left ear shows the angle between the RWM in pink and the OSL in orange measured at 46.2°. **b** The corresponding OCT image demonstrates the same relationship with a measured angle of 45°, confirming OCT accuracy for quantifying orientation relevant to cochlear implant insertion strategies.

Fig. 3a, b). These anatomical characteristics were used to assess the suitability of different electrode designs, particularly for perimodiolar arrays requiring sufficient diameter and a relatively straight insertion trajectory.

For example, in temporal bone specimen TB2, initial imaging at a depth of 2.9 mm suggested that the anteroinferior portion of the RWM provided a relatively straight and wide access (>0.8 mm) route into the ST, appearing suitable for insertion of the CI32 electrode. However, deeper imaging at 5.8 mm revealed a pronounced curvature of the proximal ST (shown in Fig. 3c), indicating a potential mismatch between the electrode trajectory and cochlear anatomy, which could increase the risk of insertion trauma or deflection. This highlights

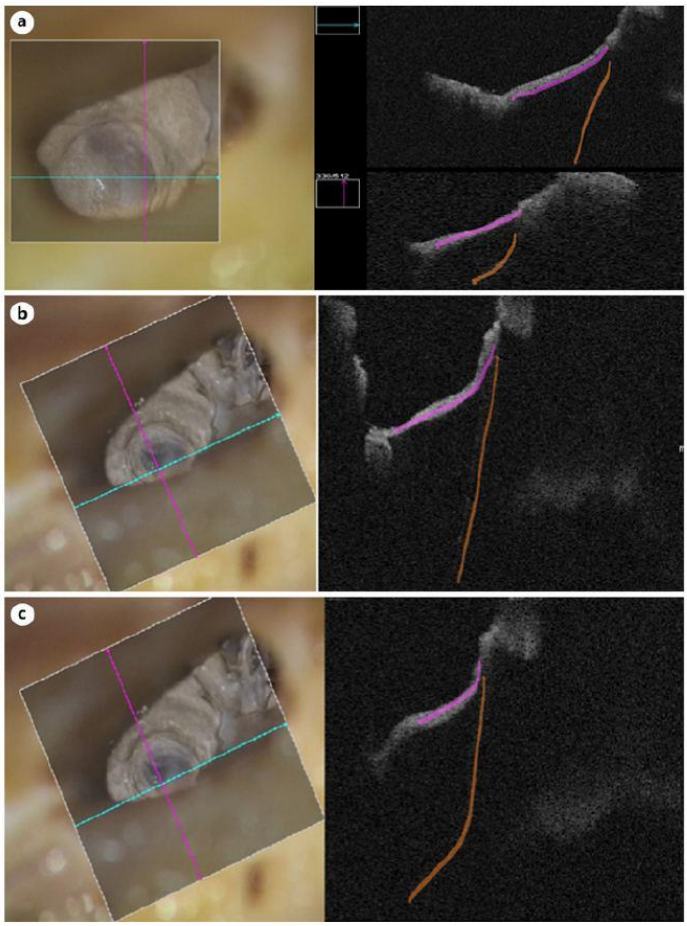

Fig. 3. OCT scans of the left ear RWM in pink from multiple orientations. All images are presented in the *Y*-axis plane (red axis), with panel A additionally displaying the *X*-axis plane (blue axis). The ST axis is defined by the position and orientation of the OSL in orange. **a** Posterior-inferior scanning shows a narrow, curved ST with the OSL in orange. Anteroinferior views (**b**) reveal a straighter, wider access at 2.9 mm depth, while deeper 5.8 mm scanning (**c**) highlights pronounced curvature influencing electrode choice.

the importance of depth-dependent OCT assessment as superficial measurements alone may lead to inappropriate electrode selection.

Predict the Most Suitable Surgical Cochlear Entry

In TB4, OCT imaging demonstrated that even in the anteroinferior quadrant, the ST was too narrow (<0.8 mm) and excessively curved to allow safe RWM insertion of the CI32 array through the RWM (shown in Fig. 4a). Under such circumstances, an extended RWM or a cochleostomy approach was, therefore, preferred (shown in Fig. 4b).

Can a Blue-Lined Cochleostomy Help Us See Deeper?

A thin bony overhang from the CF generated a shadowing artifact. Blue-lining of the cochleostomy, achieved by drilling until only a thin osseous layer covering the endosteum remained, still did not allow direct visualization through the site as the residual bone continued to generate optical shadowing. By shifting the OCT focal plane from the blue-lined cochleostomy site to the RWM, it was, nevertheless, possible to indirectly delineate the cochleostomy margins. This adjustment enabled identification of the drilled area and informed how far the cochleostomy should be extended to achieve

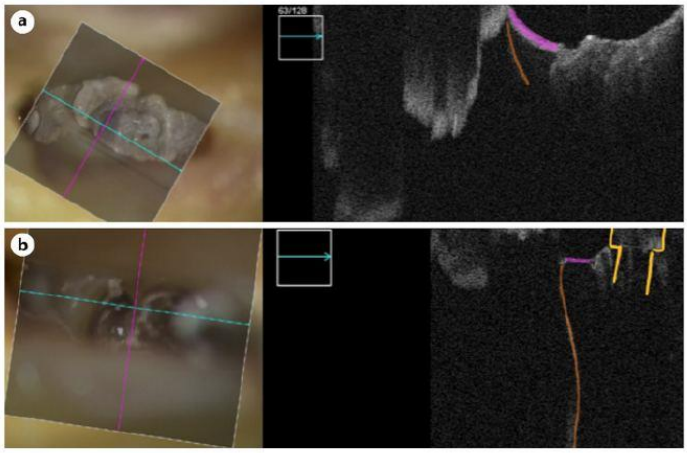

Fig. 4. OCT imaging of the right ear. In panel **a**, anteroinferior scanning through the RWM in pink reveals a narrow, curved ST unsuitable for CI32 insertion. In panel **b**, imaging through an anteroinferior cochleostomy shows the sheath and stopper in yellow aligned with the OSL in orange, enabling improved trajectory.

both an adequate diameter and optimal alignment with the ST axis for insertion of the CI32 electrode (shown in Fig. 5).

Can the Electrode Insertion Trajectory Be Followed?

An interesting observation was made during insertion of the Slim Straight CI22 array via the RWM: OCT imaging through the RWM enabled tracking of the 22 electrode insertion behavior within the first 3–5 mm of advancement following the natural curvature of the OSL (lateral wall) with remarkable precision (shown in Fig. 6).

With the CI32 electrode, the insertion sheath can be tracked in real time. OCT enabled not only the monitoring of the sheath pathway but also the adjustment of its orientation during insertion to achieve a more rectilinear trajectory aligned with the ST axis. As illustrated in Figure 7, this capability was particularly evident when the electrode was advanced through a cochleostomy, where the system allowed continuous visualization and trajectory correction.

Clinical Applicability on 2 Temporal Bones

In TB7, a full insertion workflow was simulated using EnFocus OCT in combination with fluoroscopy. The RWM was scanned with OCT in multiple axes and showed a ST diameter was consistently measured at >0.8 mm along the proximal 5 mm of the scala, indicating that insertion of the CI32 should be feasible (shown in Fig. 8a). Subsequently, the RWM was vertically opened with a 23 G needle, and the electrode was advanced under fluoroscopic guidance to evaluate the behavior of the array during insertion. The sheath remained straight and well aligned with the ST axis, with no evidence of deflection. Following full insertion, the EA showed no tip fold-over and appeared to follow a physiologically appropriate trajectory, although confirmation of its exact intracochlear course would require postoperative imaging (shown in Fig. 8b).

In TB8, EnFocus OCT imaging through the RWM revealed ST diameters of <0.8 mm at all measured points, indicating that CI32 sheath insertion through the RWM was not feasible. Fluoroscopy during attempted insertion demonstrated progressive sheath deformation, thereby confirming the OCT-based preoperative prediction (shown in Fig. 9).

Discussion

The OCT is a non-invasive imaging modality that offers micrometer-scale resolution and real-time visualization of biological tissues. While extensively used in ophthalmology and dermatology [16], its application in otologic surgery, particularly in cochlear implantation, remains limited. The key advantage of OCT lies in its ability to visualize critical intracochlear structures through the intact RWM.

This study was designed as a feasibility and observational investigation rather than a formal quantitative validation of OCT against micro-CT. While representative comparisons demonstrated anatomical

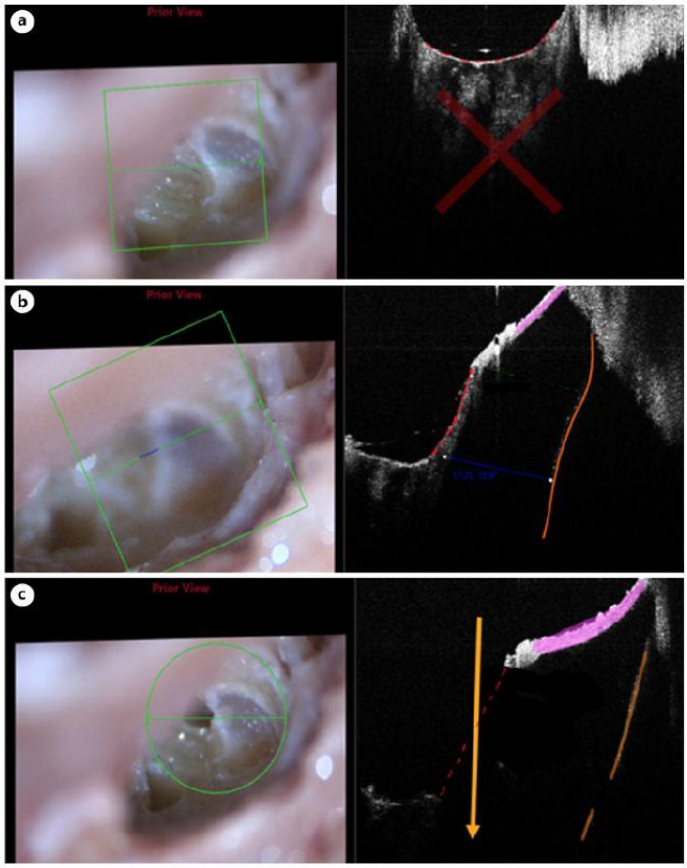

Fig. 5. OCT views of the left ear cochleostomy. Panel **a** shows a blue-lined site with residual bone shadowing artifact marked by a red cross. Panels **b** and **c**, imaged through the RWM in pink, highlight the cochleostomy site outlined by dotted red lines, demonstrating the required extension of the cochleostomy to achieve sufficient diameter and alignment with the ST axis defined by the OSL in orange, accommodating the CI32 indicated by an orange arrow.

concordance, systematic point-to-point co-registration between modalities remains challenging due to differences in imaging physics, sensitivity to acquisition angle, and variability in optical properties of cochlear tissues. Therefore, OCT should currently be considered a qualitative and semi-quantitative intraoperative tool.

We demonstrated again that the hook region, which includes the proximal ST, is a highly variable anatomical area and one of the most common sites of intracochlear trauma during electrode insertion [11, 12, 17–19]. In this study, OCT enabled detailed imaging of structures such as the OSL, CF, and SL through the intact RWM. This allowed for individualized assessment of ST curvature and diameter, factors that directly influence the feasibility of perimodiolar array atraumatic RWM insertion. Importantly, the anatomical relationships observed in this study are consistent with previously published OCT-based descriptions of the human cochlear hook region. Prior work by Kerkhofs et al. and Starovoyt et al. [12, 13] demonstrated that OCT enables reliable visualization of key intracochlear structures, including the OSL, spiral ligament, basilar membrane, and CF, as well as their spatial orientation through the RWM. The present findings reproduce similar anatomical configurations under intraoperative conditions, supporting the robustness and reproducibility of OCT-based anatomical interpretation.

Previous studies, such as that by Pau et al. [20], demonstrated the feasibility of OCT imaging in otologic specimens, but were limited to fixed temporal bones and

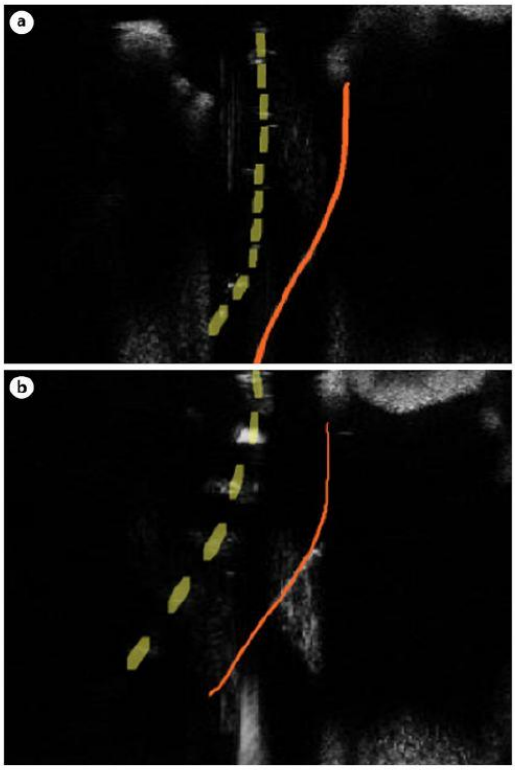

Fig. 6. OCT tracking of CI22 electrode insertion through the left ear RWM in pink. In panel **a**, a yellow dotted line indicates electrode alignment with the OSL in orange over the first 2.9 mm. Panel **b** extends visualization to 5.8 mm, confirming atraumatic trajectory along the ST.

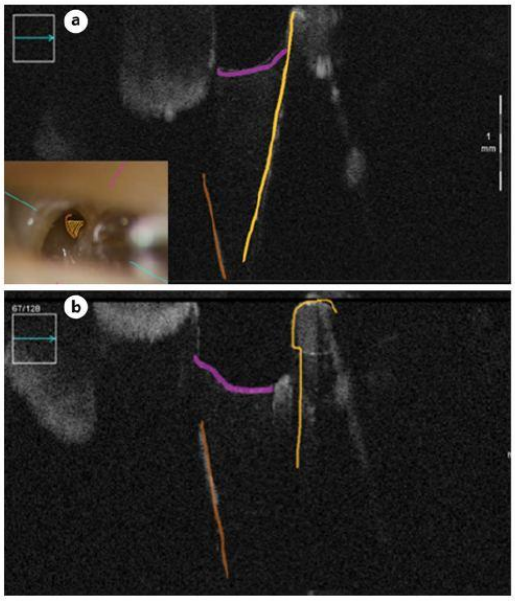

Fig. 7. OCT imaging of CI32 sheath insertion in the right ear through a cochleostomy, with monitoring performed via the RWM in pink. Panel **a** shows the sheath and stopper in yellow advancing and initially contacting the OSL in orange; removal of the membrane confirms sheath-OSL contact for anatomical correlation. Panel **b** illustrates trajectory adjustment during progression, reducing trauma risk and achieving better alignment with the ST while avoiding critical structures.

relied on cochleostomy access to visualize inner ear structures. Their system achieved resolution in the range of 4–15 µm, with a penetration depth of 1–3.5 mm. In contrast, our study used fresh-frozen cadaveric specimens and achieved resolutions down to 3 µm with a maximum imaging depth of 5.8 mm, representing a significant advancement in both anatomical fidelity and clinical relevance.

Originally developed for ophthalmology, OCT operates in tissues with relatively homogeneous refractive indices (≈1.38 in the retina and cornea). In the cochlea, however, the optical environment is more complex: the RWM exhibits values between 1.40 and 1.44, while perilymph is closer to 1.33 [8, 13]. The refractive index of dry temporal bone ranges between 1.1 and 1.7, while that of fresh tissue may reach 1.4–2.2 [13]. Even small mismatches of this order can produce geometric distortions in OCT images, particularly when scanning across curved or oblique surfaces as the RWM. Such artifacts may lead to axial distortion and misrepresentation of tissue thickness or vector angles. Therefore, it may affect depth accuracy and the estimation of tissue thickness or orientation [13]. Advances in telecentric optics and polarization-sensitive detection have already reduced part of this error, but accurate intraoperative imaging will ultimately require refined correction algorithms and a better characterization of the refractive properties of cochlear tissues [16].

While Starovoyt's OCT platform offered detailed anatomical insights, it was not clinically applicable due to a working distance limitation of 25.1 mm. In contrast, the surgical microscopes evaluated in our study allowed

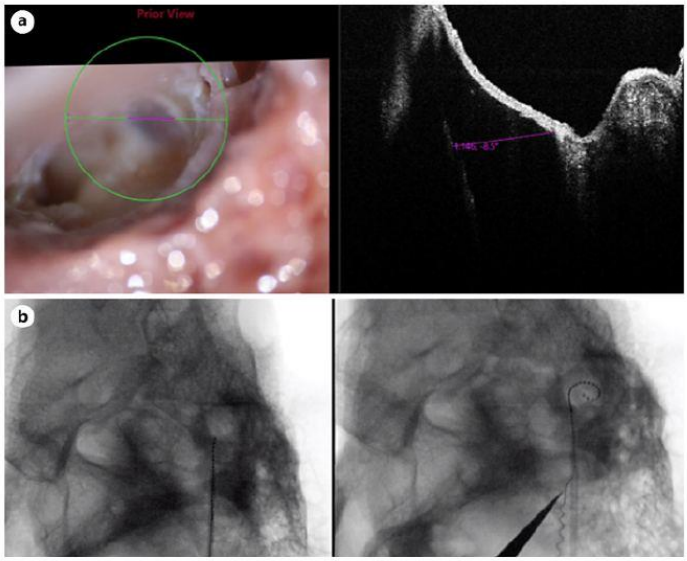

Fig. 8. Combined OCT and fluoroscopy in the left ear. Panel **a** shows OCT imaging through the RWM, with ST diameter measured between the CF and OSL, consistently above 0.8 mm. Panel **b** shows fluoroscopy confirming CI32 sheath remains straight after insertion.

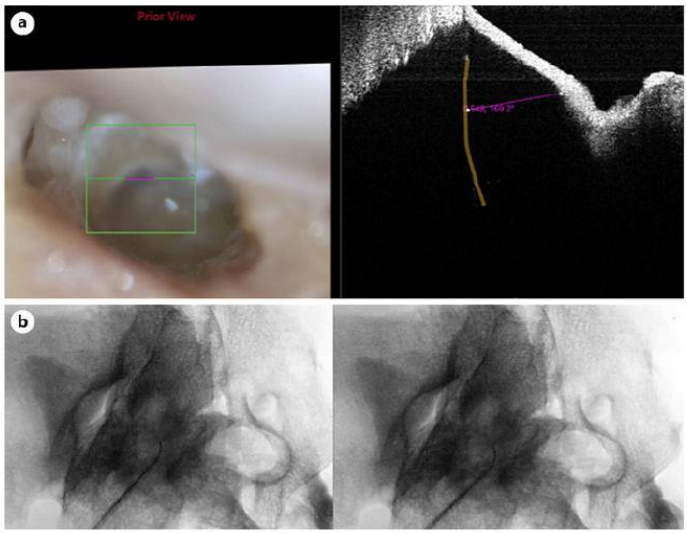

Fig. 9. OCT and fluoroscopy of the right ear. Panel **a** shows RWM with ST diameter between CF and OSL in orange below 0.8 mm. Panel **b** fluoroscopy demonstrates CI32 sheath deforming during insertion, confirming OCT prediction of unsuitable round window access.

for working distances between 175 and 225 mm, enabling comfortable intraoperative integration and enhanced scan stability. Notably, the EnFocus system also incorporated adaptive focusing and an automatic XY-Z tracking feature, which compensated for minor

movements in the surgical field and improved scan consistency during dynamic procedures.

The originality of this work lies in the use of microscope-integrated OCT, allowing imaging at a surgical working distance and within a standard operative workflow. This approach represents an important step toward the clinical translation of OCT as an intraoperative guidance tool in cochlear implantation.

Assess Cochlear Microanatomy

This allowed preopening assessment of curvature and RWM thickness and offered insight into the orientation, diameter and depth of the proximal ST segment (hook region). Significant variability of these structures was seen which has been extensively described in the literature [6–9]. These findings illustrate that, through its high spatial resolution, OCT provides detailed visualization of individual critical intracochlear landmarks. This enables precise determination of the ST axis and orientation.

Predict the Electrode Type

In this study, two EAs from Cochlear® were evaluated: the CI22 (diameter: 0.3 mm) and the CI32 with an insertion sheath measuring 0.8 mm in diameter and 5.5 mm in length. Owing to the ability of intraoperative OCT to delineate key anatomical landmarks, including the CF, the SL, and the OSL, it was possible to define the axis and diameter of the ST. This information may, in turn, facilitate the selection of the most appropriate EA.

The CI22 electrode, being slim and straight, posed no such challenge and was inserted without resistance in multiple specimens. Given its compatibility with narrower hook regions, it did not require fluoroscopic validation. These findings align with previous literature suggesting that lateral wall arrays are more forgiving in difficult anatomies, though they may offer less modiolar proximity in the long term [21].

Predict the Most Suitable Surgical Cochlear Entry

One of the key questions in atraumatic cochlear implantation is whether insertion can be achieved via the round window, thereby avoiding drilling [22]. Given that OCT is capable of delineating critical intracochlear structures, it is reasonable to assume that it may assist not only in selecting the most appropriate EA but also in determining the optimal surgical approach, whether RWM, extended RWM, or cochleostomy, based on both the diameter and the curvature of the proximal ST. This issue, which represents a central focus of our investigation, is particularly relevant for perimodiolar electrodes, which are inherently less flexible and larger due to the presence of their insertion sheath [21].

Can a Blue-Lined Cochleostomy Help Us See Deeper?

Thus, OCT provides not only the capacity to guide the choice between a RWM and an extended RWM/cochleostomy approach, but also, when an extended RW (eRW) or CS is required, the ability to determine the precise extent of drilling necessary to ensure the straightest and least traumatic insertion possible. In summary, intraoperative OCT emerges as a pivotal decision-making tool in tailoring the surgical approach to the patient's individual cochlear anatomy.

Can the Electrode Insertion Trajectory Be Followed?

Our findings highlight the potential of intraoperative OCT to actively guide electrode advancement and to minimize the risk of structural damage, thereby supporting safer and more atraumatic cochlear implantation. However, it should be noted that electrode trajectory can only be visualized and followed within the cochlea as far as the imaging depth and resolution of the OCT system allow, which may vary depending on the microscope model and its technical specifications.

Clinical Applicability on 2 Temporal Bones

These examples illustrate the role of intraoperative OCT in anticipating risk and guiding real-time decisions on electrode type and insertion vector. Despite recent imaging advances, OCT remains limited by bone shadowing, particularly in the basal turn where the dense otic capsule obstructs light penetration. Optimization of static scan mode and deliberate adjustment of imaging angles may help reduce these constraints. In our study, improvements in scan depth, lateral resolution, and rotational scanning, particularly with the EnFocus system, enabled a more comprehensive visualization of the hook region. Compared with earlier platforms, the ability to acquire images along multiple axes (two perpendicular planes, parallel sweeps, and rotational paths) provided greater flexibility and broader anatomical coverage [20].

The RESCAN 700 system, although offering real-time visualization within a familiar surgical workflow, was restricted by its fixed scan angle, absence of intraoperative measurement tools, and limited adaptability. These shortcomings frequently resulted in shallow scan planes or artifacts, especially in specimens with narrow ST morphology. In contrast, the EnFocus OCT, integrated into a surgical microscope with foot pedal-

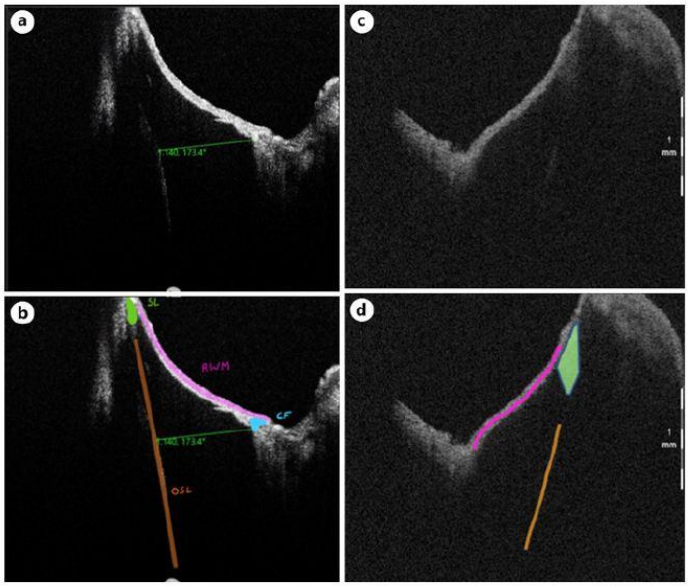

Fig. 10. Comparative intraoperative OCT imaging of cochlear anatomy. EnFocus system images (**a**, **b**, right ear) show the RWM in pink and OSL in orange, with precise visualization of the spiral ligament in green and CF in blue, and allow direct morphometric assessment of ST diameter (1.14 mm). Rescan 700 images (**c**, **d**, left ear) delineate the RWM and OSL but depict the spiral ligament and SSL only coarsely in light green.

controlled zoom and focus, overcame many of these limitations. It combined real-time measurements, rotational scan modes, and a superior axial resolution (<4 μm at ≥32,000 A-scans/sec) with extended working distance and higher scan density. This configuration allowed deeper and clearer visualization of cochlear microstructures. For instance, the cochlear fenestra (CF) and spiral lamina (SL) were distinctly imaged, whereas their delineation was less reliable with the Rescan 700 system (shown in Fig. 10). Nevertheless, distinguishing between the SSL and SL remains beyond current resolution capabilities.

A formal agreement analysis between OCT and micro-CT measurements (e.g., Bland-Altman) was not performed as it requires systematically paired measurements obtained under standardized conditions across all specimens. Future studies using dedicated acquisition protocols and analysis pipelines will be necessary to enable such quantitative validation. Collectively, these findings highlight the potential of OCT not only as a tool for anatomical assessment but also as a surgical guide, particularly in complex cochlear anatomies where conventional visual inspection may underestimate trajectory mismatches.

To unlock the full potential of OCT in otologic surgery, several technical improvements are needed. Increasing the signal-to-noise ratio, optimizing image processing algorithms, and implementing adaptive optics would improve both image quality and intraoperative usage. Enhancing scanning density and increasing light intensity (within safe limits) could facilitate deeper imaging and sharper resolution of cochlear structures. Additionally, software integration with automatic cochlear segmentation and real-time 3D reconstruction would assist in evaluating RWM transparency, ST curvature, and ossicular chain mobility. Ultimately, the development of an ENT-specific surgical microscope, optimized for cochlear imaging and integrating OCT with customized optics and dedicated software, may be the next step toward achieving true intraoperative guidance and trauma-free insertion.

Conclusion

This cadaveric study demonstrates the feasibility of the intraoperative usage of microscope-integrated OCT in cochlear implant surgery. It provides accurate, real-time visualization of cochlear microanatomy in the complex region behind the RWM, improves pre-insertion assessment, and enables tailored electrode selection based on individual anatomy. The integration

of such imaging tools into the surgical workflow represents a paradigm shift toward personalized, anatomy-driven cochlear implantation.

Some practical and technical improvements are required to translate OCT into real-time, intraoperative use. Nevertheless, this study lays an important foundation for the evolution of cochlear implantation from a tactile, blind procedure into one guided by precision imaging and dynamic anatomical feedback.

Statement of Ethics

This study was performed in accordance with the Declaration of Helsinki and was approved by the Royal Victorian Eye and Ear Hospital Human Research Ethics Committee (HREC), Approval No.: 15/1221h/20. Written informed consent to participate in the study was obtained from all donors (or their parent/legal guardian/next of kin, where applicable).

Conflict of Interest Statement

The authors declare no conflicts of interest. The Leica and Zeiss microscopes used in this study were rented exclusively for research purposes and only for the duration of the study.

Funding Sources

The present study did not require funding.

Author Contributions

G.G. conceptualized the study, collected the data, and was the lead author in drafting and revising the manuscript. P.H.R. and S.W. performed the statistical analysis, contributed to data collection interpretation, and assisted in manuscript preparation. J.M.G., S.O.L., and P.P. provided supervision throughout the project, critically revised the manuscript, and contributed to the interpretation of the findings. All authors meet the ICMJE criteria for authorship and approved the final version of the manuscript.

Data Availability Statement

All data necessary for a comprehensive understanding of the present study are fully available within this article. Further inquiries can be directed to the corresponding author.

References

1 Woodson EA, Reiss LAJ, Turner CW, Gfeller K, Gantz BJ. The Hybrid cochlear implant: a review. Adv Otorhinolaryngol. 2010;67:125–34. https://doi.org/10.1159/000262604

2 Schaefer S, Sahwan M, Metryka A, Kluk K, Bruce IA. The benefits of preserving residual hearing following cochlear implantation: a systematic review. Int J Audiol. 2021;60(8):561–77. https://doi.org/10.1080/14992027.2020.1863484

3 Aschendorff A, Kromeier J, Klenzner T, Laszig R. Quality control after insertion of the nucleus contour and contour advance electrode in adults. Ear Hear. 2007;28(2 Suppl l):75S–9S. https://doi.org/10.1097/aud.0b013e318031542e

4 Finley CC, Holden TA, Holden LK, Whiting BR, Chole RA, Neely GJ, et al. Role of electrode placement as a contributor to variability in cochlear implant outcomes. Otol Neurotol. 2008;29(7):920–8. https://doi.org/10.1097/MAO.0b013e318184f492

5 Hoskison E, Mitchell S, Coulson C. Systematic review: radiological and histological evidence of cochlear implant insertion trauma in adult patients. Cochlear Implants Int. 2017;18(4):192–7. https://doi.org/10.1080/14670100.2017.1330735

6 Li PMMC, Wang H, Northrop C, Merchant SN, Nadol JB. Anatomy of the round window and hook region of the cochlea with implications for cochlear implantation and other endocochlear surgical procedures. Otol Neurotol. 2007;28(5):641–8. https://doi.org/10.1097/mao.0b013e3180577949

7 Schart-Morén N, Agrawal SK, Ladak HM, Li H, Rask-Andersen H. Effects of various trajectories on tissue preservation in cochlear implant surgery: a micro-computed tomography and synchrotron radiation phase-contrast imaging study. Ear Hear. 2019;40(2):393–400. https://doi.org/10.1097/AUD.0000000000000624

8 Starovoyt A, Pyka G, Putzeys T, Balcaen T, Wouters J, Kerckhofs G, et al. Human cochlear microstructures at risk of electrode insertion trauma, elucidated in 3D with contrast-enhanced microCT. Sci Rep. 2023;13(1):2191. https://doi.org/10.1038/s41598-023-29401-6

9 Snels C, IntHout J, Mylanus E, Huinck W, Dhooge I. Hearing preservation in cochlear implant surgery: a meta-analysis. Otol Neurotol. 2019;40(2):145–53. https://doi.org/10.1097/mao.0000000000002083

10 Atturo F, Barbara M, Rask-Andersen H. On the anatomy of the "hook" region of the human cochlea and how it relates to cochlear implantation. Audiol Neurootol. 2014;19(6):378–85. https://doi.org/10.1159/000365585

11 Erixon E, Högstorp H, Wadin K, Rask-Andersen H. Variational anatomy of the human cochlea: implications for cochlear implantation. Otol Neurotol. 2009;30(1):14–22. https://doi.org/10.1097/MAO.0b013e31818a08e8

12 Kerkhofs L, Starovoyt A, Wouters J, Putzeys T, Verhaert N. Optical coherence tomography-based atlas of the human cochlear hook region. J Clin Med. 2022;12(1):238. https://doi.org/10.3390/jcm12010238

13 Starovoyt A, Putzeys T, Wouters J, Verhaert N. High-resolution imaging of the human cochlea through the round window by means of optical coherence tomography. Sci Rep. 2019;9(1):14271. https://doi.org/10.1038/s41598-019-50727-7

14 Starovoyt A, Quirk BC, Putzeys T, Kerckhofs G, Nuyts J, Wouters J, et al. An optically-guided cochlear implant sheath for real-time monitoring of electrode insertion into the human cochlea. Sci Rep. 2022;12(1):19234. https://doi.org/10.1038/s41598-022-23653-4

15 Schoovaerts M, Ourak M, Borghesan G, Putzeys T, Poorten EV, Verhaert N. OCT-based intra-cochlear imaging and 3D reconstruction: ex vivo validation of a robotic platform. Int J Comput Assist Radiol Surg. 2024;19(5):917–27. https://doi.org/10.1007/s11548-024-03081-7

16 Drexler Drexler W, Fujimoto JG. Optical coherence tomography technology and applications: Springer; 2015.
17 Breinbauer H, Praetorius M. Variability of an ideal insertion vector for cochlear implantation. Otol Neurotol. 2015;36(4):610–7. https://doi.org/10.1097/MAO.0000000000000719
18 Avci E, Nauwelaers T, Hamacher V, Kral A. Three-dimensional force profile during cochlear implantation depends on individual geometry and insertion trauma. Ear Hear. 2017;38(3):e168–79. https://doi.org/10.1097/AUD.0000000000000394
19 McRackan TR, Balachandran R, Blachon GS, Mitchell JE, Noble JH, Wright CG, et al. Validation of minimally invasive, image-guided cochlear implantation using Advanced Bionics, Cochlear, and Medel electrodes in a cadaver model. Int J Comput Assist Radiol Surg. 2013;8(6):989–95. https://doi.org/10.1007/s11548-013-0842-6
20 Pau HW, Lankenau E, Just T, Behrend D, Hüttmann G. Optical coherence tomography as an orientation guide in cochlear implant surgery? Acta Otolaryngol. 2007;127(9):907–13. https://doi.org/10.1080/00016480601089408
21 Dhanasingh A, Jolly C. An overview of cochlear implant electrode array designs. Hear Res. 2017;356:93–103. https://doi.org/10.1016/j.heares.2017.10.005
22 Wanna GB, Noble JH, Carlson ML, Gifford RH, Dietrich MS, Haynes DS, et al. Impact of electrode design and surgical approach on scalar location and cochlear implant outcomes. Laryngoscope. 2014;124(06):S1–7. https://doi.org/10.1002/lary.24728

Contribution to the existing literature

Optical coherence tomography of the human cochlea had previously been performed on benchtop platforms with working distances incompatible with surgery. This study evaluates a microscope-integrated system at a genuine surgical working distance and shows that the structures of the hook region, in particular the osseous spiral lamina, the crista fenestra and the spiral ligament, can be identified through the intact round window membrane before it is opened. It therefore provides micrometre-scale information that none of the imaging modalities currently available in the operating room can resolve, and which could be used to verify, and if necessary to rectify, an insertion trajectory planned preoperatively. The study further suggests that intraoperative imaging could help to anticipate whether a perimodiolar array can be inserted atraumatically in a given cochlea, a question that would warrant dedicated studies to assess the full potential of these arrays. The design is descriptive and cadaveric, and the contribution is therefore one of feasibility, together with the identification of its current limitations, chiefly bone shadowing in the basal turn.

3.2 During the Insertion Phase: Robotic-Assisted Cochlear Implant Surgery (RACIS)

3.2.1 State of the Art

3.2.1.1. Interindividual Variability in Cochlear Implant Outcomes

Auditory outcomes achieved after cochlear implantation in adults exhibit marked interindividual variability, which constitutes a major challenge in otology. This heterogeneity persists despite standardized technical procedures and seemingly similar clinical profiles, suggesting the involvement of multiple factors, anatomical, technological, cognitive, motivational, and environmental, interacting in a complex manner. As a result, an individualized approach is required, and inter-patient comparisons should be interpreted within a statistical and multifactorial framework rather than considered in isolation, since each trajectory is unique and shaped by a constellation of interdependent variables.

Among the principal determinants identified are the duration of preoperative deafness, the age at implantation, the presence and quality of residual hearing, pre-implantation auditory performance, the selected coding strategy, the technological generation of the implant, as well as the patient's cognitive, motivational, and attentional capacities. A key additional factor is cerebral plasticity, which plays a particularly critical role during the first years following implantation [169].

This variability also necessitates a rigorous and personalized preoperative assessment, encompassing not only audiological and anatomical data, but also psychological, familial, and environmental contexts. Regular auditory stimulation from the surrounding environment, particularly by close relatives, is essential for optimizing auditory learning and facilitating rehabilitation. In this context, expectations must be realistic and statistically tailored to each individual.

Performance disparities are not limited to cochlear implants, but are also observed with other auditory rehabilitation devices, underscoring the importance of intrinsic factors such as the

duration of sensory deprivation or the level of residual hearing. Each technology places differing demands on the plasticity of the central auditory system:

- With conventional hearing aids, the individual exploits residual auditory capacity, enventually limited to a narrow frequency band, associated with disturbed loudness and temporal cues.
- Frequency compression devices require adaptation to newly accessible sounds, necessitating specific decoding learning.
- Cochlear implants entail a complete frequency, loudness and temporal cues remapping, making rehabilitation longer and more complex, particularly in older patients or those with prolonged auditory deprivation.
- In bimodal stimulation, the patient must adapt to two different modes of stimulation and integrate them simultaneously, despite their potential redundancy. When successful, this integration can provide broader and enriched access to acoustic cues.

3.2.1.2. Performance Heterogeneity: Perceptual and Neurobiological Factors

Neural Degeneration and Its Impact on Auditory Outcomes

In patients with severe to profound hearing loss, progressive degeneration of the auditory nerve is frequently observed, typically beginning at the level of the peripheral dendrites and evolving toward the loss of spiral ganglion cell bodies [170–172]. However, the effectiveness of a cochlear implant depends on the functional integrity of a sufficient number of residual auditory neurons capable of transmitting auditory signals to the central nervous system. This prerequisite raises a fundamental question: how many neurons are required to ensure effective speech perception after implantation? Otte et al. [153] proposed an arbitrary threshold of approximately 10,000 spiral ganglion neurons, representing one-thirds of the normal neuronal population, as a prerequisite for meaningful speech discrimination, with sufficient neural density required in the apical cochlear region (at least 3,000 of these must be located in the apical 10 mm). However, a histopathological analysis conducted on 62 human cochleae from patients with profound deafness revealed that only 45% of them reached this threshold [153,173–175].

Moreover, several post-mortem studies have shown that neural degeneration worsens with the duration of deafness and typically begins in the basal region of the cochlea, the very area primarily targeted by the implant's electrode array [173–175]. These observations justify implantation as early as possible, in order to maximize the likelihood of stimulating still-functional auditory fibers.

Despite the gradual lowering of the age at implantation, the long-term fate of residual auditory fibers following implantation remains an open question. If neural degeneration continues after the implant is placed, auditory outcomes may be compromised in the long term. This hypothesis was suggested by Pfingst in an experimental study conducted in implanted macaques [176]. He observed a progressive drift in perceptual thresholds over time. However, this study presents several important methodological limitations, including the absence of post-mortem histological analysis to confirm neuronal degeneration as the underlying cause of threshold increases, and the identification by the authors themselves of at least two distinct mechanisms underlying these changes, suggesting that threshold variations may reflect alterations in the electrode–neuron interface or tissue properties rather than progressive neuronal degeneration.

Moreover, in contrast to the hypothesis of progressive degeneration, substantial evidence supports the concept of neural preservation induced by electrical stimulation, particularly in human post-mortem studies. Histopathological investigations in humans, notably the study by Seyyedi et al. (2013) on 26 pairs of human temporal bones, demonstrated that chronic electrical stimulation significantly improves the survival of spiral ganglion cells in cochlear segments containing electrodes compared to contralateral non-implanted ears [177]

The underlying neuroprotective mechanism has been further elucidated by recent studies on human temporal bones showing that electrical stimulation increases the expression of brain-derived neurotrophic factor (BDNF) in spiral ganglion neurons [178]. These human findings are supported by multiple animal studies demonstrating a synergistic effect of electrical stimulation combined with neurotrophic factors such as GDNF and BDNF on neuronal survival [179,180].

Longitudinal clinical data from large cohorts of cochlear implant users further indicate that electrical thresholds generally stabilize within 6–12 months after device activation. Analysis of more than 10,000 implants suggests that age at implantation, rather than duration of stimulation, is the primary determinant of auditory nerve responsiveness, with evidence of positive peripheral neural plasticity in younger individuals [181].

It should be noted, however, that not all studies have demonstrated a protective effect of electrical stimulation alone. Some experimental data suggest that chronic electrical stimulation may not prevent spiral ganglion cell degeneration under certain conditions [182,183], and that acute high-intensity electrical stimulation may induce synaptic alterations in the peripheral auditory system [184].

Nevertheless, the current body of evidence overall supports a predominantly neuroprotective role of chronic electrical stimulation, particularly when initiated early, highlighting the complexity of interpreting long-term electrophysiological changes following cochlear implantation.

Taken together, these findings highlight that long-term changes in auditory performance after cochlear implantation should not be interpreted as a simple marker of progressive neural degeneration, but rather as the result of complex and potentially reversible interactions between neural survival, electrode–tissue interface, and central auditory plasticity.

These findings have led to the development of strategies aimed at minimizing intracochlear trauma during electrode insertion. Innovations in this area include the adoption of atraumatic sealing techniques [185,186], the administration of pharmacological agents with anti-inflammatory properties to protect neural structures [187,188], and the introduction of robotic-assisted surgery to improve precision and consistency of the surgical procedure [189,190].

In clinical practice, in vivo assessment of the auditory nerve status in implanted patients remains a major challenge. Several indirect approaches have been proposed to estimate the degree of neural degeneration. From a psychoacoustic perspective, the presence of cochlear “dead regions”, areas with no functional auditory response, can be identified. These influence the quality of stimulation and may be targeted for electrode-specific deactivation, thereby optimizing coding strategies and prolonging device lifespan [191,192]. However, such methods do not provide direct information about neuronal density, but rather about local sensitivity to specific types of stimulation.

Another approach relies on the analysis of electrophysiological responses, notably auditory brainstem responses (eABRs) and compound action potentials of the auditory nerve (eCAPs). Prado-Gutierrez et al. demonstrated in an animal model that pulse phase duration and inter-phase gap (IPG) modify the intensity–response curves of these signals [193]. They revealed a strong correlation between these parameters and spiral ganglion neuron density, with curve modifications being attenuated or even absent in cases of pronounced degeneration.

Based on these findings, Ramekers et al. proposed a refined method for analyzing the characteristics of eCAPs recorded under each electrode, allowing for estimation of the local degenerative state of nerve fibers [194]. This approach, still under investigation, could pave the way for advanced individualization of stimulation parameters, tailoring coding strategies to the patient's precise neurofunctional profile at each stage of the implantation journey.

Preservation of Residual Hearing and Benefits of Electro-Acoustic stimulation

In adults, high-frequency sensorineural hearing loss is the most frequently encountered form. It is generally associated with a combination of etiologies, including age-related degeneration, genetic predisposition, metabolic and inflammatory processes, as well as environmental factors such as noise exposure and ototoxic treatments, and primarily affects the basal region of the cochlea. In this context, apical hair cells may remain functional, allowing for some perception of low-frequency sounds. However, the perception of consonants, rich in high frequencies crucial for speech intelligibility, remains significantly impaired. This spectral dissociation often results in very poor word recognition scores, especially since acoustic amplification becomes ineffective when thresholds exceed 65 dB HL in high frequencies [195,196].

To address this limitation, cochlear implantation surgery has progressively evolved toward so-called atraumatic techniques aimed at preserving residual hearing. This shift has led to the development of technical strategies such as partial insertion of long electrodes and the use of shorter or more flexible electrode models [101,103,197–200]. These advances have expanded the indications for cochlear implantation to a new population of patients with partial deafness, particularly those presenting with high-frequency hearing loss and preserved apical hearing.

This paradigm shift has favored the emergence of electro-acoustic stimulation (EAS), which combines electrical stimulation of high frequencies via the implant with acoustic stimulation of low frequencies via a hearing aid. This hybrid approach optimizes overall perception, particularly in noisy environments. Gantz et al. [201] reported that, in EAS patients, the speech recognition threshold in noise is strongly correlated with the average hearing threshold at 125, 250, and 500 Hz ($r = 0.62$; $p < 0.05$). Among responders to EAS treatment (i.e., patients who achieved significant improvement in speech perception through combined electric-acoustic processing), preoperative intelligibility and duration of deafness accounted for 33% of the variance in outcomes, compared to 91% among non-responders (i.e., patients who did not achieve significant speech perception improvement despite EAS).

Dorman et al. [202] confirmed this benefit, observing an average improvement of 19% in speech understanding scores in the EAS condition, along with a significant reduction in interindividual variability compared to the implant-alone condition. These results are comparable to those historically obtained by Helms et al. [203] in the implant-alone setting, confirming that the observed advantage indeed results from the additional acoustic input.

Beyond EAS, the presence of functional contralateral residual hearing is also a favorable factor in bimodal stimulation. It significantly improves speech perception in noise [204,205].

However, the influence of preoperative residual hearing on the implanted side remains controversial [205–207]. Adunka et al. [207], in a study with one-year follow-up after implantation, found no significant performance differences between two matched patient groups, suggesting that the mere presence of residual hearing is not a reliable predictive factor. This finding contradicts other studies that identified a moderate correlation between preoperative intelligibility and post-implantation outcomes [208,209].

The evolving profile of implanted patients, with residual hearing becoming increasingly frequent, complicates the interpretation of longitudinal series. Tyler et al. [210] illustrated this transformation through an improvement in preoperative thresholds at 250 Hz between 1986 and 1999, reflecting a progressive broadening of candidacy criteria [77,78,210]. However, the 250 Hz threshold may be biased by vibratory sensations, and Van Dijk et al. [211] suggested that the 1000 Hz threshold would be a better predictor of post-implantation outcomes.

Thus, beyond the mere presence of residual hearing, it is its capacity to provide complementary spectral, temporal, and harmonic information, particularly through low-frequency encoding of fundamental frequency, temporal envelopes, and distortion products, and its functional integration into hybrid strategies, such as bimodal or electro-acoustic stimulation, that appear to be most determinant for improving outcomes.

3.2.1.3. Robotic-Assisted Cochlear Implant Surgery

3.2.1.3.1. Introduction and Evolutionary Context of Cochlear Implantation

Auditory Restoration with Structural Preservation and Functional Optimization

CIs have become, over recent decades, the reference treatment for severe-to-profound sensorineural hearing loss. Initially reserved for patients with little or no residual acoustic hearing, they were long considered incompatible with the preservation of intracochlear structures. From the 1980s onward, this paradigm was challenged by studies demonstrating both the feasibility and the importance of preserving cochlear anatomy and certain sensory functions, including residual acoustic hearing [212]. This conceptual shift led to the emergence of EAS, introduced by von Ilberg et al. [198], whose first clinical trials using short electrode arrays (6–10 mm) demonstrated the feasibility of hearing preservation [213].

Despite substantial technological progress, the overall auditory performance of CI users has shown limited improvement over recent decades [214,215]. In contrast, the ability to preserve residual hearing has emerged as a key determinant for optimizing post-implantation outcomes. The benefits of EAS include improved speech understanding in noise, more accurate spatial localization, enhanced music perception, and improved quality of life [101,216–218]. These findings have been further corroborated by studies demonstrating functional superiority compared with exclusively electric stimulation [200,201].

Even in the absence of usable acoustic hearing, the occurrence of insertion-related trauma has been identified as a predictive factor for reduced neuronal survival and poorer long-term outcomes [113,219]. Despite modern hearing-preservation techniques, complete anatomical integrity of the cochlea remains difficult to guarantee.

Limitations of Manual Insertion and the Emergence of Robotic Assistance

In the majority of cases, electrode array insertion is still performed manually. This approach presents major limitations related to human motor variability and the surgeon's limited sensitivity to the forces applied within the cochlea.

Immediate postoperative hearing loss often reflects acute intracochlear trauma. However, a significant proportion of patients experience delayed hearing loss, occurring several months to several years after initial hearing preservation [220,221]. This observation suggests that even minimal trauma may trigger an inflammatory and fibro-osseous cascade responsible for the progressive deterioration of residual hearing.

So-called "atraumatic" techniques aim to minimize this acute trauma [222]. Nevertheless, the inherent limitations of manual insertion are well documented:
– the minimal force required to damage intracochlear tissues is below the threshold of human tactile perception,
– insertion speed and regularity vary between surgeons,
– these variations result in an inability to reliably guarantee a truly atraumatic insertion [223–225].

These limitations explain why approximately 50 % of patients with immediate hearing preservation experience a significant loss (>10–20 dB) over time. Furthermore, complete loss of residual hearing occurs in approximately 20–25% of patients with initially preserved hearing at long-term follow-up, although this rate varies considerably between studies (range 10–50%), depending on electrode design, surgical technique, and follow-up duration [90,101,122,154,155,199,226]. A meta-analysis by Snels et al. [227] confirmed a declining trend in hearing preservation outcomes over time, regardless of the surgical approach or electrode type used.

In this context, otologic robotics has emerged to provide more precise, more stable, and less invasive access to the cochlea [228]. Robotic assistance for electrode array insertion represents one of the most promising advances, aiming to overcome the intrinsic limitations of human motor control.

3.2.1.4. General Philosophy of RACIS

All of these systems share a common objective: to provide controlled, regular, and stable electrode insertion, surpassing the limitations of human motor control.

The shared conceptual principles include:
– reduction of insertion forces,
– reduction of intracochlear pressure peaks,
– prevention of scalar trauma,
– potential improvement in hearing preservation.

These principles support the idea that robotics may contribute to standardizing the surgical gesture, reducing inter-operator variability and opening the way to new approaches in cochlear implantation.

3.2.2 Robotic Platforms for Surgical Assistance: Principles and Classification

3.2.2.1. Existing Robotic Systems and Design Philosophies

Over the past decade, several robotic platforms dedicated to otologic microsurgery, and more specifically to cochlear implantation, have emerged. Among the most significant developments are:

- **RobOtol® (Collin Medical, Bagneux, France), designed by Sorbonne University / AP-HP** [229,230],
- **HEARO®**, developed at the University of Bern [231],
- **OTODRIVE®** (CASCINATION AG, Switzerland and MED-EL, Austria),
- **iota-SOFT Insertion System** (iotaMotion Inc., Iowa City, USA) [232,233]
- Automated insertion tool developed at Hannover Medical School, Germany [234,235].
- **Micro-stereotactic frames** developed at Vanderbilt University Medical Center [236].

Robotic Insertion Systems Using the Conventional Surgical Approach

Some systems (RobOtol®, iotaSOFT®, and OTODRIVE®) are based on the conventional surgical approach (mastoidectomy and posterior tympanotomy) and provide motorized assistance aimed at stabilizing and regularizing electrode insertion, while reproducing the trajectory of a manual approach.

These systems allow compatibility with all electrode array types, following a philosophy of graduated assistance rather than replacement of the surgeon's manual gesture.

Commercially available systems fitting this paradigm include:
- **iota-SOFT® Insertion System** (iotaMotion Inc., Iowa City, USA) [232,233],
- **RobOtol®** (Collin, France) [229,230],
- **OTODRIVE®** (CASCINATION AG, Switzerland and MED-EL, Austria).

These platforms provide controlled motorized kinematics, enabling reproducible insertion velocities and optimized trajectories.

RobOtol®: A Versatile Teleoperated System for Otologic Microsurgery

The RobOtol® surgical robot (Collin®, Bagneux, France) is a teleoperated system designed as a multitask platform tailored to the requirements of otologic microsurgery. Its objectives are to:
- improve gesture precision,
- optimize ergonomics,
- provide a stable platform for micro-instrumentation or endoscopy,
- enable the exploration of new surgical procedures.

RobOtol® has reached the clinical stage, where its use has proven to be safe and controllable, particularly for cochlear implant electrode array insertion [237] (Fig. 33).



Figure 33. RobOtol® (Collin®, Bagneux, France). Left: robotic workstation with operator interface. Right: robotic arm equipped with an electrode holder carrying a MED-EL FLEX24 electrode array. Reproduced from Barriat et al. (2021) [238].

Robotic Systems Using Direct Tunnel Access (Percutaneous Approach)

Other systems, such as HEARO®, Rosa® [239], and certain micro-stereotactic frames, adopt a radically different design philosophy: they create a narrow, direct tunnel between the cortical bone of the temporal bone and the cochlea, enabling percutaneous, image-guided access.

This type of approach requires specific stabilization solutions for the electrode array, because:
- the tunnel reduces the length of excess electrode cable,
- the fixed trajectory limits parasitic movements but does not guarantee the absence of migration,
- additional fixation (e.g., BonePate) remains recommended.

Available clinical series report the absence of electrode migration in cases of robotic insertion, although cohort sizes remain limited [240–243].

3.2.3 Robot-Assisted Procedure: Insertion Mechanisms, Safety, and Trauma

Control of Insertion Parameters: Speed, Force, and Precision

The central principle of RACIS is based on the use of a reduced and constant insertion speed, combined with lower insertion forces and a more reproducible trajectory than during manual insertion [244].

Safety and Precision of the Insertion Axis

Alignment of the electrode insertion axis is a critical determinant of intracochlear trauma: improper alignment increases the risk of scalar injury and translocation [245].

The RobOtol® system can be used safely and in a controlled manner as a support for micro-instruments or an endoscope; no complications directly related to the robot were reported in a clinical series of 32 cases, including 10 cochlear implantations. In this series, 7 of the 10 electrode insertions were located entirely within the scala tympani [237].

The mental representation of the optimal insertion axis depends strongly on the surgeon's experience, with substantial variability related to anatomical complexity; expert operators demonstrate superior accuracy [246]. In an experimental study on four human temporal bones, a semi-automated RobOtol®-based approach was evaluated, in which the optimal insertion trajectory was preoperatively planned from cone-beam CT imaging according to the scala tympani axis and facial nerve position; following electromagnetic registration, the robotic arm automatically positioned and oriented the insertion tool along this preplanned trajectory, a process that concerned the alignment of the instrument rather than an automated insertion of the cochlear electrode itself. The angular error between the insertion tool and the optimal reference axis was thereby reduced to 3.4° ± 1.56°, compared with 8.3° ± 2.82° for the manual procedure and 8.6° ± 2.83° for navigation-assisted manual alignment [247].

An optimized approach combining robotic alignment along the ideal axis (defined as the trajectory aligned with the longitudinal axis of the scala tympani, see Section 5.2) with a motorized insertion tool operating at a constant speed (0.25 mm/s) resulted in a significant increase in the number of electrodes fully positioned within the scala tympani compared with manual insertion ($P = 0.03$) [111].

Generation of Intracochlear Forces and Effects of Insertion Speed

The introduction of an EA into the cochlea generates several components of intracochlear forces arising from distinct mechanisms:

1. **Direct contact with cochlear structures.** The mechanical interaction of the EA with the lateral wall, the basilar membrane, and the osseous spiral lamina constitutes a primary source of force. These stresses increase when the electrode bends or deforms upon contact with an obstacle [248]. Initial resistance typically appears at a depth of approximately 5 mm and increases markedly between 8 and 10 mm, when the electrode tip reaches the basal turn or the posterior wall [249].
2. **Friction forces.** A second mechanism corresponds to friction between the EA and the endosteum, modulated by the lubricating effect of the perilymph [250]. Friction increases with the contact surface area, explaining the progressive rise in forces as insertion advances [251]. The relationship between insertion speed and friction, however, is complex: some models demonstrate minimal friction at very low speeds, a peak at intermediate speeds, and a decrease at higher speeds [250], whereas other studies do not identify a significant correlation [251].
3. **Intracochlear hydraulic pressure.** Displacement of perilymph by the EA generates pressure variations within the scala tympani. Pressure peaks observed during rapid insertions are comparable to extremely high acoustic exposures, such as explosive noise capable of inducing hair cell damage, with equivalent levels ranging from 134 to 174 dB SPL [252,253]. Slow and regular insertion, typically achieved through robotic assistance, allows more gradual perilymph displacement and improved pressure equalization, thereby reducing the frequency and amplitude of these pressure peaks [225,253,254], although some studies do not consistently confirm this relationship [255–257].

Overall, insertion speed appears to be one of the major determinants of intracochlear force generation: in a synthetic model, progressive increases in insertion speed resulted in higher mean and peak forces, with the lowest tested speed (≈ 0.16 mm/s) being associated with the lowest forces [244]. Several studies have confirmed this trend, regardless of electrode type or

insertion technique [234,235]. In cadaveric temporal bones, higher forces correlate with increased rates of cochlear trauma, particularly during passage through the basal turn [258,259]. Robotic assistance also reduces force variability (irregularities, jerks) typically observed during manual insertions [260] (Fig. 34).

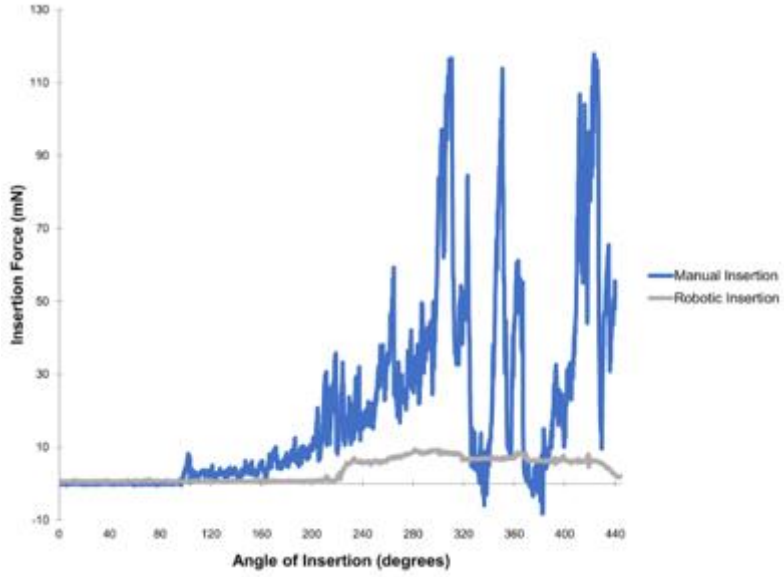

Figure 34. Force profiles obtained during a trial comparing manual and robot-assisted insertion. A PTFE phantom model, as described by Clark et al. [261], was used with a FLEX24 electrode array and a 10% soapy solution. A surgeon performed insertions as slowly as possible, first manually and then robot-assisted using the iotaSOFT system. Forces were recorded using a six-axis sensor. The resulting profiles are representative of data comparing automated and manual insertions [234,256,262]. Reproduced from Kashani et al. (2024) [223].

Reduction of Intracochlear Trauma

Extremely low forces are sufficient to alter cochlear micro-architecture. A pressure of approximately 42 mN can induce damage, with even lower thresholds for fragile structures such as the basilar membrane (26–35 mN) and Reissner's membrane (4.2 mN).These values reflect structural damage thresholds of cochlear tissues rather than forces typically applied during electrode insertion, and should therefore not be interpreted as representative of surgical conditions.

In controlled experimental conditions, insertion forces have been shown to remain within a range generally below 0.3 N, with critical thresholds often considered around 0.1 N for potential intracochlear damage, as demonstrated in temporal bone studies using force sensors [263]. Recent in vivo measurements using force-sensitive insertion tools have reported forces at the end of insertion ranging from 17.2 to 43.6 mN, with maximal peak forces between 44.8 and 102.4 mN, providing the first direct clinical quantification of intracochlear insertion forces [264].

The synthesis by Bas et al. identifies several major mechanisms that may lead to deterioration of auditory function [265]:

1. direct injury to hair cells along the basilar membrane;
2. activation of an inflammatory response evolving toward fibrosis;

3. damage to the spiral ligament and the stria vascularis, disrupting the endocochlear potential;
4. rupture of the basilar membrane resulting in scalar translocation;
5. high pressure peaks damaging sensory cells, analogous to acoustic trauma.

These traumatic events induce the expression of mediators such as TNFα and IL-1β, triggering hair cell apoptosis [266,267]. Intracochlear pressure peaks reproduce the effects of intense acoustic exposure, with accumulation of free radicals, oxidative stress, and tissue alterations [258]. Disruption of cochlear compartmentalization, mixing of perilymph and endolymph, or loss of the endocochlear potential secondary to strial injury further aggravate the functional deficit. The resulting trauma and inflammation promote intracochlear fibrosis, which is closely associated with reduced residual hearing and diminished cochlear implant performance [219,221,268].

The correlation between insertion force and intracochlear trauma has been clearly demonstrated [258]. The use of a motorized insertion tool has been shown to produce a more controlled and predictable force profile compared with manual insertion techniques, characterized by fewer abrupt force peaks and reduced variability, despite similar overall force momentum between techniques [263]. This effect is primarily attributed to the ability of motorized systems to maintain a constant insertion velocity and a stable insertion axis, thereby limiting sudden mechanical interactions with intracochlear structures.

Available data also highlight that insertion speed is a critical determinant of intracochlear force generation and its temporal profile. Surgeons generally aim to maintain a slow and stable insertion speed; however, human capabilities do not allow reliable achievement of the very low speeds considered optimal. The average speed achievable during continuous manual insertion is approximately 0.87 mm/s, whereas a speed of 0.25 mm/s is virtually unattainable for a human operator, as demonstrated by Kesler et al. [269].

Robotic assistance directly addresses this limitation by enabling highly controlled, constant, and very low insertion speeds, thereby reducing intracochlear forces [234] and certain forms of trauma such as tip fold-over [270]. This technological advantage complements its ability to stabilize the insertion axis, contributing to a more reproducible and atraumatic insertion process. Optimized robotic insertion has also been associated with less intracochlear trauma than manual insertion ($P = 0.04$) [111], with reduced force variability and fewer high-amplitude peaks, which are strongly associated with microstructural damage and scalar translocation, although quantitative force values are not systematically reported in these studies.

However, the relationship between insertion speed and intracochlear trauma is not strictly linear. Avci et al. did not observe significant differences in forces for speeds ranging from 0.05 to 2 mm/s [271], whereas Dhanasingh et al. described a non-linear relationship in which certain moderately low speeds paradoxically generated higher forces, although the overall trend still favored the lowest speeds [272]. Similarly, Kaufmann et al. showed that ultra-slow speeds (0.01 mm/s) increased maximal forces in synthetic models, without reproducing this effect in cadaveric temporal bones [260].

These findings suggest that excessively low speeds may increase prolonged mechanical contact, reduce the lubricating effect of perilymph, and exacerbate friction or transient pressure peaks. Such discrepancies are partly explained by differences between experimental models: synthetic models exhibit variable friction coefficients, whereas cadaveric temporal bones more accurately

reproduce cochlear mechanics, particularly due to the elasticity of the basilar membrane, albeit at the cost of anatomical variability [259,273]. Additional factors, including measurement methods, electrode design, insertion technique, and the physicochemical properties of the lubricating environment, further contribute to variability in reported results [273].

Thus, while a slow and stable insertion speed remains a major objective, selection of the optimal speed profile must take into account these experimental limitations and the complex mechanical interactions within the cochlea.

Traumatic insertions (scalar translocation or rupture of the basilar membrane) exhibit more irregular force profiles, with an early peak of approximately 30 ± 18.2 mN, corresponding to the initial contact of the electrode with the lateral wall of the cochlea [258]. This value should be interpreted as an early localized peak occurring during electrode–wall interaction, whereas higher thresholds around 0.1 N correspond to more global critical force levels associated with an increased risk of structural damage. At identical insertion depths, forces differ significantly between traumatic and atraumatic insertions ($p < 0.001$) [258]. The region between 150° and 180° of insertion angle represents a particularly high-risk zone for scalar translocation with certain straight electrode arrays [245].

Taken together, these findings suggest that not only the absolute magnitude of insertion forces, but also their temporal profile and variability, play a critical role in determining intracochlear trauma, with insertion speed emerging as a key modulator of these dynamics and a major lever for optimization through robotic-assisted techniques.

Finally**,** it should be noted that incorporation of dexamethasone into the electrode carrier silicone does not increase insertion forces and therefore does not appear to increase the risk of trauma [274].

Assessment of Intracochlear Trauma Associated with Robotics

Robotic insertion has been associated with a significantly lower number of traumatic events, notably a reduction in scalar translocation, compared with manual techniques [111].

This reduction in intracochlear trauma has important clinical and experimental implications, particularly regarding the preservation of residual hearing and the mechanistic understanding of insertion-related damage.

Preservation of Residual Hearing and the Importance of Atraumatic Insertion

Up to 80% of current cochlear implant candidates retain residual acoustic hearing, a proportion that is expected to increase further [275]. The literature robustly demonstrates that patients in whom this residual hearing is preserved achieve superior postoperative outcomes. The combination of acoustic stimulation (hearing aid) and electric stimulation (CI) improves pitch perception [276], speech understanding [277,278], listening in noise [216,279], and music appreciation [218,280]. However, residual hearing is lost in nearly half of patients, either early after surgery or progressively over several years [217].

Several studies, as previously discussed, suggest that reducing insertion speed may promote better clinical outcomes. Rajan et al. compared two insertion speeds (0.25 mm/s versus 1 mm/s) using the same electrode array and showed that slow insertion was associated with better

hearing preservation, more complete insertion, and a reduction in vestibular symptoms during the first 24 postoperative hours [224]. Confirmation of these benefits in terms of long-term auditory performance and quality of life, however, requires further studies.

Even in patients without usable residual hearing, atraumatic insertion remains essential. Intracochlear lesions may affect spiral ganglion neurons, which are the target structures of electrical stimulation [175,281]. Insertion trauma also triggers an inflammatory response leading to peri-electrode fibrosis, which increases electrical impedance, displaces the electrode away from the modiolus, and reduces stimulation efficiency [282]. This fibrosis has been associated with poorer scores on consonant–vowel–consonant word tests, a key indicator of auditory performance [141].

A meta-analysis estimated the overall rate of electrode scalar deviation (passage from the scala tympani to another cochlear compartment) at 12.66% (95% CI: 4.82–20.51%), being less frequent with robotic middle ear access (6.4%) and more common with robotic electrode insertion (17.1%) [283]. Scalar deviation was more frequent in the subgroup of robotic electrode insertion (17.11%) than in that of robotic access to the middle ear (6.43%) [283]. Navigation systems can be used to assess and improve surgeons' mental representation of the scala tympani axis, particularly in cochlear implant surgery [246].

Experimental Data on Robotic Systems: OTODRIVE and Others

The study by Chen et al. evaluated the safety and efficacy of the OTODRIVE system for cochlear implant electrode array insertion [57]. Fifteen human cadaveric temporal bones were implanted with different electrode arrays (FLEX26, FLEX28, FLEXSOFT, FLEX34). The OTODRIVE system maintained a constant insertion speed of 0.1 mm/s. Specimensimens were subsequently analyzed using SR-PCI to quantify intracochlear trauma (Fig. 35).

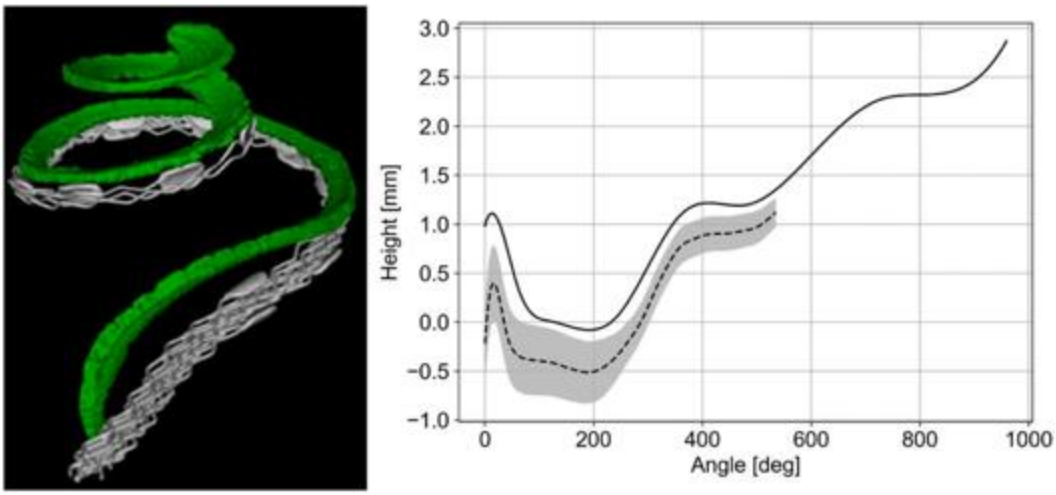

Figure 35. Left: example of 3D segmentation of the basilar membrane (green) and the electrode array (gray). Right: trauma evaluation curve, where the solid line represents the height of the basilar membrane, the dashed line the electrode center, and the shaded area the silicone body of the electrode array. Reproduced from Chen et al. (2025) [284].

The mean linear insertion depth was 24.8 ± 3.5 mm (min. 17.7; max. 31.4 mm), and the mean angular insertion depth was 527° ± 81° (min. 337°; max. 681°), corresponding to a mean cochlear coverage of 74% ± 7% (56–85%) [285]. The mean trauma score, according to the Eshraghi scale (Table 1), was 0.27 (min. 0; max. 2).

Grade of trauma	Extent of cochlear trauma
Grade 0	No observable trauma/ intact basilar membrane
Grade 1	Basilar membrane elevation
Grade 2	Scala media translocation
Grade 3	Scala vestibuli translocation
Grade 4	Osseous spiral lamina fracture
Grade 5	Osseous spiral lamina fracture and translocation

Table 2. Extent of cochlear trauma graded by the Eshraghi scale [111].

No cases of severe trauma were observed: there were no instances of tip fold-over, translocation into the scala vestibuli (Grade 3), fracture of the osseous spiral lamina (Grade 4), or combined fracture and translocation (Grade 5) [284]. Only three traumatic events were identified:
- one case of partial translocation into the scala media (Trauma Grade 2) (Fig. 36), in which the electrode tip had entered the scala media while the 11 basal contacts remained within the scala tympani, observed at an insertion angle of 535°;
- two cases of basilar membrane elevation at the apical end of the electrode array (Trauma Grade 1).

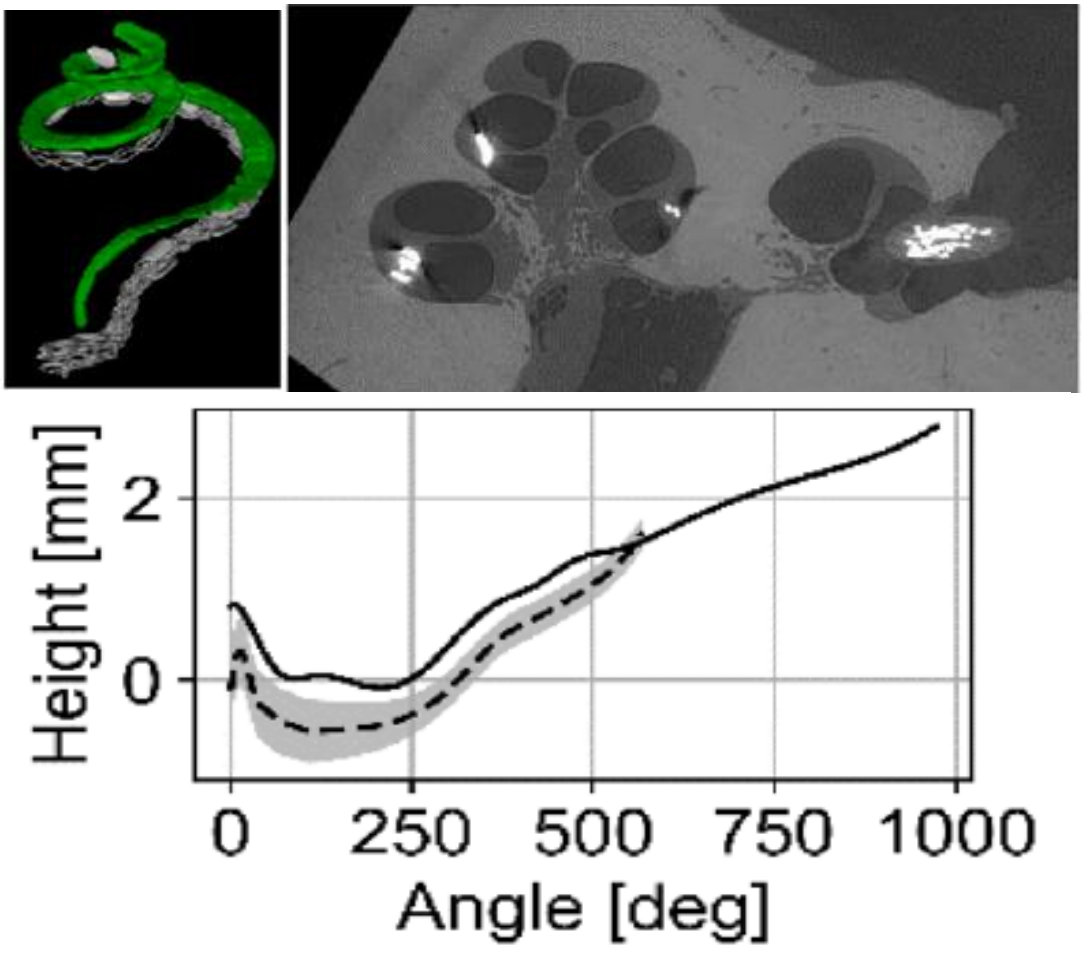

Figure 36. Example of a case showing partial translocation into the scala media (Trauma Grade 2). The solid line represents the height of the basilar membrane, the dashed line the electrode center, and the shaded area the silicone body. Upper right: 3D rendering of the basilar membrane and the electrode array; upper left: mid-modiolar sections obtained from SR-PCI imaging after robotic insertion. Reproduced from Chen et al. (2025) [284].

These results confirm that the OTODRIVE system enables precise and globally atraumatic insertion, with a low mean trauma score (0.27) and only minor events. Notably, no signs of trauma were observed in seven cases in which the insertion depth exceeded 500°, up to a maximum of 681° [284].

The conclusions of Chen et al. are consistent with those of Kaufmann et al., who compared manual and robot-assisted insertions [260]. In that study, manual insertions exhibited a mean trauma score of 3.1, compared with 0.9 for robot-assisted insertions. Manual insertions showed a high proportion of severe events: 25% scala vestibuli translocations, 17% fractures of the osseous spiral lamina, and 33% combined fracture and translocation injuries, whereas these events were absent in the robotic group (8%, 0%, and 0%, respectively) [260]. Robot-assisted insertions exhibited only minor trauma, mainly basilar membrane elevation (33%) and scala media translocations (17%) [260].

These experimental data highlight the potential of robotic systems to reduce intracochlear trauma, preserve structural integrity, and improve hearing preservation. However, clinical trials are still required to confirm these long-term benefits and to establish the superiority of robotic methods over conventional manual techniques in routine clinical practice.

Choice of Electrode Array and Surgical Approach for RACIS

The systematic review by Van de Heyning et al. [286] aimed to determine the electrode array type best suited to reducing complications during cochlear implant surgery, whether robot-assisted or conventional [286]. The complications analyzed included electrode tip fold-over (ETFO), electrode scalar deviation (ESD), and electrode migration (EM).

Electrode Tip Fold-Over (ETFO)

ETFO refers to a situation in which the tip of the EA becomes trapped and folds back on itself within the scala tympani, potentially leading to:
– a short circuit between apical contacts,
– pitch confusion,
– reduced speech understanding, sometimes by up to 20% on the Bamford–Kowal–Bench Speech Test (BKB) or the Hearing In Noise Test (HINT), although some cases report performance levels of up to 80% in quiet [287–289],
– co-stimulation of the facial nerve, vertigo, and potentially damage to the basilar membrane leading to fibrosis, hydrops, and ossification.

Surgical revision or deactivation of the involved contacts generally improves speech perception and resolves symptoms of facial nerve co-stimulation and vertigo [287,289]. Intraoperative imaging has been proposed as a means of detecting ETFO during surgery, allowing immediate correction [287,290].

ETFO is significantly more frequent with precurved electrode arrays (5.3%) than with straight electrodes (0.5%) [286]. This difference may be related to premature withdrawal of the stylet

or polymer sheath, orientation of the contacts away from the modiolar wall during insertion, or cochlear anatomical variations. Experimental studies on cadaveric temporal bones have shown that robotic insertion, by applying a constant speed along an optimized axis, can reduce intracochlear trauma [111]. It can therefore be expected that RACIS may reduce the frequency of traumatic insertions, although no evidence has yet demonstrated a reduction in ETFO rates for precurved electrodes. The future integration of haptic pressure feedback could help detect an electrode tip becoming trapped.

Electrode Scalar Deviation (ESD)

ESD corresponds to perforation of the basilar membrane, resulting in the presence of part of the apical contacts within the scala vestibuli. It occurs primarily between 90° and 180° of insertion angle and is associated with intracochlear fibrosis, neo-osteogenesis, and irreversible neuronal degeneration [141]. The resulting mixing of perilymph and endolymph may lead to complete loss of residual hearing.

ESD represents the most frequent severe intracochlear complication and is clearly associated with poorer auditory outcomes [291–293]. A meta-analysis showed that ESD reduced speech perception scores in patients implanted after post-lingual deafness and significantly decreased the likelihood of complete scala tympani placement [291]. O'Connell concluded that insertions strictly confined to the scala tympani provided better auditory outcomes and that ESD negatively affected low-frequency residual hearing [293].

In the review by Van de Heyning et al., ESD was more frequent with precurved electrodes (28.7%) than with straight electrodes (11%) [286]. Several factors contribute to this difference:

1. anatomical variability of the cochlear base and cochlear duct trajectory;
2. the standard orientation of the insertion axis, which directs precurved electrodes toward the modiolar wall; delayed withdrawal of the sheath or stylet may prevent the electrode from correctly following the cochlear spiral;
3. the intrinsic curvature of precurved electrodes, which may direct them upward toward the osseous spiral lamina rather than laterally;
4. the multidirectional flexibility of straight electrodes, which may reduce the risk of modiolar wall injury [294].

Robotic systems have demonstrated superiority in terms of directionality and precision. Doudi et al. compared 40 manually operated patients with 20 patients implanted with robotic assistance and observed a lower rate of ESD for straight electrodes in the robotic group [115]. Barriat et al. reported a mean hearing preservation of 13.60 ± 7.70 dB, correlated with a lower insertion speed (0.88 ± 0.12 mm/s) achieved using RobOtol® [238]. Animal studies show that more flexible electrodes result in less ESD, reduced intracochlear fibrosis, and better hearing preservation [295].

The cochlear approach also influences the incidence of ESD. Early cochleostomy series reported higher rates of scalar deviation [296], whereas more recent studies did not confirm a significant difference between cochleostomy and RW approaches [297]. However, several meta-analyses demonstrate that the RW approach is associated with a lower incidence of ESD compared with cochleostomy [130,298]. A consensus statement has recommended the RW approach, supported by histopathological observations suggesting less trauma [299] and by a clinical study showing greater hydrops and fibrosis in the scala tympani and scala vestibuli after

cochleostomy than after RW insertion [300]. In living subjects, no ESD was observed following RW insertion, in contrast to cochleostomy [300].

Thus, robotic surgery centered on round window access aims to ensure minimally traumatic access consistent with normal anatomy [301]. Cadaveric studies show that slow, coaxial motorized insertions reduce the incidence of ESD [247]. Nevertheless, ESD may still occur with precurved electrodes even under robotic assistance [242]. For straight electrodes, robotics improves accuracy of scala tympani placement, limits injury to scalar walls, and provides optimal orientation, thereby reducing human error and inter-surgeon variability [246,247].

Electrode Migration (EM)

EM corresponds to displacement of the electrode out of the cochlea, which may occur at the end of surgery, in the immediate postoperative period, or at a later stage. It is associated with increased impedances and decreased speech recognition [302]. EM is more frequent with straight electrodes (3.2%) than with precurved electrodes (0.53%) [286].

Precurved electrodes benefit from a natural retention force against the modiolar wall, estimated to be 5–10 times greater than that of straight electrodes [303]. For straight electrodes, migration is often related to the recoil ("spring-back") force generated by the excess cable coiled within the mastoid cavity. Secure fixation at the level of the tympanotomy is therefore recommended. An alternative consists of creating a groove between the facial nerve and the chorda tympani, in which the cable is placed to limit its mobility (Fig. 37) [304]. Some authors also recommend the use of bone dust mixed with fibrin glue to stabilize the EA [305].

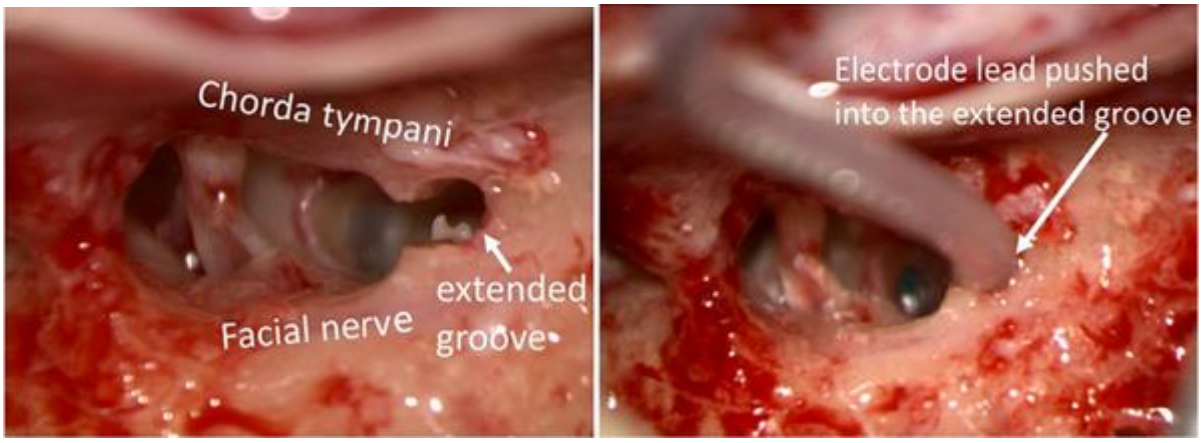

Figure 37. Example of electrode stabilization: the cable is pushed into an enlarged groove between the facial nerve and the chorda tympani to reduce the risk of migration (image courtesy of Joachim Müller, Munich, Germany) [286,304]. Reproduced from Van de Heyning et al. (2022) [286].

Electrode Rigidity

Finally, electrode rigidity plays an important role. A prototype with relatively high rigidity (6.8) resulted in significantly poorer auditory outcomes and a higher peak maximal force (56 ± 23.8 mN) than a low-rigidity prototype (0.8; 26 ± 8.7 mN). Cochlear examination showed that incorrect EA positioning or the presence of fibrosis was associated with hearing loss ≥ 40 dB at high frequencies (e.g., 16 kHz in animal models). This observation suggests that mechanical trauma, potentially exacerbated by increased electrode rigidity, may lead to structural damage and subsequent fibrotic changes.

Therefore, to preserve residual hearing, electrode design and insertion strategy should aim to minimize mechanical trauma by favoring thin and flexible arrays that facilitate atraumatic placement within the scala tympani and reduce the risk of fibrosis [295].

Conclusion on Electrode Type for RACIS

The literature reviewed in this chapter suggests that electrode choice plays an important role in insertion-related complications during RACIS. Available data tend to favor the use of straight electrodes, which are associated with lower rates of insertion trauma, particularly ETFO and ESD, compared with precurved electrodes, as reported in systematic reviews including Van de Heyning et al. [286]. However, this conclusion should be interpreted in light of the underlying mechanical factors discussed in this chapter, including insertion forces, stiffness, and trajectory control, which are key determinants of intracochlear injury. Furthermore, it must be emphasized that no dedicated clinical trial has yet directly compared RACIS outcomes between straight and precurved (perimodiolar) electrode arrays; the apparent superiority of straight electrodes observed in the literature may therefore partly reflect a selection bias rather than a true device-specific effect.

Among these lesions, ESD is considered an irreversible intracochlear injury and its prevention should be an absolute priority, whereas ETFO and EM are most often correctable. RACIS systems offer additional potential for trauma reduction through slow, regular, and controlled insertion, a prerequisite for residual hearing preservation. Nevertheless, the use of straight electrodes requires anticipation of secondary migration risk and implementation of appropriate fixation strategies.

Overall, RACIS appears to be a promising technique, likely to further reduce electrode insertion complications and improve future outcomes of cochlear implant surgery. By providing more controlled and reproducible insertion kinetics, RACIS may also help mitigate the specific risks associated with perimodiolar electrode insertion, a hypothesis that remains to be tested prospectively.

3.2.4 Clinical and Functional Outcomes of RACIS

This section provides an integrated overview of the clinical and functional outcomes of robot-assisted cochlear implantation, encompassing surgical feasibility and safety, audiological performance, intracochlear tissue responses, and the influence of key surgical parameters such as insertion depth and frequency–place matching.

3.2.4.1 **Clinical Feasibility and Surgical Complications**

Several clinical feasibility studies have demonstrated that robot-assisted cochlear implantation is feasible in both adult and pediatric populations [111,243].

The iotaSOFT® system (iotaMotion Inc., USA) was one of the first single-use robotic insertion devices to be evaluated in a clinical setting. Its safety and utility were demonstrated in the first-in-human trial of a single-use robotic surgical device [306], and subsequently confirmed in the study by Khan et al., which specifically focused on its clinical performance [228].

A recent meta-analysis estimated the overall rate of postoperative complications following RACIS at 11.85% (95% CI: 0.00–23.86%), which appears comparable to the 12.8% overall

complication rate reported for conventional manual cochlear implantation in large pooled series [80]. Complications ranged from minor events such as bruising, edema, or mild wound dehiscence to rare major complications, including cerebrospinal fluid leakage or extracochlear electrode placement compromising implant function. However, direct comparison remains limited by the wide confidence interval reflecting heterogeneity across RACIS studies, the relatively small number of cases, and the absence of stratification by electrode type, which introduces a significant and uncontrolled source of bias [283].

3.2.4.2 Audiological Performance and Quality of Electrode Placement

Impact on Audiological Performance and Quality of Electrode Placement

Insertion speed has been identified as a major determinant of auditory and vestibular preservation following cochlear implantation, as discussed previously [224,244,286,307]. Experimental data further suggest that controlled, slow, and regular insertion may limit acute intracochlear trauma and promote early functional recovery [263].

In parallel with technological advances in robotics, electrode array designs have evolved to more closely conform to cochlear anatomy. A meta-analysis examining surgical and technical factors did not demonstrate clear superiority of one electrode array model over others in terms of hearing preservation based on electrode length alone [308]. However, more recent studies, including comparisons across different manufacturers, suggest that shorter, flexible lateral wall arrays such as the MED-EL FLEX24 may be associated with improved low-frequency hearing preservation [309]. These observations, together with systematic reviews reporting lower rates of insertion-related adverse events with straight electrodes, support their preferential use in the context of RACIS [286,310].

The study by Khan et al. compared manual and robot-assisted insertions under intraoperative electrocochleographic (ECochG) monitoring [311]. Insertion assisted by the iotaSOFT® system was associated with a clinically meaningful trend toward better hearing preservation and more stable thresholds at one year, with a preservation rate of 85% in the robotic group compared with 71% in the manual group. Although this 14% difference did not reach statistical significance, likely due to the limited sample size and the already high preservation rate in the manual group, it remains clinically relevant.

This 85% preservation rate is particularly noteworthy when considering that previously published hearing preservation rates for FLEX20 and FLEX24 electrodes, defined as a pure-tone average (PTA) change ≤ 15 dB at one year, were 48.8% and 50%, respectively [312]. Comparable results were also reported with RobOtol®, in which the robotic group demonstrated an approximately 12% improvement in hearing preservation compared with the manual group [313].

In the study by Khan et al. [311], five patients in the robotic group received a longer electrode array (FLEX26), whereas no patient in the manual group did, which could theoretically bias the results against robotics. Conversely, no patient in the robotic group implanted with a FLEX20, the shortest model, experienced hearing loss, whereas three of the seven subjects who lost hearing in the manual group were implanted with a FLEX20. The absence of functional hearing loss after initial activation in the robotic group is particularly striking and suggests that assisted insertion may attenuate the acute trauma responsible for the inflammatory cascade and tissue remodeling involved in delayed hearing loss.

Robotic assistance also facilitates integration of intraoperative ECochG, providing the surgeon with real-time functional feedback on the impact of each insertion step [119]. The main limitations of this study nevertheless lie in its retrospective design, despite prospective data collection, as well as in the small sample size included [228].

Meta-analysis of Robotic Strategies and Hearing Preservation

In the meta-analysis dedicated to RACIS, procedures were classified into three categories according to the degree of robotic involvement [283]:

1. **fully robotic procedures**, in which all key steps are performed by the robot;
2. **robotic access to the middle ear with manual electrode array insertion**;
3. **robotic electrode insertion following manual drilling**.

The overall success rate, defined as the proportion of procedures completed without conversion to a manual technique, was 97.2% (95% CI: 94.03–100.00%). By subgroup, this rate reached 98.70% (95% CI: 95.28–100.00%) for robotic electrode insertion (only insertion phase is automated), 88.44% for robotic access to the middle ear (automated approach while insertion is performed manually), and 86.95% for fully robotic procedures (both access and insertion), with no statistically significant difference between subgroups ($p = 0.08$) [283].

Preservation of residual hearing was reported in 60.69% of patients (95% CI: 23.21–98.18%), albeit with very high heterogeneity ($I^2 = 98.41\%$), reflecting the wide diversity of indications, electrode types, and surgical and audiological protocols.

Finally, RobOtol® was evaluated in a pilot study involving two patients with residual hearing, under intraoperative ECochG monitoring [228]. A usable ECochG response was recorded after complete electrode insertion in both subjects, and residual hearing at the tested frequencies was preserved one month after surgery [228]. Integration of ECochG into robotic cochlear implantation thus represents an additional tool enabling dynamic adaptation of insertion based on cochlear responses, with real potential for optimizing hearing preservation.

Impedance Outcomes and Intracochlear Tissue Remodeling in the Context of Atraumatic (Robotic-Assisted) Cochlear Implantation

In the context of RACIS, which aims to minimize intracochlear trauma through controlled, slow, and highly reproducible electrode insertion, understanding impedance evolution and intracochlear tissue remodeling is essential to interpret postoperative functional outcomes and long-term cochlear preservation.

Even with optimized electrode arrays and atraumatic insertion techniques, cochlear alterations may still occur, and residual hearing may deteriorate over time. Intracochlear neural injury may manifest either immediately following mechanical trauma or secondarily as a result of chronic processes. This delayed deterioration has been attributed to persistent inflammatory responses, fibrosis, or neo-osteogenesis triggered by trauma or by an immunological foreign-body reaction [307,314]. These phenomena may disrupt cochlear physiology, compromise residual hearing, and limit postoperative performance [315].

Within this framework, even subtle differences in insertion mechanics, such as those potentially mitigated by robotic-assisted techniques, may influence the magnitude of the subsequent inflammatory and fibrotic response.

Intracochlear fibrosis is frequently observed after implantation, presenting as a fibrotic sheath surrounding the electrode array. It may result from traumatic events (such as scalar deviation) or from a foreign-body reaction even in the absence of major trauma [314]. This process plays a major role in outcome degradation by disturbing the physiological environment of the inner ear and reducing residual hearing [315]. Cochlear fibrosis has also been associated with increased electrical impedances, which may compromise implant function [316]. In addition, larger volumes of intracochlear new bone formation correlate with poorer word recognition scores [141].

Impedance values vary depending on whether electrodes are stimulated or not; in adults, higher impedances are generally associated with higher thresholds and lower comfort levels, although this relationship is less clear in children [232].

The typical temporal profile of postoperative impedances includes:
– low intraoperative baseline values,
– an early increase during the wound-healing phase,
– a secondary decrease after device activation, without complete return to baseline values [317].

This evolution reflects the formation of deposits on the electrode surface (partially removed by stimulation) and the development of a connective tissue sheath that prevents full normalization. Long attributed solely to inflammation, impedance increases are now considered the result of both inflammatory processes and stimulation-related mechanisms. In the absence of pre-existing inflammation, increasing the stimulation pulse width has been shown to normalize elevated impedances [317].

Growth of connective tissue around the electrode array is a major determinant of cochlear implant efficiency and a primary contributor to chronic impedance elevation [233]. Experimental data demonstrate a correlation between the volume of newly formed tissue surrounding the electrode array and the magnitude of impedance changes. Dexamethasone-eluting (DEX) electrode arrays significantly reduce fibrotic tissue growth and impedance increases during the first three months. Although the volume of fibrous tissue at 91 days is not correlated with hearing loss, it is strongly associated with impedance elevation, suggesting that impedance could serve as an in vivo marker of intracochlear fibrosis [233]. Incorporation of DEX into the electrode silicone allows delivery of a biologically active intracochlear dose, making DEX-eluting cochlear implants a promising strategy to reduce fibrosis and impedance increases [233].

Electrical stimulation itself induces rapid and dynamic impedance changes: after implantation, impedance increases and then decreases within minutes following stimulation onset, remaining low as long as stimulation continues [318]. This decrease is mainly related to the polarization component, indicating that stimulation primarily affects electrode surface properties rather than the global tissue environment. This phenomenon persists for several years after implantation in chronic in vivo models, supporting the concept that stimulation modifies the electrode–tissue interface rather than the surrounding tissue or fluid [318].

Longitudinal impedance monitoring is recommended, as impedance variations may reflect device malfunction, periods of non-use, hormonal influences, or perceived changes in sound quality [319]. Data beyond three years remain limited but suggest progressive stabilization of impedances after initial fluctuations, with a downward trend in apical electrodes [319]. Larger-scale studies are required to determine the functional significance of these changes.

At the microscopic level, electrical stimulation causes immediate loss of cells covering the electrode surface, reflecting localized changes in cell adhesion at commonly used stimulation levels [108]. The similarities between in vivo and in vitro impedance variations support the validity of experimental models, although the underlying mechanisms may differ. Under in vitro conditions, changes in the porosity of the cellular layer have been proposed to explain these variations, providing further insight into the dynamic processes at the electrode–tissue interface [108].

Finally, the relationship between impedance and functional performance is complex: a recent clinical study found no direct correlation between impedance variations and speech perception scores, suggesting that impedance alone cannot predict cochlear implant failure or poor performance [320].

Histopathological analyses of implanted human temporal bones nevertheless show that cochlear implantation, despite the biocompatibility of current electrode arrays, induces immediate insertion trauma followed by a delayed inflammatory response with fibrosis and neo-osteogenesis [141]. In these specimens, fibrous tissue and newly formed bone were found in all cases. CNC word scores correlated positively with the number of spiral ganglion cells and negatively with the percentage of new bone volume in the scala tympani, scala media/vestibuli, and the cochlea as a whole, but not with the volume of fibrous tissue [141]. Neo-osteogenesis in the scala media/vestibuli was strongly associated with the severity of insertion trauma, particularly basilar membrane injury. These observations underscore that residual neuronal survival and the degree of neo-osteogenesis are major determinants of postoperative auditory performance, reinforcing the importance of minimizing insertion trauma and further improving electrode biocompatibility [141].

Altogether, these findings support the rationale for robotic-assisted cochlear implantation strategies, which aim to reduce insertion-related trauma and, consequently, limit the cascade of inflammatory, fibrotic, and impedance-related changes that may negatively impact long-term auditory outcomes.

Insertion Depth and Frequency–Place Mismatch

Slow EA insertion facilitates full-depth placement with minimal resistance, thereby optimizing preservation of cochlear function [224]. Maintaining the EA entirely within the scala tympani, without scalar translocation, is correlated with better clinical outcomes, as it ensures an optimal electrode–neuron interface [286].

Robot-assisted surgery, combined with atraumatic lateral-wall electrodes, theoretically allows deeper and more controlled insertions, thereby improving cochlear coverage. By minimizing insertion forces and limiting scalar translocations and intracochlear lesions, robotics facilitates advancement of long lateral-wall electrodes toward the second cochlear turn. This deep and controlled trajectory provides improved access to neural structures in the apical and mid-apical

regions and supports a more structural coding strategy, in which frequency allocation more closely follows the tonotopic organization of the cochlea.

Long lateral-wall electrodes offer additional advantages: they reduce frequency-to-place mismatch, as demonstrated by Canfarotta et al. [321], and increase angular separation between adjacent contacts, which may improve channel independence and speech coding. These characteristics have been associated with better speech recognition scores [321].

The study by Canfarotta et al. [321] characterized variability in AID of lateral-wall electrodes and its consequences for frequency–place mismatch in cochlear implant users [321]. For complete insertions, the mean AID of the most apical contact varied significantly according to electrode type (Fig. 38):
- **FLEX24**: 428° ± 34.3°,
- **FLEX28**: 558° ± 65.4°,
- **FLEXSOFT/Standard**: 636° ± 9°.

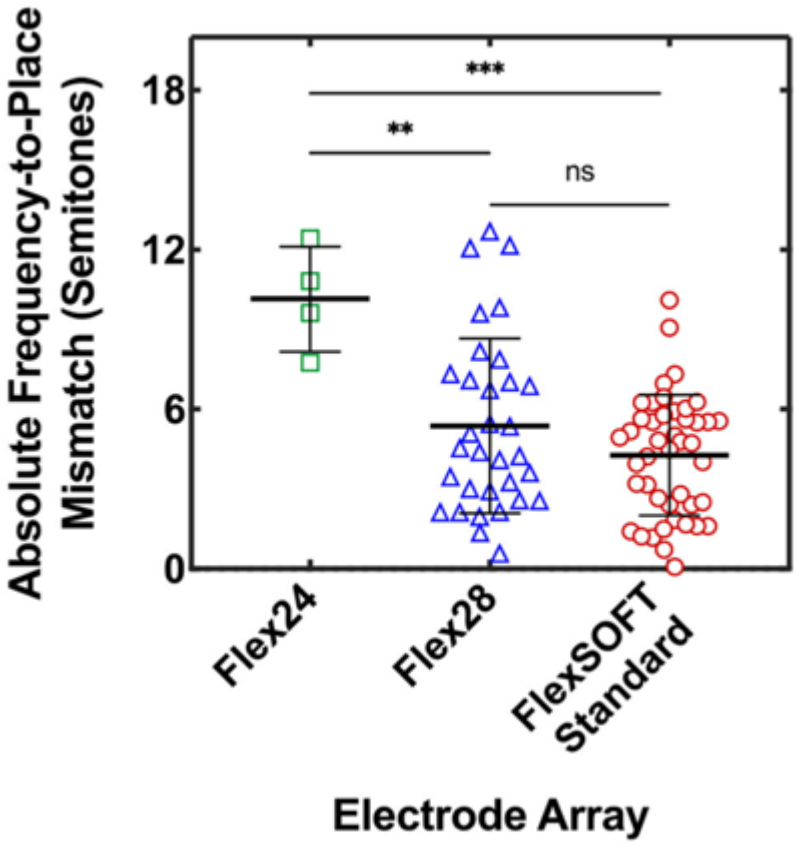

Figure 38. Relationship between frequency–place mismatch at 1500 Hz (a spectral region crucial for speech) and electrode array type in CI-only users with complete insertions; the figure shows that longer electrodes tend to reduce this mismatch. Reproduced from Canfarotta et al. (2020) [321].

These results confirm that longer electrodes reach greater apical AIDs, which are strongly correlated with electrode type and individual cochlear length (Fig. 39). Even for a given electrode length, AID varies widely among patients, such that the cochlear region being stimulated does not always correspond to the default frequency assigned by the processor. This results in heterogeneous frequency–place mismatch.

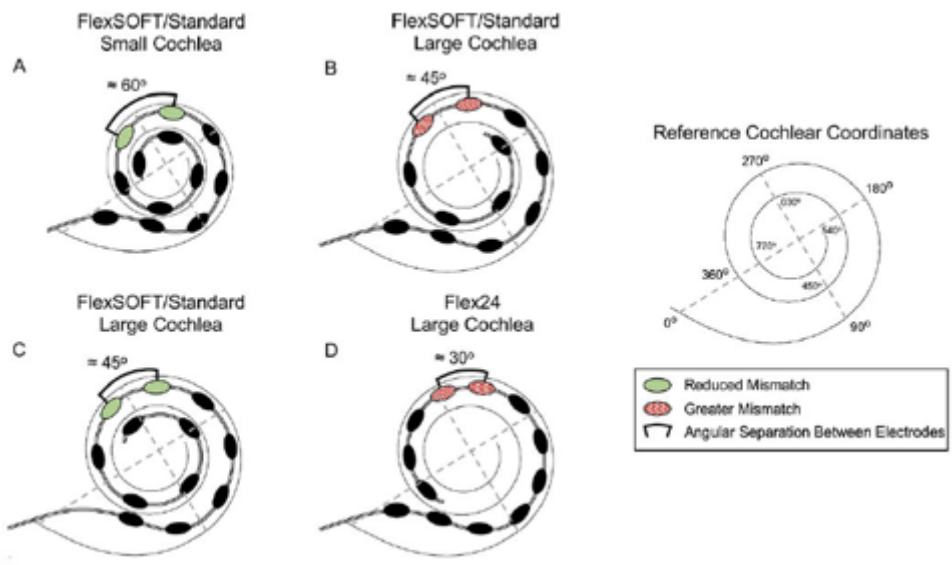

Figure 39. Four schematics illustrate the relationship between frequency–place mismatch and angular separation between adjacent contacts. Contacts located in the 1–2 kHz region of the spiral ganglion (224°–333°) are highlighted in green or red to indicate relatively low or high mismatch, respectively. Variations in cochlear length (panels A vs. B), basal insertion depth (B vs. C), and contact spacing between electrode types (A–C vs. D) jointly determine the degree of mismatch and angular separation. Reproduced from Canfarotta et al. (2020) [321].

The study showed that the use of default frequency filters tends to minimize this mismatch in CI-only users benefiting from deep insertions (long electrodes). In contrast, short electrodes and EAS configurations exhibited more pronounced mismatches, with deviations exceeding one octave in some cases [321]. Crucially, Canfarotta et al. demonstrated a direct link between this mismatch and speech performance: in CI-only users, lower mismatch, particularly in low frequencies, was associated with better CNC word scores at six months postoperatively [321]. The discussion emphasizes that the improved performance observed with longer electrodes does not rely on a single mechanism but rather on the independent contribution of two factors:

1. reduction of frequency–place mismatch through deeper insertion;
2. reduction of peripheral masking via increased angular separation between contacts.

A mismatch exceeding seven semitones may represent a critical threshold beyond which speech perception is durably impaired [321].

A systematic review by Breitsprecher et al. analyzed 23 studies to assess the impact of insertion depth on speech perception outcomes [322]. Mean AIDs ranged from 330° to 608°, and linear insertion depths (LID) from 18.9 to 24.3 mm. Fifteen studies reported a significant correlation or positive effect between deeper insertion and improved speech perception, primarily attributed to better tonotopic matching when the electrode covers more than one cochlear turn. Seven studies found no significant correlation, and one study even reported a negative correlation, suggesting that excessive insertion could result in over-insertion or suboptimal basal contact positioning. Electrode design (lateral-wall vs. perimodiolar) and insertion site (scala tympani vs. scala vestibuli) emerged as key interacting factors with AID, with scala tympani insertion generally associated with the best outcomes. The authors nevertheless emphasize methodological limitations, including high heterogeneity among studies, numerous confounding factors (duration of deafness, etiology, residual hearing, coding strategy, rehabilitation intensity), and correlation between AID and modiolus proximity. In conclusion,

insertion depth should be considered a contributory factor rather than the sole determinant of speech performance; prospective controlled studies are required to isolate its specific effect [322]. In this context, robotic-assisted cochlear implantation may provide a technological framework to better control insertion depth and trajectory, potentially reducing variability and avoiding both under- and over-insertion. By enabling slow, stable, and reproducible advancement of the electrode array, RACIS could contribute to achieving an optimal insertion depth tailored to individual cochlear anatomy, thereby maximizing tonotopic alignment while minimizing insertion-related trauma.

Finally, the retrospective study by Spiegel et al. [168] evaluated variability in cochlear morphology, particularly CDL, in 108 implanted patients using the tablet-based planning software OTOPLAN. Analysis of 108 preoperative CT scans revealed a CDL ranging from 30.4 to 40.2 mm, with a mean of 36.2 ± 1.8 mm, corresponding to a variability exceeding 30% and justifying an individualized approach. A significant sex-related difference was observed, with men exhibiting a longer mean CDL than women [168]. Post-implantation, angular insertion depth differed significantly according to electrode type, with FLEXSOFT™ providing a mean cochlear coverage of 75.8% compared with 63.9% for FLEX28™. Notably, the theoretical target of two cochlear turns (720°) was not achieved in any patient [168]. The authors conclude that the wide variability in CDL necessitates personalized preoperative anatomical assessment, and that tools such as OTOPLAN are essential for selecting the appropriate electrode length (FLEX28™ or FLEXSOFT™), optimizing cochlear coverage, and preventing complications such as tip fold-over. The study questions the clinical relevance of a fixed 720° threshold and confirms the central role of preoperative planning in optimized cochlear implant surgery [168]. These findings highlight the importance of patient-specific preoperative planning, which is directly relevant to robotic-assisted cochlear implantation strategies. Indeed, tools such as OTOPLAN can be integrated into a broader image-guided surgical workflow, allowing surgeons to define individualized insertion targets that can then be executed with high precision using robotic-assisted systems. In this perspective, RACIS not only facilitates atraumatic insertion but also enables accurate translation of preoperative anatomical planning into controlled intraoperative electrode placement. This integration of imaging-based planning and robotic execution represents a key step toward fully personalized cochlear implant surgery.

3.2.5 **Conclusion and Perspectives**

Taken together, current data indicate that RACIS, when combined with atraumatic electrode arrays, represents a meaningful evolution toward implantation strategies that are more respectful of cochlear anatomy and function. Beyond mere technical feasibility, RACIS is part of a broader effort to standardize the surgical gesture, aiming to reduce inter-operator variability and to secure critical insertion parameters, with a measurable clinical impact.

Experimental and clinical results consistently show that this approach promotes better preservation of the intracochlear environment, as reflected by improved rates of hearing preservation, more frequent electrode positioning within the scala tympani, and impedance profiles compatible with a limitation of fibro-inflammatory remodeling. These findings suggest that RACIS is not limited to technical optimization alone, but may durably influence the quality of the electrode–neuron interface and, consequently, the long-term functional performance of the cochlear implant.

By facilitating more reliable insertions of long lateral-wall electrodes, robotic assistance also opens important perspectives in terms of cochlear coverage and frequency matching. Improved

correspondence between electrical stimulation and the individual tonotopic organization of the cochlea appears to be a central lever for reducing frequency–place mismatch and optimizing speech perception, particularly in cochlear implant–only users. This approach fully aligns with a more structural and personalized coding strategy, taking into account interindividual cochlear anatomical variability.

Finally, the integration of intraoperative functional feedback, such as electrocochleography, in synergy with robotic systems represents a further step toward adaptive cochlear implantation, guided in real time by cochlear responses. The combination of robotic insertion with intraoperative electrocochleography is expected to enhance the reliability and interpretability of electrophysiological signals, enabling more precise incident detection, improved predictive value for trauma or insertion-related events, and more refined intraoperative electrode position corrections. While the available results are encouraging, prospective randomized clinical trials, including long-term functional outcomes and direct comparisons between robotic platforms, remain essential to establish the definitive clinical benefit of RACIS.

Thus, robot-assisted cochlear implantation emerges as a reliable and maturing technique, with the potential to contribute to sustained improvements in auditory outcomes, while supporting the ongoing transition toward more precise, more personalized cochlear surgery focused on functional preservation.

3.2.5.1 **RACIS and Cochlear Health**

Cochlear Health and Future Perspectives

Functional outcomes following CI are now widely recognized as the result of complex interactions between peripheral, central, technological, and psychosocial factors. Nevertheless, speech recognition performance after cochlear implantation exhibits substantial interindividual variability [98,323,324], which is partly attributable to the condition of the auditory nerve, the structure directly stimulated by the electrode array. Animal studies and human post-mortem investigations have demonstrated that spiral ganglion neuron density is reduced in the presence of hearing loss, decreases with advancing age, and varies along the cochlear spiral from base to apex [173,175,194,325].

Within this context, the concept of *cochlear health* has progressively emerged as a major determinant of auditory performance, moving beyond a purely prosthetic view of cochlear implantation to embrace a more comprehensive, biological, and neurofunctional approach to the auditory system.

As previously described, cochlear health encompasses the status of the sensory, synaptic, and neuronal structures of the inner ear (Fig. 40). It notably includes the integrity of inner and outer hair cells, the preservation of afferent synapses, as well as the density and functional integrity of spiral ganglion cells and the auditory nerve. Although cochlear implants bypass normal sensory transduction by directly stimulating auditory nerve fibers, the quality of the remaining neural substrate remains critical for efficient transmission of electrical information and for optimal auditory perception. From a physiological standpoint, cochlear implantation effectively bypasses the sensory partition of the organ of Corti as well as the mechano-electrical and synaptic transduction mechanisms of inner hair cells. In contrast, the integrity of the neuronal compartment, including spiral ganglion neurons, the auditory nerve, and brainstem structures,

becomes an essential prerequisite for proper cochlear implant function. This functional dissociation between bypassed structures and required neural substrates forms the conceptual foundation of the modern notion of cochlear health and underpins the growing interest in the direct assessment of neural health in cochlear implant users.

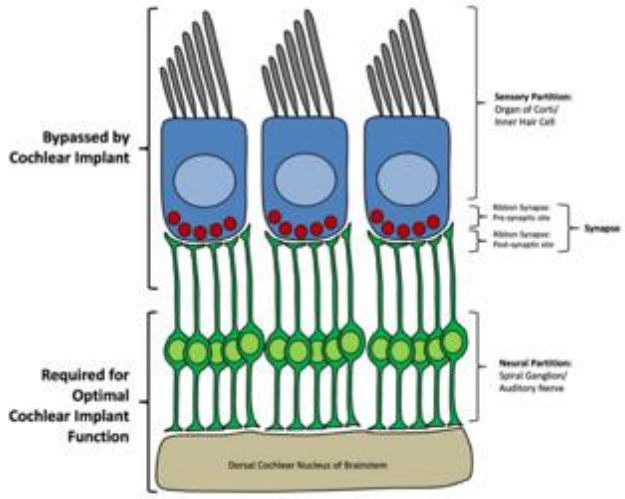

Figure 40. Schematic overview of the peripheral auditory system, highlighting the physiological principles underlying cochlear implant function. Inner hair cells, the sensory partition, as well as the pre- and postsynaptic components of the synapse are bypassed by the electrical stimulation delivered by the cochlear implant. In contrast, the integrity of the auditory nerve, the spiral ganglion, and brainstem structures is essential to ensure optimal cochlear implant performance. Reproduced from Shearer and Hansen (2019) [326].

An increasing body of evidence suggests that the etiology of hearing loss constitutes a major predictive factor of post-implantation outcomes (Fig. 41) [327,328]. Recent data from clinical and genetic studies indicate that otogenetics may account for up to 50% of post-lingual hearing loss, with substantial heterogeneity in the underlying pathophysiological mechanisms. Some mutations primarily affect sensory structures, whereas others involve synaptic elements or the neuronal compartment, the latter being associated with poorer auditory performance following cochlear implantation. The results reported by Tropitzsch et al. [329] demonstrate that variability in post-implantation performance among patients with genetic hearing loss is strongly influenced by the type of cochlear involvement: mutations affecting non-neuronal sensory structures (for example *GJB2*, *TMPRSS3*, *MYO15A*, *LOXHD1*, *SLC26A4*, and *USH2A*) are associated with better auditory outcomes, whereas mutations involving neuronal components, particularly the spiral ganglion, predict poorer performance, thereby supporting the "spiral ganglion" hypothesis. A refined characterization of the genetic etiology and the site of cochlear involvement is therefore essential to anticipate the true functional potential of the implant and to optimize patient management.

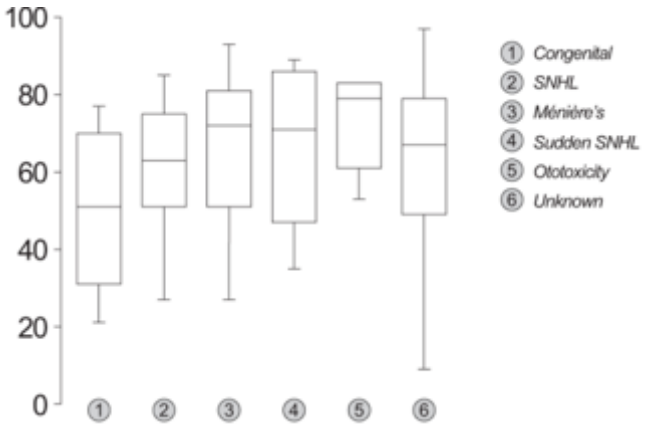

Figure 41. Distribution of post-implantation word recognition scores stratified according to the underlying etiology of hearing loss, illustrated using box-and-whisker plots. Reproduced from Bartholomew et al. (2024) [328].

In parallel, the concept of *cochlear health* cannot be dissociated from the preservation of residual hearing. The integrity of apical cochlear structures, often associated with residual low-frequency hearing, indirectly reflects the overall quality of the cochlear and neuronal environment. When preserved, this residual hearing not only contributes to improved auditory performance in quiet and in noise, but also constitutes an indirect marker of better cochlear health.

In non-implanted ears, whether exhibiting normal hearing or hearing loss, auditory nerve function is closely associated with speech recognition performance. Age-related neuronal alterations contribute in particular to the decline of more complex speech perception tasks, such as speech understanding in noise or at rapid speech rates [330–332]. Similar observations have been reported in cochlear implant users. In this population, age has little influence on speech recognition performance under simple listening conditions, such as speech perception in quiet, but exerts a more pronounced impact in acoustically complex situations [323,324,333]. Although age-related cognitive factors are known to contribute to this functional decline, the condition of the auditory nerve appears to be a central determinant of performance, particularly in cochlear implant users who are predominantly older than 65 years [79,334]. Previous studies indeed suggest that age-related performance declines may be partially explained by reduced engagement and increased dyssynchrony of auditory nerve activity [330]. In cochlear implant users, this disengagement is likely related to a reduction in the number of auditory nerve fibers, as peripheral cochlear mechanisms associated with hair cell pathology, such as reduced endocochlear potential or synaptopathy, are not relevant in the context of direct electrical stimulation. Because mechanisms of auditory nerve disengagement related to hair cell damage are largely inoperative under cochlear electrical stimulation, the term *auditory nerve density* is commonly used to characterize this disengagement in cochlear implant users. Auditory nerve dyssynchrony is defined as a reduction in the synchrony of the summed activity of auditory nerve fibers.

Cochlear health is not limited to the anatomical integrity of intracochlear structures. It also encompasses functional dimensions that can be objectively assessed in clinical practice and that reflect the condition of the neuronal substrate effectively stimulated by the cochlear implant (i.e., neural health). From this perspective, electrophysiological biomarkers represent particularly relevant tools, as they provide direct access to the functionality of the electrode–neuron interface. Among these, electrically evoked compound action potentials (ECAPs) and

electrocochleography (ECochG) have emerged as robust indicators of neural health and predictors of speech perception outcomes.

Recent advances in electrophysiology have substantially improved the ability to assess *cochlear health* in vivo. Auditory nerve disengagement in cochlear implant users can be estimated using ECAP measures. ECAPs reflect the synchronized response of a population of auditory nerve fibers to electrical stimulation. Beyond their technical dimension, they capture biological properties related to neural excitability, synchrony, and the quality of the electrode–neuron interface. In animal models, suprathreshold ECAP parameters (amplitude, slope of the amplitude growth function [AGF], and recovery function) are correlated with spiral ganglion neuron density, allowing in vivo estimation of auditory nerve health [194,325,335,336]. In humans, spiral ganglion neuron density or total neuron count, assessed post-mortem or through non-invasive measures such as ECAPs, is positively associated with speech recognition performance following cochlear implantation [337,338]. Large ECAP amplitudes suggest a higher density of spiral ganglion neurons in the vicinity of the stimulated electrode [325]. However, the mediolateral distance of the electrodes also contributes to ECAP amplitude [325,339,340]. Certain ECAP measures, particularly the effect of the interphase gap (IPG) on peak amplitude or AGF slope, are considered to reflect auditory nerve disengagement in humans (Fig. 42). These measures are correlated with spiral ganglion neuron density and speech recognition performance, while being independent of electrode position, in contrast to fixed-IPG measures that are influenced by the electrode–modiolus distance [325,339,340]. Overall, these findings indicate that reduced spiral ganglion neuron density is associated with poorer speech perception outcomes, and that specific ECAP parameters may serve as functional markers of this relationship.

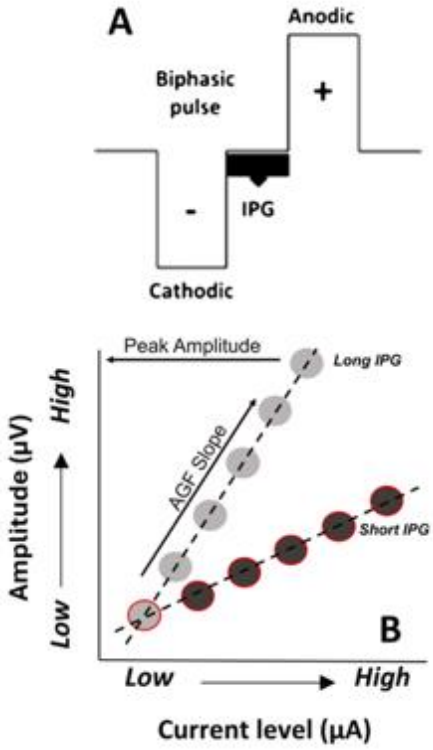

Figure 42. *Panels (A) and (B) schematically illustrate the influence of the IPG on the linear slope of the ECAP. In panel (A), a biphasic electrical pulse typically used for CI stimulation is shown, comprising a leading cathodic (negative) phase followed by an anodic (positive) phase. These two phases are separated by a brief interval with no net charge delivery, defined as the IPG, whose duration can be systematically adjusted during ECAP*

measurements. Panel (B) demonstrates that extending the IPG duration modifies ECAP parameters that have been associated with spiral ganglion neuron (SGN) density, notably the response amplitude and the linear slope of the amplitude growth function (AGF). As stimulation current increases, the N1–P2 ECAP amplitude correspondingly grows. When the IPG is prolonged while other stimulation parameters remain unchanged, both ECAP amplitude and AGF slope increase. Such IPG-dependent modulations of ECAP features are interpreted as reflecting variations in underlying SGN survival. Reproduced from Schvartz-Leyzac et al. (2025) [341].

Several studies have demonstrated significant relationships between specific ECAP parameters, such as N1–P2 latency, total refractory period, and the IPG effect, and speech recognition performance, particularly in noisy listening environments [341–343]. These parameters account for up to nearly 50% of the variance in speech-in-noise recognition scores, highlighting their high prognostic value [342].

To capture auditory nerve dyssynchrony in cochlear implant users, another ECAP-based metric can be employed: the N1–P2 interpeak latency (Fig. 43). The N1–P2 interpeak latency is analogous to the half-width reported in non-implanted older adults [332]. When the latencies of individual ECAP peaks vary substantially from trial to trial, the averaged ECAP waveform exhibits a broader N1–P2 interpeak latency, analogous to an increased half-width and greater neural dyssynchrony. Conversely, when individual peak latencies are more consistent across trials, the averaged ECAP waveform displays a narrower N1–P2 interpeak latency, analogous to a reduced half-width and improved neural synchrony.

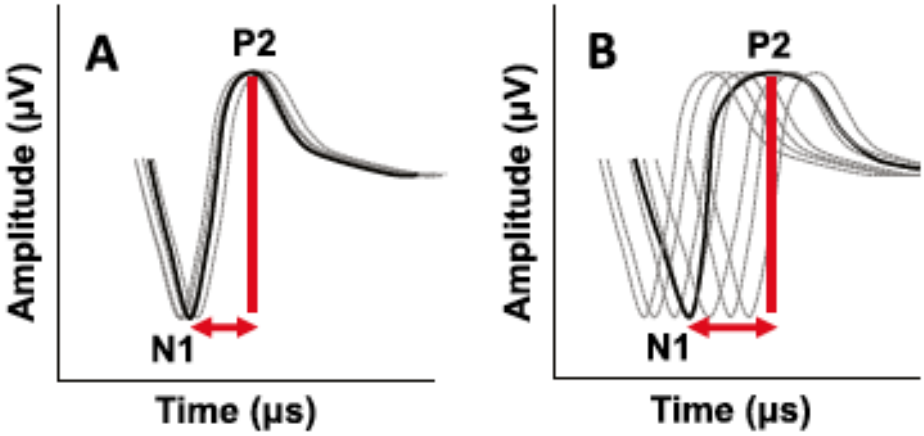

Figure 43. *Panel A illustrates a neural response characterized by low trial-to-trial temporal variability and a high degree of synchrony, with individual traces exhibiting highly consistent latencies and response widths. Panel B, in contrast, depicts a less synchronized response, characterized by increased temporal jitter across trials, resulting in a prolonged N1–P2 interpeak interval as well as an overall broadening of the evoked response. The thick black curve represents the trial-averaged N1–P2 response, whereas the grey dotted traces correspond to individual responses. Interpeak latency is defined as the duration separating the N1 and P2 components. Reproduced from Schvartz-Leyzac et al. (2025) [341].*

The associations between ECAP measures and functional outcomes are further supported by correlational analyses derived from standardized speech perception tests. Specifically, performance on the AzBio sentence test at +10 dB signal-to-noise ratio (% correct) decreases as ECAP N1–P2 latency increases, with a statistically significant relationship ($R^2 = 0.26$; $p = 0.013$). This finding suggests that longer latencies, potentially indicative of less efficient or less synchronized neural activation, are associated with poorer speech understanding in noise (Fig. 44) [341].

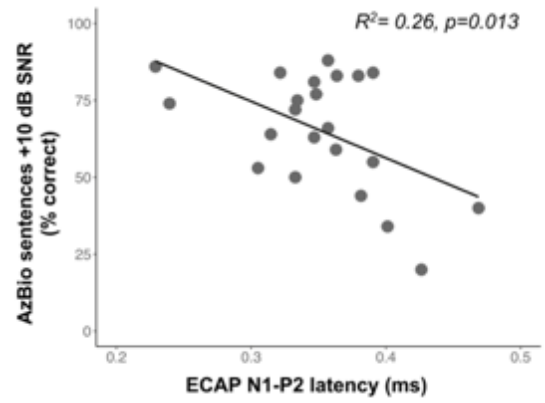

Figure 44. Relationship between the ECAP N1–P2 interpeak latency (in milliseconds) and speech-in-noise performance measured with AzBio sentence recognition at a +10 dB signal-to-noise ratio (SNR). Speech recognition outcomes are expressed as the percentage of correctly identified items on the y-axis. Reproduced from Schvartz-Leyzac et al. (2025) [341].

In addition, the ECAP IPG effect (expressed in µV/nC) is positively correlated with AzBio scores at +10 dB SNR ($R^2 = 0.21$; $p = 0.029$), indicating that a larger IPG effect, interpreted as reflecting greater neural responsiveness to variations in electrical stimulation, is associated with better functional outcomes (Fig. 45). Along the same lines, combined ECAP indices have been reported to explain up to 47% of the variance in AzBio speech-in-noise performance [343].

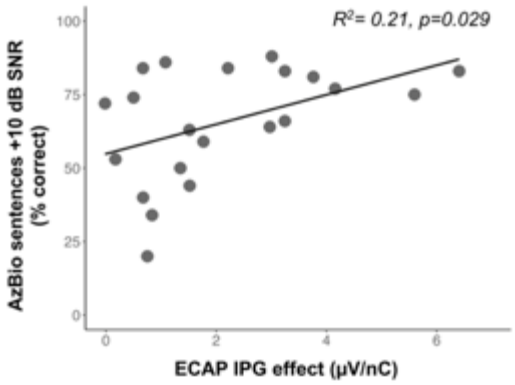

Figure 45. Relationship between the ECAP IPG effect, quantified by the linear slope (µV/nC; x-axis), and speech-in-noise performance assessed using AzBio sentence recognition at a +10 dB SNR. Performance is reported as the percentage of correct responses on the y-axis. Reproduced from Schvartz-Leyzac et al. (2025) [341].

Finally, Dawson et al. [343] identified several major determinants of auditory performance in cochlear implant users by jointly analyzing sound processor fitting parameters, electrode position, neural health markers, electrode impedances, as well as cognitive and individual factors. Collectively, these variables accounted for between 33% and 60% of the variability in performance outcomes. Multivariate analyses highlighted four key factors that were consistently associated with poorer results: substantially underfitted sound processor MAP thresholds, higher average bipolar thresholds, greater total refractory time, and a larger IPG offset. The presence of scalar translocation, certain cognitive variables, and other patient-specific factors were also found to be predictive of performance across several outcome measures, albeit less consistently.

Complementarily, ECochG has emerged as one of the strongest predictors of auditory outcomes following cochlear implantation. By simultaneously reflecting hair cell activity and auditory nerve function, ECochG provides an integrated assessment of residual cochlear function, thereby explaining its high predictive value.

Preoperative total ECochG response is strongly correlated with short- and medium-term word recognition performance. The electrocochleography total response (ECochG-TR) is a composite electrophysiological measure that aggregates acoustically evoked potentials across multiple frequencies (250–2000 Hz), calculated as the cumulative sum of spectral peaks from the first harmonics of each stimulus frequency. It integrates contributions from the cochlear microphonic (CM) generated by outer hair cells, the summating potential (SP) from inner hair cells, and neural components including the compound action potential (CAP) and auditory nerve neurophonic (ANN), thereby reflecting both sensory and neural function [118].In particular, ECochG-TR explains 43% of the variance in CNC word scores at 6 months postoperatively ($p < 0.001$), with a strong correlation ($r = 0.71$; $p < 0.0001$) [344,345], and up to 49% of the variance at 3 months [346]. This relationship is illustrated by a positive linear association between ECochG-TR and CNC performance at 6 months. Thus, higher ECochG responses are associated with better early lexical recognition outcomes, conferring ECochG the role of an integrative biomarker encompassing both sensory and neuronal dimensions [347].

Taken together, electrophysiological biomarkers such as ECAPs and ECochG allow objective characterization of cochlear health well beyond conventional audiometric evaluation. They provide a direct window into the functional state of the neuronal substrate stimulated by the cochlear implant and represent promising tools for prognostic stratification, longitudinal monitoring, and personalized optimization of stimulation strategies.

Beyond peripheral factors, recent evidence highlights the growing importance of neurocognitive mechanisms in speech perception among cochlear implant users. Speech understanding relies on bidirectional processing that combines bottom-up mechanisms, related to the quality of the peripheral auditory signal, and top-down mechanisms, dependent on central cognitive functions. Speech recognition performance, particularly in noisy environments, is associated not only with peripheral auditory function but also with general cognitive abilities (Montreal Cognitive Assessment [MoCA], nonverbal reasoning) and specific cognitive domains (working memory, processing speed, and selective auditory attention) (Fig. 46) [347]. This multidimensional framework is commonly referred to as cognitive health.

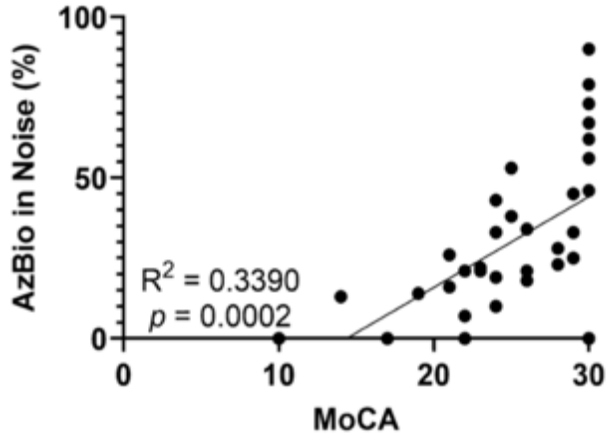

Figure 46. MoCA score exhibits a moderate linear relationship with speech-in-noise performance. Reproduced from Walia et al. (2022) [347].

Accordingly, the cochlear implant can no longer be regarded as a simple device for peripheral hearing restoration, but rather as a central component of a complex functional ecosystem in which cochlear health, neural integrity, individual clinical characteristics, technological choices, and neurocognitive mechanisms interact closely. Functional outcomes and quality of life in cochlear implant recipients emerge from this dynamic interplay, extending well beyond a strictly audiometric approach.

This integrated perspective paves the way for a truly personalized medicine of cochlear implantation, based on more refined candidate selection, atraumatic surgical strategies aimed at cochlear preservation, a rational choice of technologies, and individualized programming of stimulation strategies. In the future, the combined integration of electrophysiological biomarkers, advanced imaging tools, cognitive data, and potentially genetic factors will enable more precise patient stratification and improved outcome prediction.

In this context, cochlear health is no longer an isolated theoretical concept but emerges as a central clinical lever at the core of future perspectives in cochlear implantation, with the ultimate goal of achieving sustained improvements in auditory performance, patient satisfaction, and quality of life.

Article 2

Journal: Audiology and Neurotology. Peer-reviewed. Published: Gersdorff G, Peigneux N, Duran U, Camby S, Lefebvre PP. Impedance and Functional Outcomes in Robotic-Assisted or Manual Cochlear Implantation: A Comparative Study. Audiol Neurotol. 2025;30:80–88. doi:10.1159/000540577.

Audiology and Neurotology

Research Article

Audiol Neurotol 2025;30:80–88
DOI: 10.1159/000540577

Received: February 14, 2024
Accepted: July 24, 2024
Published online: August 23, 2024

Impedance and Functional Outcomes in Robotic-Assisted or Manual Cochlear Implantation: A Comparative Study

Guillaume Gersdorff[a] Nicolas Peigneux[a] Unal Duran[b] Severine Camby[a] Philippe P. Lefebvre[a]

[a]Department of Oto-Rhino-Laryngology, Head and Neck Surgery, Liège University, CHU de Liège, Liège, Belgium; [b]Department of Diagnostic Radiology, Liège University, CHU de Liège, Liège, Belgium

Keywords
Cochlear implants - Robot-assisted surgery - Impedance · Hearing preservation

Abstract
Introduction: Preservation of residual hearing, mainly the low frequencies, is the current main objective of cochlear implantation. New electrode arrays and the development of minimally invasive surgery have allowed electroacoustic stimulation. Over the past several years, robotic-assisted cochlear implant surgery aimed to improve the insertion process while respecting inner ear structures. However, the introduction of a foreign body inside the cochlea can lead to the development of fibrous tissue around the electrode array, or even induce osteogenesis. These histological changes disrupt the parameters of the cochlear implant, resulting in elevated impedance. In addition, long-term auditory performance can be affected, with a deterioration in word comprehension. We evaluated the potential impact of RobOtol® on impedance changes over time, leading to potentially positive functional outcomes. ***Methods:*** Cochlear implant surgery with a round window approach was performed under general anesthesia. Fifteen Med-El Flex24 electrode arrays were inserted manually and 24 using RobOtol®. All subjects underwent pure-tone audiometry tests before the surgery and at regular intervals up to 1 year after the surgery. Based on the pure-tone average at the low frequencies from 250 to 1,000 Hz, we divided the patients according to the degree of auditory preservation (full preservation ≤15 dB, partial preservation 15 dB–30 dB, significant loss >30 dB). These different groups were compared in terms of impedance changes and auditory performance, specifically word recognition score. ***Results:*** We found proportionally fewer patients who experienced significant low-frequency hearing loss after robotic insertion (53.33% in the manual group compared to 41.67% in the robot-assisted insertion group). Impedance changes at the apex of the electrode array, especially at the first electrode ($p = 0.04$), after robotic surgery, with less overall variability, a continuous decreasing trend without secondary elevation, and lower values in cases of complete residual hearing preservation (for the three first electrodes: $p = 0.017$, $p = 0.04$, $p = 0.045$). The speech intelligibility amelioration over time showed favorable evolution in patients with complete residual hearing preservation regardless of the insertion method. However, in the absence of auditory preservation, the positive evolution continued more than 6 months after robotic surgery but stagnated after manual insertion (difference at 1 year, $p = 0.038$; median auditory capacity index 83% vs. 57%). ***Conclusion:*** Atraumatic electrode array insertion with consistent, slow speed and the assistance of

karger@karger.com
www.karger.com/aud

© 2024 S. Karger AG, Basel

Correspondence to:
Philippe P. Lefebvre, pp.lefebvre@uliege.be

RobOtol® minimizes disturbances in the delicate neurosensory structures of the inner ear and leads to better auditory performance. © 2024 S. Karger AG, Basel

Introduction

Cochlear implants (CIs) have revolutionized the treatment of severe to profound sensorineural hearing loss. Since the first electrode array implantation performed by Djoo and Eyries in 1957, their evolution has continued to progress to the minimally invasive technique it is today.

The current main objective was protection of delicate intracochlear structures with preservation of residual hearing, mainly at low frequencies. Therefore, the criteria for hearing implant placement have been broadened to allow for electroacoustic stimulation. This significantly improves CI performance, including speech understanding in noise, music appreciation, and sound localization [1].

For more than a decade, several otological robots have been developed in the field of cochlear implantation. RobOtol® was the first to obtain European certification for clinical use. Robotic-assisted cochlear implant surgery (RACIS) aims to optimize the insertion process and could lead to less intracochlear trauma, potentially improving long-term audiological outcomes [2]. An electrode array (EA) placed completely inside the scala tympani (ST) with no scalar deviation is associated with better outcomes for patients by creating an optimal electrode-neural interface [3]. The clinical feasibility of robotic cochlear implantation has already been demonstrated in both adults and children. Robot-optimized insertion reduces inner ear trauma and allows a greater number of well-positioned electrodes into the ST [4, 5].

Our preliminary results were comparable to Torres data, with greater hearing preservation and no radiological inner ear trauma when the EA is inserted at a slow and constant speed in the inner ear using RobOtol® [6]. The robotic insertion allows insertion forces to be reduced, as well as pressure changes within the cochlea, increasing the likelihood of insertion in the ST axis. Nevertheless, its association with speech perception was not analyzed. The speed of electrode insertion has a significant positive impact on the preservation of hearing and vestibular function [3, 7–9].

EAs have constantly evolved to be as adapted to the cochlea as possible. According to a meta-analysis [10], no electrode design has shown a clear advantage in hearing preservation. However, Med-El Flex24 has been reported to have the best median hearing preservation score at low frequencies due to its highly flexible electrode array and ideal insertion depth. This was confirmed by a review of the literature supporting the use of straight electrodes for RACIS [3, 11].

However, EA insertion can still induce changes in the cochlea, and residual hearing loss remains possible. Intracochlear neuronal damage may by early onset (mechanical) or late onset. The hypothesis of delayed changes has been put forth on the basis of a chronic inflammatory reaction, fibrosis, or neo-osteogenesis induced by trauma, as well as on the basis of an immunological reaction to a foreign body [9, 12]. Subsequently, the normal physiology of the inner ear could be disrupted by these reactions, leading to a deterioration of the residual level of hearing and a limitation in good results [13]. Furthermore, postoperative word recognition scores have been reported to negatively correlate with the percentage volume of new bone within the cochlea [14]. In addition, fibrosis has been described as being associated with increased electrical impedance leading to lower hearing thresholds, less comfortable listening levels, less compliance level, and reduced sound quality [2, 15–17].

Overall, combining RACIS with atraumatic electrodes appears to improve the preservation of residual hearing. The aim of this study was to determine whether these changes improve postoperative impedance over time and lead to positive functional outcomes.

Materials and Methods

Study Design

We performed a retrospective single-center study to evaluate impedance measurements and audiometric outcomes in a population of patients who underwent manual or robot-assisted cochlear implantation.

Study Participants

Individuals, who met the general eligibility criteria for CI surgery, were ≥18 years old, and fluent in French were included in this study. The exclusion criteria were pregnancy or anatomical malformations of the middle or inner ear. We also excluded patients with low-frequency pure-tone average (PTA; 250 to 1,000 Hz) ≥100 dB to evaluate the potential residual hearing level. A total of 24 subjects in the robotic-assisted insertion group and 14 subjects in the manual insertion group gave written informed consent and were subsequently enrolled in the study. One patient in the manual insertion group had bilateral CIs.

Type of Electrode Arrays

All subjects had Med-El CIs and the same type of EA (Flex24) that was 24 mm long with an active length of 20.9 mm. To enable more flexibility at the tip, the five most apical electrode contacts were single, whereas the basal seven electrodes were paired. This reduced the diameter of the tip to 70% of the standard Med-El Combi40+ electrode.

Surgical and Robotic Procedure

CI surgery via the conventional surgical approach was performed under general anesthesia. The same senior surgeon performed all surgeries. A posterior tympanotomy was created with respect to the facial nerve and chorda tympani. The bony overhand of the round window niche was carefully drilled to expose the round window membrane. The RobOtol® (Collin, Bagneux, France) robot was used to introduce the EA into the cochlea. The RobOtol® arm with the insertion tool mounted on it was placed in the surgical field in the view of the posterior tympanotomy and the round window membrane. We descended the inserter's tip into the posterior tympanotomy using the robot. The robotic insertion tool was retracted 30 mm with respect to the trajectory of the insertion through the round window. The EA was clipped on the instrument 10 mm from the full insertion marker ring. The round window membrane was gently opened with the tip of a Rosen needle toward the perilymph. The axes of freedom of the robot were blocked, so the robot could only move linearly toward the round window. The insertion tool was moved gently toward the tip of the EA and inserted into the cochlea under guidance of a fork. The manual speed insertion of the EA was calculated by reviewing the videos of the procedures and the time needed to insert 5 of the 12 electrodes. The robotic speed insertion was fixed from 0.1 to 0.2 mm/s. After it was inserted completely, the EA was gently unclipped from the insertion instrument. We did not use any IV or local steroids during the surgery. Round window sealing and array fixation in the mastoid were performed using fibrin glue (Tisseel®). For the manual insertion group, CIs were inserted within the round window manually and as slowly as possible.

Outcome Measures

Audiological fitting was performed according to our standard routine, which comprises activation and initial fitting 10 days postoperatively and at regular intervals for 12 months after the surgery (1 month, 3 months, 6 months, and 12 months). An audiological evaluation was performed using the PTA, the average of hearing threshold levels (in dB HL) at a set of specified frequencies. For this study, we assessed the PTA at the range of frequencies including 250, 500, 1,000, 2,000, and 4,000 Hz. Then, we focused on the low frequencies: 250, 500, and 1,000 Hz. Postoperatively, patients were divided into three groups with regard to preservation of the low-frequency PTA (250–500–1,000 Hz): those who considered having complete preservation or no residual hearing trauma (≤15 dB HL), partial preservation or minor residual hearing trauma (15–30 dB HL), and a significant loss or major residual hearing trauma (>30 dB). This classification was selected from the consensus on hearing preservation proposed by Skarzynski et al. [18].

Electrode impedance (kOhms) was calculated according to Ohm's law (voltage = current × impedance). Impedance measurements were performed using a MED-EL Cochlear Implant System. Impedance of the 12 electrodes was measured postoperatively from CI activation onwards and at the same regular intervals.

Postoperatively, speech intelligibility performance was measured by the articulation function using the auditory capacity index (ACI). The ACI was defined as the average speech discrimination score obtained at 40, 55, and 70 dB SPL. We used words from Fournier's dissyllabic list in French, which were pronounced to the patient through a loudspeaker. Measurements were recorded at 40, 55, and 70 dB SPL and at regular intervals for 12 months after the surgery (1 month, 3 months, 6 months, and 12 months).

Imaging Analysis

All patients underwent a preoperative or postoperative, high-resolution cone beam CT of the temporal bone, which was analyzed using OTOPLAN® (CE-certification number: G1 17 10 95657 003). The software allows the analysis of the electrode array insertion angle in the cochlea.

Statistical Analysis

The data were analyzed using standard statistical software R version 3.6.1. Impedance value comparisons were made between each group using the Welch non-parametric test which is an adaptation of the t test, for comparing two independent samples. Variance comparisons were performed using the Levene test. The interaction effect of two independent factors was analyzed by a two-way ANOVA test, type two. The results were considered significant when $p \leq 0.05$.

Table 1. Audiological data

	Manual			Robot-assisted		p value
	N	mean±SD		*N*	mean±SD	
Preoperative PTA	15	84.27±9.93			82.58±13.79	0.34
Low-frequency preoperative PTA	15	76.67±13.79			73.26±13.16	0.21
Loss at low frequencies	*N*	%		*N*	%	
Preservation group						
Full (≤15 dB)	6	40	46.67	8	33.33	58.33
Partial (15–30 dB)	1	6.67		6	25	
Loss >30 dB	8	53.33		10	41.67	

Results

Participants

Thirty-eight participants took part in this study and were divided into two main groups depending on whether they were implanted manually (14 patients, 1 had bilateral CIs) or robot-assisted (24 patients). The mean age at implantation was 60 years (SD = 10) and 55 years (SD = 19), respectively. The etiologies of hearing loss for the two groups were: unknown (26.7–46%), genetic hearing loss (33.3–21%), sudden sensorineural hearing loss (20–21%), meningitis (6.7–4%), ototoxicity (none–8%), Meniere's disease (6.7%–none), multi-operated cholesteatoma (6.7%–none). All of the patients were implanted with a MED-EL Flex 24 EA by the same senior surgeon. Surgical videos of 5 randomly selected patients in the manual insertion group were reviewed to measure the speed of insertion of five electrodes of the Flex 24 EA. The mean speed was 2.48 ± 0.52 mm/s. In contrast, for robotic insertion, the speed was fixed at 0.1–0.2 mm/s. The electrode arrays insertion depth was measured using the Otoplan program after a cone beam CT of the temporal bone. When the postoperative images were not available, the preoperative were used and the putative insertion angle for the flex 24 electrode array was calculated. The insertion depth was not significantly different between the manual (419.89 ± 49.19°) and the robot-assisted (428.6 ± 37.6°) insertion in the cochlea (Mann-Whitney *Z* score = 0.707, *p* value = 0.477).

Audiological Analysis

In the manual insertion group, the preoperative PTA for five frequencies (250, 500, 1,000, 2,000, and 4,000 Hz) was 84.27 ± 9.93 dB and the preoperative low-frequency PTA (250, 500, and 1,000 Hz) was 76.67 ± 11.25 dB. In the robot-assisted insertion group, the preoperative PTA for the same five frequencies was 82.58 ± 13.79 dB and the preoperative low-frequency PTA was 73.26 ± 13.16 dB. These two groups were comparable; there was no significant difference between them ($p = 0.34$ and $p = 0.21$; Table 1). We divided each group into three subgroups based on the severity of hearing loss at the low frequencies and, thus, the degree of preservation or, conversely, the degree of residual hearing trauma. Eight patients had a loss of this PTA >30 dB in the manual insertion group and 10 in the robot-assisted group, which represents a proportion of 53.33% and 41.67%, respectively. Therefore, we found that, proportionally, 27.98% more patients had a loss >30 dB at low frequencies after manual insertion. This means that 1 out of 4 patients experience a significant loss in their residual hearing when the EA is inserted manually. However, with respect to the loss of hearing greater than 30 dB, there is no significant difference in the PTA between the two modes of insertion. Since the insertion depth can have an influence on hearing preservation [19], an analysis of the effect the insertion angle of electrode 1 on hearing preservation was performed and no significant correlation was found.

Impedance Analysis

First, we compared between the two main groups the impedance of the different electrodes at each timepoint with particular focus on the most distal electrodes, those that can reach the low-frequency region depending on the insertion and cochlear morphology. Before 12 months, we did not find any significant differences between manual and a robot-assisted insertion. The impedance data for the first five electrodes at 12 months are provided in Table 2. At this time, a difference appeared when we compare the two subgroups with a >15 dB decrease in residual hearing. This regroups the patients with minor and major residual hearing trauma who had significantly higher impedance values for the first electrode 1 year after the surgery when the EA was manually inserted ($p = 0.04$). The impact of the insertion method and degree of hearing loss (cutoff 15 dB), two independent factors, on the impedance values analyzed by two-way ANOVA demonstrates a significant combined effect for

Table 2. Impedance (in kOhms) at 12 months for the first five electrodes

	≤15 dB				>15 dB				>30 dB			
	mean	median	SD	*N*	mean	median	SD	*N*	mean	median	SD	*N*
Manual												
E1	4.73	4.61	1.22	6	6.86	6.49	1.80	9	7.06	6.58	1.81	8
E2	3.70	3.52	0.96	6	5.18	5.04	1.56	9	5.44	5.10	1.45	8
E3	3.47	3.81	1.14	6	5.07	5.28	1.66	9	5.31	5.34	1.60	8
E4	3.66	3.68	0.84	6	4.83	5.18	1.64	9	5.14	5.18	1.45	8
E5	3.60	3.49	0.76	6	4.99	5.00	1.43	9	5.20	5.11	1.38	8
Robot-assisted												
E1	5.91	6.17	1.75	4	5.22	4.63	1.11	8	5.56	4.66	1.29	5
E2	5.25	4.98	2.00	4	4.97	4.73	1.22	8	5.37	4.92	1.18	5
E3	4.44	4.29	1.39	4	4.01	4.08	0.85	8	4.42	4.60	0.82	5
E4	3.81	3.38	1.06	4	3.84	3.82	0.64	8	4.03	3.73	0.54	5
E5	4.89	3.55	3.17	4	3.95	3.69	0.87	8	4.27	3.72	0.96	5

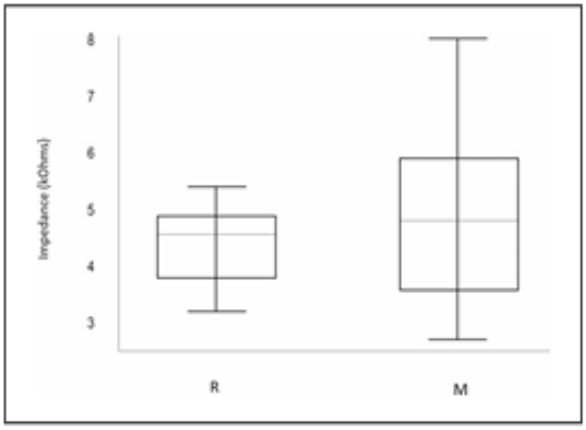

Fig. 1. Impedance disparity for the robot-assisted and manual insertion groups. The data are from electrode 1–5, the more representative electrode. The bold line represents the median; the box includes all patients from P25 to P75, with the error bar equivalent to 1 SD. One patient in the manual insertion group had an extreme impedance value.

the first, third, and fifth electrode ($p = 0.03$, $p = 0.05$, and $p = 0.05$, respectively). One other major difference between the two main groups is the consistency of values, without significant differences across the three subgroups, in the robot-assisted insertion group. In contrast, there is a clear disparity in values among these same subgroups in the manual insertion group. At 12 months, this disparity is marked by a significant difference for the first three electrodes when comparing the ≤15 dB and >15 dB subgroups ($p = 0.017$, $p = 0.04$, $p = 0.045$) and for the first five electrodes when comparing the ≤15 dB and >30 dB subgroups ($p = 0.014$, $p = 0.02$, $p = 0.03$, $p = 0.018$, $p = 0.03$). This difference in impedance disparity is illustrated in Figure 1. Finally, we observed a different evolution over time, with a continued decrease beyond 6 months for the robot-assisted insertion group (all patients included), whereas, after manual insertion, this decrease slowed and even tended to reverse, with values that slightly increased at 1 year (Fig. 2). In addition, the evaluation of the insertion angle on the electrode impedances was assessed and no correlation could be found for the first 5 electrodes (E1: $p = 0.837$, E2: $p = 0.379$, E3: $p = 0.919$, E4: $p = 0.813$ and E5: $p = 0.123$) demonstrating that the insertion depth has no influence on the impedances variations. The same analysis was performed for the manual and the robotic insertion cohorts and no correlation could be demonstrated. These covariance analysis allow to exclude the influence of the insertion depth on the impedance difference between the manual and the motorized insertion procedures.

Speech Intelligibility

The speech intelligibility performance based on the ACI is provided in Table 3. Overall, it appears that speech intelligibility improved up to 6 months in both groups, but this improvement ceased to progress in the manual insertion group. In contrast, in the robot-assisted group, the

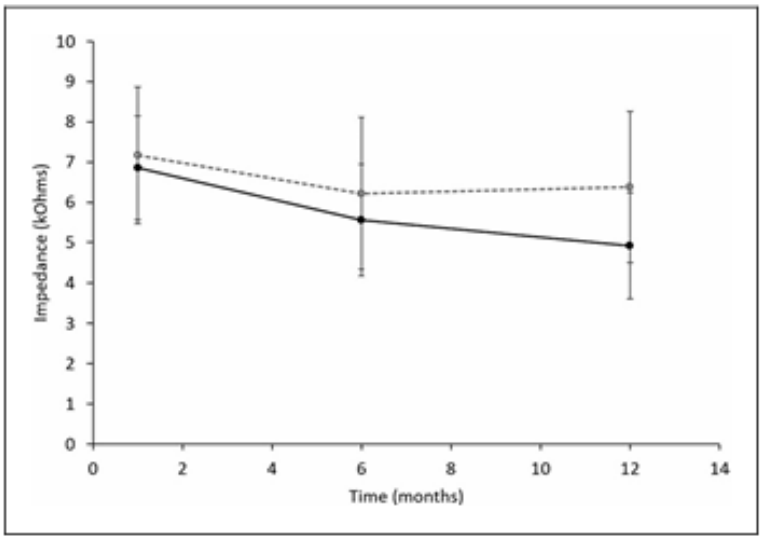

Fig. 2. Impedance evolution in electrode 1 from 1 to 12 months based on the insertion group. The solid line represents the impedance evolution for the robot group, whereas the dotted line represents the evolution for the manual group.

improvement continued over a longer time period. In fact, the overall median score for manual insertion patients decreased from 6 to 12 months due to the patients who experienced a loss >15 dB. However, patients in the same group who retained complete hearing preservation still showed a positive trend in their speech intelligibility scores. All of the patients who experienced complete hearing preservation had a generally comparable evolution regardless of the insertion method. The difference became evident when comparing patients with residual hearing loss (>15 dB), with a significant difference between the two groups that experienced significant loss (>30 dB) at 1 year ($p = 0.038$). This evolution over time in these two subgroups is illustrated in Figure 3. It appears that, even in cases of significant residual hearing loss with robotic insertion, auditory performance is not affected and patients show very good speech perception scores at 1 year (median 83%).

Discussion

CI surgery is constantly evolving, with a particular focus on making EA insertion as minimally traumatic as possible in order to preserve the structures of the inner ear. The main objective of this effort was to preserve the low-frequency range as much as possible in order to enable electroacoustic stimulation and improve CI performance, including speech understanding in noise, music appreciation, and sound localization [1]. Furthermore, significant residual postoperative hearing improves speech perception scores in patients who receive electric-only stimulation compared to those without residual postoperative hearing [20]. Conversely, patients who do not have preoperative residual hearing may benefit from atraumatic CI insertion, as this has been found to be a favorable factor for hearing performance [21, 22]. To achieve less traumatic surgery, the round window approach is preferred over cochleostomy because it allows greater preservation of the residual hearing level [23]. In addition, the design and properties of the EA may impact results. Manufacturers are paying more and more attention to the shape, the size, the diameter, and the flexibility. Therefore, to promote atraumatic surgery, the trend is to favor shorter, more flexible, and thinner EAs. The Med-El Flex24 results in fewer, if any, signs of inner ear trauma, such as scalar dislocation, than the longer arrays and has the best median low-frequency hearing preservation score [11, 24]. All of the subjects in the present study were implanted with the Med-El Flex24 EA using a round window approach.

The philosophy of RACIS is a lower insertion speed, which is associated with lower insertion forces and mainly allows more consistent CI insertion than manual insertion [7, 25]. High insertion speeds cause a significant increase in the forces that induce inner ear trauma and, therefore, are responsible for the deterioration of residual hearing. Robotic insertion results in significantly less inner ear trauma, such as a reduced translocation rate, than manual insertion [4]. A slower EA insertion speed appears to facilitate full electrode insertion with less resistance and, thus, to promote preservation of inner ear function [8].

Table 3. ACI values over time

Months	Overall			≤15 dB			>15 dB			>30 dB		
	mean	median	SD	mean	median	SD	mean	median	SD	mean	median	SD
Manual												
1	35.40	30.00	25.27	36.75	33.50	33.30	34.50	30.00	21.94	35.40	30.00	24.41
3	43.53	47.00	31.68	51.17	50.00	32.31	38.44	37.00	32.11	36.63	30.00	33.83
6	60.93	58.50	21.21	65.50	61.50	20.62	57.50	58.50	22.37	57.57	60.00	24.17
12	63.67	57.00	16.77	68.50	70.00	21.50	60.44	57.00	13.18	58.88	57.00	13.16
Robot-assisted												
1	41.90	40.00	24.30	39.86	50.00	21.55	42.93	38.50	26.29	44.25	35.00	29.55
3	42.73	41.50	25.26	37.86	33.00	15.98	45.00	47.00	28.81	47.56	60.00	26.74
6	62.27	61.50	27.43	63.86	60.00	14.74	61.53	70.00	32.15	66.70	73.50	32.24
12	73.05	73.00	18.48	73.71	73.00	14.94	72.21	76.50	20.54	78.00	83.00	20.72

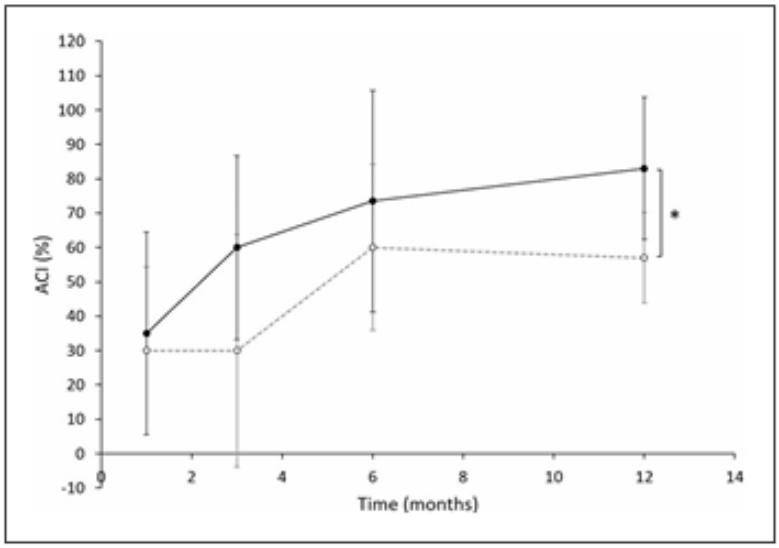

Fig. 3. ACI over time for the two subgroups that experienced residual hearing loss >30 dB. The solid line represents the robot group. The dotted line represents the manual group. The significant difference at 1 year is marked by the asterisk.

Our hearing outcomes in the low-frequency range follow the same trend as our preliminary study, with a higher rate of residual hearing preservation observed in robotic-assisted insertion cases [6]. Jia et al. [5] did not observe any difference in residual hearing outcomes after robotic-assisted insertion, but the patients' preoperative hearing was poor, generally >95 dB. An animal model study showed that we can expect a hearing loss limitation of up to 15 dB after a slow, controlled speed insertion with a robotic arm and using a flexible EA [26].

Hearing loss after cochlear implantation is related to EA position in the cochlea, but also to fibrosis in the ST. The presence of fibrous tissue surrounding the EA is associated with elevated electrical impedance and reflects the electrode-to-tissue status [27]. In the present study, the impedance values of the most apical electrode 1 year after the surgery were significantly less elevated when a patient seemed to have had initial inner ear trauma with a robotic insertion compared to a manual insertion. This suggests that, even in cases categorized as initially traumatic, the development of fibrous tissue could be less important over time. This is also supported by the evolution over time, in which a consistent decrease was observed after robotic surgery, whereas, after manual surgery, a break and upward trend in the impedances at the apex of the EA were observed from the sixth month onwards.

Scar tissue formation around the EA caused by the insertion of the CI changes the mechanical properties of the basilar membrane and can decrease residual hearing [13]. The degree of tissue encapsulation around the EA varies among subjects but is usually most pronounced in the basal turn of the cochlea, modifying the vibration of the basilar membrane apically, which may impact native low-frequency hearing [13]. This fibrous tissue can extend apically beyond the distal end of the electrode in the low-frequency range and cause a delayed residual hearing loss from 3 months to 3 years after implant surgery [12]. Unfortunately, one limitation of our study is the lack of audiological follow-up in some patients, which prevented us from accurately measuring the time interval between surgery and hearing loss.

The impedance measurements in the manual insertion group varied greatly, whereas the values in the robotic insertion group were much more homogeneous. We think that this reflects more random insertion by the human hand and much more consistent insertion with robotic assistance. Significant variations in insertion depth significantly impact impedance fluctuations. Therefore, the insertion angle of electrode 1 was measured and no difference was found between the manual and the robot-assisted procedure allowing to rule out a potential effect the insertion depth on the impedances of the electrodes. In addition, no correlation could be found between the insertion depth and the impedances for the first 5 electrodes reinforcing the hypothesis of the influence of the motorized insertion on the fibrosis due to the insertion trauma.

Finally, we investigated the clinical aspect of hearing performance after cochlear implantation. The two groups, i.e., manual or robot-assisted insertion procedures, can be compared because the assessment of the insertion depth showed no significant difference between the 2 cohorts of patients. This was important to rule out since insertion depth of the electrodes exerts an influence on speech intelligibility. In addition, no correlation was found between the insertion angle and the hearing preservation. Evolution of the word recognition score was comparable regardless of the insertion method when there was full residual hearing preservation but, as soon as there was partial residual hearing loss, a certain slowing down became apparent in the manual insertion group. This is significant in patients with residual hearing loss >30 dB. Even if fibrous tissue extends the length of the EA and beyond the tip in most cases, the degree of fibrous tissue alone does not significantly correlate with the word recognition score or intracochlear insertional trauma [14]. In contrast, these authors found that auditory performance correlated with residual spiral ganglion cell counts and the degree of intracochlear new bone formation associated with the trauma to the inner ear. Our results suggest that, in the major residual hearing loss group, the consequences of CI insertion result in deeper damage to the structures of the inner ear and in a poor electrode-neural interface.

Conclusion

The RobOtol® surgical robot allows for safe and slow CI electrode array insertion in the cochlea. This results in a reduced risk of deterioration of residual hearing at low frequencies. This gentle insertion seems to impact the degree of fibrous tissue formation around the EA tip, resulting in stable impedance. Even in the presence of residual hearing loss, the auditory performance is not affected, suggesting better preservation of the delicate neurosensory structures of the inner ear.

Acknowledgments

The authors thank the audiologists of the Department of Otorhinolaryngology for outstanding clinical work.

Statement of Ethics

This study was performed according to the regulation of the University Faculty Hospital Ethics Committee of CHU Liège (Liège, Belgium) and the principles outlined in the World Medical Association Declaration of Helsinki. The study was approved by the Local Ethics Committee of CHU Liège (Ethics Committee number 707; ref: 2023-23). Written informed consent was obtained from participants before enrollment in the study.

Conflict of Interest Statement

The authors have no conflicts of interest to declare.

Funding Sources

This study has no specific funding source.

Author Contributions

P.P.L. performed the surgeries. Clinical evaluation was assessed by G.G. and P.P.L., U.D. performed clinical assessment based on CT-scan images. G.G. and N.P. reviewed the electronic medical records. S.C. performed the statistical analyses, draft review, and editing for final manuscript.

Data Availability Statement

All data generated or analyzed during this study are included in this article. Further inquiries can be directed to the corresponding author.

References

1 Woodson EA, Reiss LAJ, Turner CW, Gfeller K, Gantz BJ. The Hybrid cochlear implant: a review. Adv Oto-Rhino-Laryngol. 2010;67:125–34. https://doi.org/10.1159/000262604

2 Jia H, Venail F, Piron J-P, Batrel C, Pelliccia P, Artières F, et al. Effect of surgical technique on electrode impedance after cochlear implantation. Ann Otol Rhinol Laryngol. 2011;120(8):529–34. https://doi.org/10.1177/000348941112000807

3 Van de Heyning P, Roland P, Lassaletta L, Agrawal S, Atlas M, Baumgartner WD, et al. Suitable electrode choice for robotic-assisted cochlear implant surgery: a systematic literature review of manual electrode insertion adverse events. Front Surg. 2022;9:823219. https://doi.org/10.3389/fsurg.2022.823219

4 Torres R, Jia H, Drouillard M, Bensimon JL, Sterkers O, Ferrary E, et al. An optimized robot-based technique for cochlear implantation to reduce array insertion trauma. Otolaryngol Neck Surg. 2018;159(5):900–7. https://doi.org/10.1177/0194599818792232

5 Jia H, Pan J, Gu W, Tan H, Chen Y, Zhang Z, et al. Robot-assisted electrode array insertion becomes available in pediatric cochlear implant recipients: first report and an intra-individual study. Front Surg. 2021;8:695728. https://doi.org/10.3389/fsurg.2021.695728

6 Barriat S, Peigneux N, Duran U, Camby S, Lefebvre PP. The use of a robot to insert an electrode array of cochlear implants in the cochlea: a feasibility study and preliminary results. Audiol Neurotol. 2021;26(5):361–7. https://doi.org/10.1159/000513509

7 Kontorinis G, Lenarz T, Stöver T, Paasche G. Impact of the insertion speed of cochlear implant electrodes on the insertion forces. Otol Neurotol. 2011;32(4):565–70. https://doi.org/10.1097/MAO.0b013e318219f6ac

8 Rajan GP, Kontorinis G, Kuthubutheen J. The effects of insertion speed on inner ear function during cochlear implantation: a comparison study. Audiol Neurotol. 2013;18(1):17–22. https://doi.org/10.1159/000342821

9 Nguyen S, Cloutier F, Philippon D, Côté M, Bussières R, Backous DD. Outcomes review of modern hearing preservation technique in cochlear implant. Auris Nasus Larynx. 2016;43(5):485–8. https://doi.org/10.1016/j.anl.2016.02.014

10 Santa Maria PL, Gluth MB, Yuan Y, Atlas MD, Blevins NH. Hearing preservation surgery for cochlear implantation: a meta-analysis. Otol Neurotol. 2014;35(10):e256–69. https://doi.org/10.1097/MAO.0000000000000561

11 Causon A, Verschuur C, Newman TA. A retrospective analysis of the contribution of reported factors in cochlear implantation on hearing preservation outcomes. Otol Neurotol. 2015;36(7):1137–45. https://doi.org/10.1097/MAO.0000000000000753

12 Foggia MJ, Quevedo RV, Hansen MR. Intracochlear fibrosis and the foreign body response to cochlear implant biomaterials. Laryngoscope Investig Otolaryngol. 2019;4(6):678–83. https://doi.org/10.1002/lio2.329

13 Choi C-H, Oghalai JS. Predicting the effect of post-implant cochlear fibrosis on residual hearing. Hear Res. 2005;205(1–2):193–200. https://doi.org/10.1016/j.heares.2005.03.018

14 Kamakura T, Nadol JB Jr. Correlation between word recognition score and intracochlear new bone and fibrous tissue after cochlear implantation in the human. Hear Res. 2016;339:132–41. https://doi.org/10.1016/j.heares.2016.06.015

15 Busby PA, Plant KL, Whitford LA. Electrode impedance in adults and children using the Nucleus 24 cochlear implant system. Cochlear Implants Int. 2002;3(2):87–103. https://doi.org/10.1179/cim.2002.3.2.87

16 Wilk M, Hessler R, Mugridge K, Jolly C, Fehr M, Lenarz T, et al. Impedance changes and fibrous tissue growth after cochlear implantation are correlated and can Be reduced using a dexamethasone eluting electrode. PLoS One. 2016;11(2):e0147552. https://doi.org/10.1371/journal.pone.0147552

17 Spitzer ER, Hughes ML. Effect of stimulus polarity on physiological spread of excitation in cochlear implants. J Am Acad Audiol. 2017;28(9):786–98. https://doi.org/10.3766/jaaa.16144

18 Skarzynski H, van de Heyning P, Agrawal S, Arauz SL, Atlas M, Baumgartner W, et al. Towards a consensus on a hearing preservation classification system. Acta Otolaryngol Suppl. 2013;133(564):3–13. https://doi.org/10.3109/00016489.2013.869059

19 O'Connell BP, Hunter JB, Haynes DS, Holder JT, Dedmon MM, Noble JH, et al. Insertion depth impacts speech perception and hearing preservation for lateral wall electrodes. Laryngoscope. 2017;127(10):2352–7. https://doi.org/10.1002/lary.26467

20 Schaefer S, Sahwan M, Metryka A, Kluk K, Bruce IA. The benefits of preserving residual hearing following cochlear implantation: a systematic review. Int J Audiol. 2021;60(8):561–77. https://doi.org/10.1080/14992027.2020.1863484

21 Aschendorff A, Kromeier J, Klenzner T, Laszig R. Quality control after insertion of the nucleus contour and contour advance electrode in adults. Ear Hear. 2007;28(2 Suppl):75S–9S. https://doi.org/10.1097/AUD.0b013e318031542e

22 Finley CC, Holden TA, Holden LK, Whiting BR, Chole RA, Neely GJ, et al. Role of electrode placement as a contributor to variability in cochlear implant outcomes. Otol Neurotol. 2008;29(7):920–8. https://doi.org/10.1097/MAO.0b013e318184f492

23 Snels C, IntHout J, Mylanus E, Huinck W, Dhooge I. Hearing preservation in cochlear implant surgery: a meta-analysis. Otol Neurotol. 2019;40(2):145–53. https://doi.org/10.1097/MAO.0000000000002083

24 Ketterer MC, Aschendorff A, Arndt S, Speck I, Rauch AK, Beck R, et al. Radiological evaluation of a new straight electrode array compared to its precursors. Eur Arch Oto-Rhino-Laryngol. 2021;278(10):3707–14. https://doi.org/10.1007/s00405-020-06434-5

25 Miroir M, Nguyen Y, Szewczyk J, Sterkers O, Bozorg Grayeli A. Design, kinematic optimization, and evaluation of a teleoperated system for middle ear microsurgery. Sci World J. 2012;2012:907372. https://doi.org/10.1100/2012/907372

26 Drouillard M, Torres R, Mamelle E, De Seta D, Sterkers O, Ferrary E, et al. Influence of electrode array stiffness and diameter on hearing in cochlear implanted Guinea pig. PLoS One. 2017;12(8):e0183674. https://doi.org/10.1371/journal.pone.0183674

27 Hughes ML, Vander Werff KR, Brown CJ, Abbas PJ, Kelsay DM, Teagle HF, et al. A longitudinal study of electrode impedance, the electrically evoked compound action potential, and behavioral measures in nucleus 24 cochlear implant users. Ear Hear. 2001;22(6):471–86. https://doi.org/10.1097/00003446-200112000-00004

Contribution to the existing literature

Comparisons between robot-assisted and manual insertion have mainly relied on radiological or audiometric endpoints obtained at a single postoperative time point. The originality of this study lies in its longitudinal design: electrode impedance, available at every follow-up visit without additional equipment, is used as an indirect marker of the intracochlear tissue response and is followed over one year. It reports lower and more stable apical impedances after robotic insertion, which supports the stability of the result over time. Its most informative finding concerns the subgroup in which residual hearing was not preserved: speech intelligibility continued to improve beyond six months after robot-assisted insertion, whereas it plateaued after manual insertion. This suggests that the benefit of robotic assistance is not confined to hearing preservation and persists in the long term when the insertion has been traumatic.

Article 3

Journal: Audiology and Neurotology. Peer-reviewed. Published: Gersdorff G, Nopp P, Camby S, Lefebvre P. Impact of Robotic-Assisted Electrode Array Insertion on Neural Health and Hearing Outcomes in Cochlear Implant Recipients. Audiol Neurotol. 2026. doi:10.1159/000552800. Received 3 December 2025; accepted 21 May 2026; published online 24 August 2026.

Audiology and Neurotology

Audiol Neurotol , DOI: 10.1159/000552800
Received: December 3, 2025
Accepted: May 21, 2026
Published online: August 24, 2026

Impact of Robotic-Assisted Electrode Array Insertion on Neural Health and Hearing Outcomes in Cochlear Implant Recipients

Gersdorff G, Nopp P, Camby S, Lefebvre P

ISSN: 1420-3030 (Print), eISSN: 1421-9700 (Online)
https://www.karger.com/AUD
Audiology and Neurotology

Disclaimer:
Accepted, unedited article not yet assigned to an issue. The statements, opinions and data contained in this publication are solely those of the individual authors and contributors and not of the publisher and the editor(s). The publisher and the editor(s) disclaim responsibility for any injury to persons or property resulting from any ideas, methods, instructions or products referred to the content.

Copyright:
© 2026 S. Karger AG, Basel

Impact of Robotic-Assisted Electrode Array Insertion on Neural Health and Hearing Outcomes in Cochlear Implant Recipients

Authors' names: Guillaume Gersdorff[a] ,Peter Nopp[b], Severine Camby[a], Philippe Lefebvre[a]

Affiliations:

a. Department of Otorhinolaryngology, CHU, Liège Belgium.
b. Med-El, Innsbruck, Austria.

Corresponding author details:
Name: Lefebvre Philippe.[1]
E-mail : pp.lefebvre@uliege.be
ORCID ID: 0000-0002-2957-7781

Keywords
Auditory nerve · Cochlear implants · Electrically evoked compound action potential· Neural health · Robotic

Abstract
Introduction: Cochlear implants (CIs) have revolutionized the treatment of severe to profound sensorineural hearing loss, offering significant auditory benefits to individuals who do not benefit adequately from conventiona hearing aids. The efficacy of CIs largely depends on the interface between the electrode array and auditory nerve fibers, with neural health playing a crucial role in postoperative outcomes. This study investigates the impact of robotic-assisted electrode array insertion on the preservation of neural health and auditory performance, evaluated through electrically evoked compound action potential (ECAP) measurements and audiometric outcomes.
Methods: A retrospective single-center study was conducted with 20 patients, divided into two groups: manual insertion (n=12) and robotic-assisted insertion (n=8). All patients received Med-El CIs with either FLEX 24 or FLEX 28 electrode arrays. The robotic-assisted insertions were performed using the RobOtol® system. ECAP measurements were taken to assess neural health. Audiometric evaluation using pure-tone audiometry (PTA) wa performed preoperatively to confirm group equivalence, while speech intelligibility was assessed both pre- and postoperatively using the auditory capacity index (ACI).
Results: Robotic-assisted insertion significantly improved neural health preservation, as evidenced by a higher mean ECAP slope difference (2.99 ± 0.69) compared to manual insertion (1.42 ± 0.68), with a significant correlation between ECAP slope difference and speech intelligibility (R^2 = 0.23, p=0.032). Additionally, patients in the robotic-assisted group demonstrated superior speech intelligibility scores (ACI: 84.5 ± 11.04%) compared to the manual group (ACI: 69.5 ± 14.29%).
Conclusion: These findings suggest that robotic-assisted cochlear implant surgeries offer substantial benefits in terms of preserving neural health and enhancing auditory outcomes.

Introduction

Cochlear implants (CIs) have revolutionized the treatment of severe to profound sensorineural hearing loss, providing significant auditory benefits to individuals who do not benefit adequately from conventional hearing aids. The success of cochlear implants is highly dependent on the interface between the electrode array and the auditory nerve fibers. Recent advancements in neural health and electrode array technology have further enhanced the efficacy of cochlear implants. One promising area of innovation is the robotic insertion of electrode arrays, which aims to improve hearing preservation by minimizing trauma during implantation.

Neural health plays a crucial role in the outcomes of cochlear implantation. Healthy spiral ganglion neurons (SGNs) as well as their neurites are essential for the effective transmission of electrical signals from the cochlear implant to the brain. Damage to these delicate neuronal structures (NSs) can result in suboptimal hearing outcomes, making the preservation of neural health a priority in cochlear implant procedures [1]. Studies have shown that atraumatic surgical techniques and the careful design of electrode arrays can significantly impact the preservation of SGNs, thereby improving postoperative auditory performance. The insertion of electrode arrays into the cochlea is a delicate process that carries the risk of damaging cochlear structures, potentially leading to a loss of residual hearing. Traditional manual insertion techniques, while effective, are limited by the precision and consistency achievable by human hands. Robotic systems have been developed to address these limitations,

offering improved precision and control during electrode array insertion. These systems are designed to reduce insertion forces and minimize trauma to the cochlea, thereby enhancing the preservation of residual hearing [2]. Emerging robotic technologies not only promise to enhance surgical precision but also offer the potential for customized, patient-specific insertion strategies. By leveraging preoperative imaging and intraoperative feedback, robotic systems can tailor the insertion process to the unique anatomy of each patient's cochlea, further improving outcomes. Preliminary studies have demonstrated the feasibility and benefits of robotic-assisted cochlear implant surgeries, marking a significant step forward in the field of otologic surgery [3] . In addition, in a previous study using the Robotol®, we have shown that all of the patients who experienced complete hearing preservation had a generally comparable evolution regardless of the insertion method. The difference became evident when comparing patients with residual hearing loss (> 15 dB), with a significant difference between the two groups that experienced significant loss (> 30 dB) at 1 year (p = 0.038). Interestingly, It appears that, even in cases of significant residual hearing loss with robotic insertion, patients show a significantly better very speech perception scores one year when compared to manual insertion, suggesting a better preservation of the neural health in the motorized electrode array insertion [4].
In this article, we explore the intricate relationship between cochlear implants, neural health evaluated by ECAP measurements, and the robotic insertion of electrode arrays with a particular focus on hearing performances in cochlear implant recipients.

Materials and Methods

Study design
We performed a retrospective single-center study to evaluate ECAP measurements and audiometric outcomes in a population of patients who underwent manual or robot-assisted cochlear implantation.
Study participants
Individuals who met the general eligibility criteria for CI surgery, were ≥18 years old, and fluent in French were included in this study. The exclusion criteria were pregnancy or anatomical malformations of the middle or inner ear. A total of 8 subjects in the robotic-assisted insertion group and 12 subjects in the manual insertion group gave written informed consent and were subsequently enrolled in the study. Patients were consecutively enrollec between 01/10/2023 and 31/12/2024 in both the manual and robotic groups.
Written informed consent to participate was not required by the University Faculty Hospital Ethics Committee of CHU Liège (Liège, Belgium).

Type of electrode arrays
All subjects had Med-El CIs and two types of EA : FLEX 24 that was 24 mm long with an active length of 20.9 mm and FLEX 28 that was 28 mm long with an active length of 23.1 mm. Seven subjects were implanted with FLEX 24 and 5 subjects with Flex 28 in manual group. Five subjects received FLEX 24 and 3 subjects received FLEX 28 in robotic-assisted group. To enable more flexibility at the tip, the five most apical electrode contacts were single, whereas the basal seven electrodes were paired. This reduced the diameter of the tip to 70% of the standard Med-El Combi40+ electrode.

Surgical and robotic procedure
CI surgery via the conventional surgical approach was performed under general anesthesia. The same senior surgeon performed all surgeries. A posterior tympanotomy was created with respect to the facial nerve and chorda tympani. The body overhang of the round window niche was carefully drilled to expose the round window membrane. The RobOtol® (Collin, Bagneux, France) robot was used to introduce the EA into the cochlea. The RobOtol® arm with the insertion tool mounted on it was placed in the surgical field in the view of the posterior tympanotomy and the round window membrane. We descended the inserter’s tip into the posterior tympanotomy using the robot. The robotic insertion tool was retracted 30 mm with respect to the trajectory of the insertion through the round window. The EA was clipped on the instrument 10 mm from the full insertion marker ring. The round window membrane was gently opened with the tip of a Rosen needle toward the perilymph. The axes of freedom of the robot were blocked, so the robot could only move linearly toward the round window. The insertion tool was moved gently toward the tip of the EA and inserted into the cochlea under guidance of a fork. The manual speed insertion of the EA was calculated by reviewing the videos of the procedures and the time needed to insert 5 of the 12 electrodes. The robotic speed insertion was fixed from 0.1

mm/s. After it was inserted completely, the EA was gently unclipped from the insertion instrument. We did not use any IV or local steroids during the surgery. Round window sealing and array fixation in the mastoid were performed using fibrin glue (Tisseel®). For the manual insertion group, CIs were inserted within the round window manually and as slowly as possible. Adequate visualization of the round window membrane was achieved in all cases. Manual electrode insertion was performed under direct microscopic visualization, with an intention to proceed as slowly and smoothly as possible.

ECAP measurement

The Med-El ECAP measurement method utilizes the ART (Auditory Response Telemetry) system, which is integrated into their Maestro cochlear implant system. Biphasic Electrical pulses are delivered to the cochlea through the implant's electrode array. The stimuli used for ECAP measurements typically consist of biphasic pulses, which are effective in eliciting neural responses while minimizing potential damage to the auditory nerve fibers. The interphase gap was modified to 10 μs and 30 μs. The recording electrode located next to the stimulating electrode measures the potential difference generated by the neural response, which is then transmitted to the external processor for analysis. The recorded ECAP waveforms are analyzed to determine key parameters such as the threshold level (the minimum stimulus level required to evoke a detectable response) and the amplitude of the response. These parameters are critical for setting the optimal stimulation levels in the cochlear implant. The recorded ECAP waveforms are analyzed automatically by the Maestro program to determine key parameters such as the threshold level (the minimum stimulus level required to evoke a detectable response) and the amplitude of the response. In particular, the slope of the amplitude growth in function of the current was determined automatically for each electrode. The mean for all electrodes was calculated for the two gap interphase paradigms stimuli (i.e. mean slope at 30 μs minus mean slope at 10 μs). This difference of slopes, also referred to as the "IPG effect on slope" or "interphase gap effect on the ECAP amplitude growth function slope" , is a representation of the neural health [5–7] .

Outcome measures

Audiological fitting was performed according to our standard routine, which comprises activation and initial fitting 10 days postoperatively and at regular intervals for 12 months after the surgery (1 month, 3 months, 6 months, and 12 months). An audiological evaluation was performed preoperatively using the pure-tone average (PTA), calculated as the mean of hearing threshold levels (in dB HL) at a set of specified frequencies. For this study, the PTA was assessed at 250, 500, 1,000, 2,000, and 4,000 Hz. This preoperative PTA was used to confirm the equivalence of the two groups before implantation.

Postoperatively, speech intelligibility performance was measured by the articulation function using the auditory capacity index (ACI). The ACI was defined as the average speech discrimination score obtained at 40, 55, and 70 dB SPL. We used words from Fournier's dissyllabic list in French, which were pronounced to the patient through a loudspeaker. Measurements were recorded at 40, 55, and 70 dB SPL and at regular intervals for 12 months after the surgery (1 month, 3 months, 6 months, and 12 months).

The ECAP measurement were performed when the patients reached a plateau in their speech intelligibility as measured by ACI.

Statistical analysis

The data were analyzed using standard statistical software R version 3.6.1. ECAP, ACI and PTA values comparisons were made between each group using the Mann-Whitney non-parametric test for comparing two independent samples. Correlation between mean ECAP slope difference and Articulation Function was tested and Pearson correlation coefficient was calculated. The results were considered significant when $p \leq 0.05$.

Results

Participants

Twenty participants took part in this study and were divided into two main groups depending on whether they were implanted manually (12 patients) or robot-assisted (8 patients). The mean age at implantation was 65.2 ± 11.7 years and 54.25 ± 13.81 years, respectively. No statistically significative difference was showed between groups in age (t test associated p-value is p= 0,063 All of the patients were implanted with a Med-El Flex 24 or Flex 28 EA by the same senior surgeon. Both groups were similar in electrode types distribution (Chi^2 test

associated p-value is 0,85). The manual insertion speed was estimated by reviewing surgical videos from five randomly selected patients. The time required to insert five electrodes of the Flex 24 array was measured. The mean insertion speed was 2.48 ± 0.52 mm/s. In contrast, robotic insertion speed was predefined and controlled a 0.1mm/s [4] .

Audiological analysis
In the manual insertion group, the preoperative PTA for five frequencies (250, 500, 1,000, 2,000, and 4,000 Hz) was 91.25 ± 13.99 dB In the robot-assisted insertion group, the preoperative PTA for the same five frequencies was 87.50 ± 13.44 db. These two groups were comparable; there was no significant difference between them (p = 0.063).

Speech intelligibility
The speech intelligibility performance based on the ACI is provided in figure 1. The maximal speech intelligibility was recorded at the plateau achieved by the patients after 6 to 12 months post implantation. ACI with implant activated and measured at the plateau was 69.5 ± 14.29 % for the manual insertion group and 84.5 ± 11.04 % foı the robotic insertion group (p = 0.0323). The ACI was measured at the time when the ECAP were recorded for the 12 electrodes. The relationship between the mean ECAP and ACI was analyzed.

ECAP analysis
The neural health was evaluated by measuring the difference of the slope average of the amplitude growth of ECAP in function of the stimulating current with an interphase gap of 30 μs and of 10 μs. ECAP slope difference with implant activated and measured at the plateau of speech intelligibility was 1.42 ± 0.68 for the manual insertion group and 2.99 ± 0.69 for the robotic insertion group (Mann-Whitney: Score Z= 2.18; U mean = 48 ; p = 0.00071). Average mean ECAP slope difference do correlate (R2=0.23) with speech intelligibility as measured by the Articulation Function (p= 0.032). Figure 2 shows ECAP results while figure 3 shows le relationship between ECAP and ACI.

Discussion

Cochlear implants (CIs) have transformed the treatment of severe to profound sensorineural hearing loss. Advances have moved towards minimally invasive techniques to ensure comprehensive cochlear health, protecting delicate intracochlear structures and reducing inflammatory responses. This approach enhances CI performance, speech understanding in noise, music appreciation, sound localization, and optimizes intracochlear drug therapies and future hearing restoration methods. Preservation of residual hearing could significantly contribute to improving speech perception scores [8–11].

Cochlear health, including neural health, is crucial for CI effectiveness. Factors such as spiral ganglion neuron (SGN) density, neuronal cell size, myelination, and synaptic function impact sound perception with CIs. Variation in SGN density accounts for significant variance in CI function measures and could be predictive of speech recognition [5,12–18]. Other factors, such as neuronal myelination, fibrosis, and osteogenesis, also affect CI outcomes [5,19–21] .

The process of electrode array insertion into the cochlea carries the risk of inducing trauma, which can significantly affect neural health and overall CI outcomes. Insertion trauma can result in mechanical damage to cochlear structures, including the basilar membrane, osseous spiral lamina, and SGNs [22]. Even minimal trauma can provoke inflammatory responses, fibrosis, and SGN loss [23], disrupting cochlear homeostasis and perception particularly in patients with residual low-frequency hearing [24].

Minimally invasive techniques, particularly robotic-assisted cochlear implant surgery (RACIS), reduce trauma, improve electrode positioning, and enhance long-term outcomes [8,25,26]. Optimal placement in the scala tympani without scalar deviation provides the best electrode–neural interface [26]. Lower insertion speeds and flexible, thin electrodes promote atraumatic surgery [27–29]. Among these, Med-El Flex24 shows superior hearing preservation, and straight electrodes are generally preferred for RACIS [26,30] . In this study, all patients received Med-El Flex24-28 arrays via the round window, guided by OTOPLAN® software.

Nevertheless, residual hearing loss may occur post-implantation due to delayed neuronal damage from chronic inflammation, fibrosis, or neo-osteogenesis [31–34]. Fibrosis has been linked to higher impedance and poorer sound quality [25,35–37]. Our prior study showed that robotic-assisted insertion leads to better long-term residual hearing preservation, stable impedance, and unaffected auditory performance compared with manual insertion [4]. Building on these findings, we observed that fibrosis and impedance are influenced mainly by

insertion quality rather than insertion depth [4]. Auditory performance correlated more with SGN counts and intracochlear new bone than with fibrotic spread [34]. In patients with >30 dB residual hearing loss, implantation may cause deeper cochlear damage and a poorer electrode–neural interface [4]. These findings suggest that the superior outcomes of robotic insertion arise from a more favorable electrode–neural interface, with reduced trauma and improved neural preservation, as evidenced by intraoperative electrophysiological markers. However in a recent study, we have shown that even in patients who lost residual hearing after implantation, robotic insertion allowed a higher speech intelligibility as compared to manual insertion, leading to the hypothesis of a better preservation of the neural components of the cochlea when the electrode array was inserted at a very slov speed [4].

Electrophysiological measures provide valuable insights into neural health. Electrically evoked compound action potentials (ECAPs), and in particular changes in amplitude growth function (AGF) slope and latency with interphase gap (IPG) variations (the "IPG Effect"), reflect the cochlear health. The underlying contributions to the IPG Effect are not yet well understood, but theoretically would relate to the ability of the stimulated cell to recover from depolarization which would likely be affected by overall neural health as reviewed in previous literature [13,14,38,39]. While not completely understood, the IPG Effect is thought to be dependent on membrane characteristics, and thus reflect temporal response properties of the auditory nerve (McKay CM ,2003 [32,33] . Similar to ECAP measures using a fixed IPG, SGN density and cell size in cochlear-implanted guinea pigs account for a significant proportion of variance (about 40–60%) when measuring the IPG Effect for ECAP amplitude and slope, but not latency [5,13,39]. This effect may be advantageous compared to fixed IPG ECAPs, as it is less influenced by varying non-neural conditions [36]. Similarly ,it has been observed that the charge required to evoke an equal-amplitude ECAP when using a short or long IPG also correlates with SGN density in acutely implanted guineapigs [40]. It is proposed that, while the IPG Effect might be affected by temporal response properties of the auditory nerve, it also reflects SGN density based on these animal studies. Human data confirm its sensitivity to auditory nerve responsiveness [40]. Increasing IPG reduces auditory nerve thresholds [30] and enhances loudness perception [32].

Clinical ECAP measures such as thresholds and AGF slope provide both baseline and supra-threshold insights into neural health [6,7]. Higher ECAP responses indicate better neural survival [41], while lower responses may suggest reduced synchronization or fewer surviving fibers [7,41]. Clinically, ECAP thresholds are favored for their ease of measurement and essential data provision on neural response. However, supra-threshold measures, such as the AGF slope, offer more nuanced insights into neural health and function [6,7].MED-EL, has developed sophisticated tools and techniques for ECAP measurement, designed to optimize CI performance and to ensure successful auditory outcomes. The Maestro system, for instance, incorporates features that facilitate the automatic and real-time recording of ECAPs. This system utilizes the ART (Auditory Response Telemetry) tool to capture ECAPs, enabling clinicians to assess the auditory nerve's response to electrical stimulation with high precision [42] . Initially, electrical stimuli are delivered through the implant's electrode array to the auditory nerve. The resulting neural responses are then recorded and analyzed to determine the auditory nerve's responsiveness. This process is crucial for the programming and fitting of the cochlear implant, as it provides insights into the optimal stimulation levels required for effective hearing [42]. ECAPs are neural responses elicited by electrical stimulation from a cochlear implant. These responses provide valuable information about the integrity and functionality of the auditory nerve fibers. By measuring ECAPs, clinicians can evaluate the performance of the cochlear implant and make necessary adjustments to the device's programming, thereby enhancing the auditory experience of the user [43].

In this paper, we have shown that neural health, evaluated by measuring the difference in the average slope of the ECAP amplitude growth function as a function of the stimulating current with interphase gaps of 30 µs and 10 µs, was significantly better when using a motorized insertion at 0.1 mm/s compared to manual insertion performed by an experienced surgeon. This finding suggests improved preservation of the neural structures of the inner ear, potentially contributing to higher speech intelligibility.

This conclusion relies on the assumption that preoperative neural health was comparable between the two groups. This assumption is supported by our preoperative audiometric evaluation, which confirmed equivalent baseline auditory thresholds between the manual and robotic groups (preoperative PTA: 91.25 ± 13.99 dB vs. 87.50 ± 13.44 dB, $p = 0.063$). As the pure-tone average reflects cochlear and neural integrity prior to implantation [6,12,18], the absence of a significant difference between groups reinforces the validity of our comparison regarding postoperative neural health. This approach is consistent with previous findings showing that similar preoperative auditory thresholds are indicative of comparable baseline neural integrity [6,7].

While our study focused on long-term neural health following robotic insertion, incorporating preoperative and early postoperative ECAP measurements in future research could help better characterize baseline neural condition and the immediate electrophysiological impact of electrode insertion. Such longitudinal ECAP monitoring, spanning from baseline through early recovery to long-term stabilization, would not directly enhance neural health but would provide a more comprehensive understanding of the temporal evolution of auditory nerve responsiveness and the degree of neural preservation achieved with robotic-assisted insertion [6,7].
The evolution of ECAP over time reflects the dynamic recovery of cochlear nerve function. Initially, patients may present higher ECAP thresholds that decrease as the electrode–tissue interface stabilizes and neural synchrony improves. Our previous study reported better impedance stability over time with robotic-assisted insertion, supporting our current findings of improved ECAP evolution [4]. Regular ECAP monitoring thus offers valuable information for optimizing cochlear implant programming and predicting auditory outcomes [41]. Although the present study assessed ECAPs after stabilization, future investigations combining baseline and early postoperative measures may further elucidate the mechanisms by which robotic techniques contribute to atraumatic insertion and long-term cochlear health.

Electrode length plays an important role in cochlear implantation outcomes, influencing both the extent of cochlear coverage and the quality of neural stimulation [6]. Patient-specific anatomy was carefully evaluated with the Otoplan program to guide electrode choice, aiming to ensure a balance between coverage and atraumatic insertion. In our series, longer electrodes such as the MedEl Flex 28 were selected for larger cochleae, with the overall goal of minimizing trauma and preserving neural health [31].

Neural health, particularly the survival and function of SGNs, remains a key determinant of CI performance and speech understanding [6,7,12,38]. Age-related decline in SGN density also influences outcomes [6,7,12]. Degeneration from long-standing deafness or traumatic insertions results in poorer encoding, underscoring the need to preserve auditory neurons [44]. Pharmacological interventions such as corticosteroids or neurotrophic factors [45,46], together with atraumatic electrode designs and robotic techniques [4], represent future avenues for optimizing CI results.

Our findings confirm that ECAP slopes and IPG-based measures are reliable indicators of neural health and correlate with speech intelligibility. Robotic-assisted insertion appears superior to manual insertion in preserving neural structures, leading to enhanced auditory outcomes [6,39]. The addition of predictive ECA (i.e., ECAP-derived parameters used to estimate the functional status of the cochlear nerve [7]), electrically stimulated auditory responses (ESA), and intraoperative electrocochleography (ECochG) could further refine monitoring [43,47].
This study has several limitations inherent to its retrospective design, including missing data and the presence of confounding variables that could not be fully controlled.

Conclusion

In conclusion, cochlear implantation provides transformative benefits, yet minimizing insertion-related trauma remains essential for optimizing long-term outcomes. Our findings confirm that robotic-assisted insertion, when combined with atraumatic electrode design, achieves superior auditory performance compared with manual techniques, even in the absence of measurable preoperative residual hearing. This advantage likely arises from reduced postoperative fibrosis and diminished neural injury, assuming comparable preoperative cochlear health as supported by equivalent preoperative audiometric thresholds between groups, resulting in a more favorable electrode–neural interface. The present ECAP study demonstrated that robotic-assisted surgery more effectively preserves neural health than conventional approaches. Integrating intraoperative electrophysiological monitoring with robotic-assisted techniques thus represents a significant advance toward safeguarding cochlear integrity and maximizing implant performance.

Statements

Acknowledgments: The authors thank the audiologist of the Department of Oto-rhinolaryngology for outstanding clinical work.

Statement of Ethics: The study was approved by the University Faculty Hospital Ethics Committee of CHU Liège (Liège, Belgium) (Ethics Committee number 707 ; ref: 2023-23). Written informed consent was not required for this study by the University Faculty Hospital Ethics Committee of CHU Liège (Liège, Belgium)

Conflict of interest: The authors have no conflicts of interest to declare. Philippe P. Lefebvre was a member of the journal's Editorial Board at the time of submission.

Funding Sources: This study has no specific funding source.

Author Contributions: Philippe P. Lefebvre performed the surgeries. Clinical evaluation was assessed by Philippe P. Lefebvre. Guillaume Gersdorff reviewed the electronic medical records and wrote the manuscript. Severine Camby performed the statistical analyses. Peter Nopp helped in reviewing the manuscript.

Data availability: All data generated or analyzed during this study are included in this article. Further enquiries can be directed to the corresponding author.

References:

1 Liu W, Wang X, Wang M, Wang H. Protection of Spiral Ganglion Neurons and Prevention of Auditory Neuropathy. Adv Exp Med Biol. 2019;1130:93–107.
2 Caversaccio M, Gavaghan K, Wimmer W, Williamson T, Ansò J, Mantokoudis G, et al. Robotic cochlear implantation: surgical procedure and first clinical experience. Acta Otolaryngol. 2017 Apr;137(4):447–54.
3 Balachandran R, Reda FA, Noble JH, Blachon GS, Dawant BM, Fitzpatrick JM, et al. Minimally Invasive Image-Guided Cochlear Implantation for Pediatric Patients: Clinical Feasibility Study. Otolaryngol Neck Surg. 2014 Apr;150(4):631–7.
4 Gersdorff G, Peigneux N, Duran U, Camby S, Lefebvre PP. Impedance and Functional Outcomes in Robotic Assisted or Manual Cochlear Implantation: A Comparative Study. Audiol Neurotol. 2024 Aug;1–9.
5 Schvartz-Leyzac KC, Colesa DJ, Buswinka CJ, Rabah AM, Swiderski DL, Raphael Y, et al. How electrically evoked compound action potentials in chronically implanted guinea pigs relate to auditory nerve health and electrode impedance. J Acoust Soc Am. 2020 Dec;148(6):3900.
6 Kim J-R, Abbas PJ, Brown CJ, Etler CP, O'Brien S, Kim L-S. The Relationship Between Electrically Evoked Compound Action Potential and Speech Perception. Otol Neurotol. 2010 Sep;31(7):1041–8.
7 Skidmore J, Xu L, Chao X, Riggs WJ, Pellittieri A, Vaughan C, et al. Prediction of the Functional Status of the Cochlear Nerve in Individual Cochlear Implant Users Using Machine Learning and Electrophysiological Measures. Ear Hear. 2021 Jan;42(1):180–92.
8 Woodson EA, Reiss LAJ, Turner CW, Gfeller K, Gantz BJ. The Hybrid cochlear implant: a review. Adv Otorhinolaryngol. 2010;67:125–34.
9 Schaefer S, Sahwan M, Metryka A, Kluk K, Bruce IA. The benefits of preserving residual hearing following cochlear implantation: a systematic review. Int J Audiol. 2021;60(8):561–77.
10 Aschendorff A, Kromeier J, Klenzner T, Laszig R. Quality Control After Insertion of the Nucleus Contour and Contour Advance Electrode in Adults. Ear & Hear. 2007;28(2):75S-79S.
11 Finley CC, Holden TA, Holden LK, Whiting BR, Chole RA, Neely GJ, et al. Role of electrode placement as a contributor to variability in cochlear implant outcomes. Otol Neurotol. 2008;29(7):920–8.
12 Schvartz-Leyzac KC, Colesa DJ, Swiderski DL, Raphael Y, Pfingst BE. Cochlear Health and Cochlear-implant Function. J Assoc Res Otolaryngol. 2023 Jan;24(1):5–29.
13 Ramekers D, Versnel H, Strahl SB, Smeets EM, Klis SF, Grolman W. Auditory nerve responses to varied interphase gap and phase duration: Spatiotemporal correlations and implications for cochlear implants. Hear Res. 2014;317:1–12.

14 Zhou N, Pfingst BE. Relationship between multipulse integration and speech recognition with cochlear implants. J Acoust Soc Am. 2014 Sep;136(3):1257.
15 Pfingst BE, Colesa DJ, Hembrador S, Kang SY, Middlebrooks JC, Raphael Y, et al. Detection of pulse trains in the electrically stimulated cochlea: Effects of cochlear health. J Acoust Soc Am. 2011 Dec;130(6):3954–68.
16 Schvartz-Leyzac KC, Colesa DJ, Buswinka CJ, Swiderski DL, Raphael Y, Pfingst BE. Changes over time in the electrically evoked compound action potential (ECAP) interphase gap (IPG) effect following cochlear implantation in Guinea pigs. Hear Res. 2019 Nov;383:107809.
17 Pfingst BE, Colesa DJ, Swiderski DL, Hughes AP, Strahl SB, Sinan M, et al. Neurotrophin Gene Therapy in Deafened Ears with Cochlear Implants: Long-term Effects on Nerve Survival and Functional Measures. J Assoc Res Otolaryngol. 2017 Dec;18(6):731–50.
18 Schvartz-Leyzac KC, Pfingst BE. Assessing the Relationship Between the Electrically Evoked Compound Action Potential and Speech Recognition Abilities in Bilateral Cochlear Implant Recipients. Ear Hear. 2018;39(2):344–58.
19 Swiderski DL, Colesa DJ, Hughes AP, Raphael Y, Pfingst BE. Relationships between Intrascalar Tissue, Neuron Survival, and Cochlear Implant Function. J Assoc Res Otolaryngol. 2020 Aug;21(4):337–52.
20 Kroon S, Ramekers D, Smeets EM, Hendriksen FGJ, Klis SFL, Versnel H. Degeneration of auditory nerve fibers in guinea pigs with severe sensorineural hearing loss. Hear Res. 2017 Mar;345:79–87.
21 Resnick JM, Rubinstein JT. Simulated auditory fiber myelination heterogeneity desynchronizes population responses to electrical stimulation limiting inter-aural timing difference representation. J Acoust Soc Am. 2021 Feb;149(2):934–47.
22 Clark G. Cochlear Implants: Fundamentals and Applications. Springer. New York; 2003.
23 Li PMMC, Somdas MA, Eddington DK, Nadol JB. Analysis of Intracochlear New Bone and Fibrous Tissue Formation in Human Subjects with Cochlear Implants. Ann Otol Rhinol Laryngol. 2007 Oct;116(10):731–8.
24 Roland PS, Wright CG. Surgical aspects of cochlear implantation: mechanisms of insertional trauma. Adv Otorhinolaryngol. 2006;64:11–30.
25 Jia H, Venail F, Piron J-P, Batrel C, Pelliccia P, Artières F, et al. Effect of Surgical Technique on Electrode Impedance after Cochlear Implantation. Ann Otol Rhinol & Laryngol. 2011;120(8):529–34.
26 Van de Heyning P, Roland P, Lassaletta L, Agrawal S, Atlas M, Baumgartner W-D, et al. Suitable Electrode Choice for Robotic-Assisted Cochlear Implant Surgery: A Systematic Literature Review of Manual Electrode Insertion Adverse Events. Front Surg. 2022 Mar;9:823219.
27 Santa Maria PL, Gluth MB, Yuan Y, Atlas MD, Blevins NH. Hearing Preservation Surgery for Cochlear Implantation. Otol & Neurotol. 2014;35(10):e256–69.
28 Kontorinis G, Lenarz T, Stöver T, Paasche G. Impact of the Insertion Speed of Cochlear Implant Electrodes on the Insertion Forces. Otol & Neurotol. 2011;32(4):565–70.
29 Miroir M, Nguyen Y, Szewczyk J, Sterkers O, Bozorg Grayeli A. Design, kinematic optimization, and evaluation of a teleoperated system for middle ear microsurgery. ScientificWorldJournal. 2012;2012:907372.
30 Shepherd RK, Hatsushika S, Clark GM. Electrical stimulation of the auditory nerve: the effect of electrode position on neural excitation. Hear Res. 1993;66(1):108–20.
31 Nguyen S, Cloutier F, Philippon D, Côté M, Bussières R, Backous DD. Outcomes review of modern hearing preservation technique in cochlear implant. Auris Nasus Larynx. 2016;43(5):485–8.
32 McKay CM, Henshall KR. The perceptual effects of interphase gap duration in cochlear implant stimulation. Hear Res. 2003 Jul;181(1–2):94–9.
33 van den Honert C, Mortimer JT. The response of the myelinated nerve fiber to short duration biphasic stimulating currents. Ann Biomed Eng. 1979 Mar;7(2):117–25.
34 Thai-Van H, Chanal J-M, Coudert C, Veuillet E, Truy E, Collet L. Relationship between NRT measurements and behavioral levels in children with the Nucleus 24 cochlear implant may change over time: preliminary report. Int J Pediatr Otorhinolaryngol. 2001 Apr;58(2):153–62.
35 Jeon EK, Brown CJ, Etler CP, O'Brien S, Chiou L-K, Abbas PJ. Comparison of Electrically Evoked Compound Action Potential Thresholds and Loudness Estimates for the Stimuli Used to Program the Advanced Bionics Cochlear Implant. J Am Acad Audiol. 2010 Jan;21(1):16–27.
36 He S, Teagle HFB, Buchman CA. The Electrically Evoked Compound Action Potential: From Laboratory to Clinic. Front Neurosci. 2017;11:339.
37 van Eijl RHM, Buitenhuis PJ, Stegeman I, Klis SFL, Grolman W. Systematic review of compound action potentials as predictors for cochlear implant performance. Laryngoscope. 2017 Feb;127(2):476–87.

38 Hughes ML, Goulson AM. Electrically Evoked Compound Action Potential Measures for Virtual Channels Versus Physical Electrodes. Ear Hear. 2011 May;32(3):323–30.
39 Schvartz-Leyzac KC, Pfingst BE. Across-site patterns of electrically evoked compound action potential amplitude-growth functions in multichannel cochlear implant recipients and the effects of the interphase gap. Hear Res. 2016 Nov;341:50–65.
40 Prado-Gutierrez P, Fewster LM, Heasman JM, McKay CM, Clark GM, Shepherd RK. Effects of interphase gap and pulse duration on electrically evoked auditory brainstem responses. Hear Res. 2006;215(1–2):47–55.
41 Abbas PJ, Brown CJ, Shallop JK, Firszt JB, Hughes ML, Hong SH, et al. Summary of results using the nucleus CI24M implant to record the electrically evoked compound action potential. Ear Hear. 1999 Feb;20(1):45–59.
42 Gärtner L, Bräcker T, Kals M, Penninger RT, Billinger-Finke M, Lenarz T, et al. ARTFit-A Quick and Reliable Tool for Performing Initial Fittings in Users of MED-EL Cochlear Implants. Life (Basel, Switzerland). 2022 Feb;12(2) DOI: 10.3390/life12020269
43 Hughes ML, Choi S, Glickman E. What can stimulus polarity and interphase gap tell us about auditory nerve function in cochlear-implant recipients? Hear Res. 2018 Mar;359:50–63.
44 Nadol JJ, Shiao J, Burgess B, Ketten D, Eddington D, Gantz B. Histopathology of cochlear implants in humans. Ann Otol Rhinol Laryngol. 2001;110(9):883–91.
45 Zeng FG, Rebscher S, Harrison W, Sun X, Feng H. Cochlear implants: system design, integration, and evaluation. IEEE Rev Biomed Eng. 2008;1:115–42.
46 Rebscher SJ, Hetherington A, Bonham B, Wardrop P, Whinney D, Leake PA. Considerations for design of future cochlear implant electrode arrays: electrode array stiffness, size, and depth of insertion. J Rehabil Res Dev 2008;45(5):731–47.

Figure Legends:

Fig. 1. ACI (Speech intelligibility) for two subgroups. The dark grey bar represents the robot group. The light grey bar represents the manual group. The significant difference is marked by the asterisk.

Fig. 2. The neural health was evaluated by measuring the difference of the slope average of the amplitude growth of ECAP in function of the stimulating current with an interphase gap of 30 µs and of 10 µs. The dark grey bar represents the robot group. The light grey bar represents the manual group. The significant difference is marked by the asterisk.

Fig. 3. ACI (Speech intelligibility) as a function of the difference of the slope average of the amplitude growth of ECAP in function of the stimulating current with an interphase gap of 30 µs and 10 µs

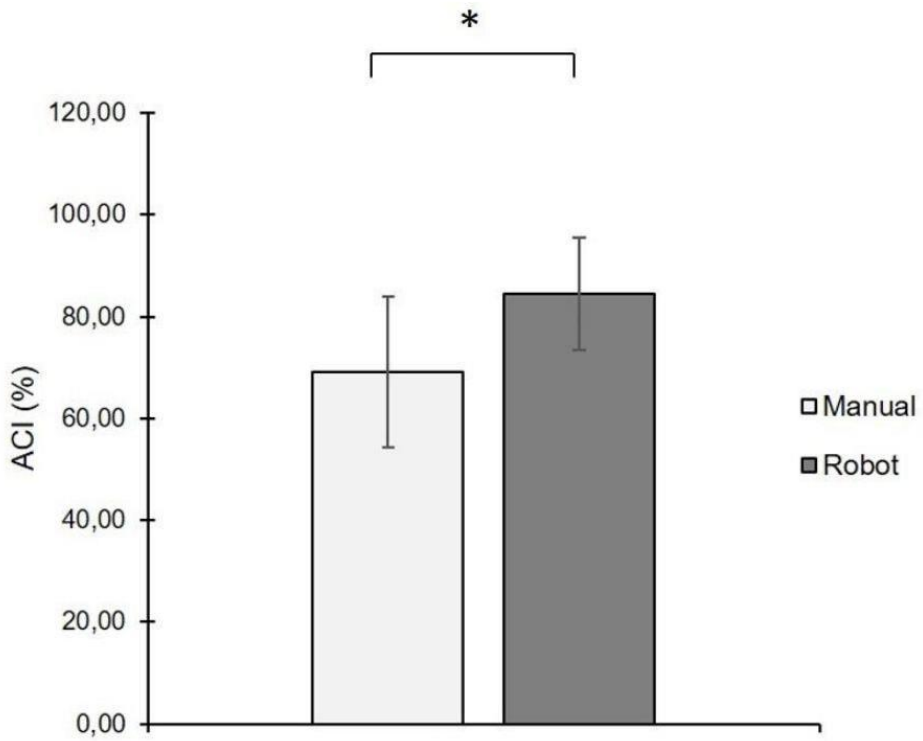
*
120,00
100,00
80,00
60,00
40,00
20,00
0,00
ACI (%)
Manual
Robot

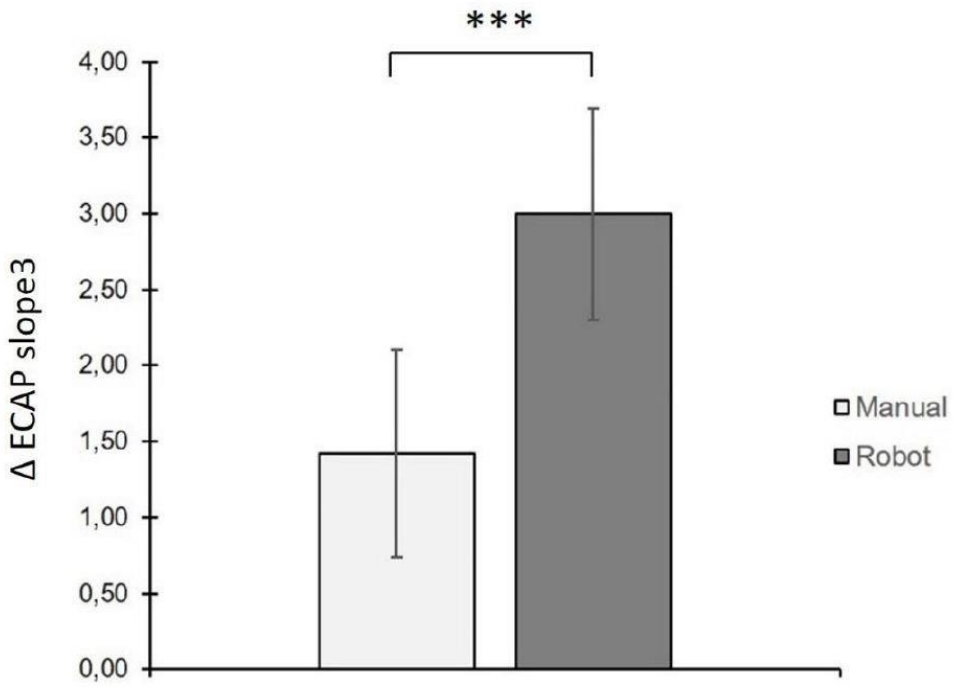
***
4,00
3,50
3,00
2,50
2,00
1,50
1,00
0,50
0,00
Δ ECAP slope3
Manual
Robot

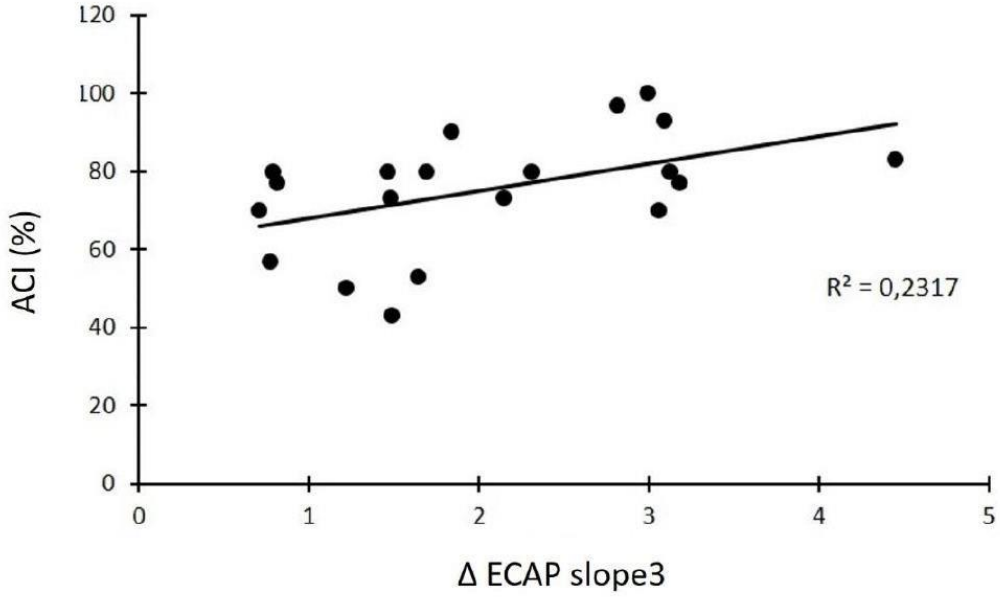
120
100
80
60
40
20
0
ACI (%)
0
1
2
3
4
5
Δ ECAP slope3
R² = 0,2317

Contribution to the existing literature

Earlier studies had shown that robot-assisted insertion may yield better functional outcomes than manual insertion, including in situations where the insertion is traumatic, without explaining why. This study offers a mechanism. Using the slope of the electrically evoked compound action potential amplitude growth function as an indirect marker of neural health, it reports a higher mean slope difference after robot-assisted insertion than after manual insertion, and a correlation between this difference and speech intelligibility. The contribution is threefold: it supports the hypothesis that robot-assisted surgery is less traumatic; it suggests that the functional advantage persists even when residual acoustic hearing is lost, because the neural structures are better preserved; and it argues for the use of electrophysiology as a predictive marker of outcome rather than as a mere verification tool. The cohort is small and retrospective, and the finding is presented as a hypothesis to be tested prospectively.

IV. Postoperative Optimization: Frequency-to-Place Mismatch

This chapter is based on two original published studies. Article 4 (Dessard L, Gersdorff G, Ivanovik N, Zoca-Assadi M, Nopp P, Camby S, Lefebvre PP. Cochlear Implant: Analysis of the Frequency-to-Place Mismatch with the Table-Based Software OTOPLAN® and Its Influence on Hearing Performance. Audiol Neurotol. 2024;29(3):239–245; doi:10.1159/000535693), of which the candidate is the second author. Article 5 (Gersdorff G, Ivanovic N, Zoka Assadi M, Nopp P, Camby S, Lefèbvre P. The importance of frequency–place mismatch in the quality of sound perceived in single-sided deafness among cochlear implant recipients. Front Audiol Otol. 2025;3:1648716; doi:10.3389/fauot.2025.1648716), of which the candidate is the first author.

The candidate is the second author of Article 4, to which he contributed the study conceptualization and methodology, the data collection, analysis and interpretation and the writing of the original draft, and the first author of Article 5, for which he reviewed the electronic medical records and drafted the manuscript. The detailed contribution of each co-author is given in the Author Contributions section of the corresponding publication.

4.1. State of the Art

4.1.1. Electrode Position within the Cochlea

Introduction

A growing body of research highlights the critical role of EA positioning within the cochlea as a key determinant of auditory outcomes following cochlear implantation. While successful insertion into the ST is an essential surgical objective, variations in EA placement, particularly in terms of insertion depth and its spatial relationship to the round window, which directly determines frequency–place mapping, have been shown to contribute significantly to interindividual differences in speech perception performance [105,109].

Importantly, clinical outcomes are now understood to depend not solely on patient-related factors such as the duration of deafness or audiological profile, but increasingly on the technical precision of electrode insertion and device programming. Even when scalar placement is achieved within the ST, discrepancies in electrode trajectory and insertion depth can result in marked variability in postoperative auditory function [105,106,109].

Modiolar Proximity and Pre-curved Arrays

Finley et al. [109] demonstrated that variations in electrode placement within the scala tympani (ST) significantly influence CI outcomes, particularly in terms of speech perception. Their clinical investigation revealed that electrodes positioned in closer proximity to the modiolus were associated with improved auditory performance. However, this anatomical advantage must be weighed against an elevated risk of intracochlear trauma, as pre-curved electrode arrays, specifically designed to achieve modiolar proximity, exhibit a higher propensity for scalar translocation.

Despite the conceptual benefit of targeted neural stimulation, pre-curved mid-scala (MH) electrodes exhibit inherent limitations in insertion depth due to their fixed curvature. Typically measuring 16–18 mm in length, these arrays rarely surpass an angular insertion of 380°- 420°, thereby restricting stimulation to frequencies no lower than approximately 500 Hz. In contrast, spiral ganglion (SG) neurons extend apically up to 660° - 720°, a range that no commercially available MH electrode is currently capable of reaching. Furthermore, the predefined curvature of these electrodes may not conform optimally to all cochlear anatomies, thereby diminishing their functional effectiveness [90].

In average-sized cochleae, the angular insertion depth of MH electrodes seldom exceeds 450°, which remains substantially below the threshold required to reach the most apical SG regions. Additionally, the modiolus narrows significantly, often to less than 1 mm in diameter, beyond the second cochlear turn, rendering electrode extraction highly traumatic and therefore clinically inadvisable [90].

Insertion Depth and Frequency-Place Matching

Although modern CI processors are capable of encoding a wide frequency range, from approximately 70 Hz to 11.5 kHz, the basal 3 - 4 mm of the cochlea, which corresponds to the highest frequencies, contributes minimally to speech perception. Consequently, this region is frequently excluded from active electrode stimulation during programming, particularly when optimizing for speech recognition [90].

From a surgical perspective, avoiding electrode insertion into the most basal 3 - 4 mm of the cochlear duct is generally recommended. This region is not only functionally marginal for speech understanding, but also more susceptible to mechanical trauma during insertion [90]. In contrast, deeper insertions reaching angular depths of approximately 450° to 600° are better aligned with the neural representation of low-frequency components of speech, which are essential for intelligibility, tonal discrimination, and prosody. However, achieving this target depth requires careful calibration. Overinsertion may result in excessive neural stimulation, increased channel interaction, and a reduction in spectral resolution. Conversely, shallow insertions risk bypassing apical SG neurons that are particularly important in individuals with steeply sloping hearing losses. Therefore, determining the optimal insertion depth involves a delicate balance between frequency-place coverage, preservation of residual hearing, anatomical constraints, and the technical limitations imposed by specific electrode designs.

This balance is particularly critical in the context of pre-curved MH electrodes, which are typically constrained to lengths of 16 -18 mm and angular insertions of only 380°-420°. These values fall substantially short of the 660°-720° range required to reach the apical SG neurons responsible for encoding frequencies below approximately 500 Hz [90]. As a result, these electrodes may fail to provide full tonotopic coverage, particularly in the apical cochlear regions.

The impact of insertion depth, expressed as angular insertion depth (AID) or linear insertion depth (LID), has been the focus of extensive investigation, though findings remain inconsistent. Some studies report a positive association between greater insertion depth and improved speech perception, while others find no correlation, and a few even report negative effects [109,136,348]. A recent systematic review found that 65% of included studies identified a statistically significant benefit of deeper insertions on speech outcomes. However, seven studies

showed no effect, and one reported a negative correlation. Across studies, reported AID values ranged from 330° to 608°, and LID values from 18.9 mm to 24.3 mm [322].

The principal mechanism proposed to explain the improved outcomes with deeper insertions is enhanced alignment between the place of electrode stimulation and the cochlea's tonotopic organization, particularly in apical regions. Nevertheless, the review also emphasized that excessive insertion depth may induce pitch confusion, inter-electrode interaction, and mechanical trauma, especially in cases of scalar translocation or electrode proximity to the lateral wall [322].

In addition to insertion depth itself, numerous confounding variables have been identified that may influence both electrode trajectory and postoperative auditory performance. These include the type of electrode array (lateral wall vs. perimodiolar), the surgical approach (round window vs. cochleostomy), the scala of insertion (scala tympani vs. scala vestibuli), cochlear duct length, and patient-specific factors such as age at implantation, etiology and duration of deafness, and preoperative speech recognition scores. For instance, insertions performed via the round window approach were more likely to result in accurate scala tympani placement, which has been associated with better consonant-nucleus-consonant (CNC) word scores. Moreover, lateral wall electrodes generally achieved greater angular insertion depths than perimodiolar arrays, although this did not consistently translate to superior clinical outcomes [322].

Cochlear Morphology and Trajectory Considerations

Anatomical variations in cochlear orientation and morphology represent critical factors influencing electrode trajectory and final positioning. Misalignment between the electrode and the modiolus wall may result in scalar translocation, compromising neural targeting. The force required to perforate the basilar membrane (BM) and induce such translocation ranges from 40 to 120 mN (mean: 88 mN), a threshold that remains challenging to monitor intraoperatively. Moreover, the inherent preset curvature of MH electrodes may cause inconsistencies in their conformational fit along the cochlear spiral, resulting in either excessive tightness or looseness depending on the individual cochlear geometry [90].

In this context, Canfarotta et al. investigated the role of cochlear anatomy, specifically ST volume, CDL, and AID, in predicting early hearing preservation following cochlear implantation with lateral wall electrodes. Their study included 45 adult patients with preoperative unaided thresholds ≤45 dB HL at 250 Hz, who were implanted with MED-EL Flex24 (24 mm), Flex28 (28 mm), or FlexSOFT (31.5 mm) electrode arrays (Fig. 47) [143].

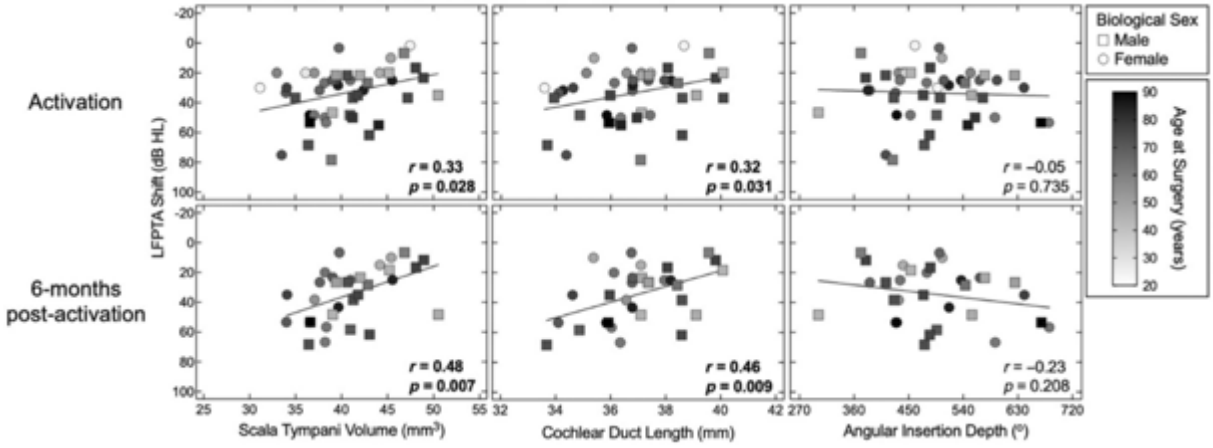

Figure 47. Preservation of low-frequency hearing at the time of device activation (n = 45) and at 6 months post-activation (n = 31) shows a significant positive correlation with both scala tympani volume and cochlear duct length, but not with angular insertion depth. Trend lines within each panel illustrate the respective correlations. The shape of the symbols represents the biological sex of each participant, while symbol color denotes age at the time of surgery, as detailed in the legend. Reproduced from Canfarotta et al. (2025) [143].

The AID varied significantly among the three electrode types: 441.1° for Flex24, 546.6° for Flex28, and 620.6° for FlexSOFT. Despite this variation, no significant correlation was found between AID and hearing preservation (p = 0.700). In contrast, ST volume demonstrated a statistically significant positive association with hearing preservation at both activation (r = 0.33, p = 0.028) and 6 months post-activation (r = 0.48, p = 0.007). CDL also showed correlation with hearing preservation, but did not emerge as a significant predictor in multivariate analyses (p = 0.367) [143].

Across the cohort, the average deterioration in low-frequency pure-tone average (LFPTA) was approximately 34 dB HL at both activation and at the 6-month follow-up. Nonetheless, 71% of patients retained functional hearing at 250 Hz (≤80 dB HL) by the latter time point. Multivariate regression identified larger ST volume (p = 0.044), younger age (p = 0.028), and female sex (p = 0.003) as independent predictors of better postoperative hearing preservation, regardless of CDL, AID, or baseline LFPTA [143].

The findings of Canfarotta et al. underscore the importance of inner ear morphology, particularly ST volume, as a determinant of low-frequency hearing preservation in the early postoperative phase. The proposed mechanism attributes this to a greater available cross-sectional area within the ST, which facilitates electrode insertion with reduced trauma. This mechanical advantage is hypothesized to minimize both direct structural disruption and insertion-induced pressure gradients. Interestingly, these results diverge from prior models that emphasized insertion depth as the dominant factor, suggesting instead that deep insertions may not compromise residual hearing when atraumatic surgical techniques and highly flexible lateral wall electrodes are employed [143].

From a clinical standpoint, the study supports the consideration of cochlear morphology during preoperative planning, particularly in patients selected for electro-acoustic stimulation (EAS). Individuals with smaller ST volumes may be more susceptible to threshold shifts and might benefit from the use of shorter electrodes or more conservative insertion depths. Conversely, patients with larger ST volumes may tolerate longer arrays that offer broader cochlear coverage and potentially improved speech outcomes if acoustic hearing is lost over time. Additionally,

the study corroborates earlier observations that both age and sex influence auditory outcomes, possibly reflecting differences in cochlear resilience or tissue compliance [143].

Despite its valuable insights, the study has limitations, including its retrospective design and the absence of a clearly defined ST volume threshold predictive of EAS success. Furthermore, all electrode insertions were performed manually, leaving open the question of whether robotic-assisted techniques could further reduce insertion-related trauma, particularly in narrow or anatomically challenging cochleae. Future prospective investigations are warranted to refine electrode selection protocols and to enable individualized, anatomy-guided surgical planning [143].

Neural Targeting and Electrode Design Constraints

Achieving effective stimulation of SG neurons remains a central challenge in CI design, primarily due to the anatomical complexity of Rosenthal's canal, where SG cell bodies are housed. This porous bony structure presents a physical barrier that complicates precise neural targeting and contributes to unavoidable cross-channel interaction during electrical stimulation.

A major point of ongoing debate concerns the functional significance of the electrode's proximity to the modiolus. While it is commonly hypothesized that reduced modiolus-to-electrode distance may enhance spatial selectivity, the evidence remains equivocal. For instance, Medina et al. [349] and De Seta et al. [350] reported minimal correlation between this distance and long-term speech perception outcomes, evaluated at 1 and 5 years post-implantation, but nonetheless advocated for deeper insertions to minimize this gap. In contrast, van der Beek et al. [351], examining straight lateral wall (LW) electrodes, found no such relationship, suggesting that electrode design may modulate the importance of proximity [90].

An illustrative example of how electrode design and insertion depth interact is provided by Spiegel et al. In their comparative analysis of the FLEX28™ and FLEXSOFT™ electrode arrays, the average CDL in both subgroups was similar (36.2 ± 2.0 mm and 36.2 ± 1.4 mm, respectively). However, the FLEXSOFT™ group achieved a significantly greater angular insertion depth (AID: 622.2 ± 35.5°) compared to the FLEX28™ group (AID: 528.3 ± 46.3°), resulting in enhanced cochlear coverage (75.8 ± 4.3% vs. 63.9 ± 5.6%) [168]. Notably, despite radiographic indications, no implant in either group attained the full 720° AID corresponding to two complete cochlear turns [168].

These findings underscore the importance of individualized electrode selection in CI surgery. Given the considerable anatomical variability among patients, preoperative measurement of CDL is essential for tailoring electrode choice. This approach facilitates full cochlear coverage while minimizing insertional complications such as kinking, tip foldover, or scalar translocation. Furthermore, achieving a sufficient AID is critical for maintaining tonotopic alignment, which is a prerequisite for accurate frequency-place matching and optimal auditory outcomes.

The study also supports the premise that electrode arrays longer than 31 mm may theoretically improve cochlear coverage and frequency mapping. However, this potential benefit must be balanced against the increased risk of trauma associated with deeper insertions - particularly in cochleae with shorter duct lengths. Ultimately, while extended-length electrodes may offer advantages in select cases, their routine use requires further validation. Additional studies are

needed to clarify the relationship between CDL, electrode trajectory, and long-term auditory performance across diverse patient populations [168].

Insertion Angle and Functional Precision

Anatomical investigations using synchrotron radiation phase-contrast imaging (SR-PCI) to analyze the morphology of the scala tympani have demonstrated that electrode trajectories can be successfully confined within a clearly defined "accommodating insertion zone." In this study, the cross-sectional diameter of the scala tympani (DST) was defined, described by Micuda et al. [142], as the diameter of the largest inscribed circle that fits within each scala tympani cross-section on mid-modiolar slices, while the distal electrode lateral extent (DELE) represents the most lateral position within the scala tympani where a 0.4 mm diameter circle can be inscribed, approximating the maximal lateral location that an electrode could theoretically occupy. This zone is delimited superiorly by the DELE trajectory and inferiorly by the center of the DST, thereby defining an anatomically accommodating region within which lateral wall electrodes can safely travel (Fig. 48) [142]. Electrodes positioned above this region would be expected to risk contact with the spiral ligament or basilar membrane, whereas electrodes located below the region would follow a more medial course with less available space. Measurements were obtained at 5-degree angular increments from the round window center across the entire cochlear spiral in 35 unimplanted and three implanted cadaveric cochleae, allowing a detailed characterization of scala tympani geometry and electrode trajectory relative to the modiolar axis. Notably, in the implanted specimens analyzed in this study, the electrode trajectories followed the DELE course and remained entirely within the accommodating insertion zone, and no scalar translocation or structural damage to the spiral ligament or basilar membrane was observed [142].

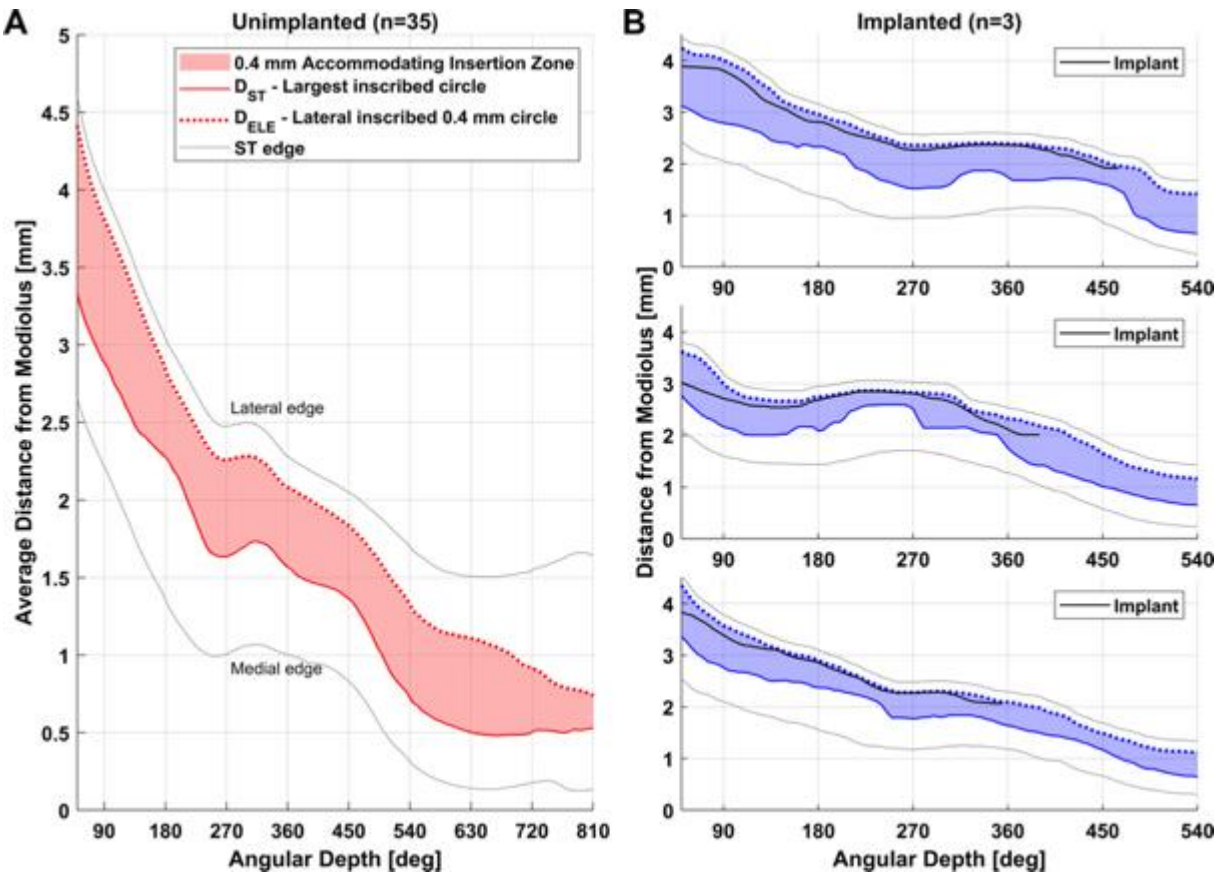

Figure 48.
(A) Mean horizontal distance from the modiolus plotted across the angular trajectory for 35 unimplanted cochleae. Shown are the average distances to the scala tympani (DST, solid red line), the distal electrode lateral extent (DELE, dotted red line), and the medial and lateral boundaries of the scala tympani (grey lines). The estimated spatial zone that can accommodate an implant is indicated by the red-shaded area.
(B) Horizontal distance measurements for three implanted cochleae are presented using the same anatomical references, but in blue. The DELE represents the maximum lateral extent that an electrode can occupy based on cochlear morphology, in both implanted and unimplanted cases. The centroid of the electrode array's sheath (black line) is plotted relative to the individual cochlear trajectories, showing that all three electrodes remain entirely within the designated accommodating region throughout their course. Reproduced from Micuda et al. (2024) [142].

Clinically, these findings support the feasibility of achieving high angular insertion depths (AIDs), which are often correlated with improved auditory performance, without compromising intracochlear integrity, even in anatomically small cochleae. For example, at an AID of 630°, the average DST measured 0.69 mm, and even the narrowest cochlea exhibited a DST of 0.52 mm. This anatomical allowance enabled the atraumatic insertion of lateral wall electrodes with standard diameters (0.4-0.52 mm), occupying only 27-43% of the available scala tympani cross-sectional area [142].

These anatomical insights confirm the safety and viability of extended insertion depths exceeding 600°, provided that electrode flexibility and insertion angle are appropriately calibrated. Such insertions effectively align with cochlear tonotopic regions encoding low-frequency sounds (<250 Hz), which are essential for speech perception and musical pitch recognition. The study contributes a robust dataset supporting the anatomical accommodation of full-length lateral wall electrodes across a wide spectrum of cochlear morphologies [142].

Emerging evidence further suggests that deeper insertions, potentially reaching the third cochlear turn, may enhance stimulation of apical low-frequency neurons and improve auditory outcomes. However, in cases where the stimulation is directed at the SG, particularly using perimodiolar arrays, angular insertions exceeding 720° appear unnecessary and may not yield additional benefits [152,155].

Targeted stimulation of low-frequency regions may necessitate smaller and more closely spaced electrode contacts. Yet, such designs carry a heightened risk of inter-electrode interaction and cross-fiber excitation [150]. Synchrotron radiation phase-contrast imaging (SR-PCI) has demonstrated that CI stimulation at angular depths beyond 360° can activate frequency regions as low as 100–300 Hz [150]. However, computational models warn that when electrodes are positioned near or beyond the apical terminus of the SG, broad excitation fields may lead to overlapping frequency zones and unpredictable pitch perception [150].

In the apical cochlea, the increasing density and close packing of neural elements, particularly SG peripheral axons, significantly hinder selective stimulation. Around 360° of angular insertion, dendritic architecture transitions from a radial to a spiral-helical trajectory, a morphological change believed to contribute to perceptual pitch shifts and to modulate the functional profile of electrical stimulation [150,152,352,353].

Multiple studies, including those involving CI users with residual low-frequency hearing, have shown that the angle of insertion, rather than depth alone, is a more reliable predictor of perceived pitch. Electrodes placed closer to the basilar membrane tend to produce more accurate pitch perception than those positioned near the modiolus [156]. Furthermore, the observed downward shift in the frequency-place function in CI users cannot be fully explained

by anatomical parameters alone, underscoring the critical importance of both insertion angle and trajectory in optimizing hearing outcomes, especially in hearing preservation cases [156,354].

Incorrect or suboptimal electrode trajectory may result in trauma to key intracochlear structures, including the outer wall, particularly the spiral ligament and its vascular supply, and the inner wall, notably the modiolus and the auditory neurons located in Rosenthal's canal [107].

Clinical Implications and Future Directions

From a surgical standpoint, the current evidence highlights the critical importance of employing atraumatic insertion techniques and tailoring electrode array selection to individual anatomical and audiological profiles. Optimizing these parameters not only enhances the safety of the procedure but also contributes to improved functional outcomes by preserving residual hearing and minimizing intracochlear trauma.

Clinically, deeper electrode insertions have been associated with enhanced stimulation of apical spiral ganglion regions, which are vital for low-frequency perception. These benefits are particularly evident in patients with residual low-frequency hearing or in those requiring broader frequency coverage. Nevertheless, the potential advantages of deeper insertion must be carefully weighed against the increased risks of trauma, scalar translocation, and degradation in sound quality associated with suboptimal electrode positioning.

The existing literature indicates that insertion depth should be considered an important, but not exclusive, factor influencing CI outcomes. It operates in conjunction with multiple variables, including electrode design, surgical approach, cochlear morphology, and patient-specific factors. As such, the interpretation of its impact requires a comprehensive, individualized approach.

To advance clinical practice, the authors of the reviewed studies advocate for future prospective, controlled investigations aimed at isolating the specific contribution of insertion depth to CI performance. Such studies are essential for establishing evidence-based guidelines that integrate anatomical metrics, audiological baselines, and device specifications to guide surgical decision-making and improve long-term auditory outcomes [322].

Conclusion

In summary, although longer electrode arrays have the theoretical advantage of extending cochlear coverage and improving alignment with the natural tonotopic organization, their clinical efficacy must be interpreted with caution. The practical benefit of extended-length arrays remains contingent upon multiple factors, including anatomical feasibility, surgical precision, and individual patient characteristics such as CDL and residual hearing capacity, as well as electrode array design characteristics that vary across manufacturers. Maximizing the advantages of longer arrays necessitates a personalized approach that integrates anatomical measurements and functional goals while minimizing the risk of insertional trauma and maintaining long-term auditory performance. Additional prospective studies are needed to elucidate the interplay between CDL, electrode positioning, and clinical outcomes. Such research will be instrumental in refining surgical strategies and optimizing device selection to meet the diverse needs of cochlear implant recipients [168].

4.1.2. Matching Electrode Position to Cochlear Frequency Maps

Achieving precise alignment between sites of electrical stimulation and the cochlea's inherent tonotopic organization remains a central objective in cochlear implantation. Accurate place-pitch correspondence enhances speech intelligibility, music appreciation, and the overall fidelity of auditory perception. This goal necessitates not only a refined surgical approach but also a comprehensive understanding of cochlear anatomy, particularly the spatial configuration of SG neurons, which constitute the principal neural targets of stimulation.

Tonotopic alignment is a critical determinant of successful frequency-place matching, especially in recipients utilizing EAS, where perceptual outcomes are highly sensitive to frequency-location mismatches [168].

The tonotopic organization of the cochlea has been classically described using Greenwood's function [355]. which correlates basilar membrane position with characteristic frequency. However, Greenwood's model is anatomically referenced to the organ of Corti (OoC), whereas electrical stimulation primarily affects SG neurons. Stakhovskaya et al. [152] addressed this discrepancy by modeling the tonotopic distribution of SG cells, revealing a spatial divergence between SG and OoC beyond 270° of angular insertion. This offset becomes increasingly significant in deep insertions and may contribute to pitch-place mismatch if not properly accounted for.

Further complexity arises from individual anatomical variability. Studies by Jiam et al. [352,353] demonstrated that intersubject differences, such as CDL and the geometry of the hook region, substantially affect the alignment between electrode position and perceived pitch. By leveraging high-resolution imaging techniques, such as computed tomography (CT), they showed that accounting for these parameters during programming improves CNC word recognition scores and pitch ranking, even when identical electrode arrays are used.

The clinical implications of anatomical variability are further supported by Rader et al. [356], who investigated place-dependent stimulation rates in patients with single-sided deafness. Their findings indicated that modifying stimulation rates to better reflect the underlying tonotopic gradient enhances pitch perception accuracy, even in cases of limited SG coverage. These results underscore the potential benefits of individualized, anatomy-driven programming protocols.

Additionally, pitch comparisons between acoustic and electric stimulation in EAS users have highlighted systematic shifts in perceived frequency, particularly in apical regions. Boëx et al. [156] and Schatzer et al. [354] observed that these mismatches challenge the validity of using default frequency maps for all patients, suggesting that such standardized programming may inadequately reflect true neural excitation sites in many cases.

From a surgical perspective, the primary goal in CI placement is the atraumatic insertion of the electrode array (EA) into the ST, with optimal alignment to the patient's cochlear frequency map. This precise placement is pivotal for maximizing pitch resolution, speech discrimination, and general auditory performance. Anatomical studies show that SG neurons extend up to approximately 660°, yet current commercial MH electrodes do not reach this depth [90]. Moreover, LW electrodes typically follow the trajectory of the OoC, offering broader cochlear coverage, while MH electrodes are targeted toward the SG regions of the basal and middle turns [90].

Given that CI processors typically encode frequencies ranging from approximately 11.5 kHz to 70 Hz, care must be taken to avoid overstimulation of the basal-most region (first 3-4 mm from the round window), which corresponds to the highest frequencies and may contribute to excessive overlap and perceptual distortion [90].

Empirical data further emphasize the relationship between electrode insertion depth, frequency-place alignment, and perceptual outcomes. Baskent and Shannon [357] have shown that successful stimulation hinges on whether electrodes interface with the SG or the OoC, an issue still under investigation. Notably, variations in the distribution of the BM and SG cells introduce further challenges to uniform programming strategies, reinforcing the need for individualized cochlear measurements [150,156,354].

As such, rigid frequency allocation tables, commonly used by default in CI programming software, may result in suboptimal stimulation patterns for many patients. Personalized frequency mapping, informed by imaging modalities such as CT, flat-panel CT, or magnetic resonance imaging (MRI), provides a route to tailor programming to the patient's unique anatomical and neural features. These individualized strategies have been shown to improve not only speech recognition and pitch perception but also user satisfaction and quality of life.

In conclusion, optimal cochlear implant outcomes depend on aligning electrode contacts with the cochlea's neuro-tonotopic structure. Standardized frequency maps fail to accommodate the substantial interindividual variability in cochlear dimensions and neural architecture. The integration of preoperative imaging, anatomical modeling, and intraoperative navigation facilitates precise electrode selection, insertion trajectories, and frequency mapping. These measures are essential to ensure effective, patient-specific programming and to maximize the potential benefits of cochlear implantation.

4.1.3. Anatomy-Based Frequency Reallocation in Cochlear Implantation: Theoretical Foundations and Clinical Implications

Default Frequency Allocation and Frequency-to-Place Mismatch

In normal hearing, each sound frequency stimulates a specific region of the basilar membrane within the cochlea. This tonotopic organization enables inner hair cells to transmit precise information to the auditory cortex via the auditory nerve [358,359]. CIs, on the other hand, analyze the acoustic signal into frequency bands, extract the temporal envelope of each band, and convert this information into electrical currents delivered to electrodes implanted within the cochlea. Ideally, electrical stimulation respects the natural tonotopic layout, but the alignment between electrode contacts and the patient's actual tonotopic map is often imperfect [360].

Cochlear implants have significantly improved speech recognition in quiet environments for individuals with severe to profound hearing loss [361], especially when conventional hearing aids prove ineffective [362]. Nevertheless, a substantial proportion of CI users continue to struggle with speech understanding in noisy environments [363,364] and with the perception of complex auditory signals [365,366].

At initial CI activation, a standard spectral allocation is typically assigned to the electrodes without accounting for individual anatomical variation or the precise intracochlear position of each electrode. This universal approach overlooks interindividual differences in cochlear length

and insertion depth [311,367]. Although manufacturers offer electrode arrays in various lengths, this does not resolve the potential mismatch between processor-assigned frequencies and the natural tonotopic location of auditory neurons, resulting in a frequency-to-place mismatch.

This mismatch is particularly problematic in postlingually deafened patients whose auditory memory relies on physiological frequency-to-place mapping. In such individuals, the discrepancy between frequencies perceived via the CI and those expected based on prior hearing experience can lead to perceptual distortions, requiring longer or incomplete adaptation [321,368].

Several studies have shown that this mismatch negatively affects speech recognition [321,369]. Although some degree of neuroplasticity allows adaptation to altered frequency distribution, this adaptation is often partial or insufficient, particularly in older adults [90,370]. One strategy sometimes employed is to deactivate certain electrodes based on subjective auditory perceptions reported by the patient, a method known as "site selection" [368]. However, this approach does not guarantee effective correction of the overall mismatch.

Limitations of Default Frequency Allocation

Studies assessing the influence of standardized frequency distributions on auditory performance report mixed results. Some show improved speech perception when frequency allocation is modified, while others find no significant benefit [369,371,372]. Perceptual adaptation to frequency-to-place mismatch is often slow and incomplete, especially when the mismatch affects critical frequency bands for speech intelligibility, notably around 1500 Hz, central to the vocal spectrum [321,373]. However, recent evidence suggests that the impact of frequency-to-place mismatch varies according to electrode type. In a large retrospective cohort, mismatch was independently associated with speech recognition only for precurved electrodes, whereas no such association was observed for straight electrodes. The authors suggested that these differences may reflect the combined influence of scalar location, modiolar positioning, and channel interaction (current spread) [374].

To date, most CI users receive a default frequency map without accounting for interindividual anatomical variability [375] or the actual electrode position within the cochlea [376]**.** This map systematically assigns frequency bands from low frequencies at the apex to high frequencies at the base according to the number of active electrodes. However, this approach does not take into account patient-specific cochlear anatomy or surgical nuances, thereby limiting its individual relevance. Several manufacturers have developed software tools enabling anatomy-based fitting strategies that use postoperative imaging to determine electrode positions and adjust frequency allocation accordingly. Recent randomized controlled trials and prospective studies demonstrate that anatomy-based fitting significantly improves speech perception in noise (10-16% improvement), consonant and vowel recognition, and music perception compared to default mapping, with 92% of participants preferring to maintain the anatomy-based configuration. These benefits appear most pronounced in the initial months following activation, though the effect may diminish over time as central adaptation occurs**.** [377–379]

Anatomical Basis for Frequency Adjustment

Numerous studies have demonstrated the anatomical variability of cochlear dimensions, based on both temporal bone dissections and CT imaging [152,226,380–383]. This variability is

further influenced by surgical specifics, leading to variation in insertion depth [380,384]. As a result, a frequent mismatch is observed between the electrical frequencies delivered by the electrodes and the natural frequencies of the stimulated cochlear sites [372].

In CI users, frequency-to-place mismatch is highly variable and depends primarily on AID, cochlear size and electrode array length. In lateral wall arrays, mismatch is generally limited to approximately half an octave within the basal turn (0–270°), but becomes substantially greater beyond 270°, reaching approximately one to two octaves in the second cochlear turn for shorter arrays [321,385].

Insertion depth influences speech recognition performance both in quiet and in noise [292,386–388]. These effects are attributed, at least in part, to improved tonotopic alignment, that is, reduced mismatch between assigned frequencies and the cochlear site's native frequencies. Conversely, several studies have shown that significant frequency mismatch can impair speech recognition, both in CI users and in simulation studies with normal-hearing subjects [389,390].

Although perceptual adaptation to spectral shifts up to three octaves has been reported [391], this adaptation is often incomplete, even after extended training or years of experience [392–394]. Canfarotta et al. [395,396] found a significant correlation between frequency mismatch at 1500 Hz (greater than seven semitones) and word recognition in quiet (CNC test), one to six months post-implantation.

Mertens et al. [397], in a retrospective study of 39 patients with normal cochlear anatomy, observed a significant negative linear correlation between average frequency-to-place mismatch (ranging from 0.47 to 1.60 octaves) and speech recognition in noise at six months post-implantation. However, this correlation was no longer significant at twelve months, suggesting potential late adaptation.

The frequency distribution along the basilar membrane follows a logarithmic organization described by Greenwood, who established an invariant relationship between cochlear position and the characteristic frequency of auditory neurons [398,399]. Integrated into the organ of Corti (OC) and the SG, the Greenwood algorithm allows estimation of the tonotopic frequency associated with each intracochlear site [152,400]. Clinical application of this model requires reliable measurement of the CDL.

Advances in high-resolution imaging, especially flat-panel detector CT, combined with 3D multiplanar reconstruction software, now allow reproducible measurement of the CDL [226] and millimetric localization of each electrode contact relative to the cochlear apex [381,401]. Based on these parameters, it becomes possible to map the individual theoretical tonotopy and to quantify, for each patient, the mismatch between the anatomical frequency map and the frequencies assigned to the electrodes [388,402–404]. A strategy to reduce this mismatch involves dynamically adjusting frequency filters to restore frequency-to-place alignment [376,405].

The development of dedicated software, such as Otoplan® (CAScination AG, Switzerland), has greatly reinforced this approach. These tools allow individualized and reproducible measurement of the CDL and AID from pre- or postoperative imaging [406,407]. Through 3D reconstruction of intracochlear electrodes, they generate an anatomically based frequency map, importable into the MAESTRO 9.0 platform (MED-EL, Austria), enabling frequency allocation tailored to each patient's specific characteristics (Fig. 49) [408].

Within this framework, personalized frequency reallocation aims to minimize the mismatch between assigned frequencies and the characteristic frequency of the stimulated auditory neurons, to optimize signal fidelity and improve speech comprehension [168,408]. The Otoplan® software automates this process by focusing frequency allocation within the critical 950 to 3000 Hz range, essential for speech intelligibility, while also integrating Fine Structure coding for low frequencies (<950 Hz) [369,373]. This combined approach, based on precise tonotopic modeling, individualized imaging, and algorithmic adjustment of frequency filters, forms the technological basis for anatomically guided fitting, with major clinical implications for auditory performance in CI users (Fig.49) [376,388,402–405].

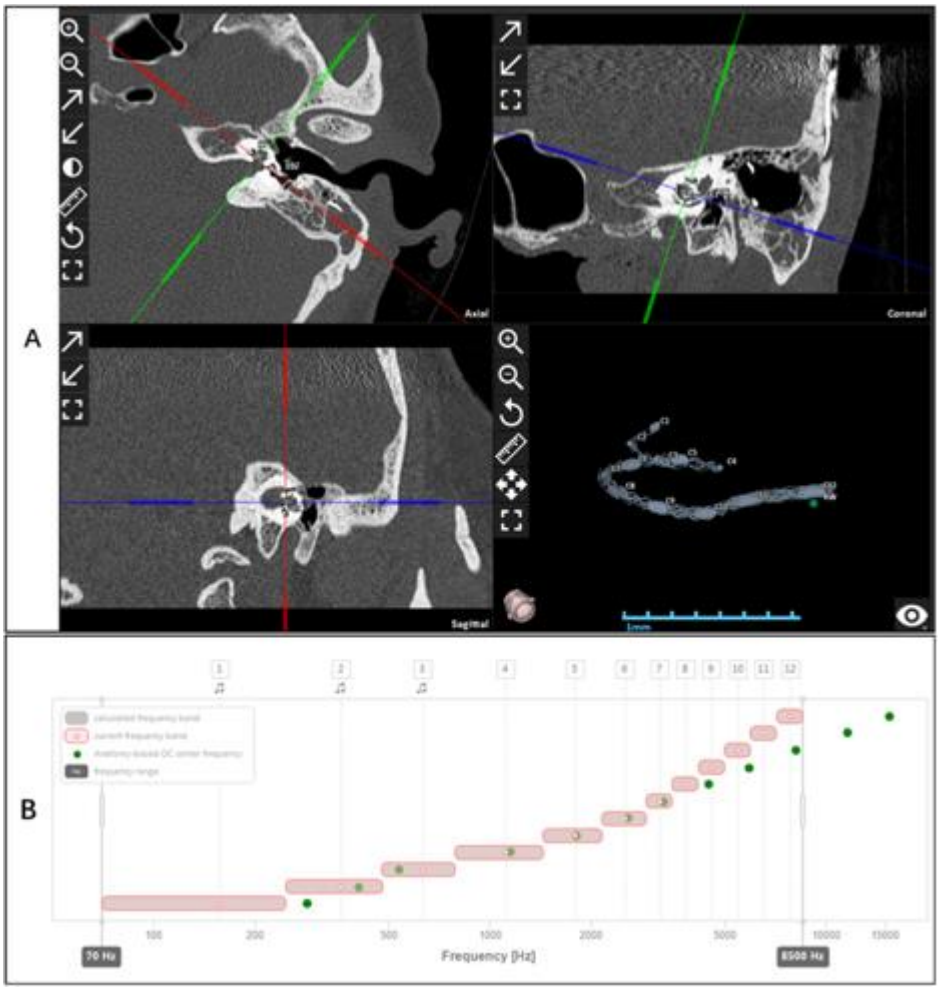

Figure 49. A. 3D reconstruction of electrodes from postoperative CT using Otoplan®, allowing measurement of AID and precise visualization of electrode trajectory. B. Data integration into MAESTRO 9.0 for anatomically personalized frequency reprogramming. Reproduced from Fan et al. (2024) [409].

Clinical Relevance of Anatomy-Based Frequency Reallocation

Despite the auditory system's plasticity, some patients never fully adapt to the frequency-to-place mismatch induced by default frequency settings [410]. This tonotopic mismatch leads to perceptual distortion, with low-frequency sounds perceived as higher-pitched, and high-frequency sounds perceived as sharper [409]. A personalized frequency reallocation strategy based on cochlear anatomy can correct these distortions by aligning the frequencies assigned to electrodes with the characteristic frequencies of the stimulated neural zones [373,408]. This

approach promotes a more natural auditory perception and improves perceived sound quality, particularly in the critical intelligibility zone around 1500 Hz [373,395,409].

The study by Creff et al. [377], a prospective, randomized, double-blind, cross-over trial, compared a tonotopic frequency (TF) setting to a conventional frequency setting in newly implanted CI users. It showed that TF significantly improved speech understanding in noise without degrading speech recognition in quiet. Auditory performance was superior at all tested SNR levels (+9 dB to 0 dB), with effect sizes ranging from 0.68 to 1.07. Frequency-to-place mismatch was significantly reduced, especially in apical and medial electrodes (E1–E8), within the critical 1200 to 3000 Hz range [411,412]. The average minimum frequency covered was reduced to 158 Hz with TF compared to 250 Hz with the conventional setting, expanding the bandwidth toward low frequencies, essential for musical and prosodic perception [377,386].

In the same study, no difference was observed in speech recognition in quiet or PTA thresholds [377], underscoring that improvements in noisy conditions did not come at the expense of performance in quiet environments. Unlike Mertens et al. [397], no significant correlation was found between average frequency mismatch and auditory performance, likely due to low interindividual variability in the study cohort [377]. Moreover, no direct correlation was found between filter width or position and observed gains, suggesting a predominant role for central mechanisms such as perceptual alignment or auditory processing efficiency [377].

The impact of this anatomical approach was also evaluated for music perception. A randomized cross-over study in 26 newly implanted adults showed significant improvements in music perception with TF compared to the conventional setting, using the Gabrielsson qualitative test, melodic contour identification, and melodic recognition tasks [413]. Aspects such as clarity, richness of sound, spatialization, and overall impression were all enhanced, and 92% of participants opted to retain the tonotopic map at the end of the study. Furthermore, speech-in-noise scores improved even after a short acclimatization period [409]. This strategy may thus be particularly valuable in older individuals or children, who may have limited capacity to adapt to default frequency mismatches.

These results contrast with those of Jiam et al. [352], who found no significant benefit of tonotopic programming after 30 minutes of acclimatization. The authors attributed these findings to the brief adaptation period, deactivation of electrodes with mismatches >7 semitones, and the use of an HDCIS strategy (70–8500 Hz). Canfarotta et al. [395], by contrast, reported a significant effect of insertion depth and mismatches >7 semitones at 1500 Hz on speech recognition in quiet, though in the context of a different FS4 coding strategy than that used in the Creff study.

The Creff et al. study [377] serves as a methodological reference: cross-over, double-blind design, six-week acclimatization period, exclusion of extracochlear electrodes, insertion depth >540°, homogeneous participants (hearing loss <5 years, mean age 60.4 years). The authors recommend expanding research to more heterogeneous populations, including individuals with longstanding deafness or alternative coding strategies. They also emphasize the need to incorporate neural plasticity phenomena when analyzing the delayed benefits of TF [392,394]. Future directions include exploring dynamic adaptive strategies and accounting for individual spectral discrimination capacity.

In conclusion, frequency reallocation based on cochlear anatomy offers robust and reproducible benefits in auditory perception, particularly in noise and musical domains. It represents a major

advancement toward personalized cochlear implant fitting, at the intersection of individual morphology, electrical coding, and neural plasticity.

Article 4

Journal: Audiology and Neurotology. Peer-reviewed. Published: Dessard L, Gersdorff G, Ivanovik N, Zoca-Assadi M, Nopp P, Camby S, Lefebvre PP. Cochlear Implant: Analysis of the Frequency-to-Place Mismatch with the Table-Based Software OTOPLAN® and Its Influence on Hearing Performance. Audiol Neurotol. 2024;29(3):239–245. doi:10.1159/000535693.

Audiology and Neurotology

Research Article

Audiol Neurotol
DOI: 10.1159/000535693

Received: October 17, 2023
Accepted: November 29, 2023
Published online: January 8, 2024

Cochlear Implant: Analysis of the Frequency-to-Place Mismatch with the Table-Based Software OTOPLAN® and Its Influence on Hearing Performance

Laura Dessard[a] Guillaume Gersdorff[a] Nicola Ivanovik[b] Masoud Zoca-Assadi[b] Peter Nopp[b] Séverine Camby[a] Philippe P. Lefebvre[a]

[a]Department of Otorhinolaryngology, CHU, Liège, Belgium; [b]Medel, Innsbruck, Austria

Keywords
Cochlear implant · Hearing performance · Frequency allocation · Cochlear length · OTOPLAN®

Abstract
Objective: The purpose of this study was to compare the originally applied frequency allocation of cochlear implant electrodes assigned by default at the time of activation with a more recent frequency allocation that is anatomy-based by a software called OTOPLAN®. Based on a computed tomography scan of the temporal bone, this software calculates the position of each electrode in the cochlea and its corresponding tonotopic frequency. We also evaluated whether patients with a significant mismatch between these two allocations present poorer speech intelligibility. ***Materials and Methods:*** Patients who underwent cochlear implantation from 2016 to 2021 at the University Hospital of Liege were included in this retrospective study. We used OTOPLAN® to calculate the tonotopic frequency allocation of each electrode according to its exact position in the cochlear duct. This anatomical frequency mapping was compared with the default frequency mapping at the time of cochlear implant activation. Finally, we compared the mismatch with the patients' auditory performance, represented by the Auditory Capacity Index (ACI). ***Results:*** Thirteen patients were included in the study. All patients had a mismatch between the two frequency maps, to a variable extent (200 Hz–1,100 Hz). Frequency shift was significantly inversely correlated with ACI and with the time needed to improve speech intelligibility. ***Conclusion:*** Our primary results show that patients with a larger mismatch between default frequency mapping and anatomically assigned frequency mapping experience poorer hearing performance and slower adaptation to a cochlear implant.
© 2024 S. Karger AG, Basel

Introduction

The cochlear implant (CI) is the first artificial neurosensory organ and allows hearing rehabilitation for patients with profound deafness. Since its first use in 1976, the intent with the CI system has been to approximate the natural organization of the cochlea. The cochlea is organized in a tonotopic mode corresponding with the maximum displacement of the basilar membrane after a sound stimulation. This movement will be maximal at the apex of the cochlea for low-frequency sounds and at the base for high-frequency sounds. Therefore, the electrical stimuli delivered by the implant will be assigned to apical electrodes for low-frequency sounds and basal electrodes for high-frequency sounds.

karger@karger.com
www.karger.com/aud
© 2024 S. Karger AG, Basel

Correspondence to:
Philippe P. Lefebvre, pp.lefebvre@uliege.be

The hearing performance of a CI can be extremely inconsistent; however, this variation is not always explainable. We know that parameters such as patient age at the time of implantation, duration of hearing loss, preoperative speech intelligibility thresholds, and cognitive abilities influence post-implant hearing performance [1, 2]. Experience with and duration of CI use also play a role with progressive improvement in speech intelligibility thresholds within 3 years post-implantation [1]. With radiological and technological improvements, more recent studies have shown that factors influencing the neuron-electrode interface also affect hearing performance, such as the depth of electrode insertion, percentage of electrodes present in the vestibular ramp, amount of fluid surrounding the electrode, and the presence of scar tissue [2–5].

When the CI is activated, a standard allocation of auditory frequencies is applied in an arbitrary and identical manner for each patient, depending on the implant model. No electrode array is designed to reach the most apical regions of the cochlea, and given the extremely variable anatomy of the cochlea (30% variability, especially by sex [6–8]), this frequency assignment will inevitably differ from the natural tonotopy of the cochlea. The result is a mismatch between the default frequency assignment of an electrode and the actual frequency of the neurons it stimulates, known as the frequency-to-place mismatch. This issue may not be as relevant for prelingually deaf CI users, who developed their speech perception through the implant, as it would be for postlingually deaf CI users, who have used normal cochlear tonotopy since birth [9].

So far, anatomical data have been difficult to incorporate into a CI fitting because of the lack of tools for measuring the cochlear duct length (CDL) [10, 11]. The tablet-based software OTOPLAN®, developed in close collaboration between CASCINATION AG (Switzerland) and MED-EL (Austria), provides an intuitive and quick way to assess the temporal bone anatomy and helps otologists plan personalized cochlear implantation to achieve the best results for each patient. It identifies the modiolus, round window, and tonotopic location of each individual electrode contact based on a computed tomography (CT) scan of the temporal bone. Canfarotta et al. [12] confirmed the reliability of OTOPLAN® for estimating the cochlear duct length (CDL) and angular insertion depth of the electrodes. These measurements are based on a formula developed by Alexiades et al. [6], which in turn is based on the third equation of Escudé [7] and on the elliptic-circular approximation [6, 8, 10, 13]. The software determines the characteristic frequency of the stimulated neurons using the Greenwood function (Greenwood 1990) and provides a tonotopic setting for patients with CI. In this study, we investigated the influence of the frequency-to-place mismatch on the hearing performance of CI users by comparing the anatomical frequency mapping defined by OTOPLAN® with the default mapping at the time of CI activation.

Materials and Methods

This retrospective study included patients with postlingual deafness implanted unilaterally with MEDEL CI from 2016 to 2021 at the University Hospital of Liege, a tertiary care center. The inclusion criteria were age ≥18 years and unilateral or bilateral postlingual hearing loss eligible for CI implantation in the deaf ear according to Belgian criteria. Exclusion criteria were age <18 years, prelingual deafness, loss to follow-up, cochlear malformations, contraindication for CT imaging, unavailable scans, poor-resolution scans, or incompatibility with the OTOPLAN® program.

All implants were activated and fitted with a processing strategy (FS4) using a standard frequency allocation map (logFS) distributed on active electrode contacts as prescribed by the manufacturer. All patients underwent a postoperative, high-resolution cone beam CT of the temporal bone, which was analyzed using OTOPLAN® (CE-certification number: G1 17 10 95657 003). The software applied automated assignment of anatomical landmarks without manual intervention (Fig. 1). With MAESTRO 9.0 anatomy-based fitting tools, an automated formula was used without manual intervention to determine a frequency allocation that followed the natural tonotopic map of the cochlea.

The default frequency assigned to each electrode at the time of fitting was compared with the frequency established by OTOPLAN®. The difference between these two values was calculated for each electrode for the frequencies corresponding to the speech spectrum (500–2,000 Hz), then averaged and presented as "average of frequency mismatch" (AFM).

Finally, the AFM was compared with the hearing results for patients as assessed by speech audiometry. We used the articulation function (AF) as an index of speech intelligibility, defined as the average speech discrimination score obtained at 40, 55, and 70 dB. The speech audiometries were performed in a soundproof booth, with the patient sitting 1 m from the sound source. We used the words of Fournier's dissyllabic list in French, pronounced to the patient through a loudspeaker. Measurements were recorded at 40–55 and 70 dB SPL to calculate the AF. All tests were performed in quiet and using the default frequency allocation.

Results

Patients

Thirteen patients were included in this retrospective study. Their demographics are shown in Table 1. Among the eight men and five women, the mean age of implantation was 57.76 years (range 39–75 years). All participants were French speaking. Eight patients were

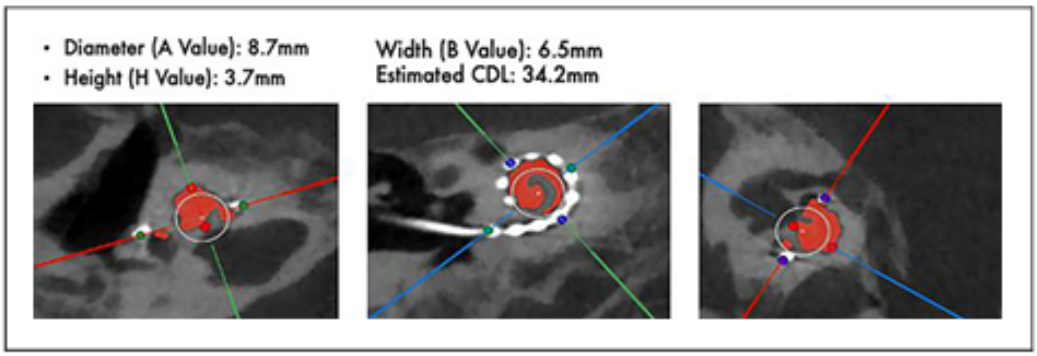

Fig. 1. CT analysis by OTOPLAN® to determine the diameter, height, and width of the cochlea for CDL estimation.

Table 1. Patient demographics

Patient	Age, years	Sex	Age at implantation, years	Etiology of deafness – right side	Etiology of deafness – left side	Other otologic symptoms	Implant type – electrode array
P1	51	M	45	Sudden hearing loss	Sudden hearing loss	None	MEDEL – FLEX 28
P2	52	M	49	Intralabyrinthine neurinoma	/	Tinnitus	MEDEL – FLEX 24
P3	55	F	50	Unknown	Unknown	None	MEDEL – FLEX 28
P4	47	M	44	/	Sudden hearing loss	None	MEDEL – FLEX 24
P5	66	F	65	Cochlear otosclerosis	Cochlear otosclerosis	Dizziness	MEDEL – FLEX 24
P6	67	M	63	Unknown	Ménière disease	Tinnitus and vertigo	MEDEL – FLEX 24
P7	46	F	40	Hereditary	Hereditary	None	MEDEL – FLEX 24
P8	70	M	68	Unknown	Unknown	Tinnitus	MEDEL – FLEX 24
P9	77	M	75	Unknown	Unknown	None	MEDEL – FLEX 24
P10	79	F	75	Sudden hearing loss	Neurinoma with radiotherapy	Tinnitus and vertigo	MEDEL – FLEX 24
P11	41	M	39	/	Trauma	None	MEDEL – FLEX 24
P12	79	F	73	Hereditary	Hereditary	None	MEDEL – FLEX 28
P13	69	M	65	Unknown	Unknown	Tinnitus	MEDEL – FLEX 28

implanted in the right ear and five in the left ear. No postoperative complications were observed. Implantation with a round window approach was performed for 12 patients, and the remaining patient was implanted using a cochleostomy approach. A MEDEL FLEX 24 (24 mm) electrode array was used for 9 patients, and 4 patients were implanted with the FLEX 28 (28 mm). Complete insertion of the electrode array was observed in 11 patients. Two patients had one extra cochlear electrode (number 12 in both cases). Subsequently, these electrodes were deactivated in accordance with the manufacturer's recommendations.

Average of Frequency Mismatch

The main objective of this retrospective study was to evaluate the outcome of speech intelligibility as a function of the difference between the default frequency mapping for each electrode and the frequency fitted by the software OTOPLAN®. All patients (100%) had a frequency mismatch of at least 200 Hz, and the average mismatch was 608.84 Hz. Five patients (38.46%) had a mismatch of <500 Hz (<500 Hz group), 4 patients (30.7%) had a mismatch of ≥500–1,000 Hz (≥500–1,000 Hz group), and 3 patients (23%) had a mismatch of ≥1,000 Hz (≥1,000 Hz group).

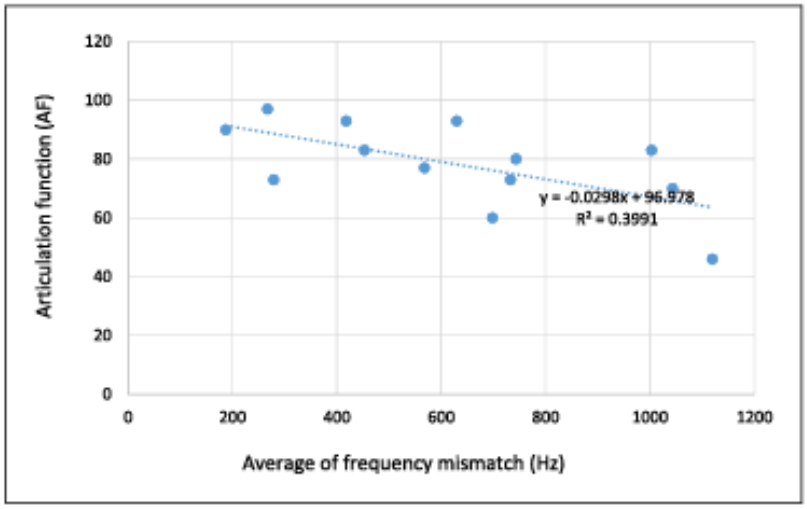

Fig. 2. A significant negative linear correlation (blue dotted line) between AF (*Y* axis) and average of frequency mismatch (*X* axis) for each patient.

Articulation Function

The relationship between AFM and AF was analyzed. AF was 75–99% in the >500 Hz group, 60–95% in the ≥500–1,000 Hz group, and 82–45% in the ≥1,000 Hz group. Average frequency mismatch correlated strongly (R^2 = 0.3991) with speech intelligibility as measured by the articulation function (p = 0.0206) (Fig. 2).

Speed of AF Acquisition

Speech intelligibility acquisition speed was evaluated in the context of average frequency mismatch using the slope reflecting the number of weeks after CI activation relative to the AF (Fig. 3). Values for these two factors showed a statistically significant negative correlation (p = 0.0286). The increase in the difference between the tonotopic frequency as defined by OTOPLAN® and the fitted frequency strongly and inversely correlated with the decreasing slope of the acquisition of speech intelligibly. Overall, the closer the match was between the adjusted and predicted frequencies, the faster speech intelligibility is acquired after CI activation.

Discussion

The principal aim of this study was to compare the default frequencies assigned to CI electrodes at the time of fitting with those based on the cochlear anatomy in OTOPLAN®. As expected, we demonstrated a systematic mismatch between these frequencies, as previously reported in several studies [9, 10, 14, 15]. The average of the mismatch was 608.84 Hz, and the magnitude of mismatch was variable, leading us to establish three groups for analysis (<500 Hz; ≥500–1,000 Hz; ≥1,000 Hz).

The secondary outcome was to compare this mismatch with the speech intelligibility reflected by the AF. We found that the group with the smallest mismatches (<500 Hz) had the best AF. Conversely, those with the greatest mismatch (≥1,000 Hz) had the worst AF. The strong negative correlation between these two factors was statistically significant (R = 0.3991).

Mertens et al. [10], which also used OTOPLAN® to calculate tonotopic frequencies, reported a similar correlation between frequency-to-place mismatch and hearing performance impairment. They showed that the mismatch was more important at the apex of the cochlea than in the base, as demonstrated in other studies [16]. This effect may be explained by the increasing difficulty of maintaining the tonotopy of the cochlea with increasing distance from its base. More importantly, these authors observed that the relationship between frequency shift and speech intelligibility deterioration disappeared 12 months after CI activation. This finding highlights the plasticity of the brain in adapting to a tonotopic frequency shift over time. Indeed, the experience of CI users is of a progressive adaptation to this discrepancy and an improvement in speech comprehension after several months of use [15–17].

Brain plasticity in this context seems to be limited to small frequency shifts, however, and is extremely variable among CI users. In addition, frequency-to-place mismatch increases the time required for CI adaptation, as Venail et al. [15] reported. They compared the frequency-to-place mismatch with the time required to reach 70–80% of

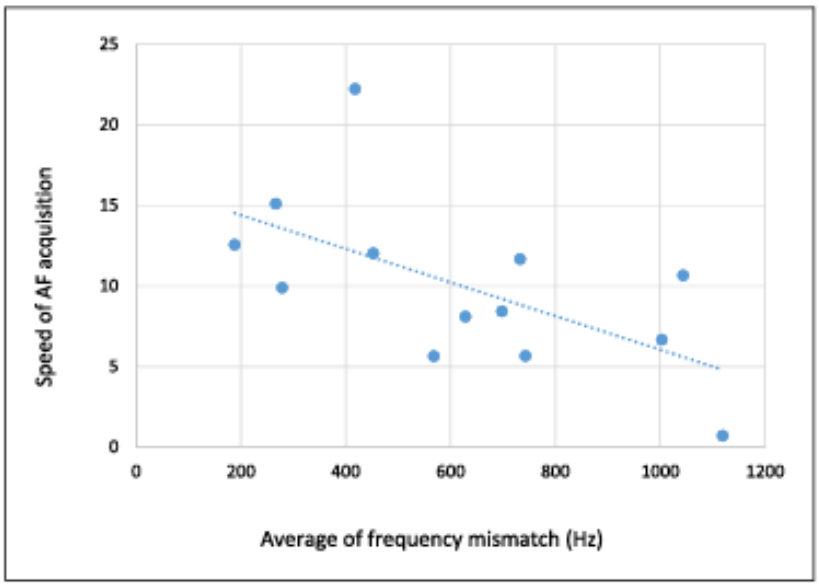

Fig. 3. A significant negative linear correlation (blue dotted line) between speed of AF (*Y* axis) acquisition and the average of frequency mismatch (*X* axis) for each patient.

maximum speech intelligibility and demonstrated a linear relationship between these two parameters [15]. This pattern is consistent with our results showing that patients with the largest AFM had the slowest AF acquisition. In addition, the subjects in our study had 1–6 years of experience with their CI but still showed a negative correlation between AFM and AF. This indicates that while adaptation does exist, it still failed to completely compensate for the negative consequences of frequency mismatch on speech perception, at least in our study cohort.

Strategies to reduce this mismatch are promising and in a constant state of development. Landsberger et al. [9] showed that this mismatch could be reduced by using longer electrode arrays or increasing the insertion depth. In this way, the frequency distribution would be closer to the natural tonotopy of the cochlea. Canfarotta et al. [14] corroborated these results in a larger patient cohort, also using OTOPLAN®. This group used the angular insertion depth to estimate the offset from the spiral ganglion and applied the Greenwood function to define the frequency mismatch. They confirmed that this mismatch could be reduced with deeper insertions and that the correlation between frequency-to-place mismatch and speech intelligibility was strongest at 1,000–2,000 Hz. Surprisingly, they also found a high degree of mismatch variability between patients carrying the same electrode array, once again demonstrating the vast anatomical variability of cochlear anatomy.

The great variability of the CDL and the lack of a standardized method are the main difficulties in calculating the mismatch [8, 18, 19]. Some studies use maps from the spiral ganglion or the organ of Corti, and some studies calculate these values based on standard X-rays [9] of the cochlea, temporal bone CT, or cone beam CT [15]. These images often present metallic artefacts, and the cochlear landmarks can be difficult to identify, requiring a certain technical and operator-dependent expertise.

Although another study by Canfarotta et al. [12] demonstrated excellent reproducibility of anatomical value identification across varying OTOPLAN® program users, subjective evaluation biases are possible, and CT analysis was time-consuming with this older version. In the newest version of OTOPLAN®, an automated evaluation of the different anatomical structures is applied, reducing potential subjective errors and processing time of each CT. The strength of our study is its use of the latest version of OTOPLAN® in combination with the MAESTRO 9.0 anatomy-based fitting tool, which is fully automated and may reduce measurement errors.

Di Mario et al. [11] also used the latest version of OTOPLAN® with the MAESTRO 9.0 tool and proposing frequency reallocation once the anatomical mapping had been established. They performed pure-tone and speech audiometry in 10 CI recipients after the patients had undergone a new anatomical frequency fitting. The speech recognition threshold was significantly lower after reallocation. These results demonstrate that the frequency-to-place mismatch has a real clinical impact on auditory performance for patients, especially when brain plasticity does not as easily facilitate adaptation to the mismatch (e.g., in elderly patients) [11]. In contrast, Lambricks et al. [16] recently published the ELEPHANT study, a single-blinded randomized controlled

trial with 14 CI recipients who were given a new anatomical frequency setting for comparison with a default setting. Recipients were randomized to switch to one of two processors for 3 months. Unexpectedly, 12 of the 14 patients preferred the standard frequency allocation setting to the anatomically based setting, and their speech intelligibility was also better with the standard fitting. The authors proposed two hypotheses for these findings. First, in anatomy-based fitting, the representation of frequencies shifts towards the high frequencies. With this factor, a patient's preference for standard fitting might arise from insufficient representation of low frequencies in the anatomical fitting. Second, the number of active electrodes differed between the two modes, with three fewer electrodes enabled in the anatomy-based compared with the standard map.

Thus, the comparison with these two studies is difficult because of a completely different methodology and design. In our study, we found a significant negative correlation between pitch-place mismatch and hearing performance, but rapidity in gaining speech intelligibility. Our results also showed a small frequency mismatch (<500 Hz) in one-third of cases, with excellent hearing results with the default fitting. This finding suggests that reallocation to anatomical mapping is not necessary in all CI patients.

Conclusion

Using the latest version of OTOPLAN®, our study showed a strong negative correlation between the default and anatomically established frequency mismatch and speech intelligibility. We also showed a correlation between the speed of speech intelligibility acquisition and this mismatch. Our results are consistent with those of other studies [9, 10, 14, 15] regarding the necessity of reducing frequency-to-place mismatch to improve hearing performance in CI users and encourages further research in the field of personalized fitting strategies.

Acknowledgments

We would like to thank Ms. Da Silva and Ms. Flas for their contribution to this study.

Statement of Ethics

This study protocol was reviewed and the need for approval and the need for informed consent for participants were waived by Comité d'Ethique Hospitalo-Factultaire Universitaire de Liège (agreement number 707).

Conflict of Interest Statement

The authors have no conflicts of interest to declare.

Funding Sources

This study was not supported by any sponsor or funder.

Author Contributions

Laura Dessard and Guillaume Gersdorff: study conceptualization and methodology, data collection, analysis and interpretation, and writing the original draft. Nicola Ivanovik, Masoud Zoca-Assadi, and Peter Nopp: study conceptualization and methodology, and draft review. Séverine Camby: data analysis, interpretation and illustration, draft review, and editing for the final manuscript. Philippe Lefebvre: study conceptualization and methodology, data analysis and interpretation, draft review, and editing for the final manuscript.

Data Availability Statement

All data generated or analyzed during this study are included in this article. Further inquiries can be directed to the corresponding author.

References

1 Blamey P, Artieres F, Başkent D, Bergeron F, Beynon A, Burke E, et al. Factors affecting auditory performance of postlinguistically deaf adults using cochlear implants: an update with 2,251 patients. Audiol Neurotol. 2013;18(1):36–47.
2 Holden LK, Finley CC, Firszt JB, Holden TA, Brenner C, Potts LG, et al. Factors affecting open-set word recognition in adults with cochlear implants. Ear Hear. 2013;34(3):342–60.
3 Van Der Beek FB, Briaire JJ, Van Der Marel KS, Verbist BM, Frijns JHM. Intracochlear position of cochlear implants determined using CT scanning versus fitting levels: higher threshold levels at basal turn. Audiol Neurotol. 2016;21(1):54–67.
4 Finley CC, Holden TA, Holden LK, Whiting BR, Chole RA, Neely GJ, et al. Role of electrode placement as a contributor to variability in cochlear implant outcomes. Otol Neurotol. 2008;29(7):920–8.
5 Buchman CA, Dillon MT, King ER, Adunka MC, Adunka O, Pillsbury HC. Influence of cochlear implant insertion depth on performance: a prospective randomized trial. Otol Neurotol. 2014;35(10):1773–9.
6 Alexiades G, Dhanasingh A, Jolly C. Method to estimate the complete and two-turn cochlear duct length. Otol Neurotol. 2015;36(5):904–7.
7 Escudé B, James C, Deguine O, Cochard N, Eter E, Fraysse B. The size of the cochlea and predictions of insertion depth angles for cochlear implant electrodes. Audiol Neurotol. 2006;11(Suppl 1):27–33.
8 Spiegel JL, Polterauer D, Hempel JM, Canis M, Spiro JE, Müller J. Variation of the cochlear anatomy and cochlea duct length: analysis with a new tablet-based software. Eur Arch Otorhinolaryngol. 2022;279(4):1851–61.

9 Landsberger DM, Svrakic M, Roland JT Jr, Svirsky M. The relationship between insertion angles, default frequency allocations, and spiral ganglion place pitch in cochlear implants. Ear Hear. 2015;36(5):e207–13.
10 Mertens G, Van de Heyning P, Vanderveken O, Topsakal V, Van Rompaey V. The smaller the frequency-to-place mismatch the better the hearing outcomes in cochlear implant recipients? Eur Arch Otorhinolaryngol. 2022;279(4):1875–83.
11 Di Maro F, Carner M, Sacchetto A, Soloperto D, Marchioni D. Frequency reallocation based on cochlear place frequencies in cochlear implants: a pilot study. Eur Arch Otorhinolaryngol. 2022;279(10):4719–25.
12 Canfarotta MW, Dillon MT, Buss E, Pillsbury HC, Brown KD, O'Connell BP. Validating a new tablet-based tool in the determination of cochlear implant angular insertion depth. Otol Neurotol. 2019;40(8):1006–10.
13 Schurzig D, Timm ME, Batsoulis C, Salcher R, Sieber D, Jolly C, et al. A novel method for clinical cochlear duct length estimation toward patient-specific cochlear implant selection. OTO Open. 2018;2(4):2473974X18800238.
14 Canfarotta MW, Dillon MT, Buss E, Pillsbury HC, Brown KD, O'Connell BP. Frequency-to-place mismatch: characterizing variability and the influence on speech perception outcomes in cochlear implant recipients. Ear Hear. 2020;41(5):1349–61.
15 Venail F, Mathiolon C, Menjot De Champfleur S, Piron JP, Sicard M, Villemus F, et al. Effects of electrode array length on frequency-place mismatch and speech perception with cochlear implants. Audiol Neurotol. 2015;20(2):102–11.
16 Lambriks L, van Hoof M, Debruyne J, Janssen M, Chalupper J, van der Heijden K, et al. Imaging-based frequency mapping for cochlear implants: evaluated using a daily randomized controlled trial. Front Neurosci. 2023;17:1119933.
17 Reiss LAJ, Turner CW, Karsten SA, Gantz BJ. Plasticity in human pitch perception induced by tonotopically mismatched electro-acoustic stimulation. Neuroscience. 2014;256:43–52.
18 Adunka O, Unkelbach M, Mack M, Radeloff A, Gstoettner W. Predicting basal cochlear length for electric-acoustic stimulation. Arch Otolaryngol Head Neck Surg. 2005;131(6):488–92.
19 Kawano A, Seldon H, Clark G. Computer-aided three-dimensional reconstruction in human cochlear maps: measurement of the lengths of organ of Corti, outer wall, inner wall, and Rosenthal's canal. Ann Otol Rhinol Laryngol. 1996;105(9):701–9.

Contribution to the existing literature

Anatomy-based frequency allocation is often discussed in theoretical terms or on the basis of simulated maps. This study quantifies, in a clinical cohort and using table-based planning software, the mismatch that actually separates the default allocation applied at activation from the allocation derived from each patient's own cochlear anatomy. Every patient in the series presented such a mismatch. The magnitude of the frequency shift was inversely correlated both with speech intelligibility and with the time required to reach it, which situates the mismatch as a determinant not only of final performance but also of the speed of adaptation. These results support the view that deeper insertions performed with less traumatic arrays, by reducing the residual mismatch, could contribute to improved outcomes.

4.2 Special Case: Single-Sided Deafness (SSD)

The postoperative follow-up of cochlear implant recipients with single-sided deafness (SSD) relies on a structured and personalized rehabilitation program, initiated as soon as the audio processor is activated. The primary objective is to facilitate gradual adaptation to electrical stimulation and encourage the integration of new auditory perceptions with the contralateral ear. It is essential to reassure the patient and their family about the expected benefits and to establish a rehabilitation plan tailored to individual needs.

This rehabilitation should include intensive stimulation sessions of the implanted ear, notably through direct signal input to the processor, in order to maximize stimulation efficiency and promote optimal adaptation. The rehabilitation program may also incorporate training specifically focused on sound localization, listening strategies, and speech understanding in various environments, as well as psychoeducational support aimed at reinforcing the patient's social skills and communication confidence.

Rigorous and periodic evaluations are essential to monitor progress and adjust the management protocol accordingly. Assessments should be conducted at 1, 3, 6, and 12 months following implant activation, with an annual evaluation thereafter. Additional consultations should remain available in the event of difficulties.

Evaluations include audiological and functional testing, particularly pure-tone audiometry to monitor hearing thresholds in the non-implanted ear before and after surgery. This is especially important for early detection of any hearing changes, particularly in patients with asymmetric hearing loss.

Speech-in-noise understanding should be assessed in a free-field sound-treated booth using validated sentence recognition tests. Listening conditions must include: (1) implant off with the contralateral ear aided, and (2) both ears aided. Background noise should be maintained at 65 dBA, and the speech level adjusted to determine the speech reception threshold, defined as the level at which 50% of sentences are correctly understood. For patients who cannot wear a hearing aid in the contralateral ear, the test can be adapted by maintaining speech at 65 dBA and adjusting the noise level. Three spatial configurations must be tested: the signal on the implanted side with noise on the contralateral side (SSSDNAH), signal from the front with noise on the implanted side (S0NSSD), and signal and noise from the front (S0N0). These measures quantify binaural benefits derived from cochlear implant use, including the head shadow effect, binaural squelch, binaural summation, and spatial release from masking.

Sound localization should be assessed in an acoustically treated room using a semicircular loudspeaker array with at least seven speakers positioned from -90° to +90°. Short, spectrally diverse sounds should be used to avoid misleading monaural cues.

The impact of the implant on quality of life should also be measured using validated and user-friendly tools, such as the abbreviated version of the “Speech, Spatial, and Qualities of Hearing” questionnaire.

Finally, in patients with tinnitus in the implanted ear, a specific assessment of tinnitus-related handicap should be conducted both before and after implantation. The Tinnitus Functional Index (TFI) is the recommended gold-standard tool due to its reliability and sensitivity to change, although other validated questionnaires may also be used.

This comprehensive postoperative follow-up protocol is based on the Belgian recommendations established by Távora-Vieira et al. [414], who defined quality standards for cochlear implantation in adults with single-sided deafness and asymmetric hearing loss.

Article 5

Journal: Frontiers in Audiology and Otology. Peer-reviewed. Published: Gersdorff G, Ivanovic N, Zoka Assadi M, Nopp P, Camby S, Lefèbvre P. The importance of frequency–place mismatch in the quality of sound perceived in single-sided deafness among cochlear implant recipients. Front Audiol Otol. 2025;3:1648716. doi:10.3389/fauot.2025.1648716.

frontiers | Frontiers in Audiology and Otology

TYPE Original Research
PUBLISHED 18 August 2025
DOI 10.3389/fauot.2025.1648716

Check for updates

OPEN ACCESS

EDITED BY
Mehdi Abouzari,
University of California, Irvine, United States

REVIEWED BY
Sasan Dabiri,
Northern Ontario School of Medicine University, Canada
Miriam Smetak,
Washington University in St. Louis, United States

*CORRESPONDENCE
Philippe Lefèbvre
pp.lefebvre@uliege.be

RECEIVED 17 June 2025
ACCEPTED 21 July 2025
PUBLISHED 18 August 2025

CITATION
Gersdorff G, Ivanovic N, Zoka Assadi M, Nopp P, Camby S and Lefèbvre P (2025) The importance of frequency–place mismatch in the quality of sound perceived in single-sided deafness among cochlear implant recipients. *Front. Audiol. Otol.* 3:1648716. doi: 10.3389/fauot.2025.1648716

COPYRIGHT
© 2025 Gersdorff, Ivanovic, Zoka Assadi, Nopp, Camby and Lefèbvre. This is an open-access article distributed under the terms of the Creative Commons Attribution License (CC BY). The use, distribution or reproduction in other forums is permitted, provided the original author(s) and the copyright owner(s) are credited and that the original publication in this journal is cited, in accordance with accepted academic practice. No use, distribution or reproduction is permitted which does not comply with these terms.

The importance of frequency–place mismatch in the quality of sound perceived in single-sided deafness among cochlear implant recipients

Guillaume Gersdorff[1], Nicola Ivanovic[2], Masoud Zoka Assadi[2], Peter Nopp[2], Séverine Camby[1] and Philippe Lefèbvre[1]*

[1]Department of Otorhinolaryngology, Centre Hospitalier Universitaire (CHU), Liège, Belgium, [2]Medel, Innsbruck, Austria

Introduction: Single-sided deafness (SSD) affects the ability to localize sounds and understand speech in noisy environments, significantly impacting the quality of life. Cochlear implants (CIs) have been explored as a solution for SSD, with varying success attributed to different factors, such as onset of deafness (pre- vs. post-lingual), duration of especially pre-lingual deafness, and compliance to rehab protocols, as well as the frequency-to-place mismatch, where the frequency assigned to CI electrodes does not align with the cochlea's natural tonotopy. The objective is to investigate the influence of frequency-to-place mismatch on hearing performance, sound quality, and patient satisfaction in SSD CI recipients by comparing default and anatomical frequency mapping.

Methods: A retrospective study was conducted on 19 SSD patients implanted with MEDEL CIs between 2014 and 2023. Post-activation, high-resolution cone beam computed tomography scans were analyzed using OTOPLAN® (Version V4) to define anatomical frequency mapping. The average frequency mismatch (AFM) between default and anatomical mapping was calculated. Speech intelligibility was assessed using articulation function (AF) scores, and sound quality was evaluated through patient questionnaires.

Results: A significant negative correlation between AFM and AF ($R = -0.47$, $p = 0.042$) was observed. Sound quality aspects, including natural sound perception and similarity to the normal ear, inversely correlated with AFM ($R^2 = 0.281$, $p = 0.05$, and $R^2 = 0.301$, $p = 0.043$, respectively). Global satisfaction scores were high (3.58 ± 0.77), unaffected by AFM.

Conclusion: Frequency-to-place mismatch impacts speech intelligibility and sound quality in SSD CI patients. Anatomical frequency mapping using tools like OTOPLAN can enhance CI outcomes, highlighting the need for individualized cochlear measurements and electrode assignment.

KEYWORDS

cochlear implant, hearing quality, frequency allocation, cochlear length, OTOPLAN®

Introduction

Hearing is a crucial sense that connects us to the surrounding world, enabling communication, fostering relationships, and enriching our overall life experiences. The human auditory system relies on the ability to differentiate between sounds and localize their source. For individuals with single-sided deafness (SSD), this natural ability is compromised, leading to a range of issues in environments where background noise and multiple speakers are prevalent. SSD refers to the condition

in which one ear has profound or severe hearing loss while the other ear maintains normal hearing or has a less severe impairment. It affects 3%–6% of the total population (Ross et al., 2010). While this condition may seem manageable in quiet settings, the difficulties become pronounced in noisy situations, making it challenging for individuals with SSD to effectively understand speech in noise and engage in social interactions. This situation requires compensatory mechanisms, and patients' quality of life may be affected by social isolation (Taylor, 2010; Tokita et al., 2014; Kitterick et al., 2015).

In recent years, advancements in auditory technology have paved the way for transformative solutions, and one such breakthrough is the use of cochlear implants (CIs) to address SSD. The first use of a CI for treating SSD was reported in 2008 (Van de Heyning et al., 2008). CIs, originally designed for individuals with bilateral hearing loss, are currently being explored as an innovative option to restore hearing in those with SSD. They can support better-ear listening and provide access to interaural intensity cues. Studies have demonstrated that CIs can improve sound localization and speech understanding in noise (Dillon et al., 2022; Wesarg et al., 2024; Park et al., 2023; Távora-Vieira et al., 2019; Seebacher et al., 2023; Mertens et al., 2017). Evidence from a previous study involving SSD children and adults has shown that CI use significantly improves performance across all three target-to-masker configurations [speech at 0° azimuth, masking noise at 0° azimuth (collocated) (S0N0), $p = 0.013$; speech front and masker to the CI or left ear (S0Nci/L), $p = 0.027$; and speech front and masker to the normal hearing or right ear (S0Nnh/R), $p < 0.001$] (Park et al., 2023). Additionally, significant improvements in Speech Reception Threshold (SRTs) with a CI, compared to the preoperative unaided condition, were found in all spatial configurations (Wesarg et al., 2024).

As we delve into the possibilities and challenges associated with CIs in the context of SSD, it becomes evident that these devices offer newfound hope for a more inclusive and enriched auditory experience. The criteria and predictive factors for recommending implantation have been recently published (Dillon et al., 2022; Park et al., 2023). During CI activation, auditory frequencies are typically assigned in a quasi-logarithmic and identical manner (which is a standard procedure) based on the specific implant model. However, due to limitations in the electrode array's ability to reach the most apical regions of the cochlea, as well as natural variability of cochlear anatomy (Alexiades et al., 2015; Escudé et al., 2006; Spiegel et al., 2022), this frequency assignment may not align with the cochlea's natural tonotopy. As a result, there is a discrepancy between the default frequency assigned to an electrode and the actual frequency of the stimulated neurons. This phenomenon is commonly referred to as the frequency-to-place mismatch. The current challenge in CI fitting lies in incorporating anatomical data (Mertens et al., 2022). A collaborative effort between CASCINATION AG (Switzerland) and MED-EL (Austria) has resulted in the development of OTOPLAN®, a tablet-based software. This innovative tool offers otologists an intuitive and efficient method to evaluate the anatomy of the temporal bone, enabling them to plan personalized cochlear implantation for optimal outcomes. By utilizing computed tomography (CT) scans of the temporal bone, OTOPLAN® accurately identifies crucial structures such as the modiolus, round window, and the tonotopic location of each electrode contact. The software's reliability was confirmed for estimating cochlear canal length and insertion angle depth of the electrodes (Canfarotta et al., 2020). Therefore, this program can provide a tonotopic setting for CI patients.

This retrospective study aims to investigate the influence of frequency-to-place mismatch on the hearing performance, sound quality, and patient satisfaction in individuals with SSD, by comparing anatomical frequency mapping defined by OTOPLAN with the default mapping used at the time of CI activation.

Materials and methods

This retrospective study included patients with post-lingual deafness implanted unilaterally with MEDEL CI from 2014 to 2023 at the University Hospital of Liege, a tertiary care center. The inclusion criteria were age >18 years and unilateral post-lingual hearing loss eligible for CI implantation in the deaf ear with normal hearing in the contralateral ear [Pure Tone Average (PTA) <20 dB for 500, 1,000, 2,000, 4,000, and 8,000 Hz]. The exclusion criteria were: age <18 years, abnormal hearing threshold in the contralateral ear (PTA >35 dB at 250, 500, 1,000, 2,000, 4,000, and 8,000 Hz), pre-lingual deafness, cochlear malformations, contraindication to CT imaging, unavailable or poor-resolution scans, or incompatibility with the OTOPLAN program.

All implants were activated and fitted with a processing strategy (FS4) using a standard frequency allocation map (logFS) distributed on active electrode contacts, as prescribed by the manufacturer. All patients underwent a post-operative, high-resolution cone beam CT of the temporal bone, which was analyzed using OTOPLAN (V4; CE-certification number: G1 17 10 95657 003). The software performed automated anatomical landmark assignment without manual intervention (Figure 1). Using the MAESTRO 9.0 anatomy-based fitting tools, an automated formula was used without manual intervention to determine a frequency allocation that followed the natural tonotopic map of the cochlea. In our calculation, we used the logFS bandpass-filter center frequencies.

The default frequency assigned to each electrode at the time of fitting was compared with the frequency established by OTOPLAN based on the position of the spiral ganglion neurons. The difference between these two values was calculated for each electrode for the frequencies corresponding to the speech spectrum (500–2,000 Hz) and then averaged and presented as "average of frequency mismatch" (AFM).

Finally, the AFM was compared with the hearing results for patients as assessed by speech audiometry. We used the articulation function (AF) as an index of speech intelligibility, defined as the average speech discrimination score obtained at 40, 55, and 70 dB. The speech audiometries were performed in a soundproof booth, with the patient sitting 1 m from the sound source and their normal-hearing ear masked using an earphone. We used the words of Fournier's dissyllabic list in French, pronounced to the patient through a loudspeaker. Measurements were recorded at 40–55 and 70 dB Sound Pressure Level (SPL) to calculate the AF. All tests were conducted in a quiet environment, using the default frequency allocation.

The patients were interviewed to fill out a satisfaction questionnaire composed of five questions on an analog scale ranging from 0 (*not at all*) to 5 (*completely*), with one exception

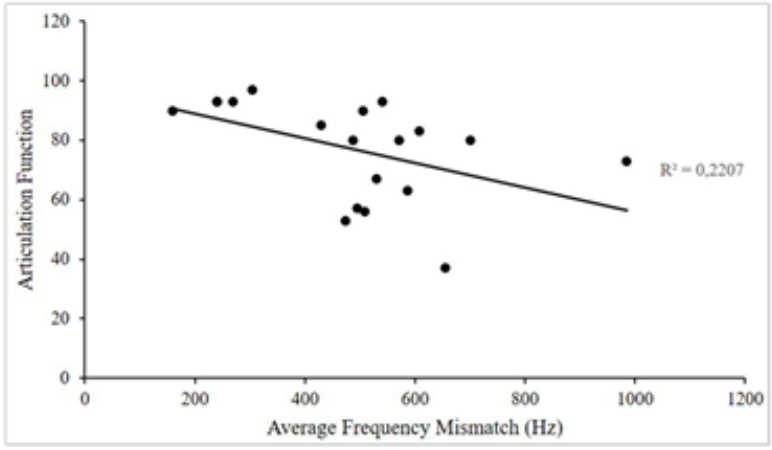

FIGURE 1
Correlation between average frequency mismatch and articulation function.

for the question on robotic sound quality, which ranged from 0 (*completely*) to 5 (*not at all*). The following aspects of satisfaction were evaluated: (1) global satisfaction of the cochlear implant, (2) sound detection (is the implant activated), (3) robotic quality of sound, (4) similarity of the sound to the normal ear, and (5) natural sound sensation.

All data sets are available upon request.

Results

Patients

Nineteen patients were included in this retrospective study. Among the 7 men and 12 women, the mean age of implantation was 60 ± 11.8 (range 44–80 years). All participants were French-speaking. Eight patients were implanted in the right ear and 11 in the left ear. No post-operative complications were observed. Implantation with a round window approach was performed for all patients; a MEDEL FLEX 24 (24-mm) electrode array was used for 13 patients, a FLEX 26 (26-mm) electrode was implanted for 2 patients, and a FLEX 28 (28-mm) electrode was implanted for 4 patients. The normal-hearing ear showed a PTA of 19.6 ± 10.99 dB, and the implanted ear showed a PTA of 93.66 ± 20.09 dB before surgery and of 38.32 ± 4.42 dB with the implant activated.

AFM

The main objective of this retrospective study was to evaluate the outcome of speech intelligibility as a function of the difference between the default frequency mapping for each electrode and the frequency fitted by the OTOPLAN software. All patients (100%) had a frequency mismatch of at least 159.8 Hz and a maximum of 985 Hz, and the average mismatch was 489.09 ± 193.21 Hz.

AF

The relationship between AFM and AF was analyzed (Figure 1). Among implant-activated patients, the AF measured at the plateau reached after implant activation was 77 ± 17.03%. The average frequency mismatch showed a significant inverse correlation ($R = -0.47$, $R^2 = 0.22$) with speech intelligibility, as measured by the Articulation Function ($p = 0.042$).

Quality of sound

The increase in the difference between the tonotopic frequency, as defined by OTOPLAN, and the fitted frequency strongly and inversely correlated with the perception of a natural sound ($R = -0.476$, $R^2 = 0.281$, $p = 0.05$) and with the similarity of the sound perceived in the normal ear ($R = -0.494$, $R^2 = 0.301$, $p = 0.043$), as assessed on an analog scale ranging between 0 and 5 (Figure 2). Robotic sound quality ($R = -0.22$, $R^2 = 0.089$, $p = 0.395$) and perception of the presence of the implant ON ($R = -0.172$, $R^2 = 0.071$, $p = 0.52$) were not significantly affected by the AFM. However, overall subjective satisfaction remained very good for all patients, with a score of 3.58 ± 0.77 ($R = -0.347$, $R^2 = 0.15$, $p = 0.17$), and was not affected by AFM.

Overall, significantly, the closer the match between the adjusted and predicted frequencies, the higher the total score for the five questions on subjective sound quality perception after CI activation ($R = -0.562$, $R^2 = 0.316$, $p = 0.0188$).

Discussion

Previous studies on frequency mapping were mainly conducted on patients suffering from bilateral hearing loss. The originality of this retrospective study was to evaluate the outcomes of speech intelligibility, as well as the quality of sound and the

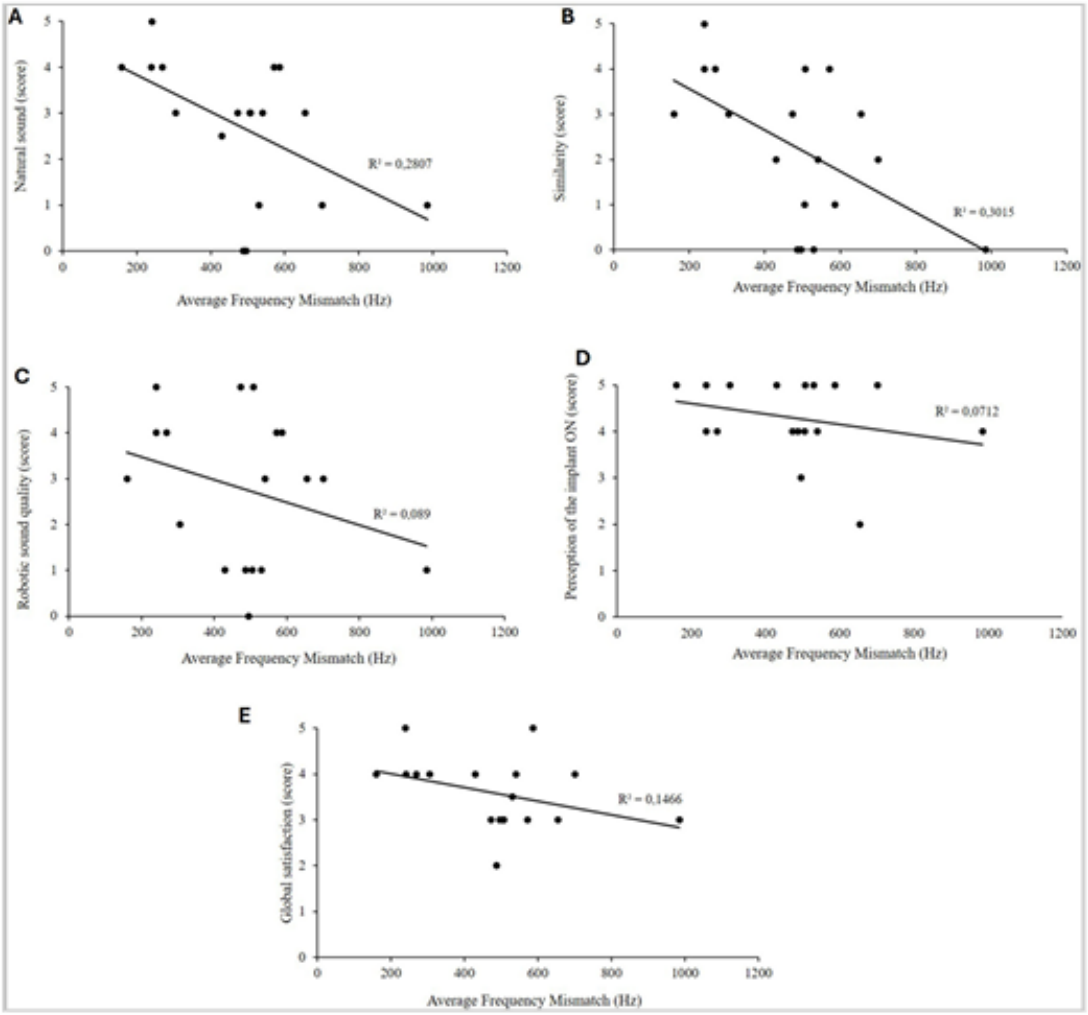

FIGURE 2
Natural sound (A), similar sound to normal ear (B), robotic sound quality (C), perception of the implant ON (D), and global satisfaction score (E) as a function of the calculated frequency placed mismatch.

global satisfaction of patients presenting a SSD, as a function of the difference between the default frequency mapping for each electrode and the frequency suggested by the software OTOPLAN based on the anatomy of the cochlea. CI implantation in the deaf ear improves binaural function rehabilitation in SSD. Sound localization can be restored, and speech understanding greatly improved after implantation, while the severity of SSD-related tinnitus can be reduced. Moreover, CI confers greater improvement in sound localization than a bone conduction hearing aid or a contralateral routing of signal device, which do not restore meaningful sound localization (Van de Heyning et al., 2008; Wesarg et al., 2024; Arndt et al., 2011; Cabral Junior et al., 2016; Kitterick et al., 2016; Thomas et al., 2016; Hempel et al., 2018).

Criteria and predictive factors for recommended implantation have been recently published (Dillon et al., 2022; Park et al., 2023), suggesting that CI is an appropriate treatment for patients with SSD. Parameters such as age at the time of implantation, duration of hearing loss, preoperative speech intelligibility thresholds, and the patient's cognitive abilities can influence post-implant hearing performance (Blamey et al., 2013). It has been established that CI tends to produce a positive effect in noise for some SSD patients (Firszt et al., 2012; Távora-Vieira et al., 2013; Gersdorff et al., 2024) and that there is a significant positive correlation between contralateral PTA and noise test results under certain conditions (Gersdorff et al., 2024; Dorbeau et al., 2018). Overall, post-operative CI hearing performance can be extremely inconsistent. Therefore,

additional unknown factors still remain. Recent studies have shown that several factors could play a role in hearing performance, including the depth of electrode insertion, the percentage of electrodes present in the scala vestibuli, and the amount of fluid and scar tissue surrounding the electrodes (Holden et al., 2014; Van Der Beek et al., 2016; Finley et al., 2008; Buchman et al., 2014). As an additional factor, the variable anatomy and dimensions of the human cochlea suggest that frequency maps could vary considerably. Therefore, the electrode frequency assignment may not align with the cochlea's natural tonotopy and may not be optimal for specific anatomical variations. Partial coverage of electrical stimulation in CI recipients with profound post-lingual deafness could lead to a frequency mismatch. In a previous study, we reported that frequency-to-place mismatch could explain the variability in results for speech intelligibility in bilaterally deaf patients. The same trend could be observed with the length and width of the cochlear base, the total cochlear volume, and the volumes of the separate compartments (Starovoyt et al., 2023). In this study, we confirm that the bigger the AFM is, the lower the intelligibility in SSD patients will be. It has been shown that matching electrodes to cochlear frequency maps is essential for optimal fitting and performance. There is a strong interaction between the optimal frequency–place mapping, electrode insertion depth, and speech recognition (Li et al., 2020; Dhanasingh and Jolly, 2017; Baskent and Shannon, 2005). Understanding and incorporating these factors into research and development efforts are essential for tailoring interventions to individual needs.

The primary outcome of this study was to compare the default frequencies assigned to the electrodes of a CI at the time of fitting with those established based on the anatomical values defined in OTOPLAN. As expected, we demonstrated a systematic mismatch between these frequencies as previously reported in several studies (Mertens et al., 2022; Canfarotta et al., 2020; Venail et al., 2015; Landsberg et al., 2015; Dessard et al., 2024). The average of the mismatch was 489.09 ± 193.21 Hz.

The secondary outcome was to compare this mismatch with the hearing performance of CI users. The maximum speech intelligibility achieved by the patients was measured at 78.95 + 13.87%. AFM showed a strong inverse correlation with speech intelligibility, as measured by the AF. This inverse correlation between the mismatch and speech performance is statistically significant. A linear correlation between frequency-to-place mismatch and hearing performance impairment was described by Mertens et al. (2022). Our results are in line with other studies (Mertens et al., 2022; Canfarotta et al., 2020; Venail et al., 2015; Landsberg et al., 2015; Dessard et al., 2024), highlighting the necessity of reducing this mismatch to improve hearing performance.

The third outcome of this study was to analyze the perception of a natural sound and the similarity of the sound perceived in the normal ear, as assessed on an analog scale ranging from 0 to 5. We showed a statistically significant negative correlation with the AFM. The closer the match between the adjusted and predicted frequencies, the higher the total score on the five questions assessing subjective perception after CI activation. However, overall subjective satisfaction remained very good for all patients, with an average score of more than 3.5. The perception of "natural" sound is inherently subjective and varies among CI users. Therefore, considering an objective measurement of the quality of life as defined by Kitterick et al. (2015) is important. It is particularly relevant for SSD patients who are able to achieve a comparison between both sides. We know that compliance could be an issue for those recipients when they consider no similarity in the perceived sound between both sides. Factors such as age at implantation, duration of deafness, and individual differences in auditory processing contribute to the diversity in user experiences. In our study, we did not take those parameters into account, but they should also be analyzed in further studies.

This study has several limitations. First, it is a retrospective analysis based on data that were not originally collected for research purposes, which may result in missing information or inaccuracies. Stratifying the sample according to potential influencing factors—such as cochlear anatomy, depth of electrode insertion, age, and others—could help with better understanding possible confounding variables. Multivariate models may also be valuable to explore these associations, but they would require a larger sample size.

This study should be considered preliminary. Further prospective research with larger cohorts is needed to confirm these findings and address these limitations.

Conclusion

In this study, we showed that sound quality and patient satisfaction in individuals with SSD are inversely proportional to the difference between the default frequency mapping for each electrode, fitted by MAESTRO 9.0, and the frequency suggested by the OTOPLAN (V4) software. In addition, we have demonstrated a systematic mismatch between the assigned default frequencies and those established based on the anatomical values defined in OTOPLAN®. We also highlighted that, in line with other studies, the average frequency mismatch correlated statistically with speech intelligibility ($p = 0.042$). CIs, originally designed for individuals with bilateral hearing loss, are currently being explored as an innovative option to address SSD. This study reinforces the hypothesis that CIs are an appropriate treatment for patients with SSD and that incorporating the concept of anatomy-based fitting into clinical practice is valuable for tailoring interventions to individual needs. Frequency-to-place mismatch could explain variability in results for test-in-noise or in localization tests. This should be considered in a further SSD prospective study.

This study encourages further research into the benefits of personalized fitting strategies for SSD patients.

Data availability statement

The raw data supporting the conclusions of this article will be made available by the authors, without undue reservation.

Ethics statement

The studies involving humans were approved by Comité d'Éthique Hospitalo-Facultaire Universitaire de Liège. The studies were conducted in accordance with the local legislation and institutional requirements. Written informed consent for

participation was not required from the participants or the participants' legal guardians/next of kin because this retrospective study is not under the law of 07 May 2004.

Author contributions

GG: Writing – original draft, Software, Writing – review & editing, Data curation. NI: Software, Writing – review & editing. MZ: Software, Writing – review & editing. PN: Supervision, Writing – review & editing. SC: Formal analysis, Writing – review & editing. PL: Writing – review & editing, Conceptualization, Investigation.

Funding

The author(s) declare that no financial support was received for the research and/or publication of this article.

Acknowledgments

The authors thank the audiologist from the Department of Oto-rhinolaryngology for outstanding clinical work.

Conflict of interest

NI, MZ, and PN were employed by Medel.

The remaining authors declare that the research was conducted in the absence of any commercial or financial relationships that could be construed as a potential conflict of interest.

Generative AI statement

The author(s) declare that no Gen AI was used in the creation of this manuscript.

Publisher's note

All claims expressed in this article are solely those of the authors and do not necessarily represent those of their affiliated organizations, or those of the publisher, the editors and the reviewers. Any product that may be evaluated in this article, or claim that may be made by its manufacturer, is not guaranteed or endorsed by the publisher.

References

Alexiades, G., Dhanasingh, A., and Jolly, C. (2015). Method to estimate the complete and two-turn cochlear duct length. *Otol. Neurotol.* 36, 904–907. doi: 10.1097/MAO.0000000000000620

Arndt, S., Aschendorff, A., Laszig, R., Beck, R., Schild, C., Kroeger, S., et al. (2011). Comparison of pseudobinaural hearing to real binaural hearing rehabilitation after cochlear implantation in patients with unilateral deafness and tinnitus. *Otol. Neurotol.* 32, 39–47. doi: 10.1097/MAO.0b013e3181fcf271

Baskent, D., and Shannon, R. (2005). Interactions between cochlear implant electrode insertion depth and frequency-place mapping. *J. Acoust. Soc. Am.* 117, 1405–1416. doi: 10.1121/1.1856273

Blamey, P., Artieres, F., Başkent, D., Bergeron, F., Beynon, A., Burke, E., et al. (2013). Factors affecting auditory performance of postlinguistically deaf adults using cochlear implants: an update with 2251 patients. *Audiol. Neurotol.* 18, 36–47. doi: 10.1159/000343189

Buchman, C. A., Dillon, M. T., King, E. R., Adunka, M. C., Adunka, O., Pillsbury, H. C., et al. (2014). Influence of cochlear implant insertion depth on performance: a prospective randomized trial. *Otol. Neurotol.* 35, 1773–1779. doi: 10.1097/MAO.0000000000000541

Cabral Junior, F., Pinna, M. H., Alves, R. D., Malerbi, A. F. D. S., and Bento, R. F. (2016). Cochlear implantation and single-sided deafness: a systematic review of the literature. *Int Arch Otorhinolaryngol.* 20, 69–75. doi: 10.1055/s-0035-1559586

Canfarotta, M. W., Dillon, M. T., Buss, E., Pillsbury, H. C., Brown, K. D., O'Connell, B. P., et al. (2020). Frequency-to-place mismatch: characterizing variability and the influence on speech perception outcomes in cochlear implant recipients. *Ear Hear.* 41, 1349–1361. doi: 10.1097/AUD.0000000000000864

Dessard, L., Gersdorff, G., Ivanovik, N., Zoca-Assadi, M., Nopp, P., Camby, S., et al. (2024). Cochlear implant: analysis of the frequency-to-place mismatch with the table-based software OTOPLAN® and its influence on hearing performance. *Audiol. Neurootol.* 29, 239–245. doi: 10.1159/000535693

Dhanasingh, A., and Jolly, C. (2017). An overview of cochlear implant electrode array designs. *Hear Res.* 356, 93–103. doi: 10.1016/j.heares.2017.10.005

Dillon, M., Rooth, M. A., Canfarotta, M. W., Richter, M., Thompson, N., Brown, K. D., et al. (2022). Sound Source localization by cochlear implant recipients with normal hearing in the contralateral ear: effects of spectral content and duration of listening experience. *Audiol. Neurootol.* 27, 437–448. doi: 10.1159/000523969

Dorbeau, C., Galvin, J., Fu, Q., Legris, E., Marx, M., Bakhos, D., et al. (2018). Binaural perception in single-sided deaf cochlear implant users with unrestricted or restricted acoustic hearing in the non-implanted ear. *Audiol. Neurootol.* 23, 187–197. doi: 10.1159/000490879

Escudé, B., James, C., Deguine, O., Cochard, N., Eter, E., Fraysse, B., et al. (2006). The size of the cochlea and predictions of insertion depth angles for cochlear implant electrodes. *Audiol. Neurotol.* 11(Suppl. 1), 27–33. doi: 10.1159/000095611

Finley, C. C., Holden, T. A., Holden, L. K., Whiting, B. R., Chole, R. A., Neely, G. J., et al. (2008). Role of electrode placement as a contributor to variability in cochlear implant outcomes. *Otol. Neurotol.* 29, 920–928. doi: 10.1097/MAO.0b013e318184f492

Firszt, J., Holden, L., Reeder, R., Waltzman, S., and Arndt, S. (2012). Auditory abilities after cochlear implantation in adults with unilateral deafness: a pilot study. *Otol. Neurotol.* 33, 1339–1346. doi: 10.1097/MAO.0b013e318268d52d

Gersdorff, G., Péan, V., Camby, S., Barriat, S., and Lefebvre, P. P. (2024). Factors predictive of binaural hearing restoration by cochlear implant in single-sided deafness. *Audiol. Neurootol.* 1, 1–11. doi: 10.1159/000540577

Hempel, J., Simon, F., and Müller, J. (2018). Extended applications for cochlear implantation. *Adv. Otorhinolaryngol.* 81, 74–80. doi: 10.1159/000485546

Holden, L. K., Finley, C. C., Firszt, J. B., Timothy, A., Brenner, C., Potts, L. G., et al. (2014). Factors affecting open-set word recognition in adults with cochlear implants. *Ear Hear.* 34, 342–360. doi: 10.1097/AUD.0b013e3182741aa7

Kitterick, P. T., Lucas, L., and Smith, S. N. (2015). Improving health-related quality of life in single-sided deafness: a systematic review and meta-analysis. *Audiol. Neurotol.* 20, 79–86. doi: 10.1159/000380753

Kitterick, P. T., Smith, S. N., and Lucas, L. (2016). Hearing instruments for unilateral severe-to-profound sensorineural hearing loss in adults: a systematic review and meta-analysis. *Ear Hear.* 37, 495–507. doi: 10.1097/AUD.0000000000000313

Landsberg, D. M., Svrakic, S., Roland, J. T., and Svirsky, M. (2015). The relationship between insertion angles, default frequency allocations, and spiral ganglion place pitch in cochlear implants. *Ear Hear.* 36, e207–e213. doi: 10.1097/AUD.0000000000000163

Li, H., Schart-Morén, N., Rohani, S. A., Ladak, H. M., Rask-Andersen, H., Agrawal, S., et al. (2020). Synchrotron radiation-based reconstruction of the human spiral ganglion: implications for cochlear implantation. *Ear Hear.* 41, 173–181. doi: 10.1097/AUD.0000000000000738

Mertens, G., De Bodt, M., and Van de Heyning, P. (2017). Evaluation of long-term cochlear implant use in subjects with acquired unilateral profound hearing loss: focus on binaural auditory outcomes. *Ear Hear.* 38, 117–125. doi: 10.1097/AUD.0000000000000359

Mertens, G., Van de Heyning, P., Vanderveken, O., Topsakal, V., and Van Rompaey, V. (2022). The smaller the frequency-to-place mismatch the better the hearing outcomes in cochlear implant recipients? *Eur. Arch. Oto-Rhino-Laryngol.* 279, 1875–1883. doi: 10.1007/s00405-021-06899-y

Park, L. R., Dillon, M. T., Buss, E., and Brown, K. D. (2023). Two-year outcomes of cochlear implant use for children with unilateral hearing loss: benefits and comparison to children with normal hearing. *Ear Hear.* 44, 955–968. doi: 10.1097/AUD.0000000000001353

Ross, D., Visser, S., Holstrum, W., Qin, T., and Kenneson, A. (2010). Highly variable population-based prevalence rates of unilateral hearing loss after the application of common case definitions. *Ear Hear.* 31, 126–133. doi: 10.1097/AUD.0b013e3181bb69db

Seebacher, J., Franke-Trieger, A., Weichbold, V., Galvan, O., Schmutzhard, J., Zorowka, P., et al. (2023). Sound localisation of low- and high-frequency sounds in cochlear implant users with single-sided deafness. *Int. J. Audiol.* 62, 71–78. doi: 10.1080/14992027.2022.2030496

Spiegel, J. L., Polterauer, D., Hempel, J. M., Canis, M., Spiro, J. E., Müller, J., et al. (2022). Variation of the cochlear anatomy and cochlea duct length: analysis with a new tablet-based software. *Eur. Arch. Oto-Rhino-Laryngol.* 279, 1851–1861. doi: 10.1007/s00405-021-06889-0

Starovoyt, A., Pyka, G., Putzeys, T., Balcaen, T., Wouters, J., Kerckhofs, G., et al. (2023). Human cochlear microstructures at risk of electrode insertion trauma, elucidated in 3D with contrast-enhanced microCT. *Sci. Rep.* 13:2191. doi: 10.1038/s41598-023-29401-6

Távora-Vieira, D., Marino, R., Krishnaswamy, J., Kuthbutheen, J., and Rajan, G. (2013). Cochlear implantation for unilateral deafness with and without tinnitus: a case series. *Laryngoscope* 123, 1251–1255. doi: 10.1002/lary.23764

Távora-Vieira, D., Rajan, G., Van de Heyning, P., and Mertens, G. (2019). Evaluating the long-term hearing outcomes of cochlear implant users with single-sided deafness. *Otol. Neurotol.* 40, e575–e580. doi: 10.1097/MAO.0000000000002235

Taylor, B. (2010). Contralateral routing of signal amplification strategies. *Semin. Hear.* 31, 378–392. doi: 10.1055/s-0030-1268036

Thomas, R., Buchman, C., Eisenberg, L., Henderson, L., He, S., Firszt, J., et al. (2016). Proceedings of the annual symposium of the american cochlear implant alliance. *Cochlear Implants Int.* 17, 211–237. doi: 10.1080/14670100.2016.1225348

Tokita, J., Dunn, C., and Hansen, M. (2014). Cochlear implantation and single sided deafness. *Curr. Opin. Otolaryngol. Head Neck Surg.* 22, 353–358. doi: 10.1097/MOO.0000000000000080

Van de Heyning, P., Vermeire, K., Diebl, M., Nopp, P., Anderson, I., De Ridder, D., et al. (2008). Incapacitating unilateral tinnitus in single-sided deafness treated by cochlear implantation. *Ann. Otol. Rhinol. Laryngol.* 117, 645–652. doi: 10.1177/000348940811700903

Van Der Beek, F. B., Briaire, J. J., Van Der Marel, K. S., Verbist, B. M., and Frijns, J. H. M. (2016). Intracochlear position of cochlear implants determined using CT scanning versus fitting levels: higher threshold levels at basal turn. *Audiol. Neurotol.* 21, 54–67. doi: 10.1159/000442513

Venail, F., Mathiolon, C., Menjot De Champfleur, S., Piron, J. P., Sicard, M., Villemus, F., et al. (2015). Effects of electrode array length on frequency-place mismatch and speech perception with cochlear implants. *Audiol. Neurotol.* 20, 102–111. doi: 10.1159/000369333

Wesarg, T., Wiebe, K., Galindo Guerreros, J. C., Arndt, S., Aschendorff, A., Voß, B., et al. (2024). Speech understanding and subjective listening effort in noise with different OTEs and sound processing technologies. *Otol. Neurotol.* 45, e91–101. doi: 10.1097/MAO.0000000000004091

Contribution to the existing literature

Studies of frequency-to-place mismatch have focused on speech intelligibility in bilaterally deafened recipients. This study addresses single-sided deafness, a situation in which the contralateral normal ear provides a direct internal reference for sound quality. It reports that the mean anatomical frequency mismatch correlates inversely with speech intelligibility and with the perceived naturalness of sound and its similarity to the normal ear, while overall satisfaction remained high and independent of the mismatch. The contribution is to extend the question beyond intelligibility, to the quality of the percept itself, in the population best placed to judge it. Since device use in single-sided deafness depends heavily on the perceived quality of the implanted ear, these qualitative aspects are directly relevant to compliance: an atraumatic, deeper insertion performed with a less traumatic array, by reducing the mismatch, could improve sound quality relative to the contralateral ear and thereby support better long-term device use.

V. Conclusions and Perspectives

This doctoral thesis is situated within a period of progressive transformation in cochlear implantation. The scope of which extends well beyond a mere technological advance and instead reflects a broader redefinition of the surgical, functional, and pathophysiological concepts that underpin this field. Initially developed as a standardized therapeutic approach for patients with bilateral profound hearing loss, primarily aimed at restoring speech understanding, cochlear implantation is now evolving toward a more holistic model of care that integrates patient-specific anatomical, neurobiological, and perceptual dimensions. The work presented in this manuscript sought to examine in an integrated manner how atraumatic surgical strategies, electrode insertion modalities, and the optimization of frequency allocation parameters interact to improve not only the preservation of intracochlear structures, but also audiometric outcomes and the overall quality of sound perception. Collectively, our findings converge toward a unified conclusion: the preservation of cochlear health represents a key determinant in reducing post-implantation outcome variability, shortening rehabilitation timelines, and promoting durable and functionally diverse auditory benefits.

Research devoted to the detailed analysis of the pre-insertion phase has highlighted the central role of a thorough understanding of cochlear anatomical complexity in preventing intracochlear trauma. The human cochlea is characterized by marked interindividual variability, both at the morphological and micro-architectural levels, particularly within the proximal regions commonly referred to as the hook region, where the initial stages of electrode insertion take place. This anatomical variability exposes surgeons to a non-negligible risk of misalignment between the intended insertion axis and the true orientation of the scala tympani. Such incongruence may result in traumatic consequences affecting the integrity of local anatomical structures, including the lateral wall, the basilar membrane, and adjacent neural elements. The findings presented herein therefore underscore the importance of integrating high-resolution intraoperative imaging tools, such as optical coherence tomography (OCT). Indeed, currently available clinical imaging modalities, including CT scan, lack the spatial resolution required for a reliable assessment of intracochlear micro-anatomy. By providing individualized, three-dimensional visualization of the initial intracochlear structures, these tools allow surgeons to move beyond indirect or empirical approaches to cochlear surgery. They pave the way for a genuine paradigm shift, transitioning from a standardized, one-size-fits-all surgical strategy toward personalized cochlear implantation guided by each patient's specific anatomy. The ability to finely tailor the surgical gesture to individual anatomical realities thus emerges as a fundamental prerequisite for any approach aiming to achieve truly atraumatic cochlear surgery.

Long-term functional outcomes may be determined as early as the electrode insertion phase, which represents a critical moment during which mechanical stresses applied to intracochlear structures can compromise their integrity. The original studies conducted within the framework of this thesis demonstrate that robot-assisted insertion techniques enable markedly improved control of insertion kinetics, particularly with respect to insertion speed, movement stability, and maintenance of the insertion axis. By limiting the repeated microtrauma associated with the variability and imprecision inherent to manual insertion, these approaches contribute to a reduction in long-term inflammatory and fibrotic responses, while promoting better preservation of neural structures and, more broadly, of neural health. In this context, our previous work has shown that robot-assisted insertion is associated with superior long-term preservation of residual hearing, increased impedance stability, and improved auditory performance over time compared with manual insertion. Analysis of these findings suggests

that the development of fibrosis and the evolution of impedance are more strongly determined by the quality of the insertion gesture than by insertion depth per se.

Furthermore, we demonstrated that the longitudinal evolution of the electrically evoked compound action potential (ECAP), considered an indirect marker of the functional status of the auditory nerve, is more favorable following robot-assisted insertion. Longitudinal ECAP monitoring reflects a dynamic recovery of cochlear neural function. During the early postoperative phase, higher ECAP thresholds may be observed, followed by a progressive decrease as the electrode-tissue interface stabilizes and neural synchrony improves. The greater impedance stability observed in our previous work with robotic-assisted insertion further reinforces these findings and supports the hypothesis of a more harmonious and durable interaction between the electrode array and intracochlear tissues. Accordingly, regular ECAP monitoring emerges as a particularly relevant tool, both for optimizing cochlear implant fitting and for refining the prediction of long-term auditory outcomes. Taken together, these results emphasize that, when biological and functional objectives are clearly defined, robotic-assisted surgery should not be regarded as a technological end in itself, but rather as a means to enhance the reproducibility, precision, and coherence of the surgical gesture in the service of cochlear and neural preservation.

Within this tissue-preservation framework, electrode array design emerges as a critical determinant. So-called atraumatic electrodes, owing to their flexibility and specifically tailored geometry, help limit the mechanical stresses exerted on intracochlear structures during insertion, while simultaneously enabling greater insertion depths. Our work further demonstrated that deeper insertions are associated with expanded cochlear coverage. This increased coverage represents a key lever for reducing frequency-related distortions and for improving the alignment between delivered electrical stimulation and the cochlea's physiological tonotopic organization.

In this way, our work, in line with numerous published studies, has demonstrated that optimization of the surgical gesture, even when relying on atraumatic electrode arrays, is not sufficient on its own to guarantee optimal functional outcomes. Post-operative programming therefore emerges as a critical step in fully capitalizing on the benefits of tissue-preserving insertion strategies. Analysis of the mismatch between the actual electrode position and the programmed frequency allocation highlights the limitations of standardized fitting strategies, which fail to account for interindividual anatomical variability and effective insertion depth. By contrast, frequency allocation adjustments that incorporate patient-specific cochlear anatomy and the true intracochlear position of the electrode array allow frequency-related distortions to be reduced and improve the perceived naturalness of the auditory signal. The findings of this thesis suggest that such anatomo-functional alignment constitutes a major determinant of perceptual quality, particularly for complex auditory dimensions such as music perception, which relies on coherent frequency representation and harmonious integration of spectral and temporal information. This issue appears especially pronounced in patients with single-sided deafness. From this perspective, these results argue for an integrated approach in which surgery and fitting should no longer be considered as independent, sequential steps, but rather as inseparable components of a coherent therapeutic continuum.

Taken as a whole, the findings of this thesis argue for a redefinition of the conceptual framework of cochlear implantation. Minimally invasive surgery, robotic assistance, atraumatic electrode design, and anatomy-based fitting should be viewed as interdependent components of a global strategy aimed at preserving the cochlear and neural health. This integrated approach

not only reduces the contribution of iatrogenic variability to postoperative outcomes, but also allows better consideration of the anatomical, neural, and functional heterogeneity of patients, which remains one of the primary determinants of post-implantation performance.

Nevertheless, several limitations must be acknowledged. With the exception of the OCT feasibility study, which follows a descriptive, technique-oriented design, the clinical studies underlying this work are retrospective in nature, and no prospective randomized controlled trial has yet been conducted; such studies represent an important direction for future research. The size of the studied cohorts, the diversity of clinical profiles, and the complexity of interactions among anatomical, neurobiological, and perceptual factors require cautious interpretation of the results. Moreover, the identification of direct causal relationships remains constrained by the multifactorial nature of auditory performance. These considerations highlight the need for larger-scale, multicenter studies incorporating standardized protocols, advanced imaging tools, and objective markers of cochlear and neural health. Such approaches will enable improved patient stratification and refinement of the clinical indications for individualized cochlear implantation strategies.

The perspectives opened by this work are numerous and align with a translational research dynamic. From a surgical standpoint, the future integration of more autonomous robotic systems, combined with advanced intraoperative imaging and real-time electrophysiological monitoring, could enable dynamic adaptation of the surgical gesture to the patient-specific anatomical constraints encountered during electrode insertion. In this context, the development of image-guided surgery, based on patient-specific preoperative imaging and intraoperative navigation, is already achievable with robot-assisted insertion systems such as RobOtol combined with CT-based guidance, represents a key step toward increased precision and reproducibility of cochlear implant surgery. From a functional perspective, the identification of reliable biomarkers of neural health and their integration into fitting strategies offer promising avenues for the progressive personalization of electrical stimulation over time. In the longer term, these advances support a broader vision of cochlear implantation as a comprehensive neuro-sensory rehabilitation process, coherently integrating anatomical, neurobiological, cognitive, and perceptual dimensions.

In conclusion, this work demonstrates that the contemporary evolution of cochlear implantation is driven by a progressive convergence of minimally invasive surgery, robotic assistance, atraumatic electrode design, and anatomically guided optimization of frequency allocation. This convergence aims not only to improve audiometric outcomes, but also to enhance the overall quality of sound perception, including music perception. Moreover, these approaches open new perspectives for the development of emerging technologies and for a broader reflection on how to access the cochlea in the least traumatic manner possible. By improving our understanding of the interactions between the surgical gesture and the intracochlear biological response, they may ultimately foster the emergence of more targeted therapeutic strategies, including genetic, immunological, and/or pharmacological interventions.

Within this context, cochlear implantation increasingly aligns with a precision medicine paradigm, grounded in the rational and individualized adaptation of each step of the therapeutic pathway to the specific anatomy and physiology of each patient.

VI. Conflict of Interest Statement

The author declares no conflict of interest with MED-EL (Innsbruck, Austria) or with Collin Medical (Bagneux, France), the manufacturer of the RobOtol® system. In the interest of full transparency, it is nevertheless disclosed that Prof. Philippe Lefebvre, promoter of this work, contributed to the development of the RobOtol® system, in particular to the addition of a fourth motor allowing an insertion speed of 0.1 mm/s and to the design of the holder used for MED-EL straight electrode arrays.

REFERENCES

1 Simmons JA. A view of the world through the bat's ear: the formation of acoustic images in echolocation. Cognition. 1989 Nov;33(1–2):155–99.
2 Poole JH, Payne K, Langbauer WR Jr, Moss CJ. The social contexts of some very low frequency calls of African elephants. Behav Ecol Sociobiol. 1988;22(6):385–392.
3 Deacon T. The symbolic species: the co-evolution of language and the brain. WW Norton. New York; 1997.
4 Fay RR. Hearing in vertebrates: a psychophysics databook. Hill-Fay A. Winnetka; 1988.
5 Enard W, Przeworski M, Fisher SE, Lai CSL, Wiebe V, Kitano T, Monaco AP, Pääbo S. Molecular evolution of FOXP2, a gene involved in speech and language. Nature. 2002 Aug;418(6900):869–72.
6 Lieberman P. The Evolution of Human Speech: Its Anatomical and Neural Bases. Curr Anthropol. 2007;48(1):39–66.
7 Warren R. Auditory Perception. Elsevier; 1982. DOI: 10.1016/C2013-0-03384-1
8 Lee CC, Sherman SM. Synaptic properties of thalamic and intracortical inputs to layer 4 of the first- and higher-order cortical areas in the auditory and somatosensory systems. J Neurophysiol. 2008 Jul;100(1):317–26.
9 Lee CC, Sherman SM. On the classification of pathways in the auditory midbrain, thalamus, and cortex. Hear Res. 2011 Jun;276(1–2):79–87.
10 Shaw EAG. The External Ear. In: Keidel WD, Neff WD, editors. Auditory System: Anatomy Physiology (Ear). Berlin, Heidelberg: Springer Berlin Heidelberg; 1974; pp 455–90.
11 Pickles J. An introduction to the physiology of hearing. 4th ed. Bingley, UK: Emerald Group Publishing Limited; 2012.
12 Pujol R. Voyage au centre de l'audition [Internet]. 2018. Available from: http://www.cochlea.eu
13 Blauert J. Spatial Hearing: The Psychophysics of Human Sound Localization. The MIT Press; 1996. DOI: 10.7551/mitpress/6391.001.0001
14 Jot J, Larcher V, Warusfel O. Digital signal processing issues in the context of binaural and transaural stereophony. Proc. 98th AES Convention. Paris; 1995.
15 Moore K, Dalley A. Clinical oriented anatomy. 4th ed. Baltimore: Lippincott Williams and Wilkins; 1999.
16 Aran J, Dancer A, Dolmazon J, Pujol R, Tran ba Huy P. Physiologie de la cochlée. 1988.
17 Robier A. Otologie. Tours: Université de Médecine de Tours; 2004.
18 Pujol R. Promenade autour de la cochlée. INSERM Montpellier; 2004.
19 Moore B. Introduction to the Psychology of hearing. 5th ed. Academic Press; 2003.
20 de Pont LMH, van Steekelenburg JM, Verbist BM, van Buchem MA, Blom HM, Hammer S. State of the Art Imaging in Menière's Disease. Tips and Tricks for Protocol and Interpretation. Curr Radiol Rep. 2020 Nov;8(11):25.
21 Tona R, Lopez IA, Fenollar-Ferrer C, Faridi R, Anselmi C, Khan AA, Shahzad M, Morell RJ, Gu S, Hoa M, Dong L, Ishiyama A, Belyantseva IA, Riazuddin S, Friedman TB. Mouse Models of Human Pathogenic Variants of TBC1D24 Associated with Non-Syndromic Deafness DFNB86 and DFNA65 and Syndromes Involving Deafness. Genes (Basel). 2020 Sep;11(10). DOI: 10.3390/genes11101122
22 Bizley JK. Audition. In: Conn PM, editor. Conn's Translational Neuroscience.

Academic Press/Elsevier; 2017. p. 579–598. DOI: 10.1016/B978-0-12-802381-5.00042-7
23 Von Békésy G. Experiments in hearing. NY: McGraw-Hill; 1960.
24 Rüttiger L, Zimmermann U, Knipper M. Biomarkers for Hearing Dysfunction: Facts and Outlook. ORL J Otorhinolaryngol Relat Spec. 2017;79(1–2):93–111.
25 Bear M, Connors B, Paradiso M. Neuroscience: Exploring the Brain. 3rd ed. Lippincott Williams and Wilkins; 2007.
26 Kandel E, Koester J, Mack S, SA S. Principles of Neural Science. 6th ed. NY: McGraw-Hill Professional; 2021.
27 Delmaghani S, El-Amraoui A. Inner Ear Gene Therapies Take Off: Current Promises and Future Challenges. J Clin Med. 2020 Jul;9(7). DOI: 10.3390/jcm9072309
28 Nobili R, Mammano F, Ashmore J. How well do we understand the cochlea? Trends Neurosci. 1998 Apr;21(4):159–67.
29 Ashmore JF, Oghalai JS, Dewey JB, Olson ES, Strimbu CE, Wang Y, Shera CA, Altoè A, Abdala C, Elgoyhen AB, Eatock RA, Raphael RM. The Remarkable Outer Hair Cell: Proceedings of a Symposium in Honour of W. E. Brownell. J Assoc Res Otolaryngol. 2023 Apr;24(2):117–27.
30 Ashmore J. Cochlear outer hair cell motility. Physiol Rev. 2008 Jan;88(1):173–210.
31 Ashmore JF, Kolston PJ. Hair cell based amplification in the cochlea. Curr Opin Neurobiol. 1994 Aug;4(4):503–8.
32 Bear M, Connors B, Paradiso M. Neuroscience: Exploring the Brain. Jones & Bartlett Learning; 2020.
33 Safieddine S, Eybalin M. Expression of mGluR1 alpha mRNA receptor in rat and guinea pig cochlear neurons. Neuroreport. 1995 Dec;7(1):193–6.
34 Zhang-Hooks Y, Agarwal A, Mishina M, Bergles DE. NMDA Receptors Enhance Spontaneous Activity and Promote Neuronal Survival in the Developing Cochlea. Neuron. 2016 Jan;89(2):337–50.
35 Gold T, Gray J. Hearing II. The physical basis of the action of cochlea. Proc R Soc B Biol Sci. 1948;135(881):492–8.
36 Johnstone BM, Patuzzi R, Yates GK. Basilar membrane measurements and the travelling wave. Hear Res. 1986;22:147–53.
37 Kiang NY, Rho JM, Northrop CC, Liberman MC, Ryugo DK. Hair-cell innervation by spiral ganglion cells in adult cats. Science. 1982 Jul;217(4555):175–7.
38 Spoendlin H. Innervation densities of the cochlea. Acta Otolaryngol. 1972;73(2):235–48.
39 Liberman MC. Single-neuron labeling in the cat auditory nerve. Science. 1982 Jun;216(4551):1239–41.
40 Liberman MC. Auditory-nerve response from cats raised in a low-noise chamber. J Acoust Soc Am. 1978 Feb;63(2):442–55.
41 Johnson DH. The relationship between spike rate and synchrony in responses of auditory-nerve fibers to single tones. J Acoust Soc Am. 1980 Oct;68(4):1115–22.
42 Liberman LD, Suzuki J, Liberman MC. Dynamics of cochlear synaptopathy after acoustic overexposure. J Assoc Res Otolaryngol. 2015 Apr;16(2):205–19.
43 Niwa M, Young ED, Glowatzki E, Ricci AJ. Functional subgroups of cochlear inner hair cell ribbon synapses differently modulate their EPSC properties in response to stimulation. J Neurophysiol. 2021 Jun;125(6):2461–79.
44 Merchan-Perez A, Liberman MC. Ultrastructural differences among afferent synapses on cochlear hair cells: correlations with spontaneous discharge rate. J Comp Neurol. 1996 Jul;371(2):208–21.
45 Heil P, Peterson AJ. Basic response properties of auditory nerve fibers: a review. Cell

Tissue Res. 2015 Jul;361(1):129–58.
46 Joris PX, Yin TC. Responses to amplitude-modulated tones in the auditory nerve of the cat. J Acoust Soc Am. 1992 Jan;91(1):215–32.
47 Eggermont JJ. Representation of spectral and temporal sound features in three cortical fields of the cat. Similarities outweigh differences. J Neurophysiol. 1998 Nov;80(5):2743–64.
48 Liang L, Lu T, Wang X. Neural representations of sinusoidal amplitude and frequency modulations in the primary auditory cortex of awake primates. J Neurophysiol. 2002 May;87(5):2237–61.
49 Oxenham AJ. Pitch perception. J Neurosci. 2012 Sep;32(39):13335–8.
50 Schalk TB, Sachs MB. Nonlinearities in auditory-nerve fiber responses to bandlimited noise. J Acoust Soc Am. 1980 Mar;67(3):903–13.
51 Kimura RS, Schuknecht HF, Sando I. FINE MORPHOLOGY OF THE SENSORY CELLS IN THE ORGAN OF CORTI OF MAN. Acta Otolaryngol. 1964 Nov;58:390–408.
52 Katsuki Y, SUmi T, Uchiyama H, Watanabe T. Electric responses of auditory neurons in cat to sound stimulation. J Neurophysiol. 1958 Nov;21(6):569–88.
53 Saenz M, Langers DRM. Tonotopic mapping of human auditory cortex. Hear Res. 2014 Jan;307:42–52. DOI: 10.1016/j.heares.2013.07.016
54 Perrot X. Anatomie et Physiologie du Système Nerveux Auditif Central. Cah l'Audioprothèse. 2010;23(6).
55 Rouiller EM, Rodrigues-Dagaeff C, Simm G, De Ribaupierre Y, Villa A, De Ribaupierre F. Functional organization of the medial division of the medial geniculate body of the cat: tonotopic organization, spatial distribution of response properties and cortical connections. Hear Res. 1989 May;39(1–2):127–42.
56 Jacomme A-V, Nodal FR, Bajo VM, Manunta Y, Edeline J-M, Babalian A, Rouiller EM. The projection from auditory cortex to cochlear nucleus in guinea pigs: an in vivo anatomical and in vitro electrophysiological study. Exp brain Res. 2003 Dec;153(4):467–76.
57 King AJ. Sensory processing: Signal selection by cortical feedback. Curr Biol. 1997 Feb;7(2):R85–8.
58 Suga N. Plasticity of the adult auditory system based on corticocortical and corticofugal modulations. Neurosci Biobehav Rev. 2020 Jun;113:461–78.
59 Heil P, Neubauer H, Irvine DRF. An improved model for the rate-level functions of auditory-nerve fibers. J Neurosci. 2011 Oct;31(43):15424–37.
60 Smith RJH, Bale JFJ, White KR. Sensorineural hearing loss in children. Lancet (London, England). 2005 Mar;365(9462):879–90.
61 Petit C, El-Amraoui A, Avan P. Audition: Hearing and Deafness. In: Pfaff D, editor. Neuroscience in the 21st Century. NY: Springer-Science; 2013.
62 Nadol JBJ. Hearing loss. N Engl J Med. 1993 Oct;329(15):1092–102.
63 Ahmed S, Sheraz S, Malik SA, Ahmed NR, Malik SA, Farooq S, Raheem A, Basheer F, Nayyar ZA. Frequency Of Congenital Hearing Loss In Neonates. J Ayub Med Coll Abbottabad. 2018;30(2):234–6.
64 Fortnum HM, Summerfield AQ, Marshall DH, Davis AC, Bamford JM. Prevalence of permanent childhood hearing impairment in the United Kingdom and implications for universal neonatal hearing screening: questionnaire based ascertainment study. BMJ. 2001 Sep;323(7312):536–40.
65 Tillaut H, Doncarli A, Da Costa V, Godey B, Roussey M, Goulet V, King L. Programme de dépistage de la surdité permanente néonatale. Bilan de mise en oeuvre en Bretagne; 2015-2016 [Internet]. 2019;Santé Publique France.

66 Caluraud S, Marcolla-Bouchetemblé A, de Barros A, Moreau-Lenoir F, de Sevin E, Rerolle S, Charrière E, Lecler-Scarcella V, Billet F, Obstoy M-F, Amstutz-Montadert I, Marie J-P, Lerosey Y. Newborn hearing screening: analysis and outcomes after 100,000 births in Upper-Normandy French region. Int J Pediatr Otorhinolaryngol. 2015 Jun;79(6):829–33.
67 Delobel-Ayoub M, Klapouszczak D, Cans C, Arnaud C, van Bakel M. Données épidémiologiques sur les surdités bilatérales sévères et profondes en France pour les générations 1997 à 2005. Bull Epidemiol Hebd. 2015;42–43:781–8.
68 Haile LM, Orji AU, Reavis KM, Briant PS, Lucas KM, Alahdab F, Bärnighausen TW, Bell AW, Cao C, Dai X, Hay SI, Heidari G, Karaye IM, Miller TR, Mokdad AH, Mostafavi E, Natto ZS, Pawar S, Rana J, Seylani A, Singh JA, Wei J, Yang L, Ong KL, Steinmetz JD. Hearing Loss Prevalence, Years Lived With Disability, and Hearing Aid Use in the United States From 1990 to 2019: Findings From the Global Burden of Disease Study. Ear Hear. 2024;45(1):257–67.
69 François M, Boukhris M, Noel-Petroff N. Schooling of hearing-impaired children and benefit of early diagnosis. Eur Ann Otorhinolaryngol Head Neck Dis. 2015 Nov;132(5):251–5.
70 Lin FR, Yaffe K, Xia J, Xue Q-L, Harris TB, Purchase-Helzner E, Satterfield S, Ayonayon HN, Ferrucci L, Simonsick EM. Hearing loss and cognitive decline in older adults. JAMA Intern Med. 2013 Feb;173(4):293–9.
71 Cunningham LL, Tucci DL. Hearing Loss in Adults. N Engl J Med. 2017 Dec;377(25):2465–73.
72 Markman TM, Quittner AL, Eisenberg LS, Tobey EA, Thal D, Niparko JK, Wang N-Y. Language development after cochlear implantation: an epigenetic model. J Neurodev Disord. 2011 Dec;3(4):388–404.
73 Lina-Granade G, Gallego S, Thai-Van H, Truy E. Appareillage auditif conventionnel par voie aérienne. Paris: Elsevier Masson SAS; 2010.
74 Hermann R, Lescanne E, Loundon N, Barone P, Belmin J, Blanchet C, Borel S, Charpiot A, Coez A, Deguine O, Farinetti A, Godey B, Lazard D, Marx M, Mosnier I, Nguyen Y, Teissier N, Virole MB, Roman S, Truy E. French Society of ENT (SFORL) guidelines. Indications for cochlear implantation in adults. Eur Ann Otorhinolaryngol Head Neck Dis. 2019 Jun;136(3):193–7.
75 SFORL - Société Française d'Oto-Rhino-Laryngologie et de Chirurgie de la Face et du Cou. Indications de l'implant cochléaire chez l'adulte et chez l'enfant. Recommandation pour la pratique clinique. 2018
76 Simon F, Roman S, Truy E, Barone P, Belmin J, Blanchet C, Borel S, Charpiot A, Coez A, Deguine O, Farinetti A, Godey B, Lazard D, Marx M, Mosnier I, Nguyen Y, Teissier N, Virole B, Lescanne E, Loundon N. Guidelines (short version) of the French Society of Otorhinolaryngology (SFORL) on pediatric cochlear implant indications. Eur Ann Otorhinolaryngol Head Neck Dis. 2019 Oct;136(5):385–91.
77 Truy E, Bouccara D, Sterkers O, Triglia J. Techniques chirurgicales d'implantation d'aides auditives en otoneurologie. EMC. Paris: Elsevier Masson SAS; 2009; pp 1–20.
78 Eshraghi AA, Frachet B, Van De Water TR, Eter E. Surdité de l'adulte: réparer ou compenser. Rev Prat. 2009 May;59(5):645–52.
79 Zwolan TA, Schvartz-Leyzac KC, Pleasant T. Development of a 60/60 Guideline for Referring Adults for a Traditional Cochlear Implant Candidacy Evaluation. Otol Neurotol. 2020 Aug;41(7):895–900.
80 Carlson ML. Cochlear Implantation in Adults. N Engl J Med. 2020 Apr;382(16):1531–42.
81 Buchman CA, Gifford RH, Haynes DS, Lenarz T, O'Donoghue G, Adunka O, Biever

A, Briggs RJ, Carlson ML, Dai P, Driscoll CL, Francis HW, Gantz BJ, Gurgel RK, Hansen MR, Holcomb M, Karltorp E, Kirtane M, Larky J, Mylanus EAM, Roland JTJ, Saeed SR, Skarzynski H, Skarzynski PH, Syms M, Teagle H, Van de Heyning PH, Vincent C, Wu H, Yamasoba T, Zwolan T. Unilateral Cochlear Implants for Severe, Profound, or Moderate Sloping to Profound Bilateral Sensorineural Hearing Loss: A Systematic Review and Consensus Statements. JAMA Otolaryngol Head Neck Surg. 2020 Oct;146(10):942–53.

82 Macherey O, Carlyon R. Cochlear implants. Curr Biol. 2014;24(18):R878–R884.

83 Zwicker E, Terhardt E. Analytical expressions for critical-band rate and critical bandwidth as a function of frequency. J Acoust Soc Am. 1980;68(5):1523–5.

84 Lawson D, Wilson B, Zerbi M, Finley C. Speech processors for auditory prostheses. NIH Contract. 1996

85 Griffin D, Lim J. Multiband excitation vocoder. IEEE Trans Acoust Speech Signal Process. 1988;36(8):1223–35.

86 Pudenz RH, Agnew WF, Yuen TGH, Bullara LA, Jacques S, Shelden CH. Adverse Effects of Electrical Energy Applied to the Nervous System. Stereotact Funct Neurosurg. 1977;40(2–4):72–87.

87 Hughes M. Objective Measures in Cochlear Implants. Plur Pub. 2013

88 Bierer JA. Threshold and channel interaction in cochlear implant users: evaluation of the tripolar electrode configuration. J Acoust Soc Am. 2007 Mar;121(3):1642–53.

89 Shannon R. Multichannel electrical stimulation of the auditory nerve in man. Hear Res. 1983;12(1):1–16.

90 Dhanasingh A, Jolly C. An overview of cochlear implant electrode array designs. Hear Res. 2017;356:93–103.

91 Moran M, Dowell R, Iseli C, Briggs R. Hearing preservation outcomes for 139 cochlear implant recipients using a thin straight electrode array. Otol Neurotoltol. 2017;38(5):678–84.

92 Gordin A, Papsin B, Gordon K. Packing of the cochleostomy site affects auditory nerve response thresholds in precurved off-stylet cochlear implants. Otol Neurotol. 2010 Feb;31(2):204–9.

93 Wilson BS, Finley CC, Lawson DT, Wolford RD, Eddington DK, Rabinowitz WM. Better speech recognition with cochlear implants. Nature. 1991 Jul;352(6332):236–8.

94 Luers JC, Hüttenbrink K-B. Surgical anatomy and pathology of the middle ear. J Anat. 2016 Feb;228(2):338–53.

95 Gersdorff M, Gérard J. Atlas of Middle Ear Surgery. Stuttgart: 2011.

96 Labadie RF, Chodhury P, Cetinkaya E, Balachandran R, Haynes DS, Fenlon MR, Jusczyzck AS, Fitzpatrick JM. Minimally invasive, image-guided, facial-recess approach to the middle ear: demonstration of the concept of percutaneous cochlear access in vitro. Otol Neurotol. 2005 Jul;26(4):557–62.

97 Eshraghi AA, Nazarian R, Telischi FF, Rajguru SM, Truy E, Gupta C. The cochlear implant: historical aspects and future prospects. Anat Rec. 2012 Nov;295(11):1967–80.

98 Holden LK, Finley CC, Firszt JB, Timothy A, Brenner C, Potts LG, Ph D, Gotter BD, Vanderhoof SS, Mispagel K, Heydebrand G, Skinner MW. Factors Affecting Open-Set Word Recognition in Adults with Cochlear Implants. Ear Hear. 2014;34(3):342–60.

99 Zwolan TA, Basura G. Determining Cochlear Implant Candidacy in Adults: Limitations, Expansions, and Opportunities for Improvement. Semin Hear. 2021 Nov;42(4):331–41.

100 Gstoettner W, Kiefer J, Baumgartner W-D, Pok S, Peters S, Adunka O. Hearing preservation in cochlear implantation for electric acoustic stimulation. Acta Otolaryngol. 2004 May;124(4):348–52.

101 Gantz BJ, Turner C, Gfeller KE, Lowder MW. Preservation of hearing in cochlear implant surgery: advantages of combined electrical and acoustical speech processing. Laryngoscope. 2005 May;115(5):796–802.
102 Lehnhardt E. Intracochlear placement of cochlear implant electrodes in soft surgery technique. HNO. 1993 Jul;41(7):356–9.
103 Lenarz T, Stöver T, Buechner A, Lesinski-Schiedat A, Patrick JF, Pesch J. Temporal bone results and hearing preservation with a new straight electrode. Audiol Neurootol. 2006;1:34–41.
104 Hoskison E, Mitchell S, Coulson C. Systematic review: Radiological and histological evidence of cochlear implant insertion trauma in adult patients. Cochlear Implants Int. 2017 Jul;18(4):192–7.
105 Aschendorff A, Kromeier J, Klenzner T, Laszig R. Quality Control After Insertion of the Nucleus Contour and Contour Advance Electrode in Adults. Ear & Hear. 2007;28(2):75S-79S.
106 Skinner MW, Holden TA, Whiting BR, Voie AH, Brunsden B, Neely JG, Saxon EA, Hullar TE, Finley CC. In vivo estimates of the position of advanced bionics electrode arrays in the human cochlea. Ann Otol Rhinol Laryngol Suppl. 2007 Apr;197:2–24.
107 Starovoyt A, Pyka G, Putzeys T, Balcaen T, Wouters J, Kerckhofs G, Verhaert N. Human cochlear microstructures at risk of electrode insertion trauma, elucidated in 3D with contrast-enhanced microCT. Sci Rep. 2023;13(1):2191.
108 Newbold C, Richardson R, Millard R, Seligman P, Cowan R, Shepherd R. Electrical stimulation causes rapid changes in electrode impedance of cell-covered electrodes. J Neural Eng. 2011 Jun;8(3):36029.
109 Finley CC, Holden TA, Holden LK, Whiting BR, Chole RA, Neely GJ, Hullar TE, Skinner MW. Role of electrode placement as a contributor to variability in cochlear implant outcomes. Otol Neurotol. 2008;29(7):920–8.
110 Wanna GB, Noble JH, Gifford RH, Dietrich MS, Sweeney AD, Zhang D, Dawant BM, Rivas A, Labadie RF. Impact of Intrascalar Electrode Location, Electrode Type, and Angular Insertion Depth on Residual Hearing in Cochlear Implant Patients: Preliminary Results. Otol Neurotol. 2015 Sep;36(8):1343–8.
111 Torres R, Jia H, Drouillard M, Bensimon J, Sterkers O, Ferrary E, Nguyen Y. An Optimized Robot-Based Technique for Cochlear Implantation to Reduce Array Insertion Trauma. Otolaryngol Neck Surg. 2018;159(5):900–7.
112 Rau TS, Lenarz T, Majdani O. Individual Optimization of the Insertion of a Preformed Cochlear Implant Electrode Array. Int J Otolaryngol. 2015;2015:724703.
113 Carlson ML, Driscoll CLW, Gifford RH, Service GJ, Tombers NM, Hughes-Borst BJ, Neff BA, Beatty CW. Implications of minimizing trauma during conventional cochlear implantation. Otol Neurotol. 2011 Aug;32(6):962–8.
114 Ibrahim HN, Helbig S, Bossard D, Truy E. Surgical trauma after sequential insertion of intracochlear catheters and electrode arrays (a histologic study). Otol Neurotol. 2011 Dec;32(9):1448–54.
115 Daoudi H, Lahlou G, Torres R, Sterkers O, Lefeuvre V, Ferrary E, Mosnier I, Nguyen Y. Robot-assisted Cochlear Implant Electrode Array Insertion in Adults: A Comparative Study With Manual Insertion. Otol Neurotol. 2021 Apr;42(4):e438–44.
116 Starovoyt A, Putzeys T, Wouters J, Verhaert N. High-resolution Imaging of the Human Cochlea through the Round Window by means of Optical Coherence Tomography. Sci Rep. 2019 Oct;9(1):14271.
117 Kerkhofs L, Starovoyt A, Wouters J, Putzeys T, Verhaert N. Optical Coherence Tomography-Based Atlas of the Human Cochlear Hook Region. J Clin Med. 2022 Dec;12(1). DOI: 10.3390/jcm12010238

118 Shoman NM. Robotics and cochlear implant surgery: goals and developments. Curr Opin Otolaryngol Head Neck Surg. 2022 Oct;30(5):314–9.
119 Kashani RG, Kocharyan A, Bennion DM, Scheperle RA, Etler C, Oleson J, Dunn CC, Claussen AD, Gantz BJ, Hansen MR. Combining Intraoperative Electrocochleography with Robotics-Assisted Electrode Array Insertion. Otol Neurotol. 2024 Feb;45(2):143–9.
120 Zhou L, Friedmann DR, Treaba C, Peng R, Roland JTJ. Does cochleostomy location influence electrode trajectory and intracochlear trauma? Laryngoscope. 2015 Apr;125(4):966–71.
121 Mostafa BE, Fiky LM El. Radiologic Evaluation of the Round Window Niche Configuration: A One-Stop Approach. J Int Adv Otol. 2021 Nov;17(6):478–81.
122 Li PMMC, Wang H, Northrop C, Merchant SN, Nadol JB. Anatomy of the round window and hook region of the cochlea with implications for cochlear implantation and other endocochlear surgical procedures. Otol Neurotol. 2007;28(5):641–8.
123 Atturo F, Barbara M, Rask-Andersen H. Is the human round window really round? An anatomic study with surgical implications. Otol Neurotol. 2014 Sep;35(8):1354–60.
124 Schart-Morén N, Agrawal SK, Ladak HM, Li H, Rask-Andersen H. Effects of Various Trajectories on Tissue Preservation in Cochlear Implant Surgery: A Micro-Computed Tomography and Synchrotron Radiation Phase-Contrast Imaging Study. Ear Hear. 2019;40(2):393–400.
125 Atturo F, Barbara M, Rask-Andersen H. On the anatomy of the "hook" region of the human cochlea and how it relates to cochlear implantation. Audiol Neurootol. 2014;19(6):378–85.
126 Briggs RJ, Tykocinski M, Stidham K, Roberson JB. Cochleostomy site: implications for electrode placement and hearing preservation. Acta Otolaryngol. 2005;125(8):6.
127 Agrawal S, Schart-Morén N, Liu W, Ladak HM, Rask-Andersen H, Li H. The secondary spiral lamina and its relevance in cochlear implant surgery. Ups J Med Sci. 2018 Mar;123(1):9–18.
128 Heutink F, Verbist BM, Mens LHM, Huinck WJ, Mylanus EAM. The evaluation of a slim perimodiolar electrode: surgical technique in relation to intracochlear position and cochlear implant outcomes. Eur Arch oto-rhino-laryngology. 2020 Feb;277(2):343–50.
129 Havenith S, Lammers MJW, Tange RA, Trabalzini F, della Volpe A, van der Heijden GJMG, Grolman W. Hearing preservation surgery: cochleostomy or round window approach? A systematic review. Otol Neurotol. 2013 Jun;34(4):667–74.
130 Wanna GB, Noble JH, Carlson ML, Gifford RH, Dietrich MS, Haynes DS, Dawant BM, Labadie RF. Impact of electrode design and surgical approach on scalar location and cochlear implant outcomes. Laryngoscope. 2014 Nov;124 Suppl(0 6):S1-7.
131 Pringle MB, Konieczny KM. Anatomy of the Round Window Region With Relation to Selection of Entry Site Into the Scala Tympani. Laryngoscope. 2021 Feb;131(2):E598–604.
132 Briggs RJ, Tykocinski M, Xu J, Risi F, Svehla M, Cowan R, Stöver T, Erfurt P, Lenarz T. Comparison of round window and cochleostomy approaches with a prototype hearing preservation electrode. Audiol Neurotol. 2006;11(SUPPL. 1):42–8.
133 Addams-Williams J, Munaweera L, Coleman B, Shepherd R, Backhouse S. Cochlear implant electrode insertion: in defence of cochleostomy and factors against the round window membrane approach. Cochlear Implants Int. 2011 Aug;12 Suppl 2:S36-9.
134 Gudis DA, Montes M, Bigelow DC, Ruckenstein MJ. The round window: is it the "cochleostomy" of choice? Experience in 130 consecutive cochlear implants. Otol Neurotol. 2012 Dec;33(9):1497–501.

135 Richard C, Fayad JN, Doherty J, Linthicum FHJ. Round window versus cochleostomy technique in cochlear implantation: histologic findings. Otol Neurotol. 2012 Sep;33(7):1181–7.
136 Adunka O, Kiefer J, Unkelbach MH, Lehnert T, Gstoettner W. Development and evaluation of an improved cochlear implant electrode design for electric acoustic stimulation. Laryngoscope. 2004 Jul;114(7):1237–41.
137 Shakeel M, Spielmann PM, Jones SE, Hussain SSM. Direct measurement of the round window niche dimensions using a 3-dimensional moulding technique--a human cadaveric temporal bone study. Clin Otolaryngol. 2015 Dec;40(6):657–61.
138 Eitutis ST, Vickers DA, Tebbutt K, Thomas T, Jiang D, de Klerk A, Clemesha J, Chung M, Bance ML. A Multicenter Comparison of 1-yr Functional Outcomes and Programming Differences Between the Advanced Bionics Mid-Scala and SlimJ Electrode Arrays. Otol Neurotol. 2023 Dec;44(10):e730–8.
139 Patro A, Lindquist NR, Schauwecker N, Holder JT, Perkins EL, Haynes DS, Tawfik KO. Comparison of Speech Recognition and Hearing Preservation Outcomes Between the Mid-Scala and Lateral Wall Electrode Arrays. Otol Neurotol. 2024 Jan;45(1):52–7.
140 Pennington-FitzGerald W, Waring NA, Hamiter M, Kuhlmey M, Kim AH. Impact of Cochlear Implant Electrode Array Design on Post-Op Speech Perception. Otolaryngol neck Surg. 2025 Mar;172(3):960–6.
141 Kamakura T, Nadol Jr JB. Correlation between word recognition score and intracochlear new bone and fibrous tissue after cochlear implantation in the human. Hear Res. 2016 Sep;339:132–41.
142 Micuda A, Li H, Rask-Andersen H, Ladak HM, Agrawal SK. Morphologic Analysis of the Scala Tympani Using Synchrotron: Implications for Cochlear Implantation. Laryngoscope. 2024 Jun;134(6):2889–97.
143 Canfarotta MW, Dillon MT, Selleck AM, Brown KD. Scala Tympani Volume Influences Initial 6-Month Hearing Preservation With Lateral Wall Electrode Arrays. Laryngoscope. 2025 May;135(5):1781–7.
144 GBD 2016 Disease and Injury Incidence and Prevalence Collaborators. Global, regional, and national incidence, prevalence, and years lived with disability for 328 diseases and injuries for 195 countries, 1990–2016: a systematic analysis for the Global Burden of Disease Study 2016. Lancet. 2017 Sep;390(10100):1211–59.
145 Olusanya BO, Davis AC, Hoffman HJ. Hearing loss: rising prevalence and impact. Bull World Health Organ. 2019 Oct;97(10):646-646A.
146 Emmett SD, Sudoko CK, Tucci DL, Saunders JE, Akhtar N. Expanding access: cost-effectiveness of cochlear implantation and deaf education in Asia. Otolaryngol Head Neck Surg. 2019;161(4):672–82.
147 Sorkin DL, Buchman CA. Cochlear Implant Access in Six Developed Countries. Otol Neurotol. 2016 Feb;37(2):e161-4.
148 Martinez-Monedero R, Niparko JK, Aygun N. Cochlear Coiling Pattern and Orientation Differences in Cochlear Implant Candidates. Otol Neurotol. 2011;32(7):1086–93.
149 Breinbauer H, Praetorius M. Variability of an ideal insertion vector for cochlear implantation. Otol Neurotol. 2015;36(4):610–7.
150 Li H, Schart-Morén N, Rohani SA, Ladak HM, Rask-Andersen H, Agrawal S. Synchrotron Radiation-Based Reconstruction of the Human Spiral Ganglion: Implications for Cochlear Implantation. Ear Hear. 2020;41(1):173–81.
151 Avci E, Nauwelaers T, Lenarz T, Hamacher V, Kral A. Variations in microanatomy of the human cochlea. J Comp Neurol. 2014 Oct;522(14):3245–61.
152 Stakhovskaya OA, Sridhar D, Bonham B, Leake P. Frequency map for the human

cochlear spiral ganglion: implications for cochlear implants. J Assoc Res Otolaryngol. 2007;8(2):220–33.
153 Otte J, Schuknecht HF, Kerr AG. Ganglion cell populations in normal and pathological human cochleae. Implications for cochlear implantation. Laryngoscope. 1978;88(8 Pt 1):1231–1246.
154 Locher H, de Groot JCMJ, van Iperen L, Huisman MA, Frijns JHM, Chuva de Sousa Lopes SM. Distribution and development of peripheral glial cells in the human fetal cochlea. PLoS One. 2014;9(1):e88066.
155 Rask-Andersen H, Erixon E, Kinnefors A, Löwenheim H, Schrott-Fischer A, Liu W. Anatomy of the human cochlea--implications for cochlear implantation. Cochlear Implants Int. 2011 May;12 Suppl 1:S8-13.
156 Boëx C, Baud L, Cosendai G, Sigrist A, Kós M-I, Pelizzone M. Acoustic to electric pitch comparisons in cochlear implant subjects with residual hearing. J Assoc Res Otolaryngol. 2006 Jun;7(2):110–24.
157 Engmér C, Laurell G, Bagger-Sjöbäck D, Rask-Andersen H. Immunodefense of the round window. Laryngoscope. 2008 Jun;118(6):1057–62.
158 Goycoolea M V, Lundman L. Round window membrane. Structure function and permeability: a review. Microsc Res Tech. 1997 Feb;36(3):201–11.
159 Su WY, Marion MS, Hinojosa R, Matz GJ. Anatomical measurements of the cochlear aqueduct, round window membrane, round window niche, and facial recess. Laryngoscope. 1982 May;92(5):483–6.
160 Clifford A, Gibson WP. Anatomy of the round window with respect to cochlear implant surgery. Ann Otol Rhinol Laryngol. 1987;96(128):17–9.
161 Singla A, Sahni D, Gupta AK, Loukas M, Aggarwal A. Surgical anatomy of round window and its implications for cochlear implantation. Clin Anat. 2014 Apr;27(3):331–6.
162 Baki FA, Shewel Y, Eshhomi M, Mehanna A. Cadaveric Study of Crista Fenestra: Revisited. J Int Adv Otol. 2021 May;17(3):245–50.
163 Angeli RD, Lavinsky J, Setogutti ET, Lavinsky L. The Crista Fenestra and Its Impact on the Surgical Approach to the Scala Tympani during Cochlear Implantation. Audiol Neurootol. 2017;22(1):50–5.
164 Gopen Q, Rosowski JJ, Merchant SN. Anatomy of the normal human cochlear aqueduct with functional implications. Hear Res. 1997 May;107(1–2):9–22.
165 Kumar R, Singh A, Sagar P, Behera C, Kumar R. Access to Round Window Niche via Posterior Tympanotomy and Impact of Drilling Its Overhangs: A Cadaveric Descriptive Study. Indian J Otolaryngol head neck Surg. 2018 Dec;70(4):510–4.
166 Roland PS, Wright CG, Isaacson B. Cochlear implant electrode insertion: the round window revisited. Laryngoscope. 2007 Aug;117(8):1397–402.
167 Perlman HB. Experimental occlusion of the inferior cochlear vein. Ann Otol Rhinol Laryngol. 1952 Mar;61(1):33–44.
168 Spiegel JL, Polterauer D, Hempel JM, Canis M, Spiro JE, Müller J. Variation of the cochlear anatomy and cochlea duct length: analysis with a new tablet-based software. Eur Arch Oto-Rhino-Laryngology. 2022;279(4):1851–61.
169 Tyler RS, Parkinson AJ, Woodworth GG, Lowder MW, Gantz BJ. Performance over time of adult patients using the Ineraid or nucleus cochlear implant. J Acoust Soc Am. 1997;102(4):2403–11.
170 Bledsoe SC, Nagase S, Miller JM, Altschuler RA. Deafness-induced plasticity in the mature central auditory system. Neuroreport. 1995;7(1):225–229.
171 Kerr A, Schuknecht HF. The spiral ganglion in profound deafness. Acta Otolaryngol. 1968;65(6):586–598.

172 Spoendlin H. Factors inducing retrograde degeneration of the cochlear nerve. Ann Otol Rhinol Laryngol. 1984;112:76–82.
173 Nadol JJ, Young Y, Glynn R. Survival of spiral ganglion cells in profound sensorineural hearing loss: implications for cochlear implantation. Ann Otol Rhinol Laryngol. 1989;98(6):411–6.
174 Zimmermann CE, Burgess BJ, Nadol JB. Patterns of degeneration in the human cochlear nerve. Hear Res. 1995;90(1–2):192–201.
175 Nadol JB. Patterns of neural degeneration in the human cochlea and auditory nerve: Implications for cochlear implantation. Otolaryngol Head Neck Surg. 1997;117(3 Pt 1):220–228.
176 Pfingst BE. Changes over time in thresholds for electrical stimulation of the cochlea. Hear Res. 1990;50(1–2):225–236.
177 Seyyedi M, Eddington DK, Nadol JBJ. Effect of monopolar and bipolar electric stimulation on survival and size of human spiral ganglion cells as studied by postmortem histopathology. Hear Res. 2013 Aug;302:9–16.
178 Wong EC, Lopez IA, Ishiyama A, Ishiyama G. Expression of Brain-Derived Neurotrophic Factor in Human Spiral Ganglia Neurons after Cochlear Implantation. Otol Neurotol. 2024 Mar;45(3):326–33.
179 Scheper V, Paasche G, Miller JM, Warnecke A, Berkingali N, Lenarz T, Stöver T. Effects of delayed treatment with combined GDNF and continuous electrical stimulation on spiral ganglion cell survival in deafened guinea pigs. J Neurosci Res. 2009 May;87(6):1389–99.
180 Leake PA, Hradek GT, Snyder RL. Chronic electrical stimulation by a cochlear implant promotes survival of spiral ganglion neurons after neonatal deafness. J Comp Neurol. 1999 Oct;412(4):543–62.
181 Larsen E, Litvak LM, Liberman MC, Maison SF. Peripheral Neural Plasticity in Cochlear Implant Users Across the Lifespan. JAMA Otolaryngol Head Neck Surg. 2026 Feb;152(2):126–34.
182 Agterberg MJH, Versnel H, de Groot JCMJ, van den Broek M, Klis SFL. Chronic electrical stimulation does not prevent spiral ganglion cell degeneration in deafened guinea pigs. Hear Res. 2010 Oct;269(1–2):169–79.
183 Chen I, Limb CJ, Ryugo DK. The effect of cochlear-implant-mediated electrical stimulation on spiral ganglion cells in congenitally deaf white cats. J Assoc Res Otolaryngol. 2010 Dec;11(4):587–603.
184 Li Q, Lu T, Zhang C, Hansen MR, Li S. Electrical stimulation induces synaptic changes in the peripheral auditory system. J Comp Neurol. 2020 Apr;528(6):893–905.
185 Burghard A, Lenarz T, Scheper V. Inflammatory response after cochlear implantation. Otol Neurotol. 2014;35(3):457–464.
186 Mamelle E, Peineau A, Sterkers O, Ferrary E, Lacour M, Bonfils P. A new sealing technique to reduce inflammation after cochlear implantation. Hear Res. 2017;353(98):106.
187 Scheper V, Hoffmann A, Gepp M, Lenarz T, Durisin M. Drug delivery in cochlear implantation. Adv Drug Deliv Rev. 2017;114:144–154.
188 Wilk M, Biggs N, Wasowski A, Skarzynski H. Drug-eluting electrodes for cochlear implants. Otolaryngol Pol. 2016;70(5):13–19.
189 Kazmitcheff G, Nguyen Y, Miroir M, Péan F, Ferrary E, Cotin S, Sterkers O, Duriez C. Middle-Ear Microsurgery Simulation to Improve New Robotic Procedures. Biomed Res Int. 2014;2014:891742. DOI: 10.1155/2014/891742
190 Nguyen Y, Kazmitcheff G, Péan F, Ferrary E, Sterkers O, Cotin S. Robotic assistance in cochlear implantation. Eur Arch Otorhinolaryngol. 2012;269(5):1321–1325.

191 Bierer JA, Faulkner KF. Identifying cochlear implant channels with poor electrode-neuron interface: Partial tripolar, single-channel thresholds and psychophysical tuning curves. Ear Hear. 2010;31(2):247–258.
192 Goldwyn JH, Bierer SM, Bierer JA. Modeling the electrode–neuron interface of cochlear implants: Effects of neural health, distance, and orientation. Hear Res. 2010;268(1–2):93–104.
193 Prado-Guitierrez P, Fewster LM, Heasman JM, McKay CM, Shepherd RK. Effect of interphase gap and pulse duration on electrically evoked potentials is correlated with auditory nerve survival. Hear Res. 2006 May;215(1–2):47–55.
194 Ramekers D, Versnel H, Strahl SB, Smeets EM, Klis SF, Grolman W. Auditory nerve responses to varied interphase gap and phase duration: Spatiotemporal correlations and implications for cochlear implants. Hear Res. 2014;317:1–12.
195 Ching TY, Dillon H, Byrne D. Speech recognition of hearing-impaired listeners: predictions from audibility and the limited role of high-frequency amplification. J Acoust Soc Am. 1998 Feb;103(2):1128–40.
196 Hogan CA, Turner CW. High-frequency audibility: benefits for hearing-impaired listeners. J Acoust Soc Am. 1998;104:432–441.
197 Gantz BJ, Turner C, Gfeller KE, Lowder MW. Conservation of low-frequency hearing in cochlear implantation. Acta Otolaryngol. 2004;124(3):272–80.
198 Von lberg C, Keifer J, Tillein J, Pfenningdorff T, Hartmann R, Stürzebecher E. Electric-acoustic stimulation of the auditory system. New technology for severe hearing loss. ORL J Otorhinolaryngol Relat Spec. 1999;61:334–340.
199 James C, Albegger K, Battmer R, Burdo S, Deggouj N, Deguine O. Preservation of residual hearing with cochlear implantation: how and why. Acta Otolaryngol. 2005;125:481–491.
200 Büchner A, Schüssler M, Battmer RD, Stöver T, Lesinski-Schiedat A, Lenarz T. Impact of low-frequency hearing. Audiol Neurootol. 2009;1:8–13.
201 Gantz BJ, Hansen MR, Turner CW, Oleson JJ, Reiss LA, Parkinson AJ. Hybrid 10 clinical trial: preliminary results. Audiol Neurootol. 2009;14(Suppl 1):32–8.
202 Dorman MF, Gifford RH, Spahr AJ, McKarns SA. The benefits of combining acoustic and electric stimulation for the recognition of speech, voice and melodies. Audiol Neurootol. 2008;13:105–12.
203 Helms J, Müller J, Schön F, Moser L, Arnold W, Janssen T. Evaluation of performance with the COMBI40 cochlear implant in adults: a multicentric clinical study. ORL J Otorhinolaryngol Relat Spec. 1997;59:23–35.
204 Potts LG, Skinner MW, Litovsky RA, Strube MJ, Kuk F. Recognition and localization of speech by adult cochlear implant recipients wearing a digital hearing aid in the nonimplanted ear (bimodal hearing. J Am Acad Audiol. 2009;20:353–373.
205 Ching TY, Incerti P, Hill M. Binaural benefits for adults who use hearing aids and cochlear implants in opposite ears. Ear Hear. 2004;25:9–21.
206 Cullen RD, Higgins C, Buss E, Clark M, Pillsbury HC, Buchman CA. Cochlear implantation in patients with substantial residual hearing. Laryngoscope. 2004;114:2218–2223.
207 Adunka OF, Buss E, Clark MS, Pillsbury HC, Buchman CA. Effect of preoperative residual hearing on speech perception after cochlear implantation. Laryngoscope. 2008;118:2044–2049.
208 Gomaa NA, Rubinstein JT, Lowder MW, Tyler RS, Gantz BJ. Residual speech recognition and cochlear implant performance in postlingually deaf adults. Audiol Neurootol. 2003;8:234–41.
209 Rubinstein JT, Parkinson WS, Tyler RS, Gantz BJ. Residual speech recognition and

cochlear implant performance: effects of implantation criteria. Am J Otol. 1999;20(445):52.
210 Tyler RS, Parkinson AJ, Wilson BS, Witt S, Preece JP, Noble W. Patients utilizing a hearing aid and a cochlear implant: speech perception and localization. Ear Hear. 2002;23:98–105.
211 Van Dijk J, Van Olphen A, Langereis M, Mens L, Brokx JP, Smoorenburg G. Predictors of cochlear implant performance. Audiology. 1999;38:109–16.
212 Boggess WJ, Baker JE, Balkany TJ. Loss of residual hearing after cochlear implantation. Laryngoscope. 1989 Oct;99(10 Pt 1):1002–5.
213 Gantz B, Turner C. Combining acoustic and electrical speech processing: Iowa/Nucleus hybrid implant. Acta Otolaryngol. 2004;124(4):344–7.
214 Gantz BJ, Hansen M, Dunn CC. Clinical perspective on hearing preservation in cochlear implantation, the University of Iowa experience. Hear Res. 2022 Dec;426:108487.
215 Boisvert I, Reis M, Au A. Cochlear implantation outcomes in adults: A scoping review. PLoS One. 2020;15:e023242.
216 Dunn CC, Perreau A, Gantz B, Tyler RS. Benefits of localization and speech perception with multiple noise sources in listeners with a short-electrode cochlear implant. J Am Acad Audiol. 2010 Jan;21(1):44–51.
217 Gantz BJ, Turner C, Gfeller KE, Lowder MW. Cochlear implantation with hearing preservation yields significant benefit for speech recognition in complex listening environments. Ear Hear. 2013;34(4):413–25.
218 Gfeller KE, Oleszewski C, Turner C, Gantz B, Oleson J. Music perception with cochlear implants and residual hearing. Audiol Neurootol. 2006;1:12–5.
219 Rahman MT, Chari DA, Ishiyama G, Lopez I, Quesnel AM, Ishiyama A, Nadol JB, Hansen MR. Cochlear implants: Causes, effects and mitigation strategies for the foreign body response and inflammation. Hear Res. 2022 Sep;422:108536.
220 Scheperle RA, Tejani VD, Omtvedt JK, Brown CJ, Abbas PJ, Hansen MR, Gantz BJ, Oleson JJ, V Ozanne M. Delayed changes in auditory status in cochlear implant users with preserved acoustic hearing. Hear Res. 2017 Jul;350:45–57.
221 Tejani VD, Yang H, Kim J-S, Hernandez H, Oleson JJ, Hansen MR, Gantz BJ, Abbas PJ, Brown CJ. Access and Polarization Electrode Impedance Changes in Electric-Acoustic Stimulation Cochlear Implant Users with Delayed Loss of Acoustic Hearing. J Assoc Res Otolaryngol. 2022 Feb;23(1):95–118.
222 Tarabichi O, Jensen M, Hansen MR. Advances in hearing preservation in cochlear implant surgery. Curr Opin Otolaryngol Head Neck Surg. 2021;29:385–90.
223 Kashani RG, Henslee A, Nelson RF, Hansen MR. Robotic assistance during cochlear implantation: the rationale for consistent, controlled speed of electrode array insertion. Front Neurol. 2024;15:1335994.
224 Rajan GP, Kontorinis G, Kuthubutheen J. The Effects of Insertion Speed on Inner Ear Function during Cochlear Implantation: A Comparison Study. Audiol Neurotol. 2012;18(1):17–22.
225 Banakis Hartl RM, Kaufmann C, Hansen MR, Tollin DJ. Intracochlear Pressure Transients During Cochlear Implant Electrode Insertion: Effect of Micro-mechanical Control on Limiting Pressure Trauma. Otol Neurotol. 2019 Jul;40(6):736–44.
226 Kawano A, Seldon H, Clark G. Computer-aided three-dimensional reconstruction in human cochlear maps: measurement of the lengths of organ of Corti, outer wall, inner wall, and Rosenthal's canal. Ann Otol Rhinol Laryngol. 1996;105(9):701–9.
227 Snels C, IntHout J, Mylanus E, Huinck W, Dhooge I. Hearing Preservation in Cochlear Implant Surgery: A Meta-Analysis. Otol & Neurotol. 2019;40(2):145–53.

228 Gawęcki W, Balcerowiak A, Podlawska P, Borowska P, Gibasiewicz R, Szyfter W, Wierzbicka M. Robot-Assisted Electrode Insertion in Cochlear Implantation Controlled by Intraoperative Electrocochleography-A Pilot Study. J Clin Med. 2022 Nov;11(23). DOI: 10.3390/jcm11237045
229 Spitzer ER, Hughes ML. Effect of Stimulus Polarity on Physiological Spread of Excitation in Cochlear Implants. J Am Acad Audiol. 2017 Oct;28(9):786–98.
230 Miroir M, Nguyen Y, Szewczyk J, Sterkers O, Bozorg Grayeli A. Design, kinematic optimization, and evaluation of a teleoperated system for middle ear microsurgery. ScientificWorldJournal. 2012;2012:907372.
231 Weber S, Gavaghan K, Wimmer W, Williamson T, Gerber N, Anso J, Bell B, Feldmann A, Rathgeb C, Matulic M, Stebinger M, Schneider D, Mantokoudis G, Scheidegger O, Wagner F, Kompis M, Caversaccio M. Instrument flight to the inner ear. Sci Robot. 2017 Mar;2(4). DOI: 10.1126/scirobotics.aal4916
232 Busby PA, Plant KL, Whitford LA. Electrode impedance in adults and children using the Nucleus 24 cochlear implant system. Cochlear Implants Int. 2002;3(2):87–103.
233 Wilk M, Hessler R, Mugridge K, Jolly C, Fehr M, Lenarz T, Scheper V. Impedance Changes and Fibrous Tissue Growth after Cochlear Implantation Are Correlated and Can Be Reduced Using a Dexamethasone Eluting Electrode. PLoS One. 2016 Feb;11(2):e0147552–e0147552.
234 Majdani O, Schurzig D, Hussong A, Rau T, Wittkopf J, Lenarz T, Labadie RF. Force measurement of insertion of cochlear implant electrode arrays in vitro: comparison of surgeon to automated insertion tool. Acta Otolaryngol. 2010;130(1):31–6.
235 Hussong A, Rau TS, Ortmaier T, Heimann B, Lenarz T, Majdani O. An automated insertion tool for cochlear implants: another step towards atraumatic cochlear implant surgery. Int J Comput Assist Radiol Surg. 2010 Mar;5(2):163–71.
236 Kratchman LB, Blachon GS, Withrow TJ, Balachandran R, Labadie RF, Webster RJ 3rd. Design of a bone-attached parallel robot for percutaneous cochlear implantation. IEEE Trans Biomed Eng. 2011 Oct;58(10):2904–10.
237 Vittoria S, Lahlou G, Torres R, Daoudi H, Mosnier I, Mazalaigue S, Ferrary E, Nguyen Y, Sterkers O. Robot-based assistance in middle ear surgery and cochlear implantation: first clinical report. Eur Arch oto-rhino-laryngology. 2021 Jan;278(1):77–85.
238 Barriat S, Peigneux N, Duran U, Camby S, Lefebvre PP. The Use of a Robot to Insert an Electrode Array of Cochlear Implants in the Cochlea: A Feasibility Study and Preliminary Results. Audiol Neurotol. 2021;26(5):361–7.
239 Klopp-Dutote N, Lefranc M, Strunski V, Page C. Minimally invasive fully ROBOT-assisted cochlear implantation in humans: Preliminary results in five consecutive patients. Clin Otolaryngol. 2021;46(6):1326–1330.
240 Caversaccio M, Gavaghan K, Wimmer W, Williamson T, Ansò J, Mantokoudis G, Gerber N, Rathgeb C, Feldmann A, Wagner F, Scheidegger O, Kompis M, Weisstanner C, Zoka-Assadi M, Roesler K, Anschuetz L, Huth M, Weber S. Robotic cochlear implantation: surgical procedure and first clinical experience. Acta Otolaryngol. 2017 Apr;137(4):447–54.
241 Caversaccio M, Wimmer W, Anso J, Mantokoudis G, Gerber N, Rathgeb C, Schneider D, Hermann J, Wagner F, Scheidegger O, Huth M, Anschuetz L, Kompis M, Williamson T, Bell B, Gavaghan K, Weber S. Robotic middle ear access for cochlear implantation: First in man. PLoS One. 2019;14(8):e0220543.
242 Torres R, Daoudi H, Lahlou G, Sterkers O, Ferrary E, Mosnier I, Nguyen Y. Restoration of High Frequency Auditory Perception After Robot-Assisted or Manual Cochlear Implantation in Profoundly Deaf Adults Improves Speech Recognition. Front Surg. 2021;8:729736.

243 Jia H, Pan J, Gu W, Tan H, Chen Y, Zhang Z, Jiang M, Li Y, Sterkers O, Wu H. Robot-Assisted Electrode Array Insertion Becomes Available in Pediatric Cochlear Implant Recipients: First Report and an Intra-Individual Study. Front Surg. 2021 Jul;8:695728.
244 Kontorinis G, Lenarz T, Stöver T, Paasche G. Impact of the Insertion Speed of Cochlear Implant Electrodes on the Insertion Forces. Otol & Neurotol. 2011;32(4):565–70.
245 Torres R, Drouillard M, De Seta D, Bensimon J-L, Ferrary E, Sterkers O, Bernardeschi D, Nguyen Y. Cochlear Implant Insertion Axis Into the Basal Turn: A Critical Factor in Electrode Array Translocation. Otol Neurotol. 2018 Feb;39(2):168–76.
246 Torres R, Kazmitcheff G, Bernardeschi D, De Seta D, Bensimon JL, Ferrary E, Sterkers O, Nguyen Y. Variability of the mental representation of the cochlear anatomy during cochlear implantation. Eur Arch oto-rhino-laryngology. 2016 Aug;273(8):2009–18.
247 Torres R, Kazmitcheff G, De Seta D, Ferrary E, Sterkers O, Nguyen Y. Improvement of the insertion axis for cochlear implantation with a robot-based system. Eur Arch oto-rhino-laryngology. 2017 Feb;274(2):715–21.
248 Bennion DM, Horne R, Peel A, Reineke P, Henslee A, Kaufmann C, Guymon CA, Hansen MR. Zwitterionic Photografted Coatings of Cochlear Implant Biomaterials Reduce Friction and Insertion Forces. Otol Neurotol. 2021 Dec;42(10):1476–83.
249 Lim YS, Park S-I, Kim YH, Oh SH, Kim SJ. Three-dimensional analysis of electrode behavior in a human cochlear model. Med Eng Phys. 2005 Oct;27(8):695–703.
250 Dohr D, Wulf K, Grabow N, Mlynski R, Schraven SP. A PLLA Coating Does Not Affect the Insertion Pressure or Frictional Behavior of a CI Electrode Array at Higher Insertion Speeds. Mater (Basel, Switzerland). 2022 Apr;15(9). DOI: 10.3390/ma15093049
251 Miroir M, Nguyen Y, Kazmitcheff G, Ferrary E, Sterkers O, Grayeli AB. Friction force measurement during cochlear implant insertion: application to a force-controlled insertion tool design. Otol Neurotol. 2012 Aug;33(6):1092–100.
252 Greene NT, Mattingly JK, Banakis Hartl RM, Tollin DJ, Cass SP. Intracochlear Pressure Transients During Cochlear Implant Electrode Insertion. Otol Neurotol. 2016 Dec;37(10):1541–8.
253 Banakis Hartl RM, Greene NT. Measurement and Mitigation of Intracochlear Pressure Transients During Cochlear Implant Electrode Insertion. Otol Neurotol. 2022 Feb;43(2):174–82.
254 Todt I, Mittmann P, Ernst A. Intracochlear fluid pressure changes related to the insertional speed of a CI electrode. Biomed Res Int. 2014;2014:507241.
255 Snels C, Roland JTJ, Treaba C, Jethanamest D, Huinck W, Friedmann DR, Dhooge I, Mylanus E. Force and pressure measurements in temporal bones. Am J Otolaryngol. 2021;42(2):102859.
256 Todt I, Ernst A, Mittmann P. Effects of Different Insertion Techniques of a Cochlear Implant Electrode on the Intracochlear Pressure. Audiol Neurootol. 2016;21(1):30–7.
257 Zagabathuni A, Padi KK, Kameswaran M, Subramani K. Development of Automated Tool for Electrode Array Insertion and its Study on Intracochlear Pressure. Laryngoscope. 2024 Mar;134(3):1388–95.
258 De Seta D, Torres R, Russo FY, Ferrary E, Kazmitcheff G, Heymann D, Amiaud J, Sterkers O, Bernardeschi D, Nguyen Y. Damage to inner ear structure during cochlear implantation: Correlation between insertion force and radio-histological findings in temporal bone specimens. Hear Res. 2017 Feb;344:90–7.
259 Mirsalehi M, Rau TS, Harbach L, Hügl S, Mohebbi S, Lenarz T, Majdani O. Insertion

forces and intracochlear trauma in temporal bone specimens implanted with a straight atraumatic electrode array. Eur Arch oto-rhino-laryngology. 2017 May;274(5):2131–40.
260 Kaufmann CR, Henslee AM, Claussen A, Hansen MR. Evaluation of Insertion Forces and Cochlea Trauma Following Robotics-Assisted Cochlear Implant Electrode Array Insertion. Otol Neurotol. 2020 Jun;41(5):631–8.
261 Clark JR, Warren FM, Abbott JJ. A Scalable Model for Human Scala-Tympani Phantoms. J Med Device. 2011 Mar;5(1). DOI: 10.1115/1.4002932
262 Bottcher-Rebmann G, Schell V, Budde L, Zuniga MG, Baier C, Lenarz T, Rau TS. A Tool to Enable Intraoperative Insertion Force Measurements for Cochlear Implant Surgery. IEEE Trans Biomed Eng. 2023 May;70(5):1643–50.
263 Nguyen Y, Kazmitcheff G, De Seta D, Miroir M, Ferrary E, Sterkers O. Definition of metrics to evaluate cochlear array insertion forces performed with forceps, insertion tool, or motorized tool in temporal bone specimens. Biomed Res Int. 2014;2014:532570.
264 Rau TS, Böttcher-Rebmann G, Schell V, Cramer J, Artukarslan E, Baier C, Lenarz T, Salcher R. First clinical implementation of insertion force measurement in cochlear implantation surgery. Front Neurol. 2024;15:1400455.
265 Bas E, Dinh CT, Garnham C, Polak M, Van de Water TR. Conservation of hearing and protection of hair cells in cochlear implant patients' with residual hearing. Anat Rec (Hoboken). 2012 Nov;295(11):1909–27.
266 Dinh CT, Goncalves S, Bas E, Van De Water TR, Zine A. Molecular regulation of auditory hair cell death and approaches to protect sensory receptor cells and/or stimulate repair following acoustic trauma. Front Cell Neurosci. 2015;9:96.
267 Yamane H, Nakai Y, Takayama M, Konishi K, Iguchi H, Nakagawa T, Shibata S, Kato A, Sunami K, Kawakatsu C. The emergence of free radicals after acoustic trauma and strial blood flow. Acta Otolaryngol Suppl. 1995;519:87–92.
268 Quesnel AM, Nakajima HH, Rosowski JJ, Hansen MR, Gantz BJ, Nadol JBJ. Delayed loss of hearing after hearing preservation cochlear implantation: Human temporal bone pathology and implications for etiology. Hear Res. 2016 Mar;333:225–34.
269 Kesler K, Dillon NP, Fichera L, Labadie RF. Human Kinematics of Cochlear Implant Surgery: An Investigation of Insertion Micro-Motions and Speed Limitations. Otolaryngol neck Surg. 2017 Sep;157(3):493–8.
270 Claussen AD, Shibata SB, Kaufmann CR, Henslee A, Hansen MR. Comparative Analysis of Robotics-Assisted and Manual Insertions of Cochlear Implant Electrode Arrays. Otol Neurotol. 2022 Dec;43(10):1155–61.
271 Avci E, Nauwelaers T, Hamacher V, Kral A. Three-Dimensional Force Profile During Cochlear Implantation Depends on Individual Geometry and Insertion Trauma. Ear Hear. 2017;38(3):e168–79.
272 Dhanasingh A, Swords C, Bance M, Van Rompaey V, Van de Heyning P. Cochlear Size Assessment Predicts Scala Tympani Volume and Electrode Insertion Force-Implications in Robotic Assisted Cochlear Implant Surgery. Front Surg. 2021;8:723897.
273 Hrncirik F, Roberts I, Sevgili I, Swords C, Bance M. Models of Cochlea Used in Cochlear Implant Research: A Review. Ann Biomed Eng. 2023 Jul;51(7):1390–407.
274 Nguyen Y, Bernardeschi D, Kazmitcheff G, Miroir M, Vauchel T, Ferrary E, Sterkers O. Effect of embedded dexamethasone in cochlear implant array on insertion forces in an artificial model of scala tympani. Otol Neurotol. 2015 Feb;36(2):354–8.
275 Sheffield SW, Jahn K, Gifford RH. Preserved acoustic hearing in cochlear implantation improves speech perception. J Am Acad Audiol. 2015 Feb;26(2):145–54.

276 Talbot KN, Hartley DEH. Combined electro-acoustic stimulation: a beneficial union? Clin Otolaryngol. 2008 Dec;33(6):536–45.
277 Gstoettner WK, van de Heyning P, O'Connor AF, Morera C, Sainz M, Vermeire K, Mcdonald S, Cavallé L, Helbig S, Valdecasas JG, Anderson I, Adunka OF. Electric acoustic stimulation of the auditory system: results of a multi-centre investigation. Acta Otolaryngol. 2008 Sep;128(9):968–75.
278 Incerti P V, Ching TYC, Cowan R. A systematic review of electric-acoustic stimulation: device fitting ranges, outcomes, and clinical fitting practices. Trends Amplif. 2013 Mar;17(1):3–26.
279 Dorman MF, Gifford RH. Speech Understanding in Complex Listening Environments by Listeners Fit With Cochlear Implants. J Speech Lang Hear Res. 2017 Oct;60(10):3019–26.
280 Gfeller K, Jiang D, Oleson JJ, Driscoll V, Olszewski C, Knutson JF, Turner C, Gantz B. The effects of musical and linguistic components in recognition of real-world musical excerpts by cochlear implant recipients and normal-hearing adults. J Music Ther. 2012;49(1):68–101.
281 Roland PS, Wright CG. Surgical aspects of cochlear implantation: mechanisms of insertional trauma. Adv Otorhinolaryngol. 2006;64:11–30.
282 Kawano A, Seldon HL, Clark GM, Ramsden RT, Raine CH. Intracochlear factors contributing to psychophysical percepts following cochlear implantation. Acta Otolaryngol. 1998 Jun;118(3):313–26.
283 Sili KN, Satar B, Serdar MA. Meta-Analysis of Robotic Cochlear Implantation. Laryngoscope. 2026 Jan;136(1):76–90.
284 Chen JM, Lin VYW, Le TN, Spiegel JL, Ungar OJ, Bajin MD, Ladak HM, Agrawal S. Synchrotron-Based Trauma Assessment of Robotic Electrode Insertions in Cochlear Implantation. Laryngoscope. 2025 Oct;135(10):3867–76.
285 Frijns JHM, Briaire JJ, de Laat JAPM, Grote JJ. Initial evaluation of the Clarion CII cochlear implant: speech perception and neural response imaging. Ear Hear. 2002 Jun;23(3):184–97.
286 Van de Heyning P, Roland P, Lassaletta L, Agrawal S, Atlas M, Baumgartner W-D, Brown K, Caversaccio M, Dazert S, Gstoettner W, Hagen R, Hagr A, Jablonski GE, Kameswaran M, Kuzovkov V, Leinung M, Li Y, Loth A, Magele A, Mlynski R, Mueller J, Parnes L, Radeloff A, Raine C, Rajan G, Schmutzhard J, Skarzynski H, Skarzynski PH, Sprinzl G, Staecker H, Stöver T, Tavora-Viera D, Topsakal V, Usami S-I, Van Rompaey V, Weiss NM, Wimmer W, Zernotti M, Gavilan J. Suitable Electrode Choice for Robotic-Assisted Cochlear Implant Surgery: A Systematic Literature Review of Manual Electrode Insertion Adverse Events. Front Surg. 2022;9:823219.
287 Sabban D, Parodi M, Blanchard M, Ettienne V, Rouillon I, Loundon N. Intra-cochlear electrode tip fold-over. Cochlear Implants Int. 2018 Jul;19(4):225–9.
288 Gomez Serrano M, Patel S, Harris R, Selvadurai D. Initial surgical and clinical experience with the Nucleus CI532 slim modiolar electrode in the UK. Cochlear Implants Int. 2019 Jul;20(4):207–16.
289 Zuniga MG, Rivas A, Hedley-Williams A, Gifford RH, Dwyer R, Dawant BM, Sunderhaus LW, Hovis KL, Wanna GB, Noble JH, Labadie RF. Tip Fold-over in Cochlear Implantation: Case Series. Otol Neurotol. 2017 Feb;38(2):199–206.
290 Garaycochea O, Manrique-Huarte R, Manrique M. Intra-operative radiological diagnosis of a tip roll-over electrode array displacement using fluoroscopy, when electrophysiological testing is normal: the importance of both techniques in cochlear implant surgery. Braz J Otorhinolaryngol. 2020 Dec;86 Suppl 1(Suppl 1):38–40.

291 Jwair S, Prins A, Wegner I, Stokroos RJ, Versnel H, Thomeer HGXM. Scalar Translocation Comparison Between Lateral Wall and Perimodiolar Cochlear Implant Arrays - A Meta-Analysis. Laryngoscope. 2021 Jun;131(6):1358–68.
292 O'Connell BP, Cakir A, Hunter JB, Francis DO, Noble JH, Labadie RF, Zuniga G, Dawant BM, Rivas A, Wanna GB. Electrode Location and Angular Insertion Depth Are Predictors of Audiologic Outcomes in Cochlear Implantation. Otol Neurotol. 2016 Sep;37(8):1016–23.
293 O'Connell BP, Hunter JB, Wanna GB. The importance of electrode location in cochlear implantation. Laryngoscope Investig Otolaryngol. 2016 Dec;1(6):169–74.
294 Dhanasingh A, Jolly C. Review on cochlear implant electrode array tip fold-over and scalar deviation. J Otol. 2019;14(3):94–100.
295 Drouillard M, Torres R, Mamelle E, De Seta D, Sterkers O, Ferrary E, Nguyen Y. Influence of electrode array stiffness and diameter on hearing in cochlear implanted guinea pig. PLoS One. 2017 Aug;12(8):e0183674–e0183674.
296 Bourn S, Goldstein MR, Jacob A. Hearing Preservation in Elderly Cochlear Implant Recipients. Otol Neurotol. 2020 Jun;41(5):618–24.
297 Helbig S, Adel Y, Rader T, Stöver T, Baumann U. Long-term Hearing Preservation Outcomes After Cochlear Implantation for Electric-Acoustic Stimulation. Otol Neurotol. 2016 Oct;37(9):e353-9.
298 Fischer N, Pinggera L, Weichbold V, Dejaco D, Schmutzhard J, Widmann G. Radiologic and functional evaluation of electrode dislocation from the scala tympani to the scala vestibuli in patients with cochlear implants. AJNR Am J Neuroradiol. 2015 Feb;36(2):372–7.
299 Rajan G, Tavora-Vieira D, Baumgartner W-D, Godey B, Müller J, O'Driscoll M, Skarzynski H, Skarzynski P, Usami S-I, Adunka O, Agrawal S, Bruce I, De Bodt M, Caversaccio M, Pilsbury H, Gavilán J, Hagen R, Hagr A, Kameswaran M, Karltorp E, Kompis M, Kuzovkov V, Lassaletta L, Yongxin L, Lorens A, Manoj M, Martin J, Mertens G, Mlynski R, Parnes L, Pulibalathingal S, Radeloff A, Raine CH, Rajeswaran R, Schmutzhard J, Sprinzl G, Staecker H, Stephan K, Sugarova S, Zernotti M, Zorowka P, Van de Heyning P. Hearing preservation cochlear implantation in children: The HEARRING Group consensus and practice guide. Cochlear Implants Int. 2018 Jan;19(1):1–13.
300 Ishiyama A, Doherty J, Ishiyama G, Quesnel AM, Lopez I, Linthicum FH. Post Hybrid Cochlear Implant Hearing Loss and Endolymphatic Hydrops. Otol Neurotol. 2016 Dec;37(10):1516–21.
301 Mueller F, Hermann J, Weber S, O'Toole Bom Braga G, Topsakal V. Image-Based Planning of Minimally Traumatic Inner Ear Access for Robotic Cochlear Implantation. Front Surg. 2021;8:761217.
302 Dietz A, Wennström M, Lehtimäki A, Löppönen H, Valtonen H. Electrode migration after cochlear implant surgery: more common than expected? Eur Arch oto-rhino-laryngology. 2016 Jun;273(6):1411–8.
303 Mittmann P, Rademacher G, Mutze S, Ernst A, Todt I. Electrode Migration in Patients with Perimodiolar Cochlear Implant Electrodes. Audiol Neurootol. 2015;20(6):349–53.
304 Loth AG, Adel Y, Weiß R, Helbig S, Stöver T, Leinung M. Evaluation of a bone groove geometry for fixation of a cochlear implant electrode. Eur Arch oto-rhino-laryngology. 2020 Feb;277(2):385–92.
305 MED-EL. FLEX electrode arrays - products information [Internet]. [cited 2021 Oct 31]. Available from: https://medel.webgate.media/en/directlink/1c9497505fe490ba/133240
306 Gantz JA, Gantz BJ, Kaufmann CR, Henslee AM, Dunn CC, Hua X, Hansen MR. A

Steadier Hand: The First Human Clinical Trial of a Single-Use Robotic-Assisted Surgical Device for Cochlear Implant Electrode Array Insertion. Otol Neurotol. 2023 Jan;44(1):34–9.
307 Nguyen S, Cloutier F, Philippon D, Côté M, Bussières R, Backous DD. Outcomes review of modern hearing preservation technique in cochlear implant. Auris Nasus Larynx. 2016;43(5):485–8.
308 Santa Maria PL, Gluth MB, Yuan Y, Atlas MD, Blevins NH. Hearing Preservation Surgery for Cochlear Implantation. Otol & Neurotol. 2014;35(10):e256–69.
309 Hallin K, Larsson U, Schart-Morén N. Do different types of cochlear implant electrode influence hearing preservation and speech perception? Acta Otolaryngol. 2024 Oct;144(10):552–7.
310 Causon A, Verschuur C, Newman TA. A Retrospective Analysis of the Contribution of Reported Factors in Cochlear Implantation on Hearing Preservation Outcomes. Otol & Neurotol. 2015;36(7):1137–45.
311 Khan MMR, Labadie RF, Noble JH. Preoperative prediction of angular insertion depth of lateral wall cochlear implant electrode arrays. J Med Imaging (Bellingham. 2020;7(3).
312 Suhling M-C, Majdani O, Salcher R, Leifholz M, Büchner A, Lesinski-Schiedat A, Lenarz T. The Impact of Electrode Array Length on Hearing Preservation in Cochlear Implantation. Otol Neurotol. 2016 Sep;37(8):1006–15.
313 Gersdorff G, Peigneux N, Duran U, Camby S, Lefebvre PP. Impedance and Functional Outcomes in Robotic-Assisted or Manual Cochlear Implantation: A Comparative Study. Audiol Neurotol. 2025;30(1):80–88.
314 Foggia MJ, Quevedo RV, Hansen MR. Intracochlear fibrosis and the foreign body response to cochlear implant biomaterials. Laryngoscope Investig Otolaryngol. 2019 Nov;4(6):678–83.
315 Choi C-H, Oghalai JS. Predicting the effect of post-implant cochlear fibrosis on residual hearing. Hear Res. 2005 Jul;205(1–2):193–200.
316 Jia H, Venail F, Piron J-P, Batrel C, Pelliccia P, Artières F, Uziel A, Mondain M. Effect of Surgical Technique on Electrode Impedance after Cochlear Implantation. Ann Otol Rhinol & Laryngol. 2011;120(8):529–34.
317 Neuburger J, Lenarz T, Lesinski-Schiedat A, Büchner A. Spontaneous increases in impedance following cochlear implantation: suspected causes and management. Int J Audiol. 2009 May;48(5):233–9.
318 Newbold C, Mergen S, Richardson R, Seligman P, Millard R, Cowan R, Shepherd R. Impedance changes in chronically implanted and stimulated cochlear implant electrodes. Cochlear Implants Int. 2014 Jul;15(4):191–9.
319 Spitzer JB, Cellum IP, Bosworth C. Stability of Audiometric Measures and Challenges in Long-Term Management of the Elderly Cochlear Implant Patient. Otol Neurotol. 2013 Dec;34(9):1636–41.
320 Pisa JFD, Almutairi WH, Mackie K, Stangherlin D, Sulkers J, Hochman JB. Impedance Change as an Indicator of Cochlear Implant Failure. Otol Neurotol. 2023 Apr;44(4):e211–5.
321 Canfarotta MW, Dillon MT, Buss E, Pillsbury HC, O'Connell BP. Frequency- to-place mismatch: Characterizing variability and impact on speech recognition outcomes in cochlear implant recipients. Ear Hear. 2020;41(6):1340–1351.
322 Breitsprecher TM, Baumgartner W-D, Brown K, Dazert S, Doyle U, Dhanasingh A, Großmann W, Hagen R, Van de Heyning P, Mlynski R, Neudert M, Rajan G, Rak K, Van Rompaey V, Schmutzhard J, Volkenstein S, Völter C, Wimmer W, Zernotti M, Weiss NM. Effect of Cochlear Implant Electrode Insertion Depth on Speech Perception

Outcomes: A Systematic Review. Otol Neurotol open. 2023 Dec;3(4):e045.
323 Holden LK, Firszt JB, Reeder RM, Uchanski RM, Dwyer NY, Holden TA. Cochlear Implants in Adults: Effects of Age and Duration of Deafness on Speech Recognition. Otol Neurotol. 2016 Oct;37(9):1238–45.
324 Jin S-H, Liu C, Sladen DP. The effects of aging on speech perception in noise: comparison between normal-hearing and cochlear-implant listeners. J Am Acad Audiol. 2014;25(7):656–65.
325 Schvartz-Leyzac KC, Colesa DJ, Buswinka CJ, Rabah AM, Swiderski DL, Raphael Y, Pfingst BE. How electrically evoked compound action potentials in chronically implanted guinea pigs relate to auditory nerve health and electrode impedance. J Acoust Soc Am. 2020 Dec;148(6):3900.
326 Shearer AE, Hansen MR. Auditory synaptopathy, auditory neuropathy, and cochlear implantation. Laryngoscope Investig Otolaryngol. 2019 Aug;4(4):429–40.
327 Goudey B, Plant K, Kiral I, Jimeno-Yepes A, Swan A, Gambhir M, Büchner A, Kludt E, Eikelboom RH, Sucher C, Gifford RH, Rottier R, Anjomshoa H. A MultiCenter Analysis of Factors Associated with Hearing Outcome for 2,735 Adults with Cochlear Implants. Trends Hear. 2021;25:23312165211037524.
328 Bartholomew RA, Hoffman SE, Juliano AF, Wu P-Z, Zhao Y, de Gruttola V, Liberman MC, Maison SF. On the Difficulty Predicting Word Recognition Performance After Cochlear Implantation. Otol Neurotol. 2024 Jun;45(5):e393–9.
329 Tropitzsch A, Schade-Mann T, Gamerdinger P, Dofek S, Schulte B, Schulze M, Fehr S, Biskup S, Haack TB, Stöbe P, Heyd A, Harre J, Lesinski-Schiedat A, Büchner A, Lenarz T, Warnecke A, Müller M, Vona B, Dahlhoff E, Löwenheim H, Holderried M. Variability in Cochlear Implantation Outcomes in a Large German Cohort With a Genetic Etiology of Hearing Loss. Ear Hear. 2023;44(6):1464–84.
330 Harris KC, Ahlstrom JB, Dias JW, Kerouac LB, McClaskey CM, Dubno JR, Eckert MA. Neural Presbyacusis in Humans Inferred from Age-Related Differences in Auditory Nerve Function and Structure. J Neurosci. 2021 Dec;41(50):10293–304.
331 Harris KC, Dias JW, McClaskey CM, Rumschlag J, Prisciandaro J, Dubno JR. Afferent Loss, GABA, and Central Gain in Older Adults: Associations with Speech Recognition in Noise. J Neurosci. 2022 Sep;42(38):7201–12.
332 McClaskey CM, Panganiban CH, Noble K V, Dias JW, Lang H, Harris KC. A multi-metric approach to characterizing mouse peripheral auditory nerve function using the auditory brainstem response. J Neurosci Methods. 2020 Dec;346:108937.
333 Schvartz-Leyzac KC, Giordani B, Pfingst BE. Association of Aging and Cognition With Complex Speech Understanding in Cochlear-Implanted Adults: Use of a Modified National Institutes of Health (NIH) Toolbox Cognitive Assessment. JAMA Otolaryngol Head Neck Surg. 2023 Mar;149(3):239–46.
334 Holder JT, Reynolds SM, Sunderhaus LW, Gifford RH. Current Profile of Adults Presenting for Preoperative Cochlear Implant Evaluation. Trends Hear. 2018;22:2331216518755288.
335 Schvartz-Leyzac KC, Colesa DJ, Buswinka CJ, Swiderski DL, Raphael Y, Pfingst BE. Changes over time in the electrically evoked compound action potential (ECAP) interphase gap (IPG) effect following cochlear implantation in Guinea pigs. Hear Res. 2019 Nov;383:107809.
336 Skidmore J, Ramekers D, Colesa DJ, Schvartz-Leyzac KC, Pfingst BE, He S. A Broadly Applicable Method for Characterizing the Slope of the Electrically Evoked Compound Action Potential Amplitude Growth Function. Ear Hear. 2022;43(1):150–64.
337 Schvartz-Leyzac KC, Pfingst BE. Assessing the Relationship Between the Electrically

Evoked Compound Action Potential and Speech Recognition Abilities in Bilateral Cochlear Implant Recipients. Ear Hear. 2018;39(2):344–58.
338 Seyyedi M, Viana LM, Nadol JBJ. Within-subject comparison of word recognition and spiral ganglion cell count in bilateral cochlear implant recipients. Otol Neurotol. 2014 Sep;35(8):1446–50.
339 Schvartz-Leyzac KC, Colesa DJ, Buswinka CJ, Rabah AM, Swiderski DL, Raphael Y, Pfingst BE. Effects of Electrode Location on Estimates of Neural Health in Humans with Cochlear Implants. J Assoc Res Otolaryngol. 2020 Jun;21(3):259–75.
340 Schvartz-Leyzac K, Pfingst B. Reexamining the effects of electrode location on measures of neural health in cochlear implant users. JASA express Lett. 2023 Jun;3(6). DOI: 10.1121/10.0019806
341 Schvartz-Leyzac KC, McClaskey CM, Dias JW, Pfingst BE, Harris KC. Contributions of Auditory Nerve Density and Synchrony to Speech Understanding in Older Cochlear Implant Users. J Assoc Res Otolaryngol. 2025 Jun;26(3):317–29.
342 Skidmore J, Oleson JJ, Yuan Y, He S. The Relationship Between Cochlear Implant Speech Perception Outcomes and Electrophysiological Measures of the Electrically Evoked Compound Action Potential. Ear Hear. 2023;44(6):1485–97.
343 Dawson P, Fullerton A, Krishnamoorthi H, Plant K, Cowan R, Buczak N, Long C, James CJ, Sismono F, Büchner A. A Prospective, Multicentre Case-Control Trial Examining Factors That Explain Variable Clinical Performance in Post Lingual Adult CI Recipients. Trends Hear. 2025;29:23312165251347136.
344 Walia A, Shew MA, Varghese J, Ioerger P, Lefler SM, Ortmann AJ, Herzog JA, Buchman CA. Improved Cochlear Implant Performance Estimation Using Tonotopic-Based Electrocochleography. JAMA Otolaryngol Head Neck Surg. 2023 Dec;149(12):1120–9.
345 Canfarotta MW, O'Connell BP, Giardina CK, Buss E, Brown KD, Dillon MT, Rooth MA, Pillsbury HC, Buchman CA, Adunka OF, Fitzpatrick DC. Relationship Between Electrocochleography, Angular Insertion Depth, and Cochlear Implant Speech Perception Outcomes. Ear Hear. 2021;42(4):941–8.
346 Walia A, Shew MA, Lefler SM, Ortmann AJ, Durakovic N, Wick CC, Herzog JA, Buchman CA. Factors Affecting Performance in Adults With Cochlear Implants: A Role for Cognition and Residual Cochlear Function. Otol Neurotol. 2023 Dec;44(10):988–96.
347 Walia A, Shew MA, Kallogjeri D, Wick CC, Durakovic N, Lefler SM, Ortmann AJ, Herzog JA, Buchman CA. Electrocochleography and cognition are important predictors of speech perception outcomes in noise for cochlear implant recipients. Sci Rep. 2022 Feb;12(1):3083.
348 Torres R, Hochet B, Daoudi H, Carré F, Mosnier I, Sterkers O, Ferrary E, Nguyen Y. Atraumatic Insertion of a Cochlear Implant Pre-Curved Electrode Array by a Robot-Automated Alignment with the Coiling Direction of the Scala Tympani. Audiol Neurootol. 2022;27(2):148–55.
349 Esquia Medina GN, Borel S, Nguyen Y, Ambert-Dahan E, Ferrary E, Sterkers O, Grayeli AB. Is electrode-modiolus distance a prognostic factor for hearing performances after cochlear implant surgery? Audiol Neurootol. 2013;18(6):406–13.
350 De Seta D, Nguyen Y, Vanier A, Ferrary E, Bebear J-P, Godey B, Robier A, Mondain M, Deguine O, Sterkers O, Mosnier I. Five-Year Hearing Outcomes in Bilateral Simultaneously Cochlear-Implanted Adult Patients. Audiol Neurootol. 2016;21(4):261–7.
351 van der Beek FB, Briaire JJ, Frijns JHM. Population-based prediction of fitting levels for individual cochlear implant recipients. Audiol Neurootol. 2015;20(1):1–16.

352 Jiam NT, Gilbert M, Cooke D, Jiradejvong P, Barrett K, Caldwell M, Limb CJ. Association Between Flat-Panel Computed Tomographic Imaging-Guided Place-Pitch Mapping and Speech and Pitch Perception in Cochlear Implant Users. JAMA Otolaryngol Head Neck Surg. 2019 Feb;145(2):109–16.
353 Jiam NT, Pearl MS, Carver C, Limb CJ. Flat-Panel CT Imaging for Individualized Pitch Mapping in Cochlear Implant Users. Otol Neurotol. 2016 Jul;37(6):672–9.
354 Schatzer R, Vermeire K, Visser D, Krenmayr A, Kals M, Voormolen M, Van de Heyning P, Zierhofer C. Electric-acoustic pitch comparisons in single-sided-deaf cochlear implant users: frequency-place functions and rate pitch. Hear Res. 2014 Mar;309:26–35.
355 Greenwood DD. Critical bandwidth and the frequency coordinates of the basila membrane. J Acoust Soc Am. 1961;33(10):13344–1356.
356 Rader T, Döge J, Adel Y, Weissgerber T, Baumann U. Place dependent stimulation rates improve pitch perception in cochlear implantees with single-sided deafness. Hear Res. 2016 Sep;339:94–103.
357 Baskent D, Shannon R. Interactions between cochlear implant electrode insertion depth and frequency-place mapping. J Acoust Soc Am. 2005;117:1405–16.
358 Campbell R, MacSweeney M, Waters D. Sign language and the brain: A review. J Deaf Stud Deaf Educ. 2008;13(1):3–20.
359 Altoè A, Shera CA. The cochlear place code for pitch: Recent advances in psychophysics and modeling. Curr Opin Otolaryngol Head Neck Surg. 2020;28(5):414.
360 Fu Q-J, Shannon R V. Effects of electrode location and spacing on speech recognition with cochlear implants. Audiol Neurootol. 1999;4(6):329–339.
361 Peterson NR, Pisoni DB, Miyamoto RT. Cochlear implants and spoken language processing abilities: Review and assessment of the literature. Restor Neurol Neurosci. 2010;28(2):237–250.
362 Nimmons GL, Kang RS, Drennan WR. Clinical assessment of music perception in cochlear implant listeners. Otol Neurotol. 2008;29:149–55.
363 Schleich P, Nopp P, D'Haese P. Head shadow, squelch, and summation effects in bilateral users of the MED-EL COMBI 40/40+ cochlear implant. Ear Hear. 2004;25(3):197–204.
364 Loizou PC, Hu Y, Litovsky R. Speech recognition by bilateral cochlear implant users in a cocktail-party setting. J Acoust Soc Am. 2009;125(1):372–383.
365 Limb CJ, Roy AT. Technological, biological, and acoustical constraints to music perception in cochlear implant users. Hear Res. 2014;308:13–26.
366 Ambert-Dahan E, Dutray S, Meyer B. Music and cochlear implants. Eur Ann Otorhinolaryngol Head Neck Dis. 2015;132(5):285–290.
367 Heutink F. Angular electrode insertion depth and speech perception in adults with a cochlear implant: a systematic review. Otol Neurotol. 2019;40(7):900–910.
368 Dutrieux N. Correlation between cochlear length, insertion angle, and tonotopic mismatch for MED-EL FLEX28 electrode arrays. Otol Neurotol. 2022;43(1):48–55.
369 Mertens G, Van de Heyning P, Vanderveken O, Topsakal V, Van Rompaey V. The smaller the frequency-to-place mismatch the better the hearing outcomes in cochlear implant recipients? Eur Arch Oto-Rhino-Laryngology. 2022;279(4):1875–83.
370 Canfarotta MW. Influence of age at cochlear implantation and frequency-to-place mismatch on early speech recognition in adults. Otolaryngol Head Neck Surg. 2020;162(6):926–932.
371 Abrahamse R, Beynon A, Piai V. Long-term auditory processing outcomes in early implanted young adults with cochlear implants: the mismatch negativity vs. P300 response. Clin Neurophysiol. 2021;132(1):258–268.

372 Landsberg DM, Svrakic S, Roland JT, Svirsky M. The Relationship between Insertion Angles, Default Frequency Allocations, and Spiral Ganglion Place Pitch in Cochlear Implants. Ear Hear. 2015;36(5):e207–13.
373 Dillon MT. Effectiveness of place-based mapping in electric-acoustic stimulation devices. Otol Neurotol. 2021;42(1):197–202.
374 DeFreese A, Berg K, Noble J, Dawant B, Holder J, Amberg S, Brown C, Burg E, Dwyer N, Sisler-Dinwiddie A, Sparrow T, Sunderhaus L, Yaras S, Bennett M, Jan T, Moberly A, O'Malley M, Patro A, Perkins E, Tawfik K, Haynes D, Gifford R. Frequency-to-Place Mismatch and Cochlear Implant Outcomes by Electrode Type. JAMA Otolaryngol Head Neck Surg. 2025;151(2):135–142. DOI: 10.1001/jamaoto.2024.4158
375 Vaerenberg B, Smits C, Ceulaer G. Cochlear implant programming: a global survey on the state of the art. Sci World J. 2014;2014(501738).
376 Jiam NT, Caldwell MT, Limb CJ. What does music sound like with a cochlear implant? Otol Neurotol. 2016;37(2):124–130.
377 Creff G, Lambert C, Coudert P, Pean V, Laurent S, Godey B. Comparison of tonotopic and default frequency fitting for speech understanding in noise in new cochlear implantees: a prospective, randomized, double-blind, cross-over study. Ear Hear. 2024;45:35–52.
378 El Shennawy A, Abdulghffar A, Ghannoum T, Sheta S. Impact of Frequency Reallocation on Cochlear Implant Outcomes. Acta Otolaryngol. 2026 Mar;1–10.
379 Wangchuk P, Umat C, Chong FY, Zaki FM, Abdullah A. Speech Perception Outcomes with the Anatomy-Based Fitting Map among Experienced, Adult Cochlear Implant Users: A Longitudinal Study. Audiol Neurotol. 2024 Nov;30(3):222–36.
380 Escudé B, James C, Deguine O, Cochard N, Eter E, Fraysse B. The size of the cochlea and predictions of insertion depth angles for cochlear implant electrodes. Audiol Neurotol. 2006;11(SUPPL. 1):27–33.
381 Sridhar D, Brown CJ, Balkany TJ. Cochlear implant electrode array insertion: Anatomic considerations and functional implications. J Am Acad Audiol. 2006;17(6):400–412.
382 Erixon E, Högstorp H, Wadin K, Rask-Andersen H. Variational anatomy of the human cochlea: Implications for cochlear implantation. Otol Neurotol. 2009;30(1):22.
383 Pelliccia P, Venail F, Bonafé A. CT-based measurements of cochlear duct length for cochlear implants: Evaluation of reliability in a multicentric study. Eur Arch Otorhinolaryngol. 2014;271(10):2515–2521.
384 Ketten DR, Skinner MW, Wang G. In vivo measures of cochlear length and insertion depth of Nucleus cochlear implant electrode arrays. Ann Otol Rhinol Laryngol Suppl. 1998;177:1–16.
385 Canfarotta MW, Dillon MT, Buss E. Frequency-to-place mismatch and speech perception in cochlear implant users. Otol Neurotol. 2022;43(1).
386 Buchman CA, Dillon MT, King ER, Adunka MC, Adunka O, Pillsbury HC. Influence of Cochlear Implant Insertion Depth on Performance: A Prospective Randomized Trial. Otol Neurotol. 2014;35(10):1773–9.
387 Connell BPO, Hunter JB, Haynes DS, Jourdan HT, Dedmon MM, Noble JH, Dawant BM, Wanna GB. Insertion depth impacts speech perception and hearing preservation for lateral wall electrodes. Laryngoscope. 2017;127(10):2352–7.
388 Canfarotta MW, Dillon MT, Buss E. Measurement and impact of frequency-to-place mismatch in cochlear implant patients. Ear Hear. 2019;40(3):484.
389 Başkent D, Shannon R V. Speech recognition under conditions of frequency-to- place mismatch in cochlear implant listeners. J Acoust Soc Am. 2004;116(6):3137.

390 Canfarotta MW, Dillon MT, Buss E, Pillsbury HC, O'Connell BP. Effects of frequency-to-place mismatch on early speech recognition performance in cochlear implant users. Ear Hear. 2020;41(3):514–523.
391 Reiss LAJ, Turner CW, Karsten SA, Gantz BJ. Plasticity in human pitch perception induced by tonotopically mismatched electro-acoustic stimulation. Neuroscience. 2007;154(2):431–438.
392 Svirsky MA, Silton-Redhouse N, Fitzgerald MB. Gradual adaptation to frequency-shifted electrical stimulation: A study in cochlear implant users. Hear Res. 2004;199(1–2):98–108.
393 Sagi E, Kaiser AR, Meyer TA, Svirsky MA. Understanding speech with a cochlear implant: Beyond the audiogram. Ear Hear. 2010;31(3):307–310.
394 Reiss LA, Perreau AE, Turner CW, Karsten SA, Gantz BJ. A randomized controlled trial of frequency-mapping techniques for cochlear implant users. Hear Res. 2014;318:91–96.
395 Canfarotta MW. Frequency-to-place mismatch: characterizing variability and the influence on speech perception outcomes in cochlear implant recipients. Ear Hear. 2020;41(5):1349–1361.
396 Canfarotta MW, Dillon MT, Buss E, Pillsbury HC, O'Connell BP. Frequency- to-place mismatch negatively impacts speech recognition in adult cochlear implant users. Otol Neurotol. 2020;41(5).
397 Mertens G, Vlaminck S, Smedts K. Frequency-to-place mismatch affects speech perception in cochlear implant users. Ear Hear. 2021;42(3):701–711.
398 Neves CA. Fully automated measurement of cochlear duct length from clinical temporal bone computed tomography. Laryngoscope. 2022;132(2):449–458.
399 Alshalan A. Cochlear implantation: the variation in cochlear height. Ear Nose Throat J. 2022
400 Greenwood DD. A cochlear frequency-position function for several species— 29 years later. J Acoust Soc Am. 1990;87(6):2592–2605.
401 Jiam NT, Lopez CA, Hatrak M. Real-world speech performance in cochlear implant users with place-based mapping. Otol Neurotol. 2019;40(5).
402 Schuman TA, Noble JH, Wright CG. Anatomic verification of a novel method for estimating the cochlear implant electrode position using CT. Otol Neurotol. 2010;31(8):1251–1256.
403 Noble JH, Labadie RF, Gifford RH, Dawant BM. Image-guidance enables new methods for customizing cochlear implant stimulation strategies. IEEE Trans Neural Syst Rehabil Eng. 2012;20(2):211–219.
404 Jiam NT, Hatrak M, Lopez CA, Limb CJ. Tonotopic vs. default frequency fitting in cochlear implants: A comparison study. Ear Hear. 2019;40(5):1149–1159.
405 Dillon M, Buss E, O'Connell BP. Acclimatization to place-based mapping in cochlear implant users. Ear Hear. 2022;43(2):531–541.
406 Cooperman SP. Influence of electrode to cochlear duct length ratio on post- operative speech understanding outcomes. Cochlear Implant Int. 2022;23(2):59–69.
407 Khurayzi T, Almuhawas F, Sanosi A. Direct measurement of cochlear parameters for automatic calculation of the cochlear duct length. Ann Saudi Med. 2020;40(3):212–218.
408 Di Maro F, Carner M, Sacchetto A, Soloperto D, Marchioni D. Frequency reallocation based on cochlear place frequencies in cochlear implants: a pilot study. Eur Arch Oto-Rhino-Laryngology. 2022;279(10):4719–25.
409 Fan X, Yang T, Fan Y, Song W, Gu W, Lu X, Chen Y, Chen X. Hearing outcomes following cochlear implantation with anatomic or default frequency mapping in

postlingual deafness adults. Eur Arch Otorhinolaryngol. 2024;281(2):719–729.
410 De Jong M. Effectiveness of phantom stimulation in shifting the pitch percept in cochlear implant users. Ear Hear. 2020;41(5):1258–1269.
411 Acoustical Society of America. American National Standards Institute S3.5-1997 (R2017)—Methods for Calculation of the Speech Intelligibility Index. 1997
412 Pavlovic C V. Speech intelligibility: a conceptual overview. In: Katz J, Chasin M, English KM, Hood LJ, Tillery KL, editors. Handbook of Clinical Audiology. 7th ed. Philadelphia, PA: Wolters Kluwer; 2018.
413 Creff G, Bernard-de-Libou X, Coudert P, Bourdon H, Pean V, Wallart N, Lambert C, Godey B. Tonotopic and Default Frequency Fitting for Music Perception in Cochlear Implant Recipients: A Randomized Clinical Trial. JAMA Otolaryngol Head Neck Surg. 2024;150(11):960–968.
414 Távora-Vieira D, Rajan G, Van de Heyning P, Mertens G. Quality standards for adult cochlear implantation in single-sided deafness and asymmetric hearing loss. B-ENT. 2020;16(4):209–2016.